Author:
Kingshott, Georgina G

Title:
The Impact of Metabolic Disturbance on Imprinting of IGF-II in Prostate and Colorectal Cancer

The Impact of Metabolic Disturbance on Imprinting of IGF-II/H19 in Prostate and Colorectal Cancer.

Georgina Kingshott

University of BRISTOL

Faculty of Health Sciences
Translational Health Sciences

A dissertation submitted to the University of Bristol in accordance with requirements of the degree DOCTOR OF PHILOSOPHY in the Faculty of Health Sciences, Translational Health Sciences.

June 2021

IGFs and Metabolic Endocrinology Group

Word count: 41,132

Abstract.

The insulin-like growth factor (IGF) axis is a complex signalling system mediates the effects of nutrition on cell growth. It is composed of two ligands, IGF-I and IGF-II, tyrosine receptors and a family of six high affinity IGF binding proteins. The IGF-II gene shares its locus with a lncRNA, H19. Both genes are subject to epigenetic regulation in the form of imprinting; a mechanism by which one parental copy of the IGF-II/H19 gene is silenced. In many malignancies, this silencing is lost, but the epigenetic events leading to this loss are yet to be determined. A link exists between cancer, type 2 diabetes (T2D) and obesity ("diabesity"). This study investigated the impact of inflammatory conditions *in vitro*, to mimic those synonymous with "diabesity"; loss of imprinting of IGF-II/H19 was induced in prostate and colorectal cancer cell lines. Loss of imprinting, determined by pyrosequencing, disrupted IGF-II/H19 mRNA expression but had no effect on secreted IGF-II peptide levels in prostate cancer; the impacts of disrupted IGF-II/H19 mRNA expression in relation to IGF-II peptide levels in colorectal cancer cell lines is yet to be determined. These data were compared with those *in vivo,* using clinical cohorts of prostate and colorectal cancer tissue. In both cohorts, approximately 30% of specimens presented with loss of imprinting of IGF-II/H19, which concurred with current evidence. Loss of imprinting increased IGF-II/H19 mRNA expression, with no changes to IGF-II peptide levels in either cohort; there was a positive correlation between IGF-II and H19 mRNA expression, regardless of imprinting status; this suggests alternative mechanisms are affecting gene transcription, in addition to imprinting loss.

Data shown by this thesis has demonstrated, for the first time, how metabolic disturbance of the cellular milieu can epigenetically affect regulation of the IGF-II/H19 gene and provides an important, additional link between T2D, obesity and cancer.

Covid 19 Mitigation Statement

Due to the recent Covid-19 pandemic, access to university laboratories was greatly restricted; the iodination required for the IGF-II radioimmunoassay, the experiment planned for inclusion in chapter 5, could not be performed in the remaining available time before submission deadline.

Acknowledgements

I would like to extend my sincere thanks and gratitude to my PhD supervisor, Dr Claire Perks. Her unwavering support over the past four years, in matters both academic and personal, has been invaluable.

I would also like to thank members of IMEG, specifically Dr Kalina Biernacka and Dr Rachel Barker; their continued encouragement over the past 4 years has kept me on the PhD path!

Publications

Kingshott, G., Biernacka, K., Sewell, A., Gwiti, P., Barker, R., Zielinska, H., Gilkes, A., McCarthy, K., Martin, R.M., Lane, J.A., McGeagh, L., Koupparis, A., Rowe, E., Oxley, J., Holly, J., Perks, C.M. The Impact of Altered Metabolism on the Regulation of IGF-II/H19 Imprinting Status in Prostate Cancer. *Cancers*. 2021; 13(4): 825

My contribution: I wrote all paper content and conducted all experiments.

Conference and academic abstracts related to this thesis.

Regulation of IGF-II/H19 imprinting status in prostate cancer.

Gordon Research Conference on IGF and Insulin System in Physiology and Disease: 10-15th March 2019, Ventura Beach Marriott, Ventura, CA, USA

Academic Awards / Grants received in relation to this thesis.

Gordon Research Conference on IGF and Insulin System in Physiology and Disease: 10-15th March 2019: Travel Award $500

Alumni Foundation Award for attendance at above conference: £1,000

Author’s declaration.

I declare that the work in this dissertation was carried out in accordance with the requirements of the University's *Regulations and Code of Practice for Research Degree Programmes* and that it has not been submitted for any other academic award. Except where indicated by specific reference in the text, the work is the candidate's own work. Work done in collaboration with, or with the assistance of, others, is indicated as such. Any views expressed in the dissertation are those of the author.

SIGNED: .....  ..... DATE: .....05/06/2021.....

Abbreviations.

4EPB-1: Eukaryotic translation initiation 4E-binding protein

ADP: adenosine diphosphate

ADT: Androgen deprivation therapy

AKT: AK-strain transforming.

ALS: Acid labile subunit

AMP: adenosine monophosphate

AMPK: activate 5' adenosine monophosphate-activated protein kinase.

ANOVA: Analysis of variance

APC: Adenomatous polyposis coli

ATCC: American Type Culture Collection

ATP: adenosine triphosphate

BMI: Body mass index

BRCA1 / BRCA2: Breast Cancer 1 and 2

BSA: Bovine serum albumin

CD: Cluster of differentiation

cDNA: Complementary DNA

CHRNA5: cholinergic receptor nicotinic alpha 5 subunit

CR: Co-repressor

CRC: Colorectal cancer

CRCM: Colorectal cancer metabolism

ddPCR: Digital droplet polymerase chain reaction

dH_2O: Doubly distilled water

DMEM: Dulbecco's modified Eagles Medium

DMR: Differentially methylated region

DMSO: Dimethyl sulfoxide

DRE: Digital rectal examination

E2F3: E2F Transcription factor 3

ECACC: European Collection of Authenticated Cell Cultures

EMEM: Eagles Minimum Essential Medium

EMT: epithelial to mesenchymal transition

ERK: Extracellular signal-regulated Kinase

EWAS: Epigenome wide association study

FBS: Foetal bovine serum

FFPE: Formalin fixed paraffin embedded.

G2E3: G2 / M phase-specific E3 ubiquitin-protein ligase

GF: Growth factor

GLRA1: glycine receptor alpha 1

GLUT: Glucose transporter

GWAS: genome-wide association studies

HDAC: Histone deacetylase

Hg: High glucose

HNPCC: Hereditary non-polyposis colon cancer

HOXB13: Homeobox B13

HPEC: Human prostate epithelial cell

IBD: Inflammatory bowel disease

ICR: Imprinting control region

IGFBP: Insulin-like growth factor binding protein.

IGF-I /- IIR: Insulin-like growth factor I / II receptor

IGF-I or II: Insulin-like growth factor I or II

IHC: Immunohistochemistry

IL: Interleukin

IMP-1, -2, -3: Insulin-like growth factor II mRNA binding protein

INS: insulin

IR: Insulin receptor

IRES: internal ribosome entry site

IRS: Insulin receptor substrate

Lg: Low glucose

lncRNA: Long non-coding RNA

LOI: Loss of imprinting

LSD: Least significant difference

M5M: McCoy's 5A medium

MEK / MAP: mitogen-activated protein

miRNA / miR-: Micro RNA

MMR: Mismatch repair

MOI: Maintenance of imprinting

MRI: Magnetic resonance imaging

mRNA: Messenger RNA

mTOR: Mammalian target of rapamycin

NaB: Sodium butyrate

NaOH: Sodium hydroxide

NF-κβ: necrosis factor–kappa-beta

NICE: National institute for clinical excellence

P: Promoter

PBS: Phosphate buffered saline.

PCa: Prostate cancer

PCR: Polymerase chain reaction

PIE: Pyrosequencing for allelic imprinted expression

PIN: Prostatic intraepithelial neoplasia

PrEvENT: Prostate Cancer Evidence of Exercise and Nutrition Trial

PSA: Prostate specific antigen

qPCR: Quantitative polymerase chain reaction.

Ras: Rat sarcoma

RASD1: rat sarcoma-related dexamethasone induced-1

RASGRF1: Ras-specific guanin nucleotide-release factor 1

RD: rhabdomyosarcoma

RFLP: Restriction fragment length polymorphism

RIA: Radioimmunoassay

RNP: Ribonucleoprotein particle

ROS: reactive oxygen species

RPM: Rotations per minute.

RPMI: Roswell Park memorial institute medium

SEM: Standard error margin

SFM: Serum free media

SLCO5A1: solute carrier organic anion transporter family 5

SNP: Single nucleotide polymorphism

SOX18: sex determining region Y-box 18.

ssDNA: Single stranded DNA

T2D: Type 2 diabetes

TB: Trypan blue

TET2: Ten-eleven translocation dioxygenase 2

TH: Tyrosine hydroxylase

TIMP4: of tissue inhibitor of metalloproteinases 4

TNF-α: Tumour necrosis factor-alpha

TNM: Tumour, Node, Metastasis

UTR: Untranslated region

List of figures.

List of tables.

Contents

CHAPTER 1: INTRODUCTION

1.1. Summary of the IGF Axis

The insulin-like growth factor (IGF) / insulin axis is a complex signalling system implicated in metabolic and mitotic growth promotion across many tissue types and organs, with each family member playing a key role in the regulation of cell proliferation, differentiation and apoptosis (Bowers, Rossi *et al*. 2015). The axis comprises three ligands: insulin-like growth factor-I (IGF-I) – also called somatomedin-C (Marshall, Underwood *et al*. 1974), insulin-like growth factor-II (IGF-II) and insulin (Blyth, Kirk *et al*. 2020); each exerts its action through binding to cell surface tyrosine kinase receptors (De Meyts and Whittaker 2002; Osher and Macaulay 2019). The effects of the IGFs can be modulated in an IGF-dependent or independent manner by a family of six high affinity IGF binding proteins (IGFBPs) (Allard and Duan 2018).

1.2 IGFs.

IGFs are growth factors implicated in numerous cellular events, such as proliferation, differentiation, and apoptosis. There are two types: IGF-I and IGF-II (Salmon and Daughaday 1957), both of which are structurally homologous to insulin.

1.2.1 IGF-I

Growth hormone, secreted by the anterior pituitary gland, induces production of IGF-I in the liver. It also regulates the paracrine production of IGF-I by many other tissues (Laron 2001; Chao and D'Amore 2008; Kasprzak, Kwasniewski *et al*. 2017).

The human IGF-I gene is located within a region of over 85 kb on the long arm of chromosome 12 (Brissenden, Ullrich *et al*. 1984) and is composed of six exons. The six exons are alternatively spliced into multiple transcripts, which are translated into different precursor polypeptides. These precursor polypeptides are subject to further post-translational modifications into isoforms of the IGF-I peptide, which have been shown to exhibit specific signaling responses (Philippou, Maridaki *et al*. 2014). Figure 1.2.1 depicts the structure of the IGF-I gene, with the six splice variants which lead to synthesis of the different isoforms of the IGF-I peptide. The total length of the human IGF-I protein is 70 amino-acids long, cross-linked with three disulphide bridges. The total weight is approximately 7.5 KDa (Rinderknecht and Humbel 1976).

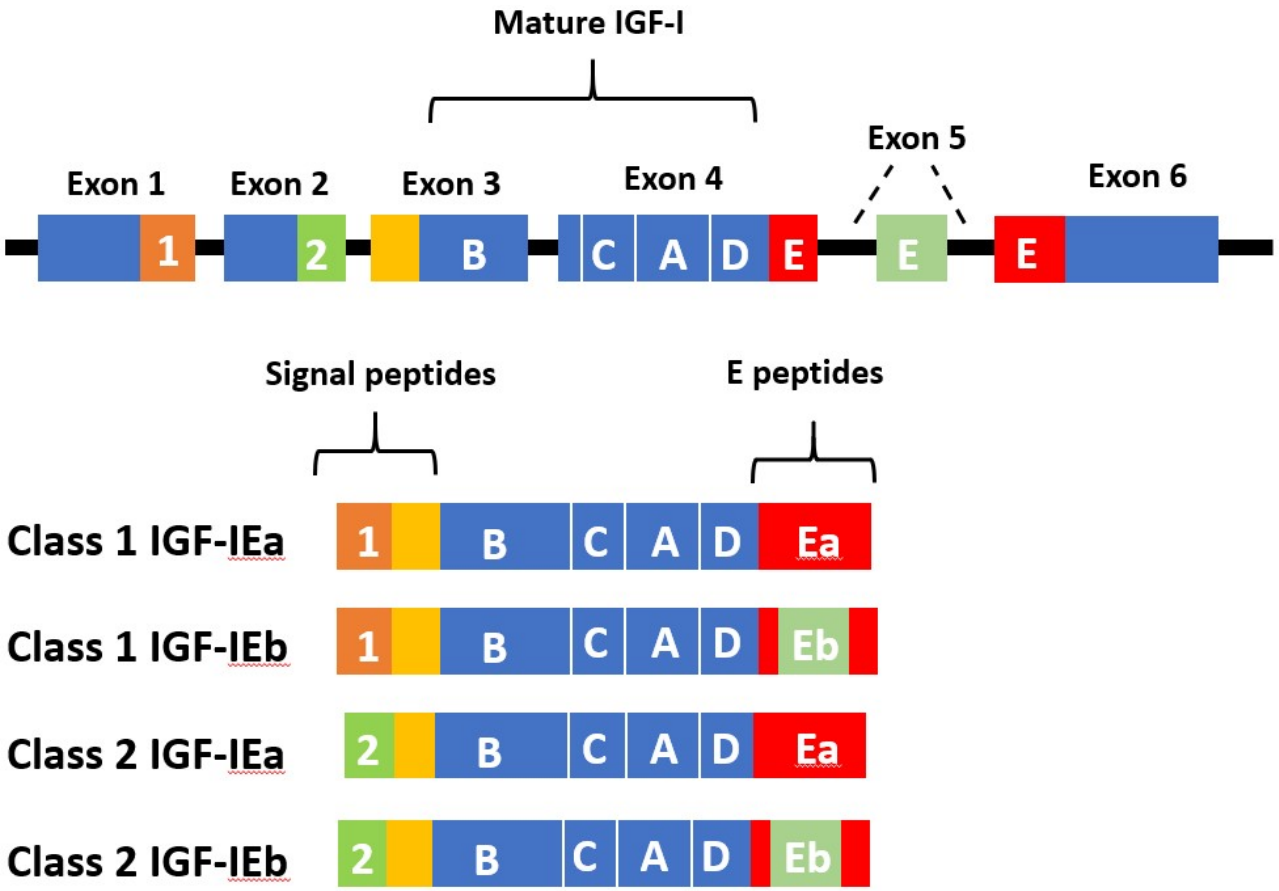

Figure 1.2.1: Gene structure of IGF-I and splice variant isoform.

The core peptide is coloured blue; exons 1-3 encode the signal peptide precursor of IGF-I (yellow); exons 5-6 encode specific sections of the E-peptides (red and light green boxes). (adapted from Vinciguerra, Musaro *et al*. 2010)

1.2.2 IGF-II

IGF-II was identified alongside IGF-I in 1957 (Salmon and Daughaday 1957). Situated within IGF-II is the long non-coding RNA (lncRNA), H19 (Doucrasy, Coll *et al*. 1993). These two genes are co-expressed primarily during embryonic and foetal development, across different tissue types. Details pertaining to IGF-II expression in foetal tissue remains unclear. However, mRNA transcript levels of IGF-II and IGF-IIR have been measured in human chorionic villus samples, where a significant positive correlation was found with birthweight (Demetriou, Abu-Amero et al. 2014). Expression of IGF-II continues throughout life, predominantly secreted by the liver (Engstrom, Shokrai *et al*. 1998; Gabory, Ripoche *et al*. 2006; Bergman, Halje *et al*. 2013).

The human IGF-II/H19 gene is located on the short arm of chromosome 11 (Brissenden, Ullrich *et al*. 1984) and consists of 9 exons (de Pagter-Holthuizen, Hoppener *et al*. 1985). The first six involve non-coding exons; control of the expression takes place from four promoters (P1-P4) and is strictly regulated (van Dijk, van Schaik *et al*. 1991). This is depicted by figure 1.2.2.

Transcripts differ in their 5'UTR (untranslated region) but have identical coding and 3'UTRs (Meinsma, Holthuizen *et al*. 1991). Transcripts derived from the promoter P3 are also subjected to further control by a family of IGFII mRNA binding proteins (IMPs1-3, which are encoded by IGF-II BP1-3). The IGF-II protein consists of 67 amino acids (Meinsma, Holthuizen *et al*. 1991) and shares 65% homology with IGF-I (Rinderknecht and Humbel 1976).

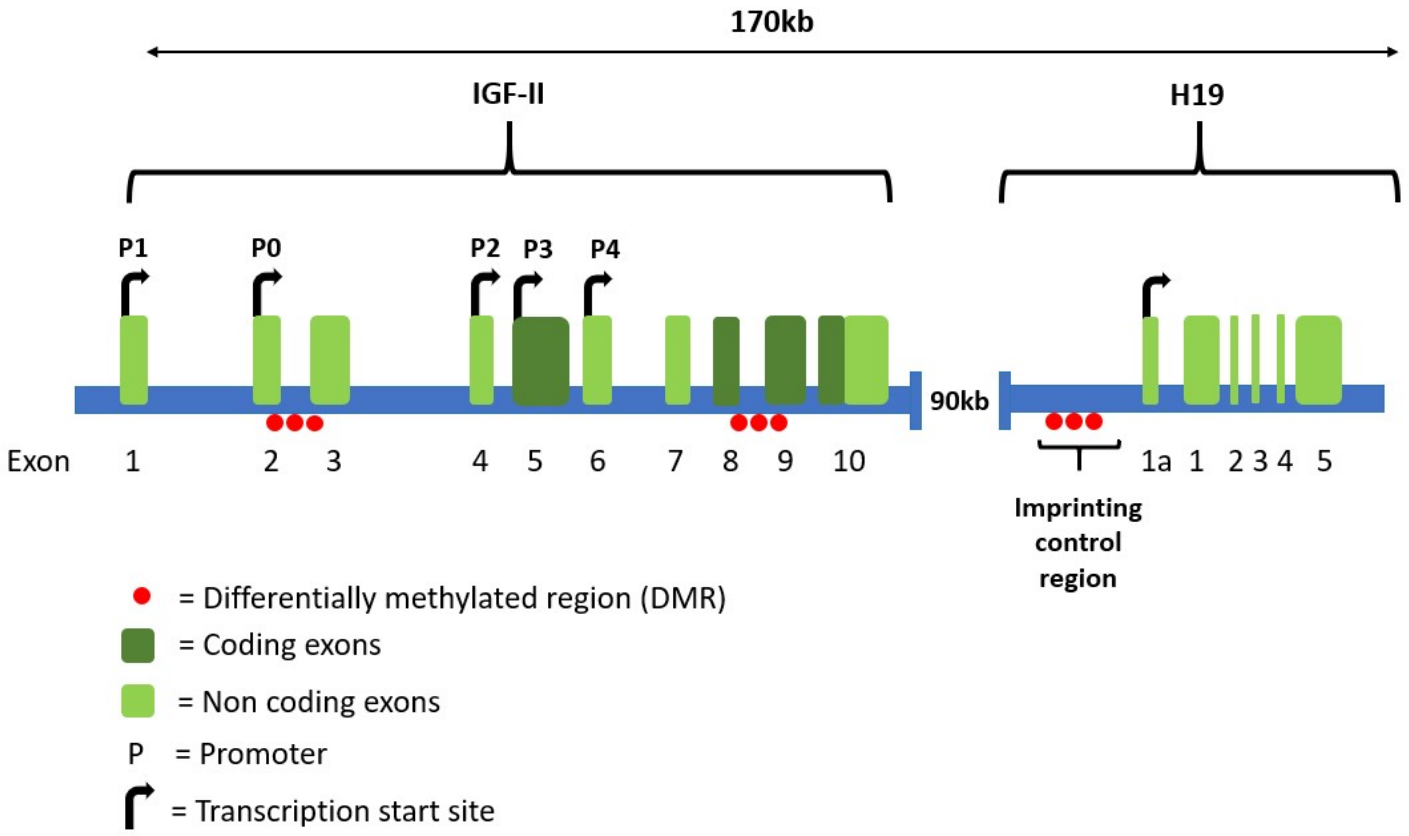

(adapted from Boissonnas, Abdalaoui *et al*. 2010; Kuffer, Gutting *et al*. 2018; Baral and Rotwein 2019)

Figure 1.2.2: Schematic of the IGF-II/ H19 gene locus: The gene consists of 10 exons in IGF-II and 5 in H19. Control of expression takes place from five promoters (P0-P4) and is strictly regulated. The imprint control region can be methylated – which blocks transcription of H19, or unmethylated – which blocks transcription of IGF-II. There are three differentially methylated regions (DMRs) across the gene.

1.2.2.1 IGF-II mRNA binding proteins (IMPs)

It was in 1999, that IGF-II mRNA-binding proteins (IMPs) were first identified (Nielsen, Christiansen *et al*. 1999); IMPs are oncofoetal proteins primarily synthesised during early embryonic development and foetal growth, with expression reoccurring in pre-cancerous and cancerous tissues (Christiansen, Kolte *et al*. 2009; Dai, Christiansen *et al*. 2013). IMPS are generally found in the cytoplasm, where they bind to target mRNA transcripts in a protective capacity to form stable protein complexes, called ribonucleoprotein particles or RNPs (Oleynikov and Singer 2003); IMPs behave as post-transcriptional modulators, regulating expression of IGF-II mRNA transcripts essential for cellular growth and proliferation (Huang, Zhang *et al*. 2018). More specifically, IMP1 is essential for cellular migration, facilitating the localisation of EMT mRNAs – such as E-cadherin, β-actin and α-actin (Gu, Katz *et al*. 2012; Nwokafor, Sellers *et al*. 2016); IMP2 has many functions across several tissue types, such as adipose, liver and muscle; it regulates the oxidation of fatty acids by the formation of RNPs, across different tissues (Dai 2020). IMP3 regulates the transport and translation of β-actin, as well as IGF-II (Zhang, Wang *et al*. 2020).

1.2.3 Insulin

After findings published in 1892 documenting the effects of pancreatic removal in dogs (Minkowski, 1892), it was in 1921 that insulin was finally identified as being the substance responsible for controlling blood glucose (Banting and Best 1922). It was first used to treat patients with diabetes the following year (Banting, Best *et al*. 1922), before being mass-produced in 1923 by the pharmaceutical company, Eli Lilly (being of bovine and porcine origin) (Rosenfeld 2002).

Insulin was first identified as a protein in 1924 after studying its biochemical behavior (Somogyi, Doisy and Shaffer, 1924). Its amino acid sequence was revealed in 1951 (Sanger and Tuppy 1951), followed almost thirty years later by characterization and sequence of the insulin (INS) gene (Bell, Pictet *et al*. 1980). Its mapped location is on the short arm (p) of chromosome 11, position 15.5, in humans (11p15.5) (Owerbach, Bell *et al*. 1981). Beta cells, within the pancreas, secrete insulin primarily in response to elevated blood glucose levels. Figure 1.2.3 depicts a simplified schematic of the insulin locus on chromosome 11, in relation to other genes.

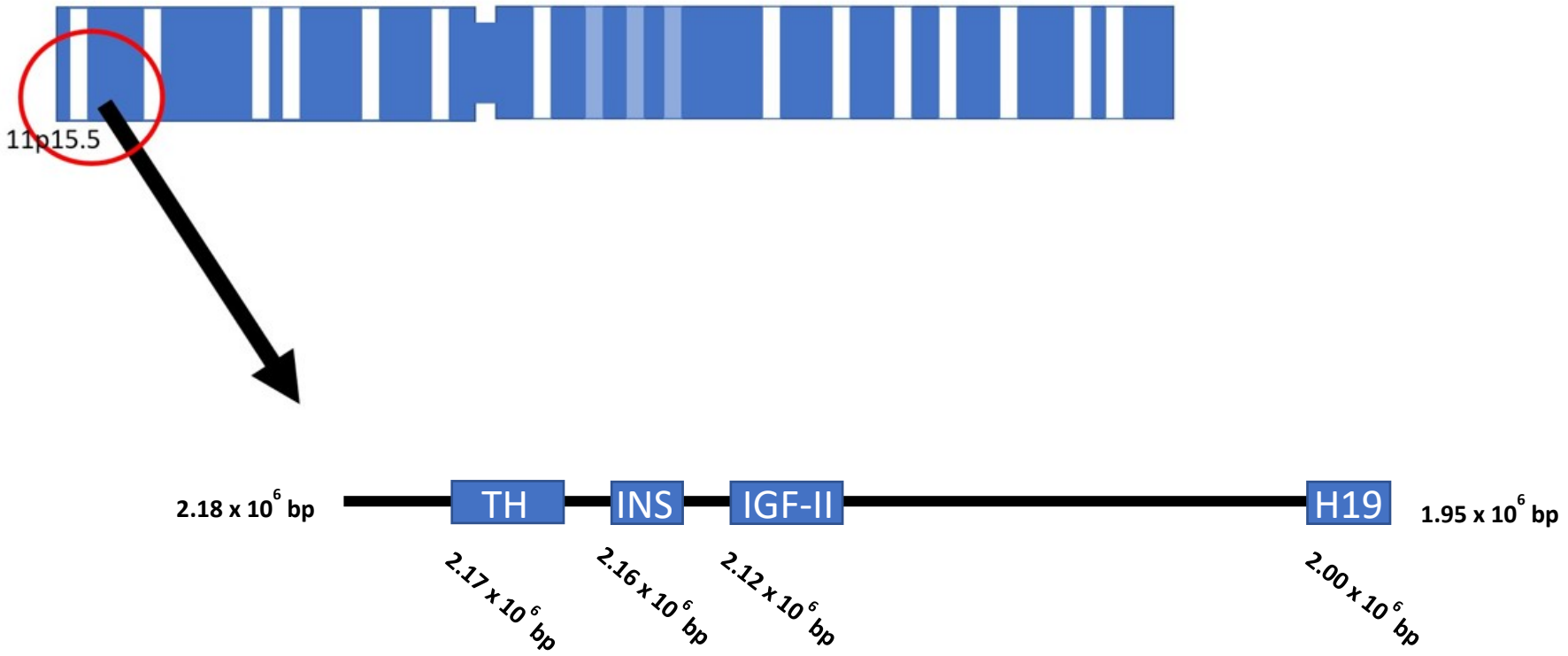

Figure 1.2.3: Position of TH/INS/IGF-II & H19 gene cluster on short arm of chromosome 11, with approximate lengths in base pairs.

TH = tyrosine hydroxylase; INS = insulin; IGF-II = insulin-like growth factor-II (adapted from Mutskov and Felsenfeld 2009; Eggermann, Bliek *et al*. 2016; Baral and Rotwein 2019)

1.3 Receptors of the IGF axis.

Growth factors (GFs) elicit their effects by binding to specific membrane receptors. There are four main receptors: insulin receptor (IR) (Massague, Pilch *et al*. 1980), type I (IGF-IR) (Zapf and Froesch 1981), type II (IGF-IIR) (Sara, Hall *et al*. 1982), and hybrid receptors (IGFIR/IR) (De Vroede, Rechler *et al*. 1986).

The IR and IGF-IR exhibit a high degree of structural similarity; both are hetero-tetrameric, composed of 2 extracellular α sub-units and 2 intra-cellular β sub-units, and both are transmembrane tyrosine kinase receptors (Massague and Czech 1982). The IR is thought to be a metabolic regulator, playing a key role in the storage and release of glucose, protein, and fats within the cell. Two forms of IR are generated: IR-A and IR-B. IR-A is formed by the exclusion of exon 11 and is primarily mitogenic in function, as it binds insulin and IGF-II with equal affinity (Frasca, Pandini *et al*. 1999). IR-B is formed when exon 11 is included and has greater metabolic function, as it predominantly binds insulin. A key role of the IGF-IR is to mediate whole body and organ growth. The IGF-IR preferentially binds to IGF-I but is also able to bind IGF-II and insulin. Ligand binding to an α sub-unit causes a conformational change that initiates receptor tyrosine kinase activity, resulting in autophosphorylation of intracellular tyrosine residues within the β sub-unit (Wang, MacDonald *et al*. 2017). Once phosphorylated, the tyrosines act as landing sites for other intracellular signalling peptides, such as IR substrate proteins 1 and 2 (IRS1 and 2) and Ras, that leads to the activation of specific signalling pathways, such as mitogen-activated protein (MAP) kinase and the canonical PI3 kinase signalling system, which regulate cell growth, survival, migration, metabolism, and blood vessel formation (Belfiore 2007; Wrigley, Arafa *et al*. 2017), depicted by figure 1.3.

Additionally, hybrid receptors can form consisting of half an IR and half an IGF-IR.

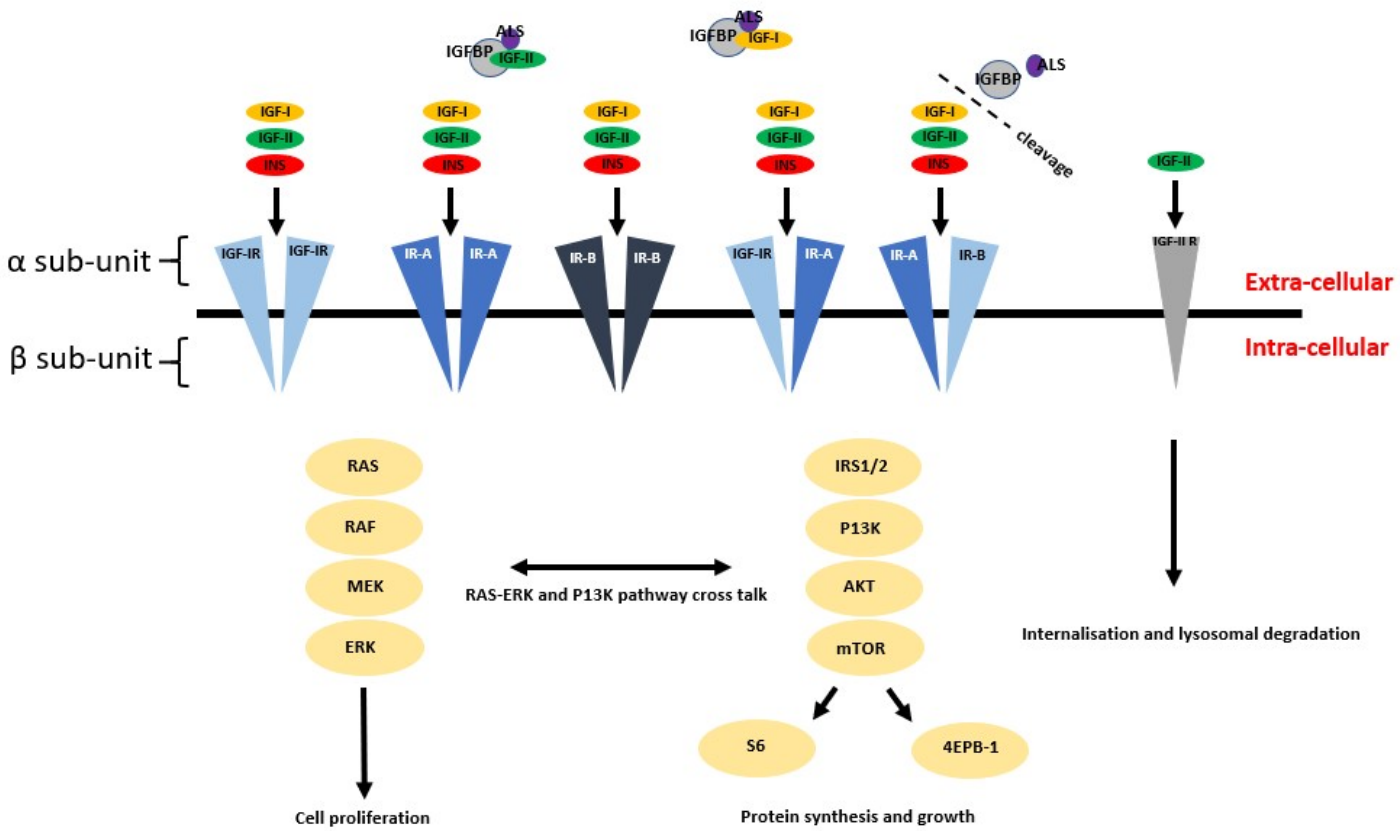

Figure 1.3: Receptors of the IGF axis.

Receptors of the IGF axis, with arrows indicating binding sites for ligands. Key: IGF-IR= IGF-I receptor; IR* = insulin receptor; IGF-IIR = IGF-II receptor; IGFBP = IGF binding protein; ALS – acid labile subunit. (Adapted from Chen and Sharon, 2013; Bowers and Ross, *et al*., 2015). This diagram is based on research conducted upon the biochemical interactions between receptors and ligands of the IGF-II axis.

The exception to the structural homology among the receptors is the type II IGF receptor (IGF-IIR; also known as the mannose 6-phosphate receptor), which lacks tyrosine kinase function. Instead, the IGF-II receptor acts to clear it from the circulation and tissues by binding and internalizing IGF-II which is then subject to lysosomal degradation (Kornfeld 1992).

1.4 IGF binding proteins (IGFBPs).

In the circulation, most IGFs (IGF-I and -II) are bound to one of 6 binding proteins: IGFBPs 1-6. In adults, most (approximately 75-90%) circulatory IGFs are bound to IGFBP-3 or -5, to a lesser extent, (Baxter 1994), along with a glycoprotein called the acid labile subunit (ALS) (Rajaram, Baylink *et al*. 1997; Allard and Duan 2018). Most IGFBP3 is secreted by the liver, with expression being regulated by GH. This allows a proportional amount of IGFBP3 to be secreted in relation to the IGF-I (Blum, Albertsson-Wikland *et al*. 1993; Allard and Duan 2018).

The bound IGF/IGFBP3/ALS molecule is too large to pass through capillary walls and, as such, it is restricted to remaining within the circulation (Lewitt, Saunders *et al*. 1994; Allard and Duan 2018). IGFs in an unbound state are unstable and have an estimated half life of as little as 10 minutes; conversely, binding to an IGFBP increases this to around 25 minutes (Guler, Zapf *et al*. 1989; Allard and Duan 2018). IGFBPs are proteolytically cleaved, releasing the IGF to bind smaller molecular weight IGFBPs in a binary complex; these complexes can pass through capillary walls, enabling transport of the IGF to the tissue site that requires it.

Additionally, IGFBPs have a more potent binding affinity for IGFs compared to their receptors and, for this reason, they can have an inhibitory effect blocking receptor binding (Mohan and Baylink 2002; Ding and Wu 2018). Most notably, IGFBPs do not bind with insulin (Firth and Baxter 2002). The IGFBPs are expressed in a tissue-specific manner and confer specificity to the IGFs; they can inhibit or enhance the actions of the IGFs (Kasprzak, Kwasniewski *et al*. 2017) and can act in a manner that is either IGF-dependent or independent (Allard and Duan 2018). Proteolytic fragments of IGFBP-5, -4, and -3, have been shown to exhibit ligand-independent biological activities (Boguszewski, Boguszewski *et al*. 2016).

1.5. Epigenetic regulation and the IGF axis.

Epigenetic regulation is one way of controlling gene expression, without affecting the DNA sequence. Typically this occurs through gene silencing by chemically editing regions of the DNA or the proteins that are immediately associated with it, such as histone proteins (Jaenisch and Bird 2003). One of the key epigenetic mechanisms implicated in gene expression is methylation. DNA methylation is an enzyme-controlled chemical alteration to the DNA structure. A methyl group ($-CH_3$) is covalently bonded to the 5-carbon on the cytosine base. Cytosines adjacent to guanine bases are known as CpG islands, and it is these that are analysed when assessing methylation patterns (Jeziorska, Murray *et al*. 2017). Methylated DNA binds to a protein complex, known as a methyl binding protein (MBP). MBP possesses a methyl-binding domain and a transcriptional repressor domain, a co-repressor molecule (CR), and a histone deacetylase (HDAC) molecule (Li, Chen *et al*. 2015); once bound to the methylated DNA, the histones around which the DNA is wrapped become deacetylated, resulting in a more condensed chromatin structure. This results in the DNA becoming inaccessible, disallowing functional transcription (Jiang and Pugh 2009).

Components of the IGF axis have been reported to be epigenetically modified, including IGFBPs-2 and -3 (Tang, Gillatt *et al*. 2019; Kumar, Singh *et al*. 2020). However, the focus of this thesis is the epigenetic regulation of IGF-II/H19 through via imprinting.

Imprinting occurs when one of the two parental copies of a gene will be silenced through structural changes to DNA, affecting expression. The phenomenon of genomic imprinting was discovered in 1984 by two separate teams of scientists – one directed by Davor Solter (McGrath and Solter 1984) in the US, and the other by Azim Surani (Surani, Barton *et al*. 1984) in the UK. Since publication of these findings, it has been observed that genomic imprinting also occurs after birth, continuing throughout life.

Insulin-like growth factor II (IGF-II) was the first imprinted gene to be identified (DeChiara, Robertson *et al*. 1991); it was observed that male mice carrying a mutation in IGF-II sired heterozygous progeny that were growth deficient. Conversely, female mice carrying the same mutation birthed heterozygous offspring with no growth defects. DeChiara *et al* concluded that this disparity in growth phenotypes must depend upon the source gamete carrying the mutation. The following year, the embedded lncRNA H19 was also identified as being subject to imprinting, resulting in paternal expression of IGF-II and maternal expression of H19 (Zemel, Bartolomei *et al*. 1992).

H19 does not encode any known peptide, rather the gene's functional product is a 2.3 kb long non-coding RNA (lncRNA) whose biochemical activities have only been explored in the last ten years (Park, Mitra *et al*. 2017), having first been identified in 1984 (Pachnis, Belayew *et al*. 1984).

One suggested role for the lncRNA is that it is the substrate used to generate two microRNAs (miRNAs), miR-675-3p and miR-675-5p (Wang, Wang *et al*. 2017). Genetic studies support a role for these miRNAs in placenta development (Keniry, Oxley *et al*. 2012) and in skeletal muscle differentiation and regeneration (Dey, Pfeifer *et al*. 2014). Furthermore, H19 can also bind miRNAs (Deng, Wang *et al*. 2016). Another proposed biochemical function is that H19 lncRNA interacts directly with transcription factor proteins, including p53, to reduce their bioactivity (Zhang, Zhou *et al*. 2017).

1.5.1 Imprinting of the IGF-II/H19 gene.

The first suggested mechanistic model of IGF-II/H19 imprinting, the 'Enhancer Competition Model', was presented in 1994 (Moulton, Crenshaw *et al*. 1994; Steenman, Rainier *et al*. 1994). In the 'Enhancer Competition Model', a CCCTC-binding factor (CTCF; a multi-zinc finger protein and transcriptional repressor), binds to an unmethylated imprinting control region (ICR) within the maternal allele of the IGF-II/H19 gene locus. This prevents transcription of IGF-II. Conversely, on the paternal allele, hypermethylation of the ICR prevents CTCF binding, resulting in IGFII expression. Figure 1.5.1 depicts the epigenetic state of the imprinted IGF-II/H19 domain on the parental genomes: on the paternal chromosome the H19 gene and the adjacent differentially methylated region (DMR) are methylated preventing H19 expression and the binding of the insulator CTCF, thus allowing enhancers access to the IGF-II gene promoting its expression. Without methylation at the DMR on the maternal chromosome bound enhancer activity is inhibited by CTCF, silencing the IGF-II gene. Notably, enhancer activity is restricted to the unmethylated H19 gene, culminating in its expression by the maternal chromosome (Park, Mitra *et al*. 2017).

Building on original findings, showed by Taniguchi *et al* (Taniguchi, Sullivan *et al*. 1995), further in-depth methylation analysis has demonstrated that hypermethylation of the ICR on both alleles causes bi-alleleic transcription of IGF-II (Kuffer, Gutting *et al*. 2018).

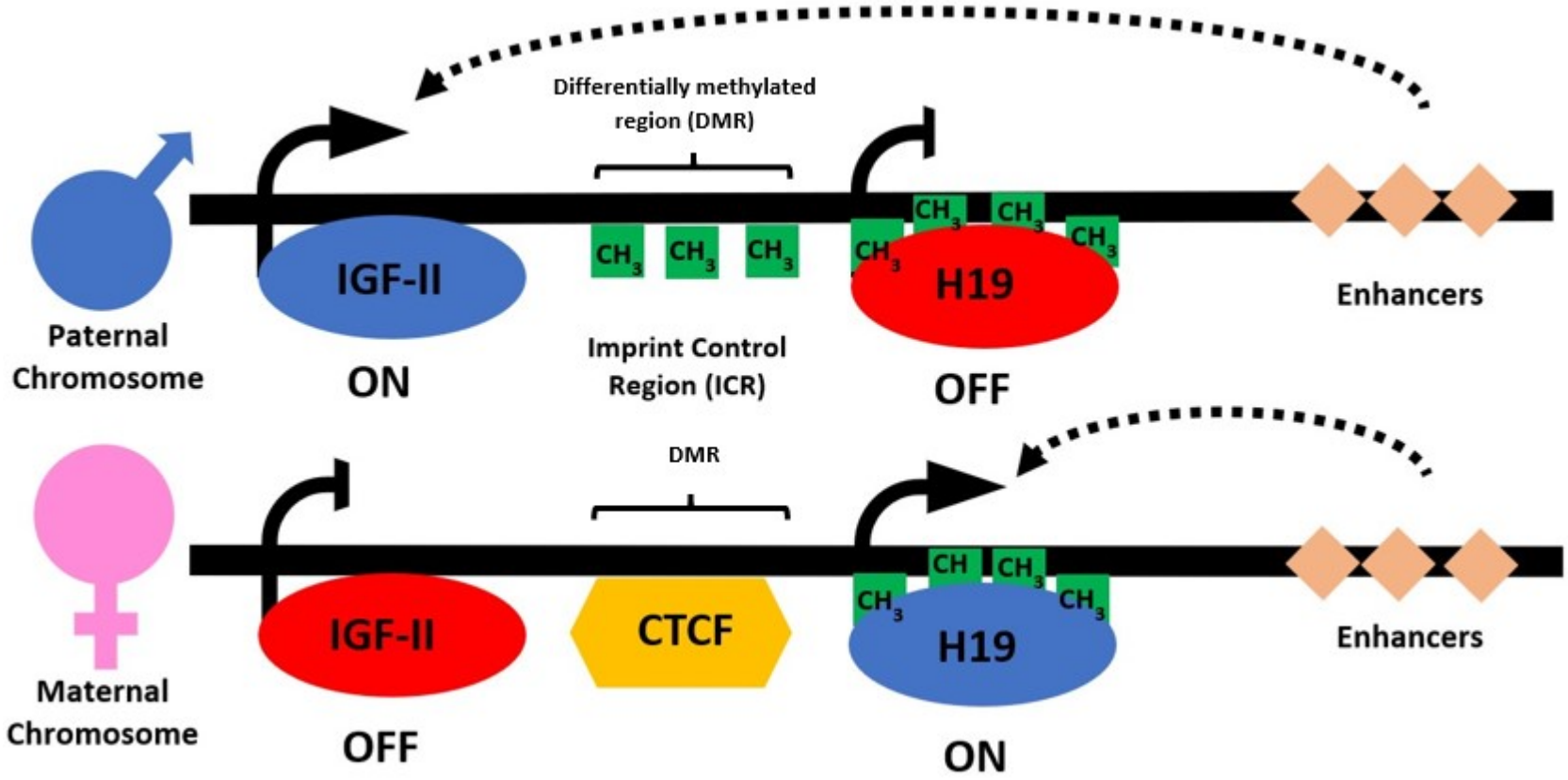

Figure 1.5.1: The epigenetic state of the imprinting IGF-II/H19 domain on the paternal and maternal genome (adapted from Reik and Murrell 2000).

1.6 Obesity and Type 2 Diabetes

An increased sedentary lifestyle across the developed world has led to an obesity crisis, with a quarter of UK adults now being classed as obese (Theis and White 2021) . It is thought that the increased adipose tissue, associated with obesity, produces over 20 hormones and cytokines that can disturb the delicate balance of the cellular environment leading to an inflammatory state (Lengyel, Makowski *et al*. 2018). The link between obesity and systemic inflammation was first identified in mice, where it was shown that increased numbers of adipocytes (fat cells) express increased amounts of the pro-inflammatory marker tumour necrosis factor-α (TNF-α) (Hotamisligil, Shargill *et al*. 1993). This was subsequently shown to also occur in humans (Kern, Ranganathan *et al*. 2001). Elevated secretion of adipocytokines leads to low grade inflammation and hypoxia, resulting in disrupted DNA methylation (Samblas, Milagro *et al*. 2019). Recently a publication reported findings concerning DNA methylation and adiposity in an Epigenome Wide Association Study (EWAS) (Crocker, Domingo-Relloso *et al*. 2020); the report explored the link between differential DNA methylation and one of three adiposity phenotypes, namely Body Mass Index (BMI), waist circumference and impedance-measured body fat. Aberrant methylation at 8264 CpG sites was shown to correlate with at least one of the three phenotypes.

There are numerous comorbidities associated with obesity including heart disease, stroke, insulin resistance and type 2 diabetes (Khaodhiar, McCowen *et al*. 1999; Quail and Dannenberg 2019; Srivastava and Goodwin 2020). Insulin resistance is said to occur when a cell's reaction to insulin becomes compromised; decreased stimulation of cellular glucose transport and metabolism by adipocytes occurs, along with weakened suppression of glucose production by the liver (Reaven 1995; Kahn and Flier 2000). Insulin resistance is a key symptom of obesity and is considered the precursor of type 2 diabetes (Reaven 2005; Czech 2017). If left untreated or unmonitored, insulin resistance leads to type 2 diabetes, the key symptom of which is hyperglycaemia (diabetes.co.uk, 2019).

Hyperglycaemia has been shown affect methylation patterns across the DNA strand. In 2012, Volkmar *et al*. (Volkmar, Dedeurwaerder *et al*. 2012; Pinzon-Cortes, Perna-Chaux *et al*. 2017) found reduced DNA methylation patterns in pancreatic tissue derived from T2D patients, which was thought to be due to disrupted glucose and insulin levels; Hall *et al*. (Hall, Dekker Nitert *et al*. 2018) showed high glucose to affect pancreatic islet gene expression, through disruption to methylation patterns. In 2018, Wang *et al*. (Wang, Tang *et al*. 2018) demonstrated that high glucose was able to affect DNA methylation levels in human oocytes, *in vitro.*

1.6.1 Obesity, Type 2 Diabetes and Cancer

The link between obesity and cancer risk has been well documented (Bandi, Minihan *et al*. 2021; Brown, Carson *et al*. 2021; Fernandez, George *et al*. 2021; Lifshitz, Ber *et al*. 2021; Liu, Pedersen *et al*. 2021; Tsekrekos, Lovece *et al*. 2021); numerous studies have consistently shown positive correlations between body mass index (BMI) and cancer risk (Jochem and Leitzmann 2016).

1.6.2 IGFs and Cancer

An increased risk and worse outcome of several cancers have been linked with the IGF axis. This has led to a growing interest in the understanding of these signalling pathways and the development of agents targeting them (Bleach, Sherlock *et al*. 2021; Gutierrez-Salmeron, Lucena *et al*. 2021; Ianza, Sirico *et al*. 2021; Mancarella, Morrione *et al*. 2021) .

In vitro studies have shown an increased expression of IGF-I and its receptors in a variety of cancer types including breast (Morimoto-Kamata and Yui 2017) , prostate (Miles, Goodman *et al*. 2017), brain (Wang, Tang *et al*. 2017), ovary (Du, Shi *et al*. 2017), colorectal (Um, Fedirko *et al*. 2017), and renal (Liao, Hofmann *et al*. 2017). This increased expression has also been associated with poorer therapeutic response to radio- and chemotherapy (Boguszewski, Boguszewski *et al*. 2016). IGFs alone, or by cross-talk with other growth factors, can promote tumour growth by affecting cell growth , differentiation, and survival (Locatelli and Bianchi 2014). Additionally, IGFs have been shown to exhibit angiogenic properties and to be able to promote metastases (Bach 2017). Aberrant expression of the IGFs, particularly IGF-II (Zhang, Zhou *et al*. 1997), is common in many malignancies, such as breast (Molnar, Meszaros *et al*. 2020), prostate (Schagdarsurengin, Lammert *et al*. 2017) brain (Oliva, Halloran *et al*. 2018) and colorectal (Lu, Cai *et al*. 2019) cancers. In some malignancies, mutations in the IGF-IIR occur, preventing degradation of IGF-II; this causes increased levels of IGF-II, which subsequently bind with other receptors inducing cell signal cascades (Iida, Salomon *et al*. 2018; Hughes, Surakhy *et al*. 2019; Liu, Zhou *et al*. 2020)

1.6.3 IGF-II/ H19, imprinting and cancer.

Aberrant expression of IGF-II was first noticed and explored in Wilms' tumour - a paediatric cancer of the kidneys (Cancer.org., 2018). In 1985, a study found increased expression of IGF-II transcripts in Wilms' tumour, compared to healthy kidney tissue (Reeve, Eccles *et al*. 1985).

Almost 10 years later, the cause of this increased expression was finally attributed to relaxed imprinting or "loss of imprinting" (LOI) in the IGF-II gene (Ogawa, Eccles *et al*. 1993). A report published in 1995 (Taniguchi, Sullivan *et al*. 1995), delved deeper into the source of imprinting loss; in a sub-set of Wilms tumours, biallelic expression of IGF-II corresponded with low levels of H19. Through methylation analysis, biallelic expression of IGF-II was shown to be caused by a reversal of the DNA methylation patterns on the maternal allele. LOI was also observed in another paediatric malignancy; in rhabdomyosarcoma, over-expression of IGF-II had also been observed and attributed to loss of imprinting (Zhan, Shapiro *et al*. 1994).

These findings from paediatric cancers were further explored in adult malignancies, with LOI found to cause upregulation of H19 in lung tumours (Kondo, Suzuki *et al*. 1995), upregulation of both IGF-II and H19 in liver tumours (Rainier, Dobry *et al*. 1995), and upregulation of IGF-II in uterine (Vu, Yballe *et al*. 1995) and prostate cancer (PCa) (Jarrard, Bussemakers *et al*. 1995). These findings demonstrate that LOI can cause independent effects on IGF-II and H19.

1.6.4 Mechanisms Underlying the Obesity-Cancer Relationship: Hyperglycaemia and Insulin Signalling.

The association of hyperglycaemia with T2D and obesity is thought to be one of the underlying causes behind increased cancer risk and poor prognostic outcome amongst this populace; as glucose is the main energy source for cells, including cancer cells, an increase in its supply can cause increased proliferative potential (Goto, Yamaji *et al*. 2020). Not surprisingly, circulatory IGF-II concentrations are higher in the obese population and have been linked with increasing BMI (Buchanan, Phillips *et al*. 2001; Livingstone and Borai 2014). Exploration into the link between IGF-II and adult obesity began in 1997, where it was noted that homozygous expression of a particular single nucleotide polymorphism (SNP) within the IGF-II gene locus showed a positive correlation with increased BMI in males (O'Dell, Miller *et al*. 1997). Subsequent findings in a mixed sex population further confirmed these findings (Gomes, Soares *et al*. 2005). Moreover, increased glucose has also been seen to increase expression of specific IGFBPs in cancer; a study published in 2013 showed high glucose to upregulate IGFBP2 in PCa, through increased acetylation of the IGFBP2-associated histones (Biernacka, Uzoh *et al*. 2013).

The issue of insulin resistance further contributes to cancer risk and development; insulin resistance affects muscle, adipose and hepatic tissue, where sensitivity to insulin is impaired. Consequently, the pancreas secretes more insulin, to overcome this issue. A combination of these two actions causes an increase in blood insulin levels (Niddk.nih.gov). By comparison, cancer tissue is not insulin resistant and, as such, it acts to facilitate glucose metabolism by the cancer cell (see review by Arcidiacono, Iiritano *et al*. 2012)

The focus of this thesis is the impact of disturbed metabolism on IGF-II/H19 imprinting in two of the most common epithelial cancers: prostate and colorectal.

1.7 Prostate Cancer.

1.7.1 The prostate

The prostate gland is a lobular organ of the male reproductive system. It is situated below the bladder and surrounds the urethra. Its function is to produce a secretion known as prostatic fluid; this is thought to compose up to 30% of ejaculate. It contains nutrients for seminal survival and prostate specific antigen (PSA), an enzyme that regulates sperm function (Corona, Baldi *et al*. 2011).

1.7.2 Incidence

PCa is the second most frequently diagnosed cancer type and the second major cause of cancer deaths amongst men (Siegel, Miller *et al*. 2016). In 2018, a global study identified approximately 1.3 million new cases of PCa, which resulted in almost 360,000 deaths (Bray, Ferlay *et al*. 2018). In the UK, PCa is the most common cancer type in men and accounted for a quarter of all new male cancer diagnoses in 2017 (Cancerresearchuk.org., 2020[1]).

1.7.3 Causes and risk factors.

Whilst the exact cause of PCa remains unclear, several risk factors have been found to contribute to disease susceptibility.

In the UK, the risk of developing PCa begins to rise after the age of 50, with most cases being diagnosed after the age of 60 (Cancerresearchuk.org., 2020[2]). Also, incidence of PCa appears to be highest in wealthier countries of the Western world, due to widely available screening and detection processes (Rebbeck 2017). Despite these, incidence of PCa remains highest amongst men of African origin, in both developed and developing countries (Rebbeck 2018; Taitt 2018). Findings published in 2019 (Dess, Hartman *et al*. 2019) found this incidence to be attributed to poor access to diagnosis and treatment, due to socio-economic reasons. Families with a history of PCa, also have an increased risk of developing the disease; likelihood doubles in those with a first-degree relationship (Goldgar, Easton *et al*. 1994). In terms of heritability, it appears that pre-disposition to the disease is due to polygenic mutations (Benafif and Eeles 2016; Brandao, Paulo *et al*. 2020). Key genes implicated in heritable cancer risk include the tumour suppressor genes Breast Cancer 1 and 2 (BRCA1 and BRCA2) (Messina, Cattrini *et al*. 2020), mutations in and/or deficiencies in mismatch repair (MMR) genes (Sedhom and Antonarakis 2019) and HOXB13 (Pilie, Giri *et al*. 2016).

A study conducted in 1997 first identified the positive correlation between increased PCa risk and elevated IGF-I levels (Mantzoros, Tzonou *et al*. 1997). This has been confirmed by further studies using other cohorts (Knuppel, Fensom *et al*. 2020). Additionally, increased IGF-I expression has been shown to contribute to disease progression (Ahearn, Peisch *et al*. 2018).

Obesity is also a contributor to PCa risk; it is thought that the long term, low levels of systemic inflammation associated with increased adiposity induces metabolic disruption, resulting in deregulation of cellular signalling systems and activation of inflammatory cytokines. These events lead to disruption of gene regulation (Adesunloye 2021).

1.7.4 Symptoms, diagnosis, and treatment

Symptoms of PCa typically begin as urinary issues such as an increase in frequency, a weak flow and difficulty when beginning to urinate. More advanced or metastatic PCa may produce symptoms such as back pain, erectile dysfunction, or blood in the urine. Unfortunately, metastatic PCa is harder to treat (Prostatecanceruk.org, 2019). Suspicion of abnormal prostatic behaviour may be further detected with a digital rectal examination (DRE), to palpate whether the prostate is enlarged or has an irregular surface. This is usually followed by a PSA measurement. Many clinicians will take a tissue biopsy (Thomson, Li *et al*. 2020) to confer disease presence, however, developments in MRI technology have led to improved diagnostic accuracy when identifying and classifying prostate malignancies (de Rooij, Hamoen et al. 2014). The "Prostate Imaging Reporting and Data System" (PI-RADS), devised and published in 2012 (Barentsz, Richenberg et al. 2012), outlined a new PCa disease classification system, using detailed multiparametric MRI (mpMRI) images of the prostate to differentiate between clinically significant (cs) and low level disease; the system ranges from PI-RADS 1 (cs disease is highly unlikely to be present) to PI-RADS 5 (cs disease is highly likely to be present) (Steiger and Thoeny 2016).

Treatments vary depending upon disease staging and classification; localised PCa may be treated by a radical prostatectomy or radiotherapy. After prostate removal, localised recurrent disease may be further treated with radiotherapy or androgen deprivation therapy (ADT). This may also be partnered with chemotherapy, should relapse be systemic (Rebello, Oing *et al*. 2021).

1.7.5 Classification of PCa

Attempts to classify PCa first began almost 70 years ago. The most successful classification system was conceived in 1966, by Donald Gleason, and is the system most widely used today (Gleason 1966). This method of scoring focused on the structural differences between glands, revealed by histological staining. The scoring system ranges from 1 to 5, depending upon the degree of tissue differentiation. The two most common tissue patterns were scored and combined to give a Gleason score, for example 4 + 2 = 6 (Gleason, Mellinger *et al*. 2017; Ong, Bagguley *et al*. 2020).

In 2014, the International Society of Urological Pathology (ISUP) incorporated the Gleason system into a new five stage grade classification (the ISUP score system) (Epstein, Egevad *et al*. 2016), to assist with diagnosis of disease severity:

Gleason	Grade	Cell morphology
6 (3 + 3)	1	Well differentiated; very slow growing tumour
7 (3 +4 =7)	2	Most cells well differentiated; tumour growth slow
7 (4 + 3 = 7)	3	Cells are beginning to show poor differentiation; tumour growth will be moderate
8 (4 + 4 = 8)	4	Some cells show very poor differentiation; tumour growth moderate to fast
9 or 10 (4 + 5 = 9, 5 + 4 = 9 or 5 + 5 = 10)	5	Most cells are poorly differentiated; tumour growth likely to be fast

(Cancerresearchuk.org., 2019[1])

A further staging system is also used, to provide a measure of disease activity and ultimately, patient prognosis; the TNM staging system (Tumour, Nodal involvement, and Metastasis) also provides the oncologist with information for selecting the correct treatment path. The stages are as follows (Macmillan.org, 2018):

T stage	Tumour location
1	Tumour is small and localised to the prostate; unable to be a palpated with digital rectal examination (DRE).
2	Tumour is small and localised to prostate, detectable with DRE. a – present in <50% of 1 of 2 lobes b – present in 50%> of 1 of 2 lobes c – present in both lobes
3	Tumour is no longer localised to prostate and may be invading nearby tissue and organs. a – tumour has spread through prostate into surrounding tissue. b – tumour has invaded seminal vesicles
4	Tumour has invaded surrounding tissue and organs, such as bladder or rectum

Nodal involvement is classed as N0, where no cancer cells are detectable in proximal lymph nodes and N1, meaning cancer cells are present in one or more proximal lymph nodes.

Metastasis is classed as either M0, meaning the tumour has not spread to other parts of the body or M1, where spread has occurred.

Another frequently used diagnostic test for PCa is to measure prostate specific antigen (PSA). PSA is secreted by healthy and malignant prostate tissue, into the blood. An enlarged, inflamed, or cancerous prostate will secrete higher levels of PSA into the blood (3ng/ml>). However, elevated PSA levels are not always a sign of cancer and are often considered on partially reliable in diagnosis (NHS.uk, 2018).

1.7.6 Loss of imprinting in PCa.

Since the identification of IGF-II/H19 imprinting loss in 1993 (Ogawa, Eccles *et al*. 1993), the phenomenon has been extensively studied across many different cancer types. Loss of imprinting - specifically biallelic expression of IGF-II - was identified in PCa in 1995 (Jarrard, Bussemakers *et al*. 1995).

In 2004, one study focused on ageing as the cause of imprinting loss in a normal human prostate epithelial cell line (HPEC) (Fu, Schwarze *et al*. 2004); cells were passaged 10 to 15 times to mimic ageing. After this time, IGF-II expression changed from mono- to biallelic. This change was also partnered with decreased expression of H19 and a two-fold decrease in CTCF, demonstrating that CTCF plays a key role in imprinting regulation by acting as a transcriptional insulator. This was further explored *in vivo,* where it was shown that LOI occurs with aging in normal prostate tissue but was more extensive in those with associated cancer (Fu, Dobosy *et al*. 2008).

In 2008, a murine study investigated the effects of diet upon IGF-II/H19 regulation in the prostate (Dobosy, Fu *et al*. 2008); it was observed that mice placed on a methyl-deficient diet showed significant upregulation of IGF-II and H19 mRNA in the prostate, which was attributed to a change in histone conformation of the IGF-II/H19 gene promoters, and not DNA methylation and, therefore, loss of imprinting.

In 2011, a study focused on IGF-II/H19 imprinting status within apparent healthy tissue, near and distal to prostate tumours (Bhusari, Yang *et al*. 2011); IGF-II LOI was observed in tumour, proximal (2mm) and distal (10mm) tissues. This correlated with increased IGF-II expression in proximal and distal tissues, but not with tumour tissue. No correlations were seen between IGF-II LOI and H19 in any of the tissue types. This LOI seen in normal tissues proximal and distal to tumour foci is known as "the field defect". The epigenetic field defect is a phenomenon that affects tissue, causing it to become pre-cancerous; such tissues look histologically normal under high magnification, but they tend to exhibit elevated numbers of epigenetic alterations – such as aberrant patterns of DNA methylation or histone acetylation (Bernstein, Nfonsam *et al*. 2013). In 2017, Damasche *et al*

(Damaschke, Yang *et al*. 2017) explored the field effect further, by generating a murine model with LOI in the prostate. The resulting biallelic expression of IGF-II, induced and increased the incidence of a type of tissue known as prostatic intraepithelial neoplasia (PIN). This confirmed that LOI in normal prostate tissue increases the likelihood of developing PCa.

Findings published in 2013 (Damaschke, Yang *et al*. 2013) described how aging-attributed disruptions to methylation patterns had led to IGF-II / H19 LOI in the prostate, resulting in biallelic expression of IGF-II. Three years later in 2016, Zhao *et al*. (Zhao, Liu *et al*. 2016) established that IGF-II / H19 LOI to be associated with chemo- and radiotherapy resistance in PCa stem cells.

Further studies pertaining to the mechanistic action of imprinting loss have yielded some interesting findings; Schagdarsurengin *et al*. (Schagdarsurengin, Lammert *et al*. 2017) demonstrated that IGF-II expression could be inhibited as a result of hypomethylation at one of the three DMRs within the IGF-II / H19 gene locus and, furthermore, identified the KL4 transcription factor to be partially responsible for transcriptional regulation of IGF-II. The following year, Küffer *et al* (Kuffer, Gutting *et al*. 2018) demonstrated that expression of IGF-II in the prostate could also be attributed to methylation of promoters 3 and 4 (P3 and P4), independent of imprinting status; IGF-II expression was found to be lower in tumour tissue compared to adjacent. This was found to be due to hypermethylation of P3 and P4.

1.8 Colorectal cancer

1.8.1 The colon and rectum

The colon and rectum are sometimes referred to collectively as the large intestine or bowel, the key function of which is to process bodily waste. The colon measures approximately 1.5- to 1.8m, with the rectum counting for the last 15 cm, which ends in the anus (Cancer.net, 2019).

1.8.2 Incidence

In the UK there are around 42,300 new bowel cancer diagnoses each year, accounting for approximately 10% of all new cases (Cancerresearchuk.org., 2020[3]). In 2018, there were approximately 1.8 million colorectal diagnoses globally, accounting for 10% of all new cancer cases, making it the fourth most common type of malignancy (Bray, Ferlay *et al*. 2018).

1.8.3 Cause and risk factors

Several factors are thought to contribute to disease susceptibility: a review of available risk data, conducted in 2015 (Henrikson, Webber *et al*. 2015), found the risk of developing CRC significantly increased in individuals with a first or second degree relative with the disease. Heritability is also a risk factor, inheriting mutations in the adenomatous polyposis coli (APC) and the hereditary non-polyposis colon cancer genes (HNPCC) also contribute to disease development (Soravia, Bapat *et al*. 1997). Inflammatory bowel disease (IBD), which encompasses ulcerative colitis and Crohn's disease, is a recurrent chronic condition affecting the bowel (Jellema, van Tulder *et al*. 2011). One study estimated the risk of developing CRC amongst individuals with inflammatory bowel disease to increase up to 80%, compared to unaffected individuals (Burisch and Munkholm 2015).

Increased expression of IGF-II has also been found to be a risk factor of CRC; a study published in 2003 showed upregulation of IGF-II, through loss of imprinting, to be present in the normal colonic mucosa in approximately 30% of CRC patients and only 10% of healthy individuals (Cui, Cruz-Correa *et al*. 2003). This was later confirmed by Sakatani *et al,* where loss of imprinting in IGF-II induced excessive growth of intestinal epithelial cells in mice (Sakatani, Kaneda *et al*. 2005).

Many studies have been conducted upon the protective effect of fibre against colorectal cancer; a recent study identified whole grains as being the most beneficial source of fibre, when linked to bowel cancer prevention (Hullings, Sinha *et al*. 2020). Proposed mechanisms by which fibre lowers CRC risk include shortening transit time of waste in the gut, leading to a reduction in exposure time of gut mucosa to carcinogenic substances in faecal matter, and bacterial fermentation processes - resulting in the release of substances, such as sodium butyrate and propionate, which inhibit proliferation and facilitate apoptosis (Baena and Salinas 2015).

Numerous studies have consistently shown positive correlations between body mass index (BMI) and colorectal cancer risk, with relative risk being higher in men compared to women (Jochem and Leitzmann 2016). As previously discussed, obesity is frequently associate with T2D; a study published in 1999 (Schoen, Tangen *et al*. 1999) explored the effect of BMI upon hyper-insulinaemia (T2D),

hyperglycaemia and CRC risk; of 102 CRC cases, individuals with fasting insulin levels above the median showed a significant association with CRC. This was also applicable to individuals with fasting glucose levels in the highest quartile, and those with a high waist measurement.

1.8.4 Symptoms, diagnosis, and treatment of CRC.

Symptoms of CRC include rectal bleeding, blood in the stool, persistent and unusual change in bowel habit, abdominal pain, and unexplained lethargy (Bowelcanceruk.org.uk[1]., 2019).

Diagnosis of CRC usually begins with a DRE to check for any rectal growths. This may be accompanied by palpating the abdomen. Sometimes a blood test may be conducted to check for anaemia. These elementary tests may be followed by a colonoscopy or a flexible sigmoidoscopy, both involve the insertion of a flexible tube with camera, allowing visualisation of the bowel. Biopsies may also be taken. Once diagnosed, these tests may be followed by a CT scan, to assess whether the cancer has metastasised (NHS.uk, 2019).

Depending on the location of the tumour (colon or bowel), treatment for CRC varies. Non-metastatic bowel tumours may be treated by surgical excision and/or chemotherapy. Rectal tumours may be treated with chemotherapy, radiotherapy, and surgery (Cancerresearchuk.org, 2019[2]).

1.8.5 Classification of colorectal cancer.

Staging and grading of colorectal cancer resembles prostate, in that the TNM staging system is applied (Bowelcanceruk.org.uk[2]., 2019)

T stage	Tumour location
1	Tumour is small and localised to the inner layer of the bowel
2	Tumour has invaded the muscle layer of the bowel wall
3	Tumour has invaded the outer layer of the bowel wall
4	Tumour has grown through the outer lining of the bowel wall

Nodal involvement is classified as:

N0 – no cancer cells detected in lymph nodes,

N1 – cancer cells found in 3 proximal lymph nodes or

N2 – cancer cells found in 4+ proximal lymph nodes.

Metastatic classification is two-stage:

M0 – no metastatic spread of tumour or

M1 – cancer has metastasised to another part of the body.

1.8.6 Loss of imprinting in colorectal cancer

Relaxation of IGF-II imprinting was first identified in colorectal tumours in 1996 (Kinouchi, Hiwatashi *et al*. 1996), where LOI was found to have occurred in both malignant and benign tissue taken from CRC patients. A subsequent study, published the following year (Cui, Horon *et al*. 1998) also witnessed LOI in normal colorectal muscosa cells derived from CRC patients. A key report published in 1997 (Barletta, Rainier *et al*. 1997), demonstrated that LOI could be reversed *in vitro* by the addition of the DNA methylation inhibitor, 5-Aza-2'-deoxycytidine.

Two years later (Takano, Shiota *et al*. 2000), a study conducted upon a cohort of 15 patients revealed IGF-II mRNA to be overexpressed in tumour tissues, compared to non-tumour tissues. Of the cohort, 2 patient samples presented with maintenance of imprinting (MOI) and 15 with LOI. These results provided further evidence that LOI of IGF-II plays an important role in the carcinogenesis of colorectal cancer.

Given the prevalence of imprinting disruption across cohort studies, the epigenetic mechanisms have also been explored in depth; a 2001 report discovered the presence of LOI in both tumour and normal colonic mucosa tissue to be caused by hypermethylation of CpG sites within the CTCF insulator region of IGF-II / H19. This suggested that hypermethylation creates a field defect, resulting in a predisposition to cancer (Nakagawa, Chadwick *et al*. 2001). Findings published a year later proposed an alternative mechanism of imprinting loss in CRC (Cui, Onyango *et al*. 2002); rather than *hyper*methylation of the DMR within the CTCF/H19 region, Cui *et al* demonstrated that it was *hypo*methylation of this DMR, as well as the DMR upstream of exon 3 within IGF-II (DMR0), to be the cause of LOI in both malignant and normal colorectal mucosa cells.

Six years later, in 2008, another study (Ito, Koessler *et al*. 2008) endeavoured to address whether this hypomethylation arose before or, as a result of carcinogenesis; methylation of DMR0 was

assessed in tumour and non-tumour tissue from 2 cohorts of CRC patients. One cohort contained tumour and non-tumour tissue gathered at diagnosis, and the second contained tissue samples gathered from patients 2-5 years prior to diagnosis. In 80% of tumour tissue from cohort 1, hypomethylation was detected at DMR0. Whereas hypomethylation of DMR0 was detected in 9.5% of tissue from cohort 2, which correlated with increased age and not cancer risk. This demonstrated that DMR0 hypomethylation was acquired, because of carcinogenesis, and not as an innate epigenetic pattern.

In 2012, Tian *et al* (Tian, Tang *et al*. 2012) showed LOI to be associated with hypomethylation of the DMR within the H19 gene in CRC tissue. A more comprehensive report (Hidaka, Higashimoto *et al*. 2018) found some DMRs to be more susceptible to hypermethylation than others – such as those within the IGF-II / H19 locus. Despite this susceptibility, there were no links found between imprinting regulation and aberrant methylation.

Other reports have further explored the downstream effects of LOI upon cell behaviour; LOI-induced over-expression of H19 in CRC has been shown to activate the epithelial to mesenchymal transition (EMT) gene, β-catenin, enhancing disease progression (Yang, Ning *et al*. 2017); Gao *et al*. (Gao, Liu *et al*. 2020) found LOI to enhance the likelihood of CRC stem cells differentiating into other cell types by promoting cancer stem cell autophagy, whilst Zhao *et al* (Zhao, Liu *et al*. 2016) demonstrated LOI to be a hallmark of chemoresistance in CRC, *in vitro*.

1.9 Summary.

- The insulin-like growth factor (IGF) / insulin axis is a complex signalling system that mediates the effects of nutrition on cell growth.
- There is a global obesity epidemic matched with an increased incidence of T2D.
- Disturbed metabolism, associated with obesity and T2D, dysregulates the IGF axis, impacting on many diseases, such as cancer.
- The IGF axis can be epigenetically modified, particularly IGF-II expression, that is subject to epigenetic regulation by imprinting.
- IGF-II expression is subject to epigenetic regulation by a mechanism known as imprinting.
- Loss of imprinting affects expression of IGF-II and H19 and is associated with cancer.

1.10 Hypothesis

Alteration of the metabolic environment to mimic that of an inflammatory state, associated with obesity and/or type 2 diabetes, will impact IGF-II/H19 imprinting status in prostate and colorectal cancer.

1.11 Aims

To prove the hypothesis, the aims of this study will be:

1) Investigate the effects of manipulating the metabolic environment to mimic those of an inflammatory state upon the imprinting status of IGF-II/H19, *in vitro,* in PCa.
2) Examine the imprinting behaviour of IGF-II/H19, *in vivo*, in PCa.
3) Investigate the effects of manipulating the metabolic environment to mimic those of an inflammatory state upon the imprinting status of IGF-II/H19, *in vitro,* in colorectal cancer.
4) Examine the imprinting behaviour of IGF-II/H19, *in vivo*, in colorectal cancer.

CHAPTER 2: MATERIALS & METHODS

2.1 Cell culture

2.1.1 Materials, equipment, & reagents

Instruments & equipment	
Pipette-boy	Fisher Scientific, Leicester, UK
Pipettes (1000, 200, 20 and 10µl)	Gilson, Dunstable, UK
Haemocytometer	Fisher Scientific, Loughborough, UK
Mini vortex	Grant Instruments, Hertfordshire, UK
Aseptic hood, BIOMAT Class II	Medical Air Technology, Manchester, UK
Sanyo, MCO-18AIC Incubator	VWR, Leicestershire, UK
Sigma Benchtop Centrifuge	Wolf Laboratories, York, UK
-70°C Freezer	VWR, Leicestershire, UK
-180°C Freezer	VWR, Leicestershire, UK

Consumables	
Cell culture flasks (T25, 75 & 175ml)	Greiner, Gloucestershire, UK
Serological pipettes	Corning, Amsterdam, Netherlands
Universal containers (25ml)	SLS, Nottingham, UK
Bijou container (5ml)	SLS, Nottingham, UK
Syringes & needles	Terumo, Leuven, Belgium
Pipette tips (1000, 200, 20, 10µl)	Bioline, London, UK
Cryogenic vials	Nunc, Roskilde, Denmark
Filters	Appleton Woods, Birmingham, UK

Media & reagents	
Dulbecco's modified Eagles Medium (DMEM) 5mM glucose (1,000mg/L)	Lonza, Slough, UK
Dulbecco's modified Eagles Medium 25mM glucose (4,000mg/L)	Lonza, Slough, UK
Eagles Minimum Essential Medium (EMEM)	Lonza, Slough, UK
McCoy's 5A medium (M5M)	Lonza, Slough, UK
Roswell Park memorial institute medium (RPMI) – 1640 with L-glutamine	Lonza, Slough, UK
Leibowitz's L-15 Medium	Lonza, Slough, UK
Trypsin-EDTA solution 0.25%	Lonza, Slough, UK
Trypsin-versene EDTA 10X Liquid	Lonza, Slough, UK
Phosphate buffered saline (PBS)	Sigma-Aldrich, Dorset, UK
Foetal bovine serum (FBS)	Gibco, Maryland, USA
Bovine serum albumin (BSA)	Sigma-Aldrich, Dorset, UK
Sodium bicarbonate	Sigma-Aldrich, Dorset, UK
Apo-transferrin (Human)	Sigma-Aldrich, Dorset, UK
L-Glutamine (stock conc.200mM)	Sigma-Aldrich, Dorset, UK
Penicillin (50 IU/ml)	Britannia Pharmaceuticals
Trypan Blue	Sigma-Aldrich, Dorset, UK
Dimethyl sulfoxide (DMSO)	Sigma-Aldrich, Dorset, UK

2.1.2 Cell Lines

2.1.2.1 PCa cell lines

Cell line	Purchased from	Details
PC3	American Type Culture Collection (ATCC)	Human prostate; derived from metastatic site in bone; epithelial; grade IV adenocarcinoma
PNT2	European Collection of Authenticated Cell Cultures (ECACC)	Human, normal prostate; epithelial; derived from 33-year-old male
VCaP	ATCC	Human prostate; derived from metastatic site in spine; epithelial
DU145	ATCC	Human prostate; derived from metastatic site in brain; epithelial
LNCaP	ATCC	Human prostate; derived from metastatic site in clavicular lymph node; epithelial

2.1.2.2 Colorectal cancer cell lines

Cell line	Purchased from	Details
HCT116	ATCC	Human colon; carcinoma; epithelial
HCT15	ATCC	Human colon; Dukes type C; epithelial
CaCO-2	ATCC	Human colon; adenocarcinoma; epithelial
HT-29	ATCC	Human colon; adenocarcinoma; epithelial; derived from primary tumour
H747	ATCC	Human colon; derived from metastatic site in common duct node; carcinoma; cecum; endothelial
SW480	ATCC	Human colon; derived from primary site; carcinoma; Dukes type B; epithelial
SW620	ATCC	Human colon; derived from metastatic site in lymph node; Dukes type C; epithelial

2.1.3 Culture media

2.1.3.1 Prostate cell lines

Cell line	**Maintenance & freezing**	**Dosing experiments (flask seeding)**
PC3 (passage numbers 18 to 31)	DMEM 4,000 mg/L glucose with 10% FBS & 1% L-Glutamine	DMEM 1,000mg/L glucose + 10% FBS & 1% L-Glutamine
PNT2 (passage numbers 13 to 17)	RPMI-1640 with 10% FBS & 1% L-Glutamine	Not Dosed (ND)
VCaP (passage numbers 11 to 21)	DMEM 4,000 mg/L glucose with 10% FBS & 1% L-Glutamine	ND
DU145 (passage numbers 14 to 19)	DMEM 4,000 mg/L glucose with 10% FBS & 1% L-Glutamine	ND
LNCaP (passage numbers 9 to 17)	RPMI-1640 with 10% FBS & 1% L-Glutamine	ND

2.1.3.2 Colorectal cell lines

Cell line	**Maintenance & freezing**	**Dosing experiments (flask seeding)**
HCT116 (passage numbers 13 to 18)	McCoy's 5A medium	DMEM 1,000mg/L glucose + 10% FBS & 1% L-Glutamine
HCT15 (passage numbers 3 to 8)	RPMI-1640 with 10% FBS & 1% L-Glutamine	ND
CaCO-2 (passage numbers 11 to 19)	EMEM	ND
HT-29 (passage numbers 14 to 18)	McCoy's 5A medium	ND
H747 (passage numbers 3 to 9)	RPMI-1640 with 10% FBS & 1% L-Glutamine	ND
SW480 (passage numbers 3 to 8)	Leibowitz's L-15 Medium	ND
SW620 (passage numbers 3 to 8)	Leibowitz's L-15 Medium	ND

2.1.3.4 Preparation of serum-free media (SFM)

For dosing experiments, cells were cultured in serum free media (SFM) using either high glucose (Hg) (25mM / 4,500 mg/L) or normal glucose (Ng) (5mM / 1,000 mg/L) containing of DMEM. SFM was prepared by supplementing DMEM (Hg / Ng) with 100 mg of BSA (final concentration of 0.02%), 600 mg of sodium bicarbonate (final concentration of 0.12%), 5 mg apo-transferrin (final concentration of 0.001%), 50 IU/ml of penicillin and a 5ml aliquot of L-glutamine (final concentration of 1%).

2.1.3.5 Preparation of phosphate buffered saline (PBS)

PBS was prepared by dissolving a single tablet in 1 L of distilled water (dH_2O). This solution was then sterilised, via autoclave, before being stored at room temperature.

2.1.4 Cell counting & viability using Trypan Blue.

Trypan Blue (TB) is a stain recommended for use in estimating the proportion of viable cells in a population. Staining enables the visualisation of cell morphology; living (viable) cells do not take up the dye, whereas dead (non-viable) cells do. Trypan blue was used as follows:
50µl of TB was added to 50µl of cell suspension. From this, a 30µl aliquot was placed in the well of a haemocytometer and covered with a cover slip. Viable cells can be visualised as bright, colourless bodies, with a surrounding "halo" of light; dead cells are visualised as round and/or broken blue bodies. For the purposes of passaging and seeding flasks, only live cells were counted.

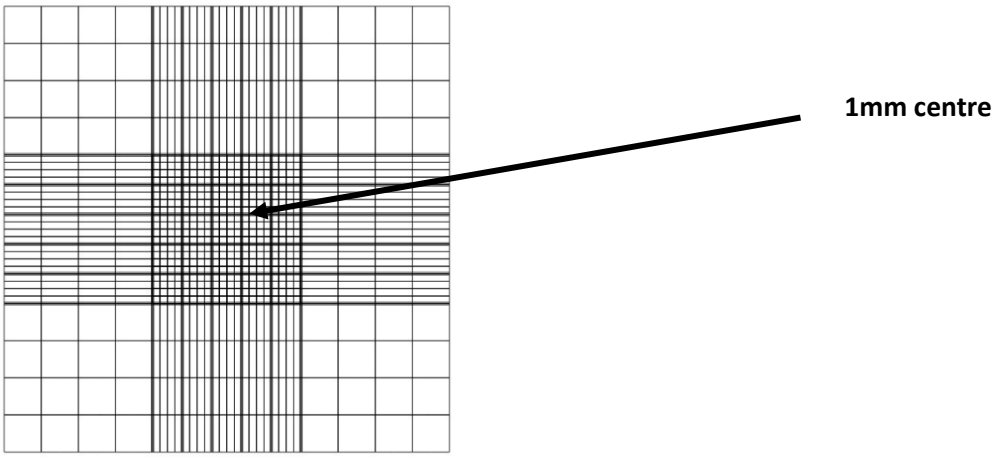

Figure 2.1.4: Chamber 1 of a haemocytometer

Starting with chamber 1 of the haemocytometer, count all the cells in the 1 mm centre square and four 1 mm corner squares (as shown in figure 2.1.4). Count cells on top and left touching middle line of the perimeter of each square. Do not count cells touching the middle line at the bottom and right sides. Repeat this method for the second chamber.

Each square of the haemocytometer, with the coverslip in place, represents a total volume of 0.1 mm^3 or 10^{-4} cm^3. This is the conversion factor for the haemocytometer. As 1 cm^3 is approximately 1 ml, the subsequent cell concentration per ml (and total cell number) can be determined using the following calculations:

Cell Density (cells per ml) =

$$\frac{\text{Nº. living cells counted}}{\text{Nº. squares counted.}} \times \text{Dilution factor} \times 10^4 \text{ (chamber conversion factor)}$$

2.1.5 Cell maintenance

Media renewal frequency varies between cell lines. The following tables outline the advised media renewal rates.

2.1.5.1 Prostate cell lines

Cell line	**Media renewal frequency**
PC3	2-3 times per week
DU145	2-3 times per week
PNT2	2-3 times per week
LNCaP	Twice per week
VCaP	Twice per week

2.1.5.2 Colorectal cell lines

Cell line	**Media renewal frequency**
HCT116	Every 2 to 3 days
HCT15	2-3 times per week
HT-29	2-3 times per week
CaCO-2	1-2 times per week
H747	Twice per week
SW480	1-2 times per week
SW620	2-3 times per week

2.1.6 Cell passaging and sub-culturing.

When cells become 75-80% confluent (i.e., the percentage of culture flask surface covered by adherent cells), they must be "split" or passaged, to enable further healthy growth. If cells become over-confluent, they begin to compete for space and nutrients that can result in cell death. Sub-culturing or splitting of cells varies between cell types.

2.1.6.1 Passaging prostate cell lines

Cell Line	**Sub-culturing**
PC3	Sub-culture at a ratio of 1:3 to 1:6
DU145	Sub-culture at a ratio of 1:4 to 1:6
LNCaP	Sub-culture at a ratio of 1:3 to 1:6
PNT2	Sub-culture at a ratio of 1:3 to 1:10
VCaP	Sub-culture at a ratio of 1:3 to 1:4

2.1.6.2 Passaging colorectal cell lines

Cell line	**Sub-culturing**
HCT-116	1:3 to 1:8
HCT-15	1:2 to 1:10
HT-29	1:3 to 1:8
CaCO-2	1:4 to 1:6
H747	1:2 to 1:4
SW480	1:2 to 1:8
SW620	1:2 to 1:10

2.1.7 Cell freezing

When freezing cells, a minimal number is required to ensure successful retrieval.

Cells cannot be frozen in media alone; they must be combined with cryopreservation mix to reduce cell damage caused by freezing.

Cryopreservation mix was prepared by combining the following, under aseptic conditions, for each 500µl of cell suspension:

- 350µl growth media,
- 100µl DMSO and
- 50µl FBS.

As the combination of DMSO, growth media and FBS causes an exothermic reaction, the freezer mix was left to cool for approximately 10 minutes before adding drop-wise to the cell suspension.

2.1.7.1 Freezing densities for prostate cell lines

Cell line	**Density (cells per cryovial)**
PC3	3×10^6
PNT2	3×10^6
DU145	3×10^6
LNCaP	6×10^6
VCaP	10×10^6

2.1.7.2 Freezing densities for colorectal cell lines

Cell line	**Density per cryovial**
HCT-116	3×10^6
HCT-15	6×10^6
HT-29	6×10^6
CaCO-2	6×10^6
H747	6×10^6
SW480	6×10^6
SW620	6×10^6

2.1.8 Cell retrieval / defrosting

Cells were removed from the liquid nitrogen store and left to thaw at room temperature. This was followed by the addition of 1ml of the relevant growth media, drop wise. The total cryovial contents were then transferred to a universal container, followed by the addition of a further 4ml of growth media. The cell solution was then centrifuged at 13000 rpm / 16,000 x g for 3 and half minutes, followed by aspiration of the supernatant. The cell pellet was resuspended in 5ml of growth media before finally being transferred to a T25 flask. The flask was placed in a humidified incubator, at 37°C (5% CO_2), and stored overnight to allow the cells to adhere to the flask surface.

2.2 DNA & RNA isolation from cultured-cell monolayers.

2.2.1 Materials, equipment, and reagents

Instruments & equipment	
Refrigerated Centrifuge	Labnet International, Berkshire, UK
Pipettes (P1000, 200, 20, 2)	Gilson, Dunstable, UK
Nanophotometer	Implen, Munchen, Germany
Thermo-Shaker	Grant Instruments, Hertfordshire, UK
Aseptic hood, BIOMAT Class II	Medical Air Technology, Manchester, UK

Consumables	
Pipette Tips (1000-, 200-, 10µl)	Bioline, London, UK
1.5ml Centrifuge Tubes	Star Lab, Milton Keynes, UK
0.5ml Centrifuge Tubes	Star Lab, Milton Keynes, UK
0.2ml Thin-walled PCR Tubes	Star Lab, Milton Keynes, UK

Reagents	
Phosphate Buffered Saline (PBS) Tablets	Sigma-Aldrich, Dorset, UK
DNAzol® Reagent	Invitrogen, ThermoFisher Scientific, Rugby, UK
RNAzol® Reagent	VWR, Leicestershire, UK
Chloroform	Fisher Scientific, Loughborough, UK
100% Ethanol	Fisher Scientific, Loughborough, UK
Isopropanol	Fisher Scientific, Loughborough, UK
Nuclease-free Water	Fisher Scientific, Loughborough, UK
Sodium Hydroxide	Fisher Scientific, Loughborough, UK
DNase 1 (Amplification Grade)	Sigma-Aldrich, Dorset, UK
High-Capacity RNA-to-cDNA Kit	Applied Biosystems

2.2.2. Protocol

Media was removed from the flask and cells were washed with PBS. This was then removed and discarded.

In the fume hood, 0.75 - 1ml RNAzol® / DNAzol® was added, per 10cm^2 culture flask area (for T25, 1ml added). The flask was tilted to lyse the cells and the lysate was transferred into a 1.5ml centrifuge tube.

1. For RNA isolation: 200µl chloroform were added to the lysate and the tubes were inverted several times to mix the contents.
2. The tube was then transferred to a centrifuge and spun at 13,500 rpm / ~17,000 x -g for 15 minutes.
3. For RNA: top colourless phase was transferred to a new centrifuge tube.

   For DNA: top viscous phase was transferred to a new centrifuge tube.

   For both: remaining pink phase was discarded.
4. For RNA: 500µl of isopropanol were added to a tube containing the colourless phase and incubated at room temperature for 10 minutes, to allow precipitation of RNA.

   For DNA: 500µl of 100% ethanol were added to the transferred viscous phase and incubated at room temperature for 3-5 minutes.
5. For RNA: the tube was transferred to a centrifuge and spun at 13,000 rpm / ~17,000 x g for 15 minutes, to sediment RNA precipitate. The supernatant was removed, followed by addition of 1ml 70% ethanol. The tubes were vortexed to dislodge RNA precipitate from the base of the tube. Tubes were then transferred to a centrifuge and spun at 7,500 rpm / ~5300 x g for 10 minutes – this was the first RNA wash step.

   For DNA: using a pipette tip, the DNA thread was transferred to a clean tube, followed by the addition of 1ml of 75% ethanol. This was transferred to the centrifuge and spun at 7500 rpm / ~5300 x g for 10 minutes; this was the first DNA wash step.

6. For RNA: the supernatant was removed and the addition of 1ml of 70% ethanol was repeated, followed by a final spin at 7,500 rpm / ~5300 x g for 10 minutes. The supernatant was removed, and the pellet was left to air dry for 5 minutes.

   For DNA: the supernatant was removed and the addition of 1ml 75% ethanol was repeated, followed by a final spin at 7,500 rpm / ~5300 x g for 10 minutes. The supernatant was removed, and the pellet was left to air dry for 5 minutes.

7. For RNA: 20µl DNAse free water was added to the pellet.

   For DNA: 40µl of 8mM sodium hydroxide (NaOH) was added to the pellet.

   The tubes were transferred to a 58°C thermo-block for 5 minutes; this step enabled the RNA / DNA to dissolve into solution.

Quantification of product was ascertained by using a nanophotometer. DNA extracts were stored at -70°C.

RNA was then treated with DNase 1, as follows:

1. 2µg of RNA in 8µl of water was added to a 0.2ml PCR tube, along with 1µl 10X reaction buffer and 1µl of DNase 1. This was mixed gently and incubated at room temperature (18-23°C) for 15 minutes.
2. After this time, 1µl of Stop Solution was added, to inactivate the DNase 1. This was heated to 70°C for 10 minutes, to denature both the DNase 1 and RNA. The resulting reaction volume was then cooled on ice.

RNA was stored at stored at -80°C.

RNA to cDNA conversion.

For each 20µl reaction, up to a maximum of 2µg of RNA (DNase treated) was used.

The volume of reaction components, per sample, was as follows:

- 2X RT Buffer - 10µl
- 20X Enzyme Mix - 1µl
- RNA Sample - up to 9µl
- Nuclease-free water - as required to increase volume of samples to 9µl, at a maximum concentration of 2µg.

1. A quantity of master mix containing RT buffer and enzyme mix was made, according to the number of RNA samples, with 11µl master mix aliquoted into each PCR tube.
2. Each RNA sample was vortexed then added to a PCR tube containing aliquoted master mix (total volume equated to 9µl at an overall concentration of 2µg).
3. PCR tubes were then briefly spun to ensure all contents were at the bottom of the tube. Tubes were then transferred to a thermocycler and heated to 37°C. They were incubated for 60 minutes, followed by a 5-minute incubation at 95°C to stop the reaction. The cDNA was then ready for use.

2.3 DNA & RNA isolation from formalin fixed paraffin embedded tissue (FFPE)

2.3.1 Materials, equipment, and reagents

Instruments & equipment	
Refrigerated Centrifuge	Labnet International, Berkshire, UK
Pipettes (P1000, 200, 20, 2)	Gilson, Dunstable, UK
Nanophotometer	Implen, Munchen, Germany
Thermo-Shaker	Grant Instruments, Hertfordshire, UK
Microtome	Leica, Milton Keynes, UK

Consumables	
Pipette Tips (1000-, 200-, 10µl)	Bioline, London, UK
1.5ml Microcentrifuge Tubes	Star Lab, Milton Keynes, UK
0.5ml Microcentrifuge Tubes	Star Lab, Milton Keynes, UK
0.2ml Thin-walled PCR Tubes	Star Lab, Milton Keynes, UK

Reagents	
RecoverAll™ Total Nucleic Acid Isolation Kit	Ambion by Life Technologies California, USA
Xylene	Fisher Scientific, Loughborough, UK
100% Ethanol	Fisher Scientific, Loughborough, UK

2.3.2 Protocol

1. 5 slices of FFPE tissue were taken from tissue blocks, at a thickness of 16µm each, using a microtome. The slices were transferred to a 1.5ml microcentrifuge tube; 1ml of xylene was added to each tube and then heated at 50°C for 5 minutes, to dissolve the paraffin wax.

2. After this time, samples were centrifuged at 13,500 rpm / ~17,000 x g for 2 minutes to pellet the tissue; the supernatant was subsequently discarded.

3. To remove residual xylene from the pellet, 1ml 100% of ethanol was added to each tube, vortexed and centrifuged at 13,500 rpm / ~17,000 x g for 2 minutes. The supernatant was discarded. This wash step was repeated twice. The pellet was left to air-dry at room temperature for 45 minutes.

4. To each pellet, 200µl of digestion buffer and 4µl of protease were added. The samples were incubated at 50°C overnight. To maximise digestion of the tissue, samples were heated at 80°C for 15 minutes, followed by the addition of another 4µl of protease and a 1-hour incubation period, at 50°C.

5. A mix containing 240µl of isolation additive and 550µl of 100% ethanol were added to each sample, followed by a brief vortex to mix.

6. For each sample, a filter cartridge was placed in a collection tube (as shown in figure 2.3); a 700µl aliquot of the sample/isolation additive mix was transferred on to the filter cartridge, followed by centrifugation for 30 seconds, at 10,000 rpm / ~9400 x g, to pass the sample mix

through the filter. The flow through was then discarded. These steps were repeated with the remaining sample mix.

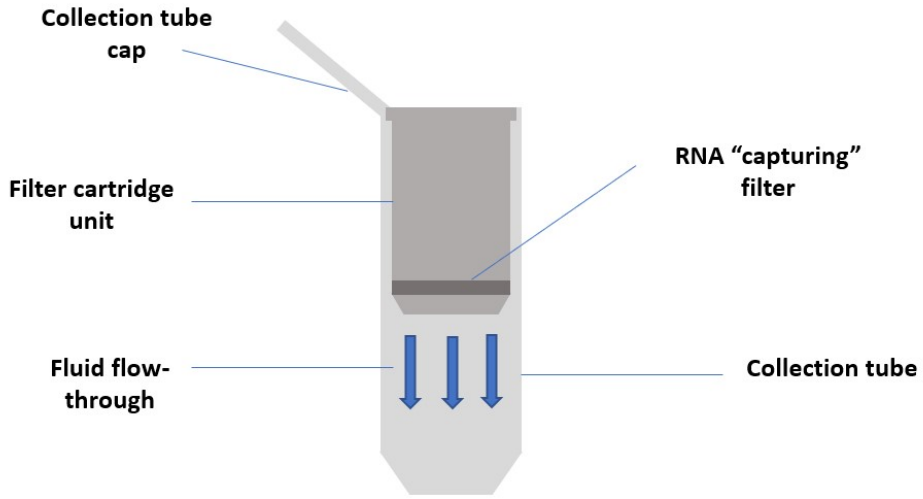

Figure 2.3: The RecoverAll ™ Total Nucleic Acid Isolation Kit Filter Cartridge & Collection Tube Assembly.

7. To the filter cartridge, 700µl of Wash 1 were added, followed by centrifugation for 30 seconds, at 10,000 rpm / ~9400 x g; the flow through was discarded. Using the same collection tube, 500µl of 2/3 Wash were added to the filter cartridge, followed by centrifugation for 30 seconds, at 10,000 rpm / ~9400 xg; the flow through was discarded. The filter cartridge and collection tube were centrifuged for a further 30 seconds at 10,000 rpm / ~9400 x g to remove any residual fluid from the filter.

8. A mix of 6µl of 10X DNase buffer, 4µl of DNase and 50µl of nuclease-free water were added to the centre of the filter cartridge and incubated for 30 minutes at room temperature (22-25°C).

9. After this time, 700µl of Wash 1 were added to the filter cartridge and incubated for 30-60 seconds at room temperate. The filter cartridge and collection tube were then centrifuged for 30 seconds at 10,000 rpm / ~9400 x g; the flow through was discarded.

10. 500µl of Wash 2/3 were added to each filter cartridge and collection tube, followed by centrifugation for 30 seconds at 10,000 rpm. This wash step was repeated a second time. The filter cartridge and collection tube were centrifuged for a further 1 minute, at 10,000 rpm / ~9400 x g, to remove any residual liquid.

11. The filter cartridge was transferred to a new collection tube for RNA elution; 30µl of elution solution were added to the centre of each filter cartridge and incubated for 10 minutes at room temperature. After this time, the cartridge and collection tube were centrifuged for 1 minute at 10,000 rpm / ~9400 x g to remove the eluate from the filter.

12. The eluate was quantified using a nanophotometer. RNA was stored at -70°C.

2.4 KingFisher™ automated RNA recovery from fresh-frozen tissue

2.4.1 Materials, equipment, and reagents.

Instruments & equipment	
KingFisher™ Duo Prime System	ThermoFisher Scientific, Paisley, UK
Pipettes (P1000, 200, 20, 2)	Gilson, Dunstable, UK
Precellys 24 Benchtop Homogeniser	Bertin Instruments, France
Nanophotometer	Implen, Munchen, Germany
Centrifuge	Labnet International, Berkshire, UK

Consumables	
Pipette Tips (1000-, 200-, 10µl)	Bioline, London, UK
KingFisher 96 deep-well plates (A48424)	ThermoFisher Scientific, Paisley, UK
KingFisher Duo elution strips (97003520)	ThermoFisher Scientific, Paisley, UK
KingFisher Duo 12-tip Comb (97003500)	ThermoFisher Scientific, Paisley, UK
Ceramic Beads 2.8mm (13114-325)	Qiagen, Manchester, UK
Screw Cap Microtubes, 1.5ml	Sarstedt, Leicester, UK

Reagents	
Omega Biotek Mag-Bind Total RNA Kit	Norcross, Georgia, USA
100% Ethanol	Fisher Scientific, Loughborough, UK

2.4.3 Protocol

1. 20mg fresh tissue and 6 ceramic beads were transferred to a 1.5ml screw cap microtube; this was followed by the addition of 450 µl OTRK lysis buffer and 20µl of proteinase K.

2. The tissue, beads, buffer, and proteinase K were homogenised for 30 seconds at 3,000 rpm / ~850 x g, followed by centrifugation for 5 minutes at 10,000 rpm / ~9400 x g.

3. A 96 deep-well plate was prepared, as follows:

Row	Reagent	Volume (µl)
A	Lysate & Binding Mix	400 + 320
B	VHB Buffer	400
C	RNA Wash Buffer II	400
D	RNA Elution Buffer DNase Digestion Mix PHM Buffer & RNA Wash Buffer II	100 52 (add at pause 1) 150 + 300 (add at pause 2)
E	RNA Wash Buffer II	400
F	Comb	NA
G	Empty	
H	Empty	

4. 320µl of binding mix were prepared, composed of 300µl of 100% ethanol and 20µl of Mag-Bind® Particles CNR. This was added to the 400µl of cleared lysate in row A and the two were mixed by gentle pipetting.

5. The elution strip wells were loaded with 30µl of elution buffer; the deep-well plate and elution strip were loaded on to the KingFisher™ machine. Program 'Omega_M6731_KFDuo_100.bdz' was used, with requisite reagents added at pause 1 and 2.

6. RNA eluate was transferred from the elution strip well to a 0.5ml microtube and quantified using a nanophotometer; RNA was subsequently stored at -70°C. The plate was removed from the machine and discarded.

2.5 Restriction fragment length polymorphism analysis (RFLP).

2.5.1 Materials, equipment, and reagents.

Apparatus / Instruments	**Manufacturer / Supplier**
Centrifuge (Microstar 17)	VWR, Leicestershire, UK
Pipettes (P1000, 100, 20, 10 and 2)	Gilson, Dunstable, UK
Thermocycler (T100)	Bio-Rad, Watford, UK
Weighing Scale	Mettler, Leicester, UK
Transilluminator / Gel Imager	Bio-Rad, Watford, UK

Consumables	**Manufacturer / Supplier**
Pipette Tips	Bioline, London, UK
1.5 ml Centrifuge Tubes	Eppendorf, Stevenage, UK
Thin Walled 0.2ml PCR Tubes	Eppendorf, Stevenage, UK

Reagents	**Manufacturer / Supplier**
10X $MgCl_2$ Buffer	Qiagen, Manchester, UK
0.1 mM dNTPs	New England Biolabs, Hitchin, UK
APA1 Primer Forward (cttggactttgagtcaaattgg)	Sigma-Aldrich, Dorset, UK
APA1 Primer Reverse (ggtcgtgccaattacatttca)	Sigma-Aldrich, Dorset, UK
Taq Polymerase	Applied Biosystems, Cheshire, UK
Nuclease -free Water	Ambion, ThermoFisher Scientific, Rugby, UK
FastDigest® APA1 Kit	ThermoFisher Scientific, Rugby, UK
Agarose	Bio-Rad, Watford, UK
Midori Green Nucleic Acid Staining Solution	Nippon Genetics, Duren, Germany
1X Tris-EDTA (TE) Buffer	Fisher Scientific, Loughborough, UK
1KB Ladder	New England Biolabs, Hitchin, UK

2.5.2 Protocol

2.5.2 PCR amplification of product

A master mix containing the following reagents, in the following quantities, was prepared:

Reagent	Volume (1X)	Volume (nX)
10X Cl Buffer	1µl	1 x n
dNTPs	0.1 µl	0.1 x n
0.1mM IGFII APA1 Primer (F)	0.5µl	0.5 x n
0.1mM IGFII APA1 Primer (R)	0.5µl	0.5 x n
Taq Polymerase	0.05µl	0.05 x n
Nuclease-free Water	9 – (Σ vol. above) = 6.85µl	(9 x n) – Σ vol. above

1. 9µl of master mix were aliquoted into each PCR tube, followed by the addition of 1µl of cDNA. Tubes were then briefly spun to ensure entire contents were at the bottom of the tube.
2. Samples were transferred to a thermocycler and the following programme was used: 95°C for 5 minutes, 94°C for 45 seconds, 62°C for 45 seconds, 72°C for 45 seconds for a total of 35 cycles, followed by 72°C for 5 minutes then 4°C for ∞.

APA1 RFLP digestion of PCR product.

A master mix containing reagents in the following quantities, was prepared:

Reagent	Volume (1X)	Volume (nX)
Nuclease-free Water	17µl	17 x n
10X FastDigest Green Buffer	2µl	2 x n
FastDigest Enzyme	1µl	1 x n

1. The 20µl of master mix were added to the PCR product to make a total volume of 30µl.

2. Tubes were spun to ensure the entire volume was at the base of the tube and were transferred to a thermocycler, using the following programme: 37°C for 20 minutes, 65°C for 5 minutes, then hold at 4°C. The digested product was then loaded on to a 2% agarose gel, for electrophoresis.

Agarose gel preparation

A 2% agarose gel was prepared by adding 2g of agarose to 100 ml of dH_2O in a conical flask. This was then microwaved on full power for 1 minute. The flask was removed from the microwave and left to cool for 2 minutes. This was followed by the addition of 5 µl of Midori green.

The flask contents were poured into a gel tray, with positioned combs, and left to set. Once set, the combs were removed.

Electrophoresis protocol

The gel was lowered into the electrophoresis tank and submerged in TE. The wells were loaded, from left to right, before closing the tank lid and leaving to run at 140 volts for 30 – 40 minutes.

The gel was visualised on a transilluminator, using ImageLab™ software (Bio-Rad).

2.6 qPCR / Real time PCR

2.6.1 Materials, equipment, and reagents.

Apparatus / Instruments	**Manufacturer / Supplier**
Pipettes (P1000, 200, 20, 10, 2)	Gilson, Dunstable, UK
qPCR Machine & Accompanying Software	Applied Biosystems (StepOne Software), Cheshire, UK
Centrifuge (Microstar 17)	VWR, Leicestershire, UK
Plate Spinner (MPS1000)	Labnet International, Berkshire, UK
Vortex	Jencon, Hemel Hempstead, UK

Consumables	**Manufacturer / Supplier**
Pipette Tips	Bioline, London, UK
1.5 ml & 0.5 ml Centrifuge Tubes	Eppendorf, Stevenage, UK
96 Well Plate	Sarstedt, Leicester, UK
Optical Adhesive Film / Plate Seal	Applied Biosystems, Cheshire, UK

Reagent	Manufacturer / Supplier
Nuclease-free Water	Ambion, ThermoFisher Scientific, Rugby, UK
qPCR Kit (containing Sybr 2X, Dye 100X)	Sigma-Aldrich, Dorset, UK
GAPDH Primer (F) CATCTTCTTTTGCGTCGCCA	Sigma-Aldrich, Dorset, UK
GAPDH Primer (R) TTAAAAGCAGCCCTGGTGACC	Sigma-Aldrich, Dorset, UK
TBP Primer (F) TGCACAGGAGCCAAGAGTGAA	Sigma-Aldrich, Dorset, UK
TBP Primer (R) CACATCACAGCTCCCCACCA	Sigma-Aldrich, Dorset, UK
IGFII Primer (F) GAGCTCGAGGCGTTCAGG	Sigma-Aldrich, Dorset, UK
IGFII Primer (R) GTCTTGGGTGGGTAGAGCAATC	Sigma-Aldrich, Dorset, UK
H19 Primer (F) CGGAACATTGGACAGAAG	Sigma-Aldrich, Dorset, UK
H19 Primer (R) GGCGAGGCAGAATATAAC	Sigma-Aldrich, Dorset, UK

2.6.2 Protocol.

A master mix containing the following reagents, in the following quantities, was prepared:

Reagent	Volume (1X)	Volume (n^{x2}X)
Sybr 2X (from kit)	5µl	n x 5
Primer - F (0.1mM conc.)	0.5 µl	n x 0.5
Primer – R (0.1mM conc.)	0.5µl	n x 0.5
Dye 100X (from kit)	0.1µl	n x 0.1
Nuclease-free Water	(9 – total vol. above) = 3.9µl	(n x 9) – total vol. above

1. 9µl of each master mix were aliquoted into the base of each well, allowing 2 aliquots per cDNA sample (each sample must be run in duplicate). Reverse pipetting was used. This was followed by the addition of 1µl of cDNA to each well.

2. The plate was sealed and transferred to a plate centrifuge, where it was briefly spun to ensure all reaction contents were at the base of each well.
3. The plate was transferred to the qPCR machine and using the software, the plate was set-up. The following program was used:
4. "Quantitation – Comparative CT (ΔΔCt)" experiment option, using "Sybr° green reagents". The PCR conditions were hold at 95°C for 10 minutes, 95°C for 15 seconds then 60°C for 1 minute for a total of 50 cycles, 95°C for 15 seconds, then 60°C for 1 minute then 95°C for 15 seconds.
5. Once the rtPCR was complete, data were exported in an excel format for analysis.

The ΔΔCt Pfaffl (Pfaffl 2001) method was used to calculate fold change in IGFII and H19. This method takes into consideration different primer efficiencies.

To calculate fold change:

Relative Quantification (RQ) = $\frac{2^{\Delta Ct(target)}}{2^{\Delta Ct(reference)}}$

= 2 [(Ct (target, calibrator) – Ct (target, test)] - [(Ct (ref, calibrator) – Ct (ref, test)]

= 2- [(Ct (target, test) – Ct (target, calibrator)] - [(Ct (ref, test) – Ct (ref, calibrator)

= $2^{-\Delta\Delta Ct}$

Target gene calibrator = Ct value of sample Ng0

Target gene in test = Ct value of test sample (e.g., Hg5)

Reference gene = Ct value of housekeeping gene (e.g., GAPDH or TBP)

2.7 Radioimmunoassay (R.I.A)

2.7.1 Materials, equipment, and reagents.

Apparatus / Instruments	**Manufacturer / Supplier**
Pipettes (P1000, 200, 20, 10, 2)	Gilson, Dunstable, UK
Magnetic Stirrer	Bibby Scientific, Stone, UK
pH Meter	
Bench-top Gamma Counter	

Consumables	**Manufacturer / Supplier**
Pipette Tips	Bioline, London, UK
0.5- & 1.5-ml Centrifuge Tubes	Eppendorf, Stevenage, UK
Weighing Boats	Sarstedt, Leicester, UK
Universal Containers	Sarstedt, Leicester, UK
Bijoux Containers	Sarstedt, Leicester, UK

Reagent	**Manufacturer / Supplier**
Protamine Sulphate	Sigma-Aldrich, Dorset, UK
Sodium Diphosphate	VWR, Leicestershire, UK
Sodium Azide	Sigma-Aldrich, Dorset, UK
EDTA	Sigma-Aldrich, Dorset, UK
TBS-TWEEN Buffer	Sigma-Aldrich, Dorset, UK
Radioactive Tracer ($I^{-125)}$	In-house
W5D2 Antibody	In-house
8M Formic Acid	VWR, Leicestershire, UK
1M Tris Base	Fisher Scientific, Loughborough, UK
BioMag Goat Anti-Mouse	Polysciences, Inc, Pennsylvania, USA
IGF-II peptide (receptor grade BBB-F01	GroPrep, Thebarton, Australia
IGF-I peptide (Media Grade BAI-O01)	GroPrep, Thebarton, Australia

2.7.3 Protocol

2.7.3.1 Protocol part 1

The assay buffer was prepared by adding the following reagents, in the following quantities, to 1 litre of ddH_2O:

Reagent	**Quantity**
Protamine Sulphate	0.4g
Sodium Diphosphate	4.68g
Sodium Azide	0.2g
EDTA	3.72g

pH was adjusted to pH 7.5 by the addition of hydrochloric acid. 0.5ml of Tween 20 was added before storing the solution at 4°C

Preparation of the Radioactive Tracer

I^{-125} labelled IGF-II was aliquoted and transferred to a lead lined container. Approximately 50µl of the labelled IGF-II was then added to 15ml of assay buffer.

50µl of the solution was added to an LP4 tube; the number of counts was measured using the bench-top gamma counter.

Preparation of the Antiserum, W5D2

20ml of assay buffer was aliquoted into a universal container, followed by addition of 10µl of antibody to give a 1:2000 dilution as stock.

Preparation of the Assay Standards

0.18g of protamine sulphate was added to 50ml of assay buffer to make the standards buffer.

An IGF-II working stock was prepared by adding 10µl stock (0.5µg/µl) to 990µl of assay buffer to make a 5ng/µl (5000ng/ml) working stock.

The IGF-II standards were prepared as follows:

Standards (ng/ml)	Assay Buffer (ml)	IGFII Working Stock
50	7.6	76µl
25	3.6	3.6ml of 50ng/ml
10	4.62	3.08ml of 25ng/ml
5	3.7	3.7ml of 10ng/ml
2.5	3.4	3.4ml 0f 5ng/ml
1	3.9	2.6ml of 1.5ng/ml
0.5	2.1	2.1ml of 1ng/ml

Standards were aliquoted in 150µl amounts into microtubes and stored at -20 °C.

Preparation of 8M Formic Acid

33.92ml of neat formic acid were added to 100ml of ddH_2O. 3-4 drops of Tween-20 were added to produce a solution of 0.05% Tween.

To prepare the 1M Tris Base, 12.11g of Tris base were added to 100ml of ddH_20.

To prepare Rh IGF-1, 10µl of 1mg/ml IGF1 stock was added to 20ml of assay buffer, to give a solution 500ng/ml IGF-II.

LP4 tubes were labelled in duplicate with the following:

TC (Total Counts)

NSB (Non-Specific Binding)

B_0 (Unbound)

Extraction Procedure

1. 50μl of each sample (including the serum control) were aliquoted into a 1.5ml Eppendorf. To this, 25μl of formic acid/tween solution was added.

2. A pipette tip was primed in acetone and then used to add 175μl of acetone to each sample. The samples were centrifuged for 30 mins at 4°C at an RCF of 3000g.

3. 100μl of tris base were then added to each of the second set of 1.5ml Eppendorf tubes. 270μl of assay buffer were added to each LP3 dilution tube except for the 1:80 serum control, to which 350μl of assay buffer were added.

4. Samples were removed from the centrifuge and a pipette tip was primed with acetone, as before. 100μl of supernatant were added to the tris base, to give a 1:10 dilution.

5. 20μl of each extracted sample were added to the 180μl of assay buffer in the corresponding dilution tubes to give a final 100 times dilution.

Assay Protocol

The reagents were added to each tube as shown in the tables below:

Serum Samples containing no media:

	Assay Buffer (µl)	Sample (µl)	Standards (µl)	Tracer (µl)	Antibody (µl)	IGF-II
TC				50		
NSB	400			50		50
B_0	350			50	50	50
Standards	300		50	50	50	50
Samples	300	50		50	50	50

Supernatant Samples:

Tube	Assay Buffer (µl)	Sample (µl)	Standards (µl)	Tracer (µl)	Antibody (µl)	Formic Acid/Acetone (µl)
TC				50		
NSB	350			50		50
B_0	300			50	50	50
Standards	250		50	50	50	50
Samples	300	50		50	50	

Once all the reagents had been added, each tube was vortexed then stored at 4^0C overnight.

2.7.3.2 Protocol part 2

1. 50µl of goat-a*nti-mouse* beads were added to each tube (except the TC tubes). Each tube was vortexed and placed in magnetic rack without magnetic base and incubated at 4^0C for 20mins. The rack was removed from the fridge and placed on magnetic base on the bench for 15mins.

2. The whole magnetic tray was taken to the sink and the liquid was poured off.

3. 1ml of assay buffer was added to each tube, vortexed gently for a few seconds and placed back into the magnetic tray on the magnetic base. They were left for a further 10-15mins, before being placed in the gamma reader.

2.8 Digital droplet polymerase chain reaction (ddPCR)

2.8.1 Materials, equipment, and reagents

Apparatus / Instruments	**Manufacturer / Supplier**
Pipettes (P1000, 200, 20, 10, 2)	Gilson, Dunstable, UK
QX200 Droplet Reader	Bio-Rad, Watford, UK
C1000 Touch thermocycler	Bio-Rad, Watford, UK
QX200 droplet generator	Bio-Rad, Watford, UK
Vortex	Jencon, Hemel Hempstead, UK
Aseptic hood, BIOMAT Class II	Medical Air Technology, Manchester, UK
ddPCR Cassette Holder	Bio-Rad, Watford, UK
Multi-channel pipette 200µl	Gilson, Dunstable, UK
FLUOstar OPTIMA plate reader	BMG Labtech, Aylesbury, UK
Plate sealer	Gilson, Dunstable, UK

Consumables	**Manufacturer / Supplier**
Pipette Tips	Bioline, London, UK
1.5 ml & 0.5 ml Centrifuge Tubes	Eppendorf, Stevenage, UK
Black Flat bottom 96 Well Plate	Sarstedt, Leicester, UK
ddPCR Cartridge inserts	Bio-Rad, Watford, UK
Rubber gaskets	Bio-Rad, Watford, UK
Plate foil	Bio-Rad, Watford, UK

Reagent	Manufacturer / Supplier
ddPCR IGF-II (fam-hex) probe	Bio-Rad, Watford, UK
ddPCR H19 (fam-hex) probe	ThermoFisher Scientific, Paisley, UK
ddPCR G2E3 (fam-hex) housekeeping probe	Bio-Rad, Watford, UK
ddPCR Supermix, no UTP	Bio-Rad, Watford, UK
Droplet generator oil	Bio-Rad, Watford, UK
Promega QuantiFluor ssDNA Kit	Promega, Wisconsin, USA
Nuclease-free water	Ambion, ThermoFisher Scientific, Rugby, UK

2.8.3 Protocol

Quantification of cDNA using QuantiFluor® ssDNA System.

TE buffer (TE) and QuantiFluor ssDNA Dye (QF) were prepared as follows:

For a full 96-well plate, including a low-concentration ddDNA set of standards:

- No. samples: 80 (2 x 40, each loaded in duplicate; diluted 1:100 i.e., 1µl cDNA in 99µl 1X TE)
- No. standards: 16 (2 x 8, each loaded in duplicate)
- Total no. wells: 80 + 16 = 96

Preparation of QF working solution:

Volume QF per well: 200µl

Volume QF required: 96 x 200 = 19,200 µl / 19.2 ml

QF Dye Concentration: 2,00X

Vol QF required: 20 ml / 2,000 = 100µl

Preparation of TE:

TE Concentration: 20X

Vol of TE required:

Standards: 1,300µl / 1.3ml

Samples: (40) 4,000µl / 4 ml

QF: 19,200 µl / 19.2ml

Total Vol: 1.3 + 4 + 19.2 = 24,500 µl / 24.5 ml (approximately 25 ml)

25,000 / 20 = 1,250 µl / 1.25 ml

1.25 ml 20X TE in 23.25ml nuclease free water

A series of standards were prepared as follows:

Standard	Vol ssDNA Standard	Vol 1X TE	ssDNA concentration (ng/µl)
A	10µl	990µl	1
B	50µl of Standard A	50µl	0.5
C	50µl of Standard B	50µl	0.25
D	50µl of Standard C	50µl	0.13
E	50µl of Standard D	50µl	0.063
F	50µl of Standard E	50µl	0.031
G	50µl of Standard F	50µl	0.016

200µl of QF working solution were aliquoted into each well.

10µl of each standard were loaded into the plate as shown in figure 2.8.3.1, where 'X' was 10µl of 1X TE:

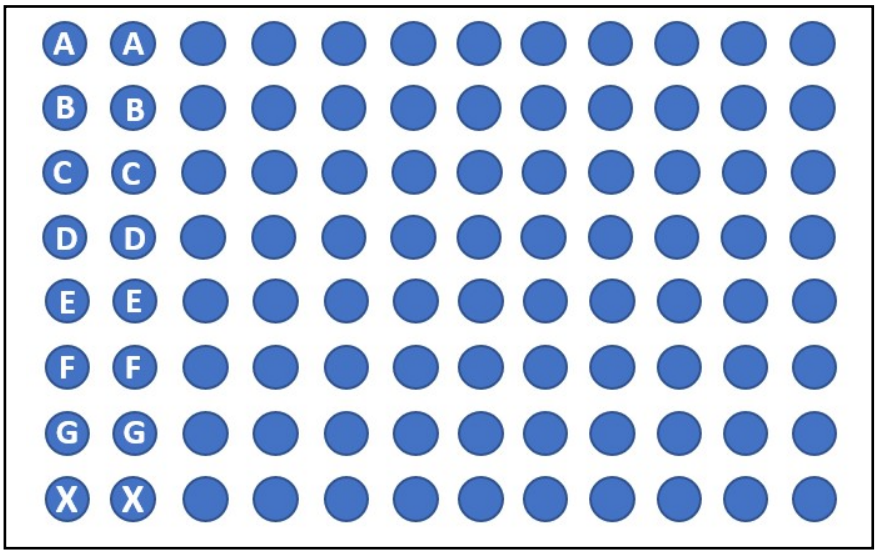

Figure 2.8.3.1: 96-well plate set-up for QF assay.

10 µl of each 1:100 diluted cDNA were added to each well, in duplicate. The plate was covered with foil and incubated for 5 minutes at room temperature (22-25 °C) on plate agitator.

After this time, fluorescence was read at 495nm, using a FLUOstar OPTIMA plate reader and Optima Control Software. Concentration was determined by the software, using a standard curve generated from the standards.

ddPCR Protocol.

To avoid contaminants, preparation of the PCR plate was conducted in a fume hood.

A master mix was prepared using the following regents:

Reagent	**1 Reaction (µl)**	**1 Reaction x 2 (µl)**	**No. samples (N)**
Supermix	11	22	N x 22
Probe (IGF-II or H19 at 500nM)	1.1	2.2	N x 2.2
Housekeeping probe G2 / M phase-specific E3 ubiquitin-protein ligase (G2E3) at 250nM)	1.1	2.2	N x 2.2
Water	7.7	15.4	N x 15.4
cDNA sample	1.1	2.2	
	Total: 10 µl	**Total: 20µl**	**Total: N x 20 µl**

1. cDNA was diluted to a concentration of 16ng in 8µl of nuclease-free water, using previously QF-determined values.
2. A cartridge insert was placed in a generator cassette and each 20µl reaction volume was loaded into the central row of wells; a 70 µl droplet of generator oil was loaded into the bottom row (as shown by figure 2.8.3.2) and a rubber gasket was placed over the cassette.

3. The filled cassette was loaded on to the droplet generator for the oil to be dispersed into the reaction volume.

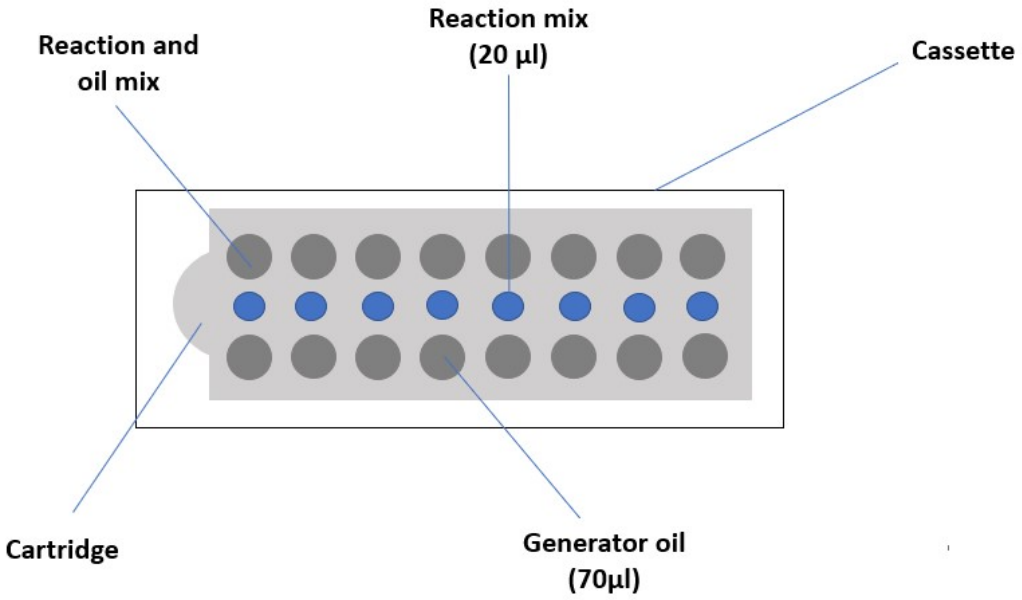

Figure 2.8.3.2: The ddPCR cartridge and cassette well lay-out.

4. The cassette was removed from the oil generator and the oil-reaction mix was transferred to a 96 well PCR plate using a multichannel pipette; the plate was heat sealed with foil before finally being transferred to the thermocycler for PCR.
5. The PCR conditions were 95°C for 10 minutes, followed by 40 cycles of 94°C for 30 seconds and 55°C for 1 minute. The plate was then read using a QX200 droplet reader. Values were analysed using Quantasoft® software, which converted droplets to copies / ng RNA, based on the RNA concentration and total volume added to the reaction dependent of Poisson distribution.
6. For normalized expression, the ratio of IGF-II/H19 concentration to control G2E3 concentration was used. Raw fluorescence amplitude data was extracted from the droplet reader.

2.9 Pyrosequencing for allelic imprinting expression (P.I.E)

2.9.1 Materials, equipment, and reagents

Apparatus / Instruments	**Manufacturer / Supplier**
Pipettes (P1000, 100, 20, 10 and 2)	Gilson, Dunstable, UK
Thermocycler (T100)	Bio-Rad, Watford, UK
Pyromark ID Pyrosequencer	Qiagen, Manchester, UK
Pyromark Vacuum Probe and Prep Table	Qiagen, Manchester, UK
Heat Block	Grant Instruments, Hertfordshire, UK
Plate agitator	Grant Instruments, Hertfordshire, UK
PSQ 96 Reagent Cartridge	Qiagen, Manchester, UK

Consumables	**Manufacturer / Supplier**
Pipette Tips	Bioline, London, UK
1.5 ml Centrifuge Tubes	Eppendorf, Stevenage, UK
96 well PCR Plate	Eppendorf, Stevenage, UK
PSQ 96 Plate Low	Qiagen, Manchester, UK

Reagent	**Manufacturer / Supplier**
HotStar Taq Plus DNA Polymerase Kit	ThermoFisher Scientific, Paisley, UK
Nuclease-free water	Ambion, ThermoFisher Scientific, Rugby, UK
Primer 1 (R) GAGCCAGTCTGGGTTGTTGC	Eurofins Genomics, Ebersberg, Germany
Primer 1 (F) ATCGTTGAGGAGTGCTGTTTCC	Eurofins Genomics, Ebersberg, Germany
Primer 2, biotinylated (R) TCGGATGGCCAGTTTACC	Eurofins Genomics, Ebersberg, Germany
Primer 2 (F) TCGGATGGCCAGTTTACC	Eurofins Genomics, Ebersberg, Germany
Sequencing Primer AGCAAAGAGAAAAGAAGG	Eurofins Genomics, Ebersberg, Germany
Pyromark Gold Q96 Reagent Pack	Qiagen, Manchester, UK
Binding Buffer	Qiagen, Manchester, UK
Denaturation Solution	Qiagen, Manchester, UK
Wash Buffer	Qiagen, Manchester, UK
Annealing Buffer	Qiagen, Manchester, UK
Streptavidin Sepharose High Performance Beads	SLS, Nottingham, UK

2.9.2 Protocol

The following protocol has been adapted from "Pyrosequencing for Accurate Imprinted Allele Expression (PIE) Analysis" (Yang, Damaschke *et al*. 2015):

Preparation of gene products.

Two stages of PCR were used to generate product for PIE analysis.

Stage 1:

A master mix was prepared containing the following reagents:

Reagent	**Volume (µl)**
10X buffer	1
dNTPs	0.1
Primer 1 (10 µM) (F)	0.5
Primer 1 (10 µM) (R)	0.5
Taq Polymerase	0.05
Nuclease-free water	6.85
cDNA	1
	Total: 10 µl

The reaction conditions for stage 1 were: 95°C for 15 minutes; 40 cycles of 95°C for 30 seconds, 54°C for 30 seconds, and 72°C for 90 seconds. PCR products from stage 1 were subsequently diluted i:10 for stage 2.

Stage 2.

A master mix was prepared containing the following reagents:

Reagent	**Volume (µl)**
10X buffer	4
dNTPs	0.4
Primer 2 (10 µM) (F)	2
Biotinylated Primer 2 (10 µM) (R)	2
Taq Polymerase	0.2
Nuclease-free water	29.4
cDNA (1:10)	2
	Total: 40 µl

Each 40 µl of reaction volume was loaded on to a 96-well PCR plate; the reaction conditions for stage 2 were: 95°C for 15 minutes; 40 cycles of 95°C for 30 seconds, 56°C for 30 seconds, and 72°C for 25 seconds.

The plate was sealed with film and stored at 4°C, prior to pyrosequencing.

Pyrosequencing Protocol.

1. Prior to use, the streptavidin beads were thoroughly vortexed to ensure all beads were uniformly dispersed in solution; a mix was prepared containing 1.5 µl of streptavidin beads and 38.5 µl of binding buffer for each Stage 2 PCR product. The plate was sealed and agitated for 5 minutes.

2. During this time, the sequencing primer and annealing buffer were prepared using the following volumes: 1.5 µl of sequencing primer and 43.5 µl of annealing buffer per sample

well. 45 µl of this mix were aliquoted into the PSQ 96 Low plate. This was positioned on the prep table, along with the plate containing the streptavidin/PCR Stage 2 mix.

The prep table configuration is shown in figure 2.9.2.1. The vacuum was started, and the probe was lowered into the water trough, to wash the probe tips.

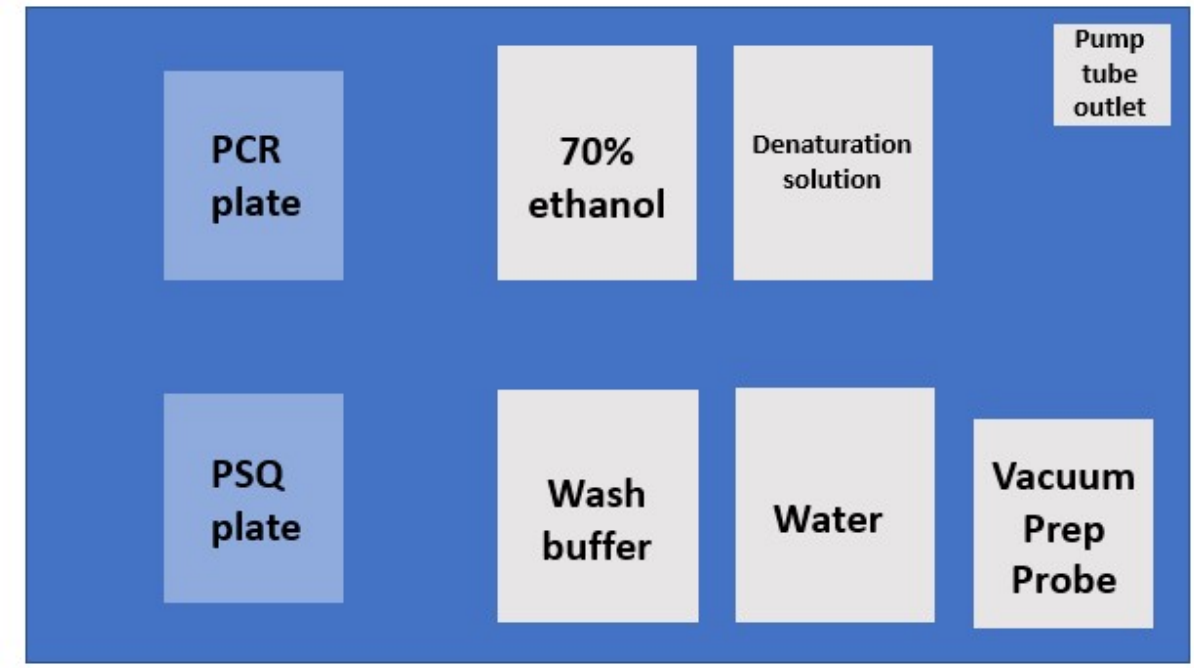

Figure 2.9.2.1: The Prep table configuration for pyrosequencing plate set-up.

3. The probe was gently lowered into the PCR plate, to allow capture of PCR product bound-streptavidin beads. The probe was then lowered into the ethanol trough and submerged for 10 seconds, followed by a 10 second submersion in the denaturation solution and finally into the wash buffer, for a final 10 second period. After this time, the probe was lifted from the wash buffer and tilted to 90°, to ensure drainage of fluids from the probe head.

4. The vacuum was switched off and the probe was lowered into the PSQ plate; gentle agitation ensured removal of PCR/beads from the probe tips. The probe was finally transferred to the water trough, where it was briefly washed of any residue.

5. The PSQ plate was incubated for 2 minutes at 80°C before being transferred to the Pyromark instrument.

6. The single nucleotide polymorphism (SNP) assay facility was selected from the PyroMark software. The sequencing primer sequence was entered, and the software generated a dispensation code. This determined the volumes of the required dNTPs for the assay run.

7. The reagent cartridge was filled with the Pyromark gold reagents; the requisite substrate (S), enzyme (E), and dNTP (guanine = G; thymine = T; adenine = A and cytosine = C) volumes were loaded in the following configuration (figure 2.9.2.2):

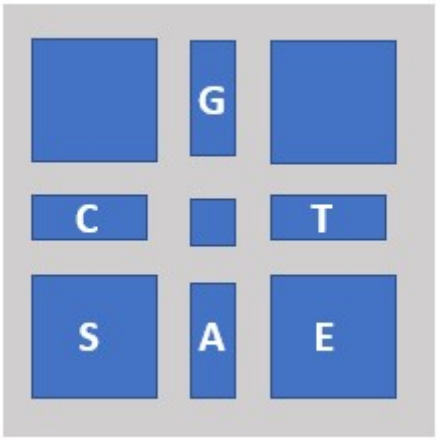

Figure 2.9.2.2: The PyroMark dNTP cartridge loading lay-out.

The cartridge was placed in the Pyromark instrument, and the assay was started. The resulting peak heights were used to calculate imprinting percentage.

To quantify imprinting as a percentage, an equation was devised using the pyrogram signal read-outs.

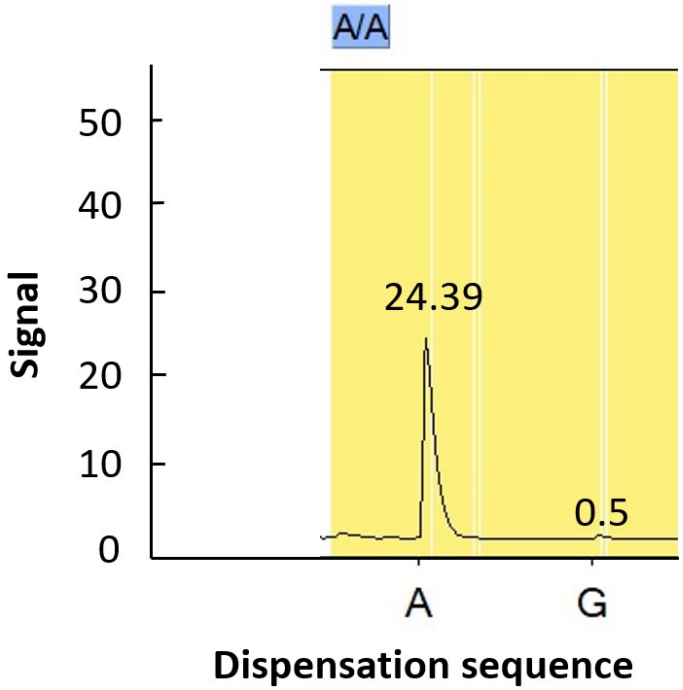

At the A/G SNP site, peak heights are indicative of allelic expression. Total peak height is calculated and expressed as 100%. Proportional expression of A and G was deduced using peak height values. Where allele A was > 50%, 50 was subtracted from its %. Where allele A was < 50%, its % was subtracted from 50. Haplotypic expression was denoted by 50. The subsequent values were multiplied by 2, to express imprinting percentage across the two parental copies.

Using the above pyrogram:

Total peak height: 24.39 + 0.5 = 24.89; 24.89 = 100%

Individual peak heights: A = 24.39 and G = 0.5

%A: 24.39 / 24.89 x 100 = 98**%**

%G: 0.5 / 24.89 x 100 = 2%

A = 98 % which is > 50

Therefore:

2 (98 – 50) = **96% imprinted**.

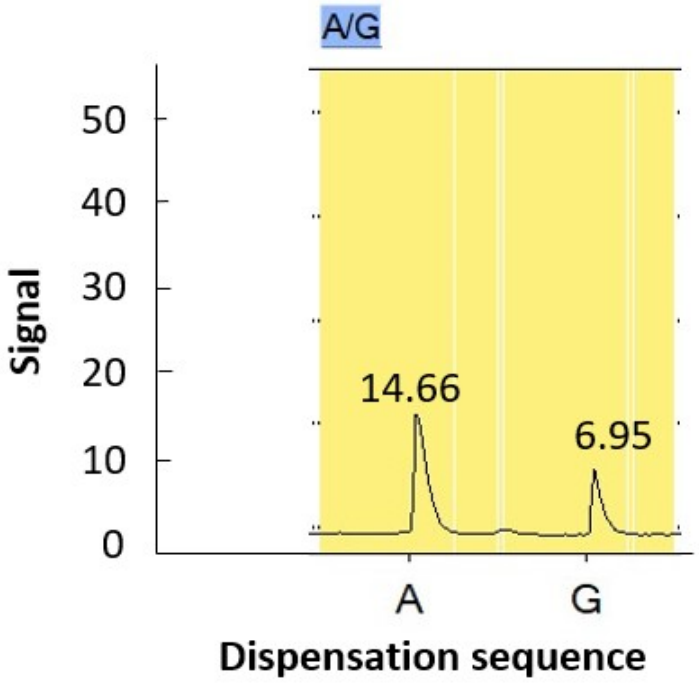

Similarly:

Total peak height: 14.66 + 6.95 = 21.61; 21.61 = 100%

Individual peak heights: A = 14.66 and G = 6.95

%A: 14.66 / 21.61 x 100 = 68**%**

%G: 6.95 / 21.61 x 100 = 32%

A = 68 % which is > 50

Therefore:

2 (68 – 50) = **36% imprinted**.

2.10 Immunohistochemistry

2.10.1 Materials, equipment, and reagents.

Apparatus / Instruments	**Manufacturer / Supplier**
Microtome	Leica, Milton Keynes, UK
Water bath	Grant instruments, Hertfordshire, UK
Pipette (P100)	Gilson, Dunstable, UK
Ventana BenchMark ULTRA™ machine	Roche, Burgess Hill, UK

Consumables	**Manufacturer / Supplier**
Pipette Tips	Bioline, London, UK
Tomo Microscope slides	Matsunami, Washington, USA
Cover slips	VWR, Leicester, UK

Reagents	**Manufacturer / Supplier**
Ventana BenchMark Ultra reagents	Roches, Burgess Hill, UK
IGF-II antibody	AbCam, Cambridge, UK
Microscope cover adhesive	VWR, Leicester, UK

2.10.2 Protocol

Using a microtome, 8µm thick slices were taken from formalin fixed paraffin embedded (FFPE) prostate tissue blocks and mounted on Tomo microscope slides (Matsunami). Slides were then stained for IGF-II peptide using an IGF-II antibody (AbCam) at a dilution of 1:600, on an automated Ventana BenchMark ULTRA™ machine (Roche). Slides were removed from the Ventana machine and covered using cover slips and adhesive.

2.10.3 Scoring

Slides were scored, in-house, using a modified version of the Allred system, combining the proportion of tissue stained (a scale of 1-5) with the stain intensity (a scale of 1-3) to give a score out of 8 (Dean, Perks *et al*. 2014), as shown in table 2.10.3. Currently, there is no standardized method of scoring prostate or colorectal cancer tissue.

Proportion of tissue stained	**Score**	**Total**	**Total score (Out of 8)**
0	0		
1% <	1		
1-10%	2		
10 – 30%	3		
30 – 65%	4		
65% >	5		
Intensity			
Absent	0		
Weak	1		
Intermediate	2		
Strong	3		

Table 2.10.3: Guidelines for adapted Allred score system

2.11 Statistical analyses

A one-way analysis of variance (ANOVA) was used for data where a comparison of more than two comparisons was required. This primarily included the data obtained from *in vitro* experiments; data are represented as a mean of three repeats, with standard error of the mean (SEM), followed by a least significant difference (LSD) post-hoc test.

For *in vivo* data analysis, a paired t-test was used to compare means of two groups.

For correlative analysis between two groups, a Pearson correlation co-efficient was used.

P-values less than 0.05 were considered statistically significant, with the following denotations: * $p \leq 0.05$, ** $p \leq 0.01$ and *** $p \leq .001$.

All data analyses were conducted using IBM SPSS statistics 24 software (IBM Corporation, version 24).

CHAPTER 3: LOSS OF IMPRINTING IN IGF-II/H19 IN PCA, *in vitro*

3.1 Introduction

PCa (PCa) is the most frequently diagnosed cancer type and the second major cause of cancer deaths amongst men (Siegel, Miller *et al*. 2016). Several factors have been found to contribute to disease susceptibility, progression, and prognosis including familial history and genetics (Giri and Beebe-Dimmer 2016), obesity (Lauby-Secretan, Scoccianti *et al*. 2016), aging (Bell, Del Mar *et al*. 2015) and ethnicity (Jones and Chinegwundoh 2014).

It is clear a link exists between obesity and cancer risk (Allott and Hursting 2015). The increased adipose tissue, associated with obesity, can disturb the delicate balance of the cellular environment, inducing an inflammatory state (Booth, Magnuson *et al*. 2015). Under inflammatory conditions, loss of epigenetic regulation occurs resulting in uncontrolled cellular activities (Fujita, Hayashi *et al*. 2019).

Obesity also increases susceptibility to type 2 diabetes (T2D) (Garg, Maurer *et al*. 2014). One key characteristic associated with T2D is hyperglycaemia. As glucose is the main energy source for cells, an increase (above the healthy range of 4- to 5.9 mM/L for an adult – according to NICE guidelines, (The National Institute for Health and Care Excellence, 2012) in its supply can cause increased proliferative potential (Chang and Yang 2016).

Insulin-like growth factor II (IGF-II) is a growth factor expressed in high quantities during early embryonic development (Liu, Greenberg *et al*. 1989). Expression continues throughout adulthood, with the liver being the primary site of synthesis (Baxter, Holman *et al*. 1995). IGF-II plays a critical role in a number of cellular events, including proliferation and survival (Resnicoff, Abraham *et al*. 1995).

In obese subjects, circulating serum levels of IGF-II are elevated and show a positive correlation with increased body mass index (BMI) (Buchanan, Phillips *et al*. 2001). Conversely, after weight loss, circulating levels of IGF-II have been shown to drop (Belobrajdic, Frystyk *et al*. 2010).

The IGF-II/H19 gene is located on the short arm of chromosome 11p.15.5 (Brissenden, Ullrich *et al*. 1984). It is composed of 10 exons and contains 5 promoters. Exons 1-4 and 6 are non-coding. Control

of expression takes place from promoters 0 to 4 and is strictly regulated. 128 kb downstream from IGF-II is a long non-coding RNA, H19, which is linked to IGF-II by an imprinting control region (ICR) (Rotwein 2018).

IGF-II was the first gene identified to be 'imprinted' (Ogawa, Eccles *et al*. 1993). This is a heritable epigenetic event whereby, through changes to the DNA structure (such as methylation or histone modification) one parental copy is silenced or imprinted (Park, Mitra *et al*. 2017). The loss of this natural silencing phenomenon (loss of imprinting – LOI) has been identified across a number of cancers, including prostate (Damaschke, Yang *et al*. 2017), breast (Mishima, Kagara *et al*. 2016), colorectal (Belharazem, Magdeburg *et al*. 2016) and lung (Zhang, Wu *et al*. 2014).

Models for the imprinting mechanism have been proposed, with the most widely accepted being the 'enhancer competition model' (Bartolomei, Webber *et al*. 1993), in which the presence of a CCCTC-binding factor (CTCF) – a multi-zinc finger protein (and a transcriptional repressor) - is able to bind to the unmethylated imprint control region (ICR) embedded within the maternal IGF-II / H19 allele. This impedes IGF-II transcription. Conversely, on the paternal allele, the ICR is hypermethylated. This blocks CTCF from binding, which permits IGF-II to be transcribed. LOI occurs when both parental copies of IGF-II / H19 are hypermethylated at the ICR, resulting in the bi-allelic expression of IGF-II (Reik and Murrell 2000).

The presence of a specific single nucleotide polymorphism (SNP) within the IGF-II/H19 gene, at restriction site 680 (rs680/ Apa1), was first used in 1993 to assess allelic expression and imprinting status of IGF-II in Wilms' tumours by Ogawa *et al*. (Ogawa, Eccles *et al*. 1993). Since then, this method has been used to assess imprinting status of IGF-II in numerous studies, specifically testing for mono- or biallelic expression of IGF-II cDNA (mRNA). Whilst sufficient for small numbers of samples, allelic analysis of larger cohorts can be time consuming. More recently, a method devised

in 2015, used pyrosequencing for rapid analysis of allelic expression in PCa tissue (Yang, Damaschke *et al*. 2015).

The function of H19 is unclear. In some cancers it is oncogenic: in gastric cancer, H19 and an embedded micro-RNA (miRNA-675) within its first exon, were found to be increased in tissue and cell lines. This over-expression led to increased cell proliferation and the inhibition of apoptosis (Yan, Zhang *et al*. 2017). In non-small-cell lung cancer, H19 expression was significantly higher in malignant lung tissue compared with normal, being at its highest in those from stage III and IV tumours (Zhou, Sheng *et al*. 2017). In contrast, H19 behaves as a tumour suppressor in some cancer types, such as colorectal (Yoshimizu, Miroglio *et al*. 2008) and prostate (Zhu, Chen *et al*. 2014). The mechanism that dictates H19 behaviour differs between cancer types.

A previous report focused on promoter methylation as a factor contributing to IGF-II transcription (Kuffer, Gutting *et al*. 2018). IGF-II mRNA and peptide levels were decreased in 80% of PCa, compared to non-neoplastic adjacent prostate and were independent of LOI status. IGF-II expression in both tumour and adjacent tissue depended on usage of the IGF-II promoters P3 and P4; decreased IGF-II expression in tumour tissue was strongly related to hypermethylation of these two promoters. The cause of hyper-methylation in this cohort was attributed to cumulative DNA damage, due to aging.

3.2 Hypothesis

Metabolic disturbances disrupt imprinting of IGF-II/H19 in PCa, *in vitro*.

3.3 Aims

1. To identify a suitable PCa cell line for investigating the effects of metabolic disturbance upon IGF-II/H19 imprinting status.
2. To explore the effects of a) hyperglycaemic (glucose concentration > 5mM/L, as defined by NICE) conditions and b) an inflammatory milieu on imprinting percentage, IGF-II & H19 mRNA expression and IGF-II peptide levels.

3.3 Materials & Methods

3.3.1 Method selection, optimisation & troubleshooting

To ascertain which cell line would be most suitable for subsequent dosing experiments, imprinting status needed to be established.

The APA1 restriction fragment length polymorphism (RFLP) digestion can identify homo- or heterozygosity of the SNP at rs680, i.e. A/A, A/G or G/G. DNA with a genotype of A/G would be informative at the preliminary level. To assess allelic expression and, therefore, imprinting status, mRNA (converted to cDNA) would require APA1 RFLP digestion. cDNA with a genotype of AA or GG would be indicative of monoallelic expression of IGF-II/H19 and, therefore, maintained imprinting status (MOI). Conversely, a genotype of A/G would be indicative of biallelic expression and, therefore, loss of imprinting (LOI). For experimental suitability, the cell line required a genotype of A/G at the DNA level, followed by AA or GG at the cDNA level.

The APA1 RFLP digestion process is lengthy and time-consuming, therefore alternative methodologies were investigated. Initially RFLP digestion was conducted using a concentrated APA1 enzyme requiring a minimum 2.5-hour incubation period for complete digestion at the restriction sites. In addition, prior to incubation, the enzyme required diluting and combining with BSA and an additional buffer. A new kit was identified excluded the step of enzyme dilution and the addition of BSA, but more importantly required a reduced incubation time of twenty-five minutes, due to a fast-acting APA1 digest enzyme. Optimal digestion time was established through serial incubations at four time points of 10-, 15-, 20- and 25 minutes. Complete digestion was observed after 15 and 20 minutes and, as such, was used for the remainder of the RFLP digestions.

Dosing with TNFα to induce IGF-II/H19 imprinting disruption had not been conducted previously. It had been used in other *in vitro* studies to investigate human neural progenitor cell survival (Kim, Jung *et al*. 2018) and osteogenic differentiation of mesenchymal stem cells (Mountziaris, Tzouanas *et al*. 2010); both studies used serial dilutions of TNFα ranging from 0 to 100ng/ml and 0 to 50ng/ml respectively. Mountziaris *et al*. used exposure time points of 24- and 48 hours, whereas Kim *et al*.

used a single time point of 24 hours. To capture any immediate or short-term mRNA responses to TNFα, an initial 6-hour exposure internal was included, in addition to the longer time points of 24- and 48 hours.

3.3.2 Culturing of immortalised PCa cell lines.

PCa cell lines PC3, LNCaP, DU145 and VCap, and a normal prostate epithelial cell line – PNT2 were used in this analysis. They were sourced and cultured as outlined in 2.1.

3.3.3 Isolation of nucleic acids

DNA and RNA were isolated from the cell lines as described in 2.X.X. They were quantified, "cleaned" and stored as described in 2.2.

3.3.4 Preparation of cDNA

RNA was converted to cDNA as outlined in 2.2.

3.3.5 Genotyping of cell lines, using RFLP analysis.

DNA and cDNA were genotyped using the single nucleotide polymorphism (SNP) in exon 7 of IGF-II, at restriction site 680 (APA1). This is described in 2.5.

3.3.6 Dosing with glucose

For all experiments, cells were seeded at a density of 1 x 10^6 per T25 flask in normal glucose-containing medium (1,000mg/L – 5mM). After 24 hours, media was exchanged for serum-free media (SFM) (composition described in 2.X.X) containing either 5mM-, 9mM- or 25mM glucose. Cells were incubated at 37°C with 5% CO_2.

At 6-, 24- and 48-hour intervals, a flask from each glucose group was removed and processed for RNA extraction and conversion to cDNA as described in 2.2.

3.3.7 Dosing with TNFα

Cells were seeded at a density of 1 x 10^6 per T25 flask in normal glucose-containing medium (1,000mg/L – 5mM). After 24 hours, media was replaced with 5mM- or 25mM glucose SFM. After a further 24 hours, cells were dosed (0 – 10ng/ml TNFα). Cells were processed for RNA extraction and conversion to cDNA, as described in 2.2.

3.3.8 Quantitative PCR (qPCR)

qPCR was performed as described in 2.X.X, using GAPDH as an internal control. Relative expression was calculated using the Pfaffl method, as outlined in 2.6.

3.3.9 Pyrosequencing

Pyrosequencing for imprinted allele expression (PIE) was conducted, as described in 2.9.

To quantify imprinting as a percentage, an equation was devised using the pyrogram signal read-outs.

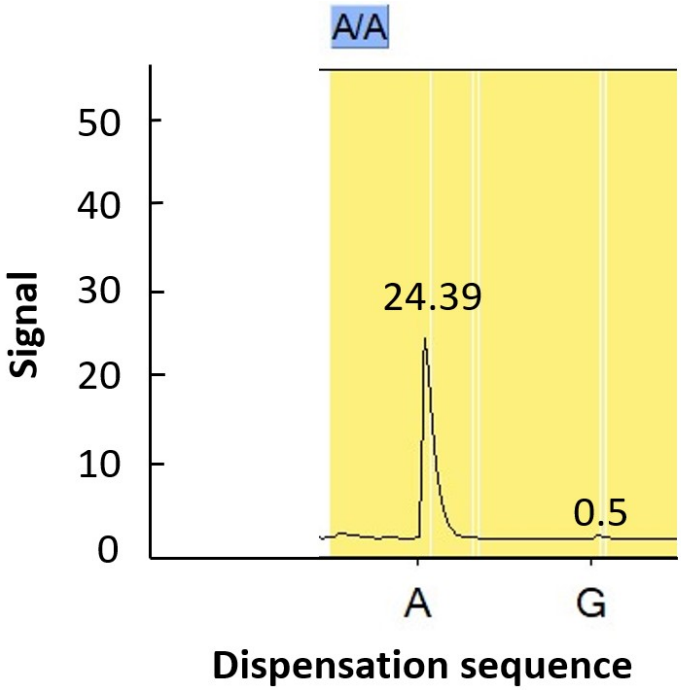

At the A/G SNP site, peak heights are indicative of allelic expression. Total peak height is calculated and expressed as 100%. Proportional expression of A and G was deduced using peak height values. Where allele A was > 50%, 50 was subtracted from its %. Where allele A was < 50%, its % was subtracted from 50. Haplotypic expression was denoted by 50. The subsequent values were multiplied by 2, to express imprinting percentage across the two parental copies.

Using the above pyrogram:

Total peak height: 24.39 + 0.5 = 24.89; 24.89 = 100%

Individual peak heights: A = 24.39 and G = 0.5

%A: 24.39 / 24.89 x 100 = 98**%**

%G: 0.5 / 24.89 x 100 = 2%

A = 98 % which is > 50

Therefore:

2 (98 – 50) = **96% imprinted**.

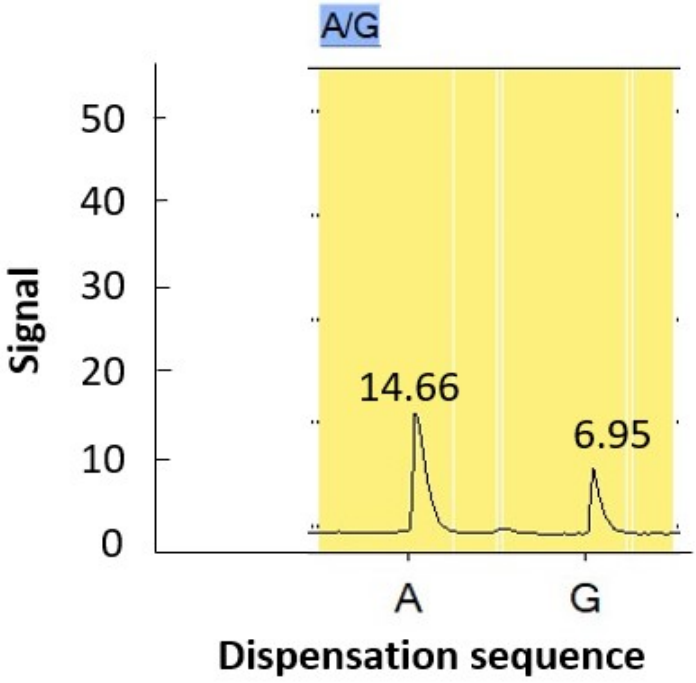

Similarly:

Total peak height: 14.66 + 6.95 = 21.61; 21.61 = 100%

Individual peak heights: A = 14.66 and G = 6.95

%A: 14.66 / 21.61 x 100 = 68**%**

%G: 6.95 / 21.61 x 100 = 32%

A = 68 % which is > 50

Therefore:

2 (68 – 50) = **36% imprinted**.

3.3.10 Radioimmunoassay (RIA)

The concentration of IGF-II peptide in cell supernatants was quantified 'in-house', using radioimmunoassay (RIA) as described in 2.7.

3.3.11 Statistical analysis

Experiments were conducted in triplicate. Analysis of variance (ANOVA) was performed followed by a least significant (LSD) post-hoc test. Analyses were conducted using IBM SPSS statistics 24 software (IBM Corporation, version 24). P-values less than 0.05 were considered statistically significant, with the following denotations: * $p \leq 0.05$, ** $p \leq 0.01$ and *** $p \leq .001$.

3.4 Results

3.4.1.1 Identification of prostate cell line suitability

To investigate the effects of metabolic conditions on LOI of IGF-II, a suitable prostate cell line needed to be determined. DNA from 4 immortalised PCa cell lines (PC3, LNCaP, DU145, VCaP, and 1 normal epithelial prostate cell line (PNT2) were genotyped using RFLP digestion at the APA1 restriction site. The VCap and PC3 cell lines were heterozygous, presenting with 2 bands of sizes 292- and 229bp, respectively (figure 3.4.1.1). These cell lines were classified as informative and would be suitable for further assessment of imprinting status. Cell lines DU145, LNCaP and PNT2 were found to be homozygous for the SNP at rs680 (i.e., the same SNP base at the same location, on both copies of the gene), resulting in a single band and, as such, were deemed non-informative.

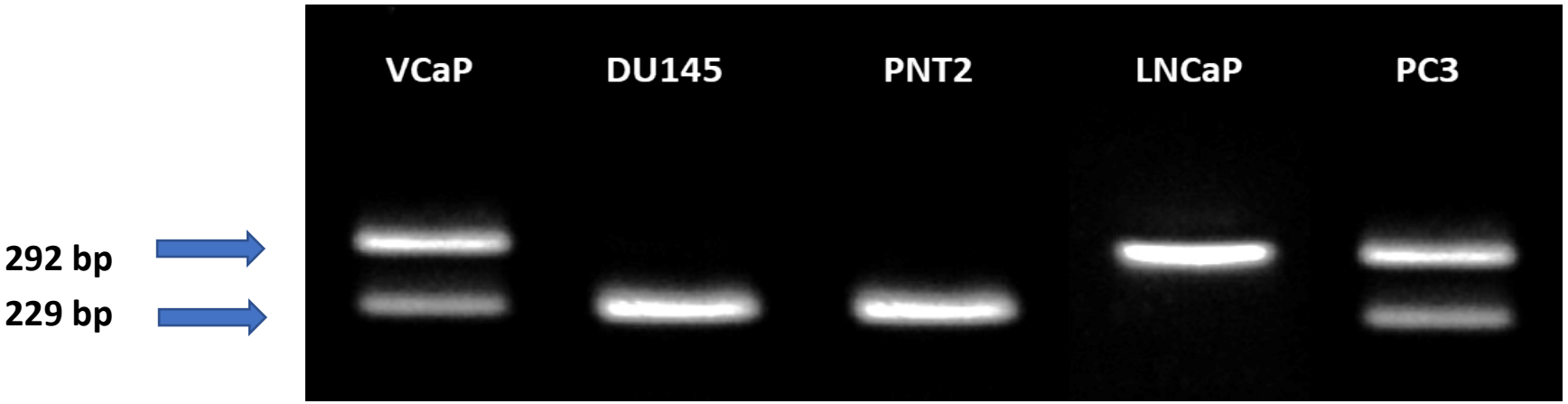

Figure 3.4.1.1: Genotyping of prostate cancer cell lines using APA1 RFLP analysis. Gel image depicting genotype results of cell lines VCaP, DU145, PNT2, LNCaP and PC3. VCaP and PC3 show two bands, sized 292- and 229bp; these cells are heterozygous for the SNP at rs680 and, therefore, informative (This is a representative gel of experiments repeated three times).

3.4.1.2 Confirmation of IGF-II imprinting status in the PC3 and VCaP cell lines

Further analysis of the PC3 and VCaP cell lines was required to establish IGF-II imprinting status. The VCaP cell line produced 2 bands of sizes 292- and 229bp, confirming bi-allelic expression of IGF-II (i.e., mRNA transcribed from 2 alleles: maternal and paternal) and, therefore, loss of imprinting (LOI) (figure 3.4.1.2). The PC3 cell line produced a single band of size 292bp, indicating mono-allelic expression of IGF-II/H19 (mRNA transcribed from a single allele) and therefore, retention of imprinting status. PC3 was determined to be the most suitable cell line for experimental use.

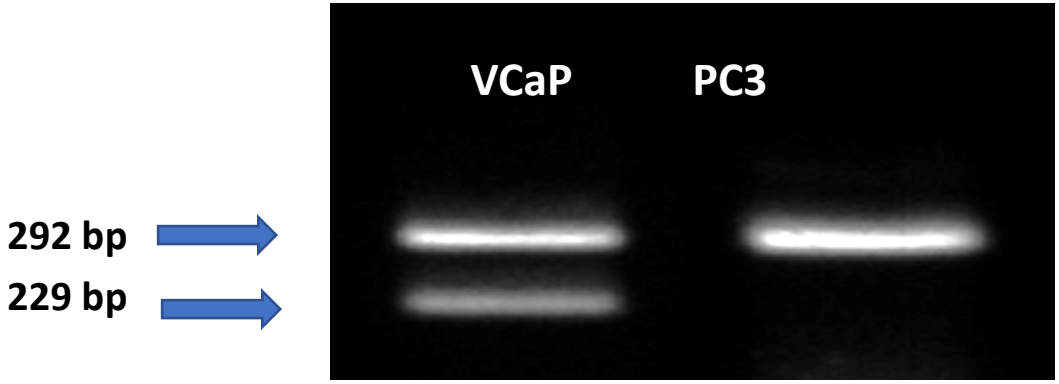

Figure 3.4.1.2: IGF-II/H19 allelic expression in prostate cancer cell lines using APA1 RFLP analysis. Gel image depicting IGF-II allelic expression. The VCaP cell line showed two bands, sized 292 and 229 bp, signifying bi-allelic expression and, therefore, loss of imprinting of IGF-II. The PC3 cell line showed a single band sized 292 bp, indicating mono-allelic expression of IGF-II and, therefore, a retention of imprinting status (This is a representative gel of experiments repeated three times).

3.4.2.1 The impact of altered levels of glucose on IGF-II/H19 imprinting status.

To investigate the effects of altered metabolic conditions upon IGF-II/H19 imprinting status, cells were cultured in media containing three different concentrations of glucose; this aimed to mimic conditions of a hyperglycaemic environment. After 6- and 24 hours, there were no changes to mono-allelic expression. After 48-hours, cells exposed to 9- and 25mM glucose-containing media showed two bands of 229- and 292bp. This indicated a change from mono- to biallelic expression and, therefore, loss of imprinting (figure 3.4.2.1).

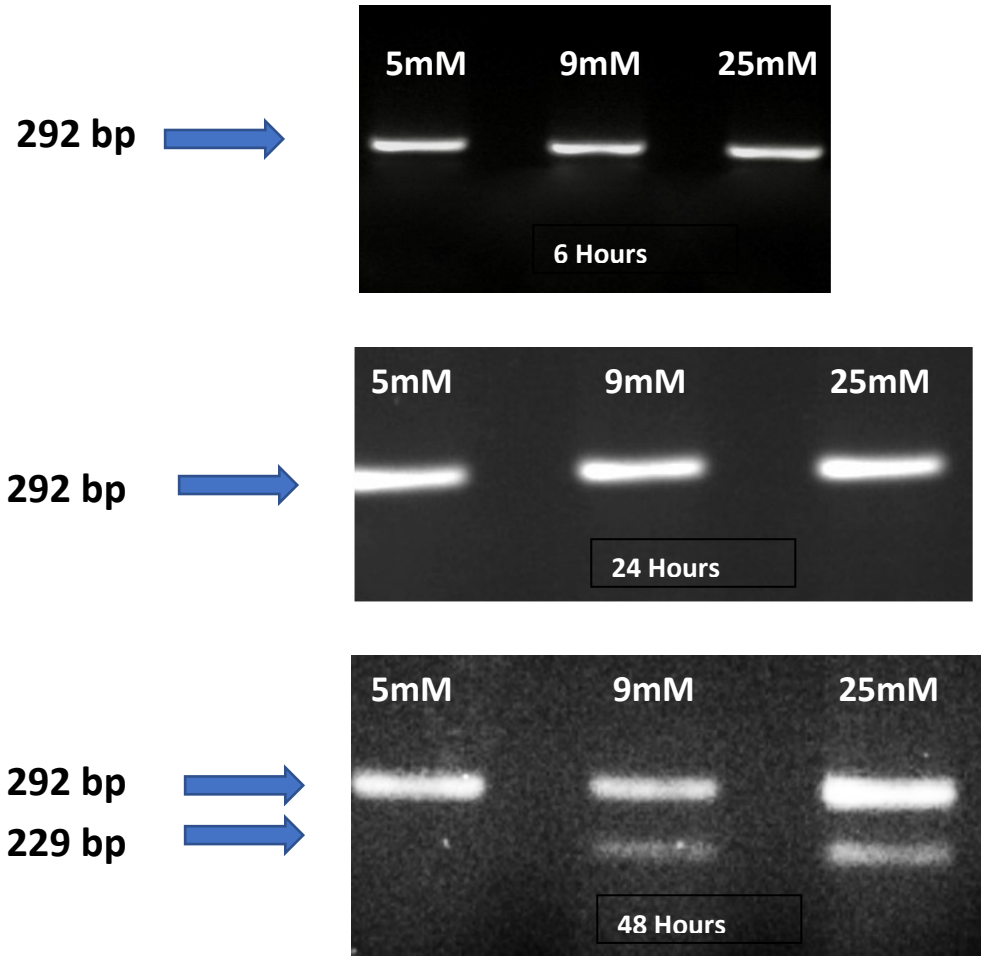

Figure 3.4.2.1: IGF-II/H19 allelic expression after treatment with glucose, using RFLP.

Gel image depicting the effects of varied glucose concentration on IGF-II/H19 allelic expression in the PC3 cell line. After 6- and 24 hours, there were no changes to mono-allelic expression. After 48 hours, cells cultured in 9- and 25 mM glucose showed two bands sized 229- and 292 bp, indicating a change from mono- to biallelic IGF-II/H19 expression and, therefore, loss of imprinting. (This is a representative gel of experiments repeated three times)

3.4.2.2 **Effect** of glucose on IGF-II/H19 imprinting percentage, using pyrosequencing.

To further clarify the change in imprinting status, pyrosequencing was used to quantify loss of imprinting as a percentage.

After 6 hours, PC3 cells cultured in 25mM glucose showed a significant ($P < .001$) decrease in imprinting percentage, compared to those cultured in 5mM glucose. After 24 hours, cells cultured in both 9- and 25mM glucose showed significant decreases in imprinting percentage ($P = 0.01$ and $< .001$ respectively), compared to those cultured in 5mM glucose; the effects of 9- and 25mM glucose were enhanced further after 48 hours ($P < .001$ and .001 respectively), when compared to those cultured in 5mM glucose (figure 3.4.2.2)

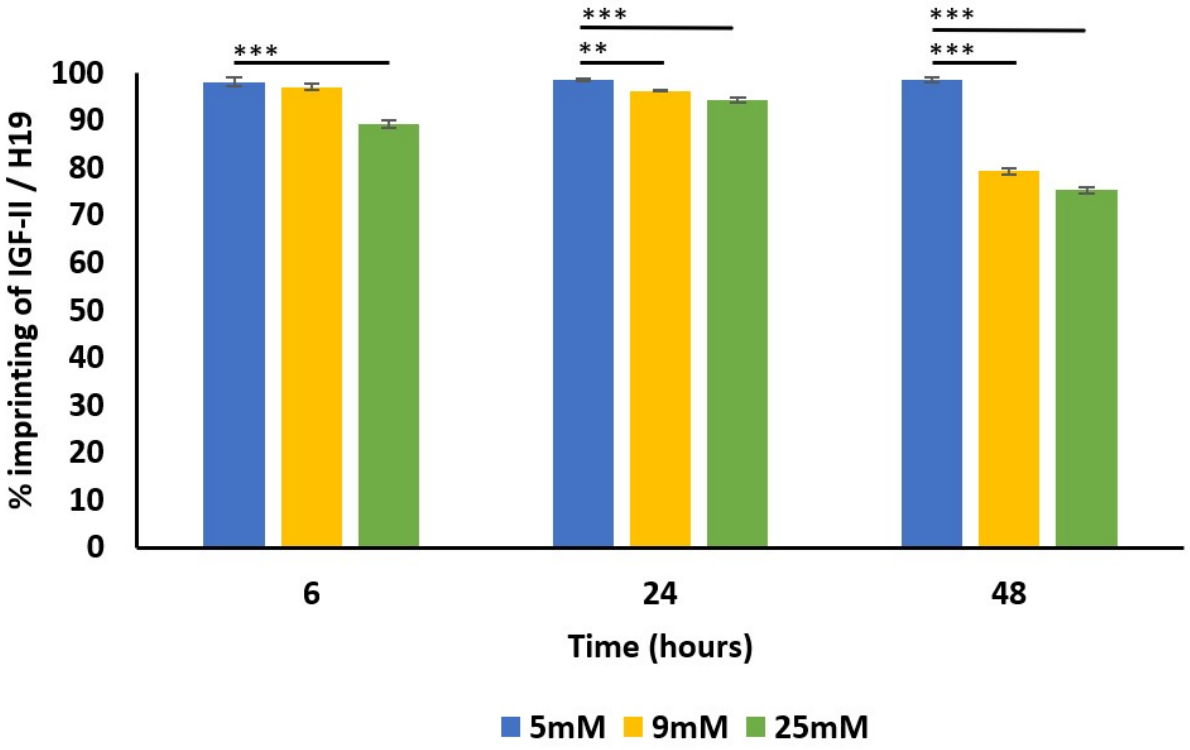

Figure 3.4.2.2: Effect of glucose on IGF-II/H19 imprinting percentage, using pyrosequencing. Imprinting percentage change of PC3 cells after exposure to glucose for 6-, 24- and 48 hours. After 6 hours, cells cultured in 25mM glucose showed a highly significant (p < .001) decrease in imprinting percentage compared to those cultured in 5mM glucose. After 24 hours, cells cultured in 9- and 25mM glucose showed significant decreases in imprinting percentage (p = 0.01 and < .001 respectively), when compared to those cultured in 5mM glucose. After 48 hours, cells cultured in 9- and 25mM glucose showed highly significant decreases in imprinting percentage (p <.001 and .001 respectively), when compared to those cultured in 5mM glucose (This is a representative set of data from experiments repeated three times).

3.4.2.3 Effect of glucose on IGF-II/H19 imprinting percentage using pyrosequencing, over three time points.

To further clarify the change in imprinting status at three different time points, pyrosequencing was used to quantify loss of imprinting as a percentage.

PC3 cells cultured in 5mM glucose for 48 hours showed a significant ($p < .001$) decrease in imprinting percentage, compared to those cultured for 6 hours. PC3 cells cultured in 9mM glucose for 24- and 48 hours showed a significant ($p = 0.003$ and $< .001$ respectively) decrease in imprinting percentage, compared to those cultured for 6 hours. PC3 cells cultured in 25mM glucose for 24- and 48 hours showed a significant ($p < .001$) increase and decrease ($p < .001$) in imprinting percentage, respectively, compared to those cultured for 6 hours (figure 3.4.2.3).

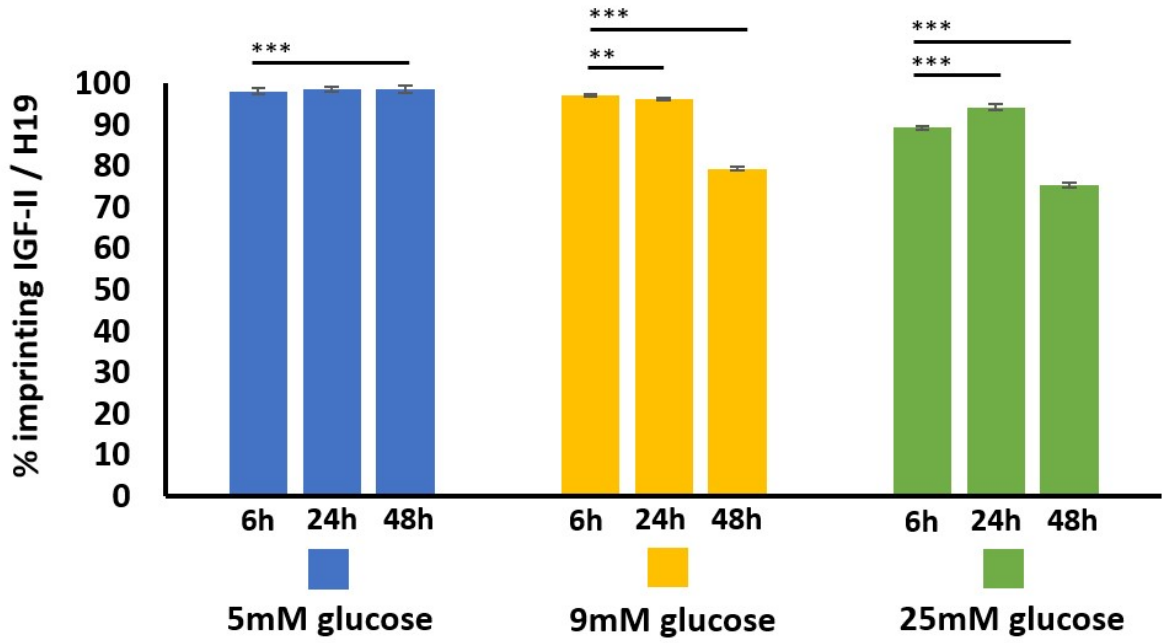

Figure 3.4.2.3 Effect of glucose on IGF-II/H19 imprinting percentage using pyrosequencing, over three time points. PC3 cells cultured in 5mM glucose for 48 hours showed a significant ($p < .001$) decrease in imprinting percentage, compared to those cultured for 6 hours. PC3 cells cultured in 9mM glucose for 24- and 48 hours showed a significant ($p = 0.003$ and $< .001$ respectively) decrease in imprinting percentage, compared to those cultured for 6 hours. PC3 cells cultured in 25mM glucose for 24- and 48 hours showed a significant ($p < .001$) increase and decrease ($p < .001$) in imprinting percentage, respectively, compared to those cultured for 6 hours (This is a representative set of data from experiments repeated three times (biological replicates).

3.4.2.4 The impact of altered levels of glucose on IGF-II and H19 mRNA expression

It was next ascertained whether changes in imprinting status and percentage, induced by increasing glucose levels, were accompanied by changes in mRNA expression IGF-II (figure A) and H19 (figure B). After 6 hours, there was a significant decrease in IGF-II mRNA in cells cultured in 9- and 25mM glucose (P = 0.01 and < .001 respectively), when compared with the control (5mM glucose). There were no significant changes to H19 mRNA expression. The same pattern of IGF-II expression seen at 6 hours, was also observed after 24 hours (P < .001 and .001 respectively), when compared with the control, and similarly there were no significant changes in H19 mRNA expression. After 48 hours, however, there was a significant increase in IGF-II mRNA in cells cultured in 25mM glucose media (P = 0.01), when compared with the control. Conversely, a significant decrease in H19 mRNA expression was observed, in cells cultured in 9- and 25mM glucose media (P < .001 and .001 respectively).

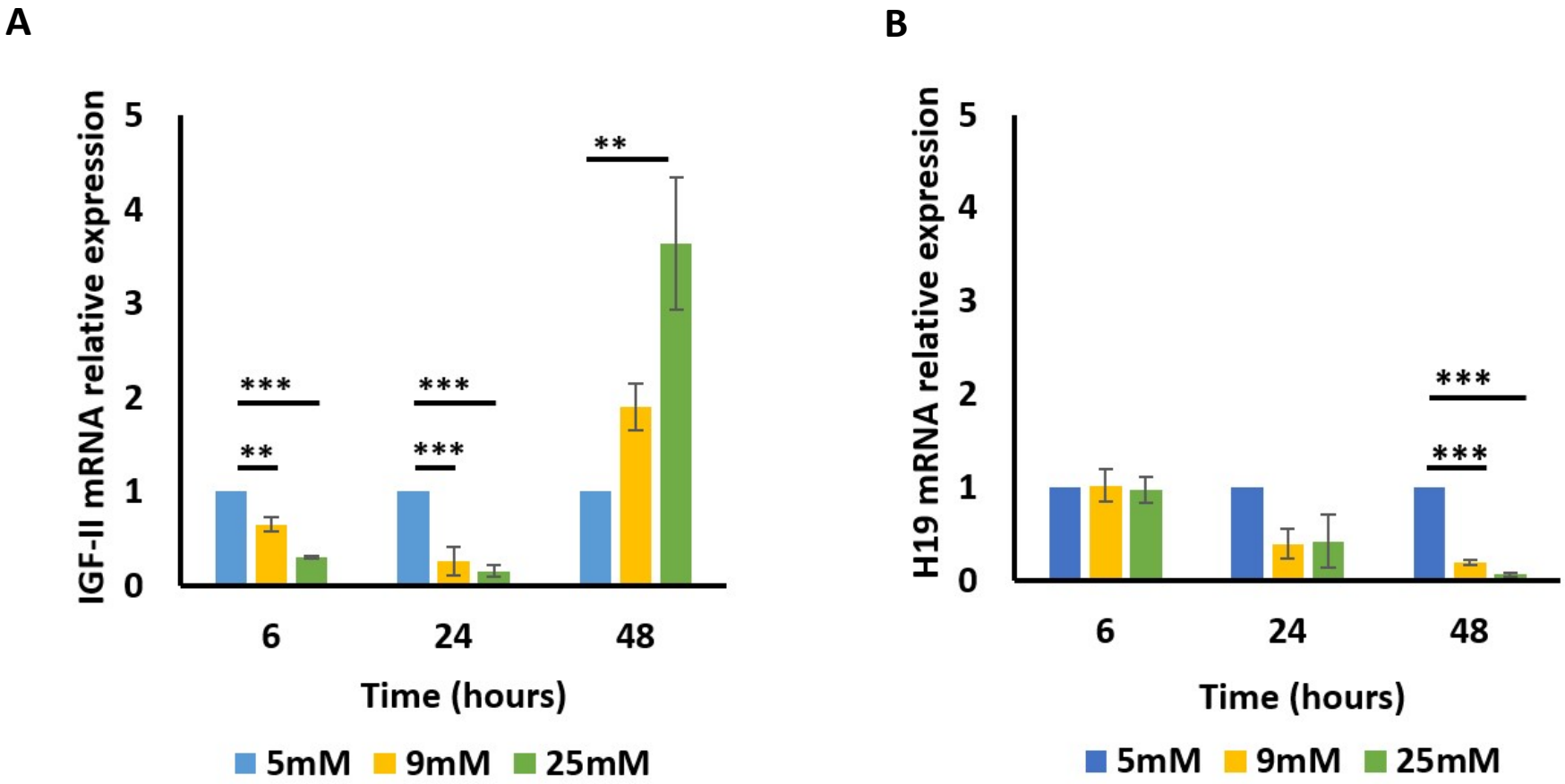

Figure 3.4.2.4 IGF-II and H19 mRNA relative expression in the PC3 cell line, after exposure to increased glucose levels. A significant increase in IGF-II mRNA expression was observed after 6-, 24- and 48-hours in 9- and 25mM glucose media (**A**). A significant decrease in H19 mRNA expression was observed after 48-hours in 9- and 25mM glucose media (**B**) (This is a representative set of data from experiments repeated three times.)

3.4.3.1 Effects of TNFα on IGF-II/H19 imprinting status in cells cultured in normal (5mM) and high (25mM) glucose media.

Having established the impact of glucose on IGF-II/H19 imprinting, the effects of an inflammatory cytokine, tumour necrosis factor-alpha (TNFα; 0-, 1-, 5- and 10ng/ml) were then assessed in PC3 cells. Cells cultured in 5 mM glucose and dosed with 10ng TNFα showed two bands sized 229- and 292 bp – which indicated a change from mono- to biallelic IGF-II expression - suggesting loss of imprinting (figure A). Cells cultured in 25 mM glucose-containing media and dosed with 1-, 5- and 10ng/ml ng TNFα showed two bands sized 229- and 292 bp. This indicated a change from mono- to biallelic IGF-II expression, suggesting loss of imprinting. The untreated cells, cultured in 25mM glucose also showed two bands of 229 and 292bp, confirming loss of imprinting with raised glucose (figure B).

A

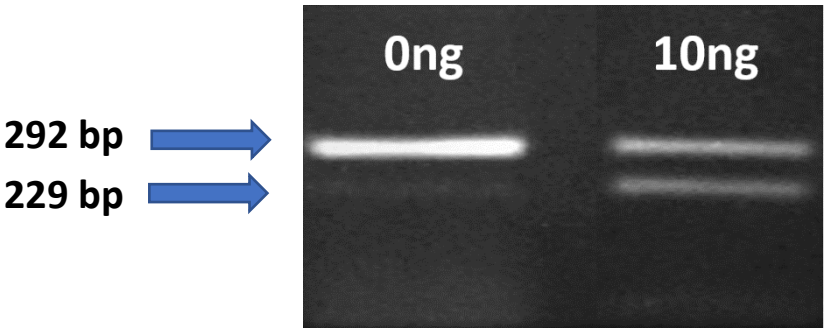

B

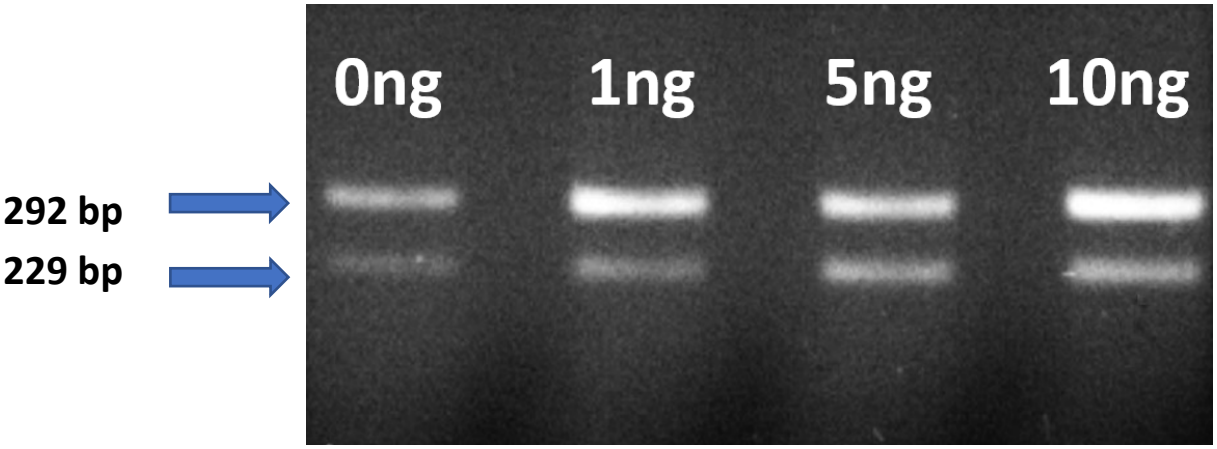

Figure 3.4.3.1: IGF-II/H19 allelic expression after treatment with TNFα, using APA1 RFLP. Cells cultured in normal (5mM) glucose and dosed with 10ng/ml TNFα showed two bands, sized 229 and 292 bp, indicating a change from mono- to biallelic IGF-II expression and, therefore, loss of imprinting (**A**). Cells cultured in high (25mM) glucose and dosed with 0-, 1-, 5- and 10ng/ml TNFα showed two bands sized 229 and 292 bp, indicating a change from mono- to biallelic IGF-II expression and, therefore, loss of imprinting (**B**) (These are representative gels of experiments repeated three times).

3.4.3.2 Effects of TNFα on the percentage of IGF-II/H19 imprinting in cells cultured in normal (5mM) and high (25mM) glucose media, using pyrosequencing.

Cells cultured in normal (5mM) glucose (figure A) and dosed with 1-, 5- and 10ng/ml for 24 hours all showed significant ($p < .001$) decreases in imprinting percentage, compared to controls. Cells cultured in high (25mM) glucose (figure B) and dosed with 5- and 10ng/ml TNFα both showed significant decreases in imprinting percentage ($p < .001$ respectively), when compared to controls.

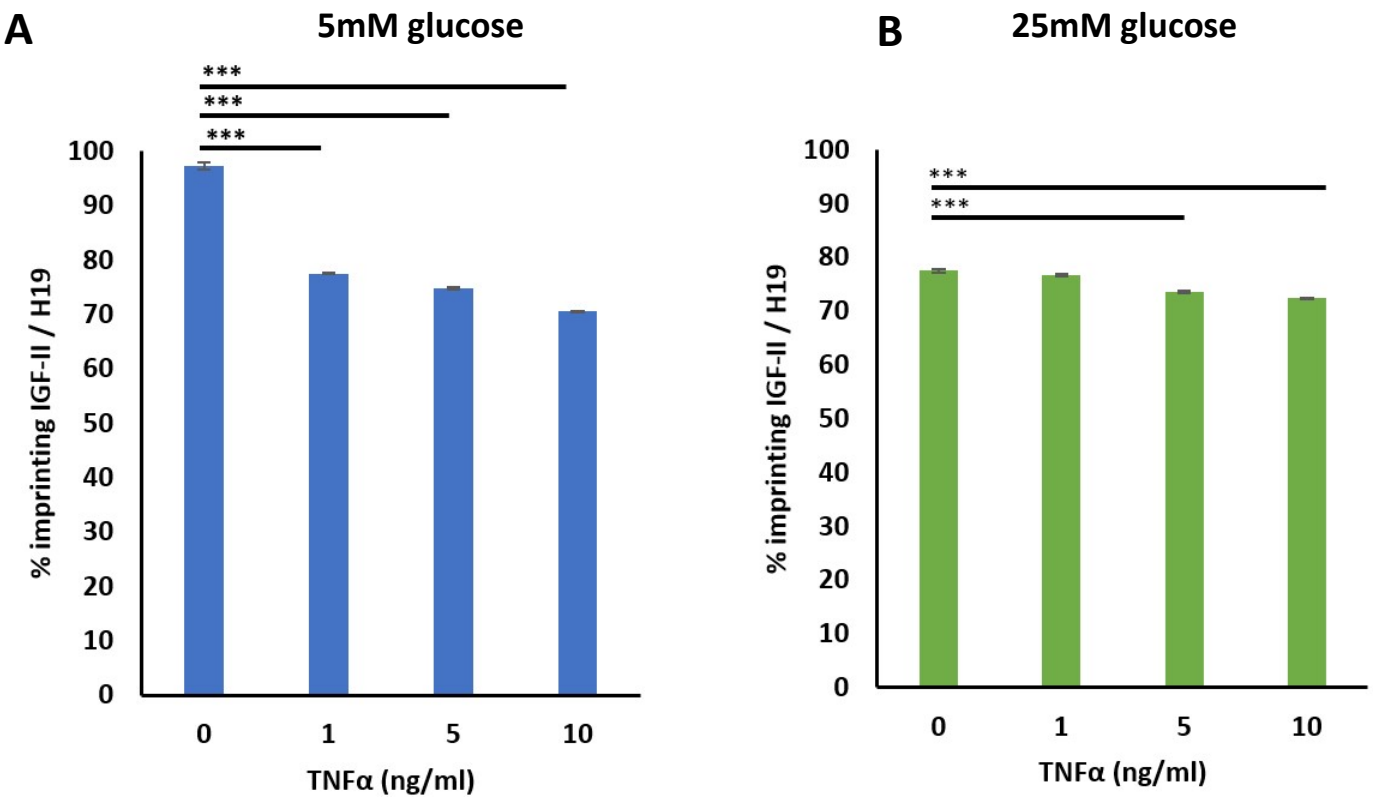

Figure 3.4.3.2 Change in IGF-II/H19 imprinting percentage in PC3 cells after exposure to TNFα for 24 hours in normal (5mM) and high (25mM) glucose media, using pyrosequencing. Cells cultured in normal (5mM) glucose media and dosed with 1-, 5- and 10ng/ml TNFα all showed highly significant (*p* <.001) decreases in imprinting percentage (**A**). Cells cultured in high (25mM) glucose media and dosed with 5- and 10ng/ml TNFα, also showed highly significant (*p* <.001) decreases in imprinting percentage when compared with the control (**B**) (This is a representative set of data from experiments repeated three times).

3.4.3.3 Effects of TNFα on IGF-II and H19 mRNA expression in cells cultured in normal (5mM) and high (25mM) glucose media.

Cells cultured in normal (5mM) glucose media for 24 hours showed a significant decrease in IGF-II mRNA expression when dosed with 1- and 5ng/ml TNFα (p = 0.01 and 0.05 respectively), compared with the untreated control. In contrast, cells treated with 10ng/ml TNFα showed a significant (p = 0.01) increase in IGF-II mRNA expression, when compared with the control. No significant fold changes in H19 mRNA expression were recorded (figure A).

Cells cultured in high (25mM) glucose showed no significant changes in IGF-II mRNA when dosed with 1- and 5ng/ml TNFα compared with the untreated control. Conversely, in 25mM glucose a significant decrease (p = 0.01) in H19 mRNA was observed in cells treated with 1ng/ml TNFα, compared with the control. A significant increase (p < .001) in H19 mRNA was observed in cells treated with 10ng/ml of TNFα, when compared with the un-dosed control (figure B).

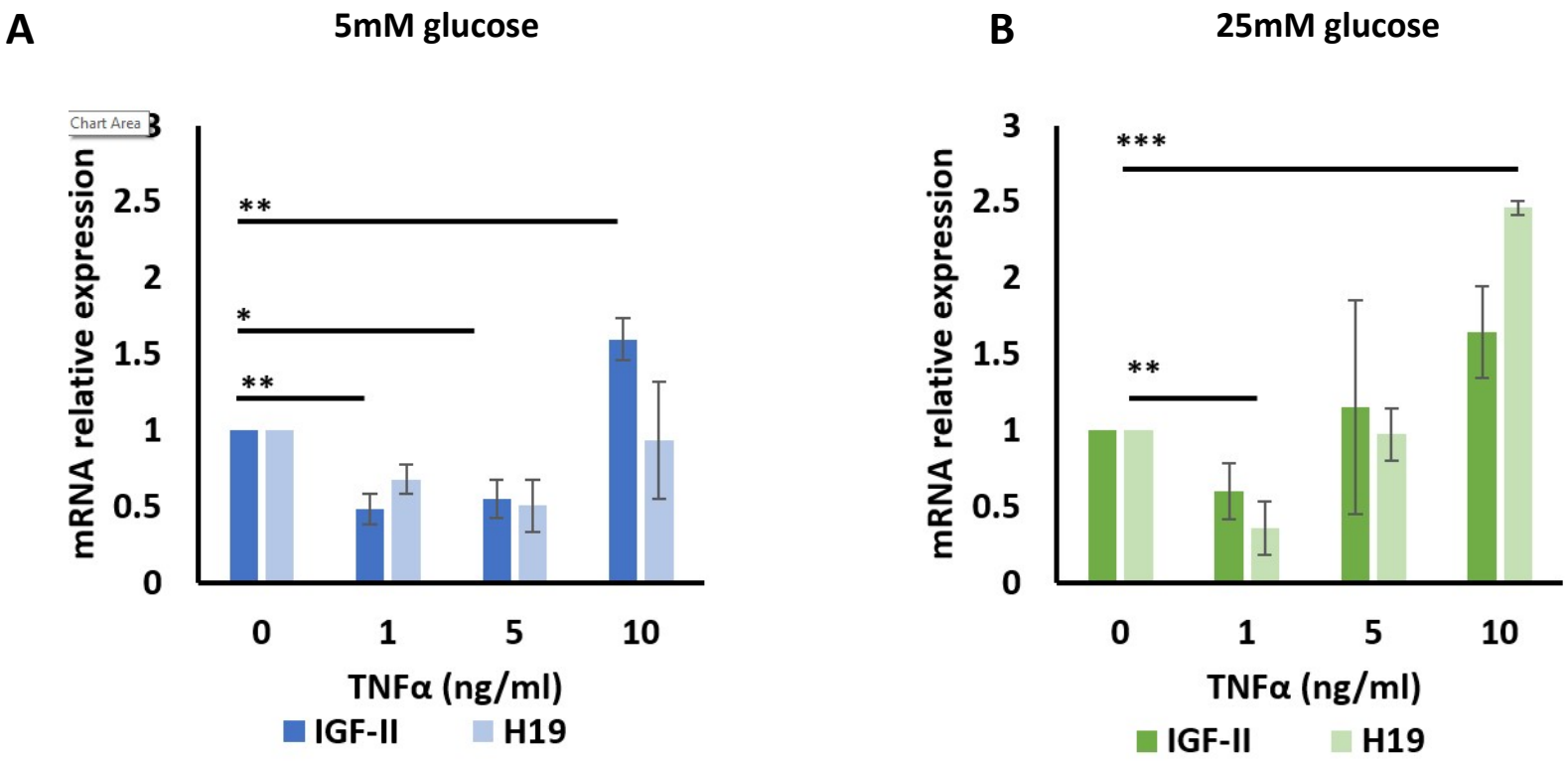

Figure 3.4.3.3: IGF-II & H19 mRNA relative expression, after treatment with TNFα in normal (5mM) and high (25mM) glucose, using qPCR. With normal (5mM) glucose, a significant increase in IGF-II was observed in cells dosed with 1-, 5- and 10ng/ml TNFα; no significant fold changes in H19 mRNA were observed (**A**). With high (25mM) glucose, no significant fold changes in IGF-II mRNA were observed; a significant decrease in H19 was found in cells dosed with 1ng/ml TNFα, whilst a significant increase was observed in those dosed with 10ng/ml TNFα (**B**) (This is a representative set of data from experiments repeated three times).

3.4.3.4 Effects of TNFα on levels of secreted IGF-II peptide

Having observed the influence of TNFα and glucose on IGF-II mRNA expression, it was next determined if this translated into secreted peptide. Cells cultured in normal (5mM) and high (25mM) glucose showed no significant changes to secreted IGF-II peptide. Cells exposed to increasing doses of TNFα (0-, 1-, 5- and 10ng/ml) in 5mM glucose, for 24- and 48 hours, showed no significant changes to secreted IGF-II peptide (figure A). This was also true of cells exposed to identical doses of TNFα cultured in high (25mM) glucose, after identical time points (figure B).

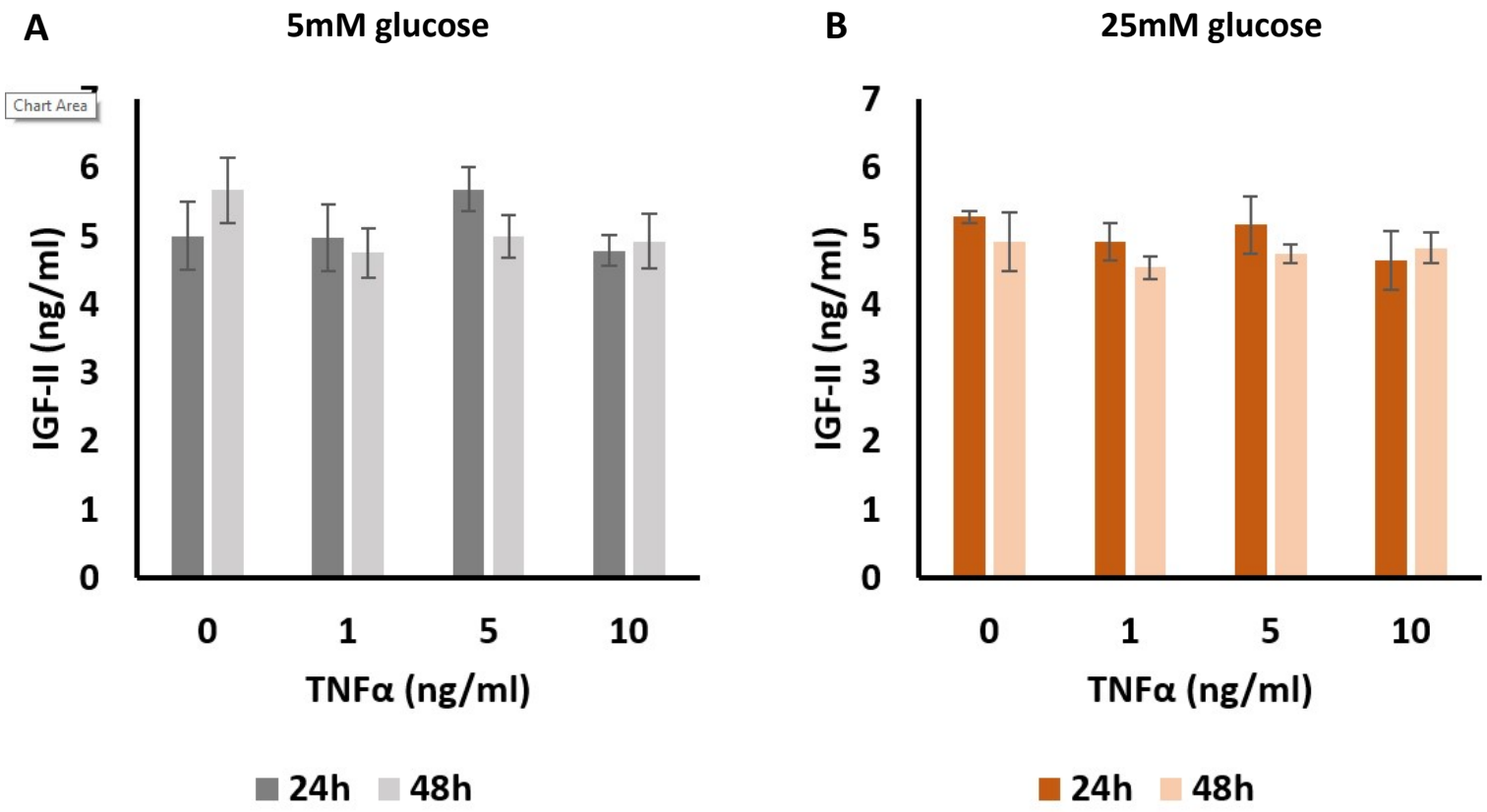

Figure 3.4.3.4: IGF-II peptide levels secreted by PC3 cells, after treatment with TNFα in normal (5mM) and high (25mM) glucose. There were no significant changes in the quantities of IGF-II peptide after 24- and 48 hours exposure to normal (5mM) glucose (**A**) or high (25mM) glucose (**B**), when combined with increasing doses of TNFα (This is a representative set of data from experiments repeated three times).

3.5 Discussion

LOI in IGF-II is a phenomenon common to many different cancer types (Bowers, Rossi *et al*. 2015). The causes and consequences remain unclear. If modifiable behaviours can be shown to influence its occurrence, this could have important implications for understanding the development and progression of cancers.

Findings in this chapter have demonstrated that under either hyperglycaemic or inflammatory metabolic conditions, loss of IGF-II imprinting can be induced *in vitro*. In high glucose (i.e above the healthy range of 4- to 5.9 mM/L for an adult – according to The National Institute for Health and Care Excellence (NICE) guidelines, (NICE, 2012) or increased inflammatory (TNFα 10ng/ml) conditions, IGF-II loses imprinting due to the introduction of a gradual expression of the silenced maternal copy. Additionally, prolonged exposure to high glucose also induces loss of imprinting. The marked increase in IGF-II mRNA did not translate into increased expression of IGF-II peptide.

Whilst the exact mechanism of imprinting loss is unclear it may be hypothesised that exposure to elevated glucose conditions and / or inflammatory cytokines may cause disruption to the methylation patterns in and around the IGF-II / H19 locus. A study published in 2018 (Hall, Dekker Nitert *et al*. 2018) documented the disruptive effects of high glucose on human pancreatic islets, *in vitro*; islets exposed to 19mM glucose exhibited significantly modified expression of 8 genes, 5 of which exhibited changes in DNA methylation. Elsewhere (Aref-Eshghi, Biswas *et al*. 2020) it was shown that prolonged exposure to high glucose was sufficient to cause epigenetic disruption; human endothelial cells were cultured in 5- and 25mM glucose for 2 and 7 days. 88 DMRs were assessed for methylation status; DNA hypermethylation was associated with increased length of exposure and glucose concentration. Similarly, it was shown by Kandilya *et al*. (Kandilya, Shyamasundar *et al*. 2020) that human neural progenitor cells showed significant disruption of DNA methylation patterns after exposure to 40mM glucose, *in vitro*.

Conversely, evidence concerning the epigenetic effects of TNFα is comparatively lacking; results published in 2019 (Lorente-Sorolla, Garcia-Gomez *et al*. 2019) showed elevated levels of TNFα, IL-6 and -10 to be linked with disrupted DNA methylation patterns in human monocytes, during sepsis. A report from the same year (Zhao, Lan *et al*. 2019) showed the addition of TNFα to induce hypomethylation-dependent and -independent activation of the IL-32 gene. Earlier findings (Verschoor, McEwen *et al*. 2017) demonstrated the existence of a positive correlation between serum levels of TNF, Interleukin (IL) -6, -8 and -10 and increased levels of DNA methylation in a cohort of community-dwelling adults.

The *in vitro* data indicated that LOI was accompanied by an increase in expression of IGF-II and a reciprocal reduction in expression of H19 consistent with the 'enhancer competition model', first posited in 1993 (Bartolomei, Webber *et al*. 1993). Further pyrosequencing to analyse methylation patterns at across the gene may provide further clarification. If disruption to the DMRs has occurred, as a result of dosing with glucose and/or TNFα, pyrosequencing will highlight the specific CpG sites where hyper- or hypomethylation may have occurred, using the untreated control as a comparative. Oxidative stress can also induce LOI, in both benign and malignant prostate tissue, by disrupting the expression of CTCF and its binding to H19 and the ICR; oxidative stress can cause binding of necrosis factor–kappa-beta (NF-κβ) to the CTCF promoter, causing a decrease in its expression (Yang, Wagner *et al*. 2014)

Whilst RFLP analysis is sufficient with regards to determining allelic expression, it is unable to provide the nuanced result of pyrosequencing; RFLP provides a binary result but will not reveal more in-depth information pertaining to imprinting. One such example are the results shown by figure 3.4.2.1; the RFLP digestion at 6- and 24 hours showed no change in allelic expression. Conversely, pyrosequencing revealed significant decreases in imprinting at these two time points, which was otherwise "invisible" by RFLP analysis.

Comparatively, RFLP analysis is relatively inexpensive requiring basic equipment held by most laboratories, whereas pyrosequencing requires expensive capital equipment and reagents available from limited suppliers. By comparison, pyrosequencing is high throughput and can assess large numbers of samples (up to 96) in a single fifteen-minute assay. The preparation of PCR product for RFLP is single stage, whereas pyrosequencing requires two stages of PCR to amplify the required gene product.

A key finding in this chapter is that no measurable change in IGF-II peptide, despite the increase of IGF-II mRNA was detected. This may be due to issues processing the mRNA transcripts i.e., post-transcriptional modification.

A key group of molecules implicated in processing IGF-II mRNA is the IGF-II mRNA-binding protein family (IMPs) (also referred to as IGF2BPs in some sources), of which there are three types: IMP1, -2 and -3.

First identified as IGF-II mRNA-binding proteins in 1999 (Nielsen, Christiansen *et al*. 1999), IMPs are primarily synthesised during early embryonic development and foetal growth and are typically missing in adult tissues. IMPS are generally found in the cytoplasm, where they bind to target mRNA transcripts in a protective capacity, to form stable protein complexes called ribonucleoprotein particles or RNPs (Oleynikov and Singer 2003). Each IMP has multiple target mRNAs, with varying effects upon each target. For example, in the context of embryonic growth, IMP1 inhibits the translation of IGF-II mRNA (Nielsen, Christiansen *et al*. 1999). Conversely, it has been shown to enhance translation of an internal ribosome entry site (IRES) mRNA in the hepatitis C virus (Weinlich, Huttelmaier *et al*. 2009); IMP2 has been shown to enhance translation of IGF-II mRNA in human rhabdomyosarcoma (RD) cells (Dai, Rapley *et al*. 2011; Dai, Christiansen *et al*. 2013) and inhibit apoptosis in pancreatic cancer (Xu, Yu *et al*. 2019); IMP3 has been shown to enhance translation of the cell adhesion protein cluster of differentiation (CD) -44, in breast cancer (Liu, Yu *et al*. 2017) and CD164 in Ewing sarcoma (Mancarella, Caldoni *et al*. 2020).

Aberrant expression of IGF-II in numerous cancer types is well documented, but elevated synthesis of IMPs, specifically IMP2, has also been identified in a number of different cancer types - such as liver (Gutschner, Hammerle *et al*. 2014; Fawzy, Hamza *et al*. 2016; Shaalan, Handoussa *et al*. 2018), ovarian (Kobel, Weidensdorfer *et al*. 2007; Kobel, Xu *et al*. 2009; Hsu, Shen *et al*. 2015), colorectal (Liu, Li *et al*. 2013; Ye, Song *et al*. 2016), breast (Liu, Li *et al*. 2015) and pancreatic (Schaeffer, Owen *et al*. 2010; Wang, Wang *et al*. 2015; Glass, Michl *et al*. 2020). Not surprisingly the dysregulation of IMP2 expression, seen across a variety of cancers, is also seen in T2D.

The link between T2D and IMP2 was first highlighted in 2007, after a series of genome-wide association studies (GWAS) which determined that a group of SNPs, within the IMP2 gene, induced an increase in the risk of developing T2D (Diabetes Genetics Initiative of Broad Institute of, Mit *et al*. 2007; Scott, Mohlke *et al*. 2007; Wellcome Trust Case Control 2007). The mechanistic behaviours of IMP2 and SNPs of IMP2 in T2D remain unclear, although a report published in 2012 (Schaeffer, Hansen *et al*. 2012) showed IMP2 to be down-regulated under high glucose conditions, inhibiting translation of laminin-β2 mRNA in rats. In the context of my *in vitro* results, the findings of Schaeffer *et al* may offer one explanation for the elevated levels of non-translated IGF-II mRNA. However, without quantification of IGF-II mRNA binding proteins using qPCR or RIA, this suggested explanation remains theoretical.

In addition to a lack/absence of IMPs, another suggested activity that may have blocked translation of IGF-II mRNA into peptide is post-transcriptional regulation by micro RNAs (miRNAs; miRs).

First identified in 2001 (Lagos-Quintana, Rauhut *et al*. 2001), miRNAs are small (approximately 20-22 nucleotides) single stranded, non-coding molecules involved in many types of genetic processes – one of which is translational repression (Ambros 2001). The three stages of translation are: initiation, elongation and termination; miRNAs aid in repression of this process by binding to the 5'-untranslated-region (UTR) of the mRNA strand at the initiation step, preventing the synthesis of peptide (Iwakawa and Tomari 2015). In the context of these findings, there may be involvement of endogenous miRNAs blocking translation of the upregulated IGF-II mRNA into peptide. Assessing

whether this process was blocking peptide synthesis would require further analysis, as there are several miRNAs which target IGF-II translation through inhibition of IMPs. Findings published in 2015 (Wang, Li *et al*. 2015) detailed the suppressive effect of miR-873 upon IMP1 in glioblastoma; a report published in 2018 (Wang, Aireti *et al*. 2019) described the inhibitory effect of miR-150 upon IMP1 in osteosarcoma, citing its behaviour as a tumour suppressor. More recently, Yan *et al*. (Yan, Wang *et al*. 2020) demonstrated miR-454-3p to inhibit cell proliferation by targeting IMP1 in oesophageal cancer.

3.6 Conclusion

Data in this chapter have demonstrated that, under high glucose (≥ 9mM) or increased inflammatory conditions (TNFα at a concentration of ≥ 10 ng/mL), imprinting status of IGF-II is gradually lost through the progressive expression of the silenced, maternal copy. It may be hypothesised that exposure to elevated glucose conditions and/or inflammatory cytokines may disrupt the methylation patterns in and around the IGF-II/H19 locus. The *in vitro* data indicates that LOI was accompanied by an increase in expression of IGF-II and a reciprocal reduction in expression of H19 consistent with the "enhancer competition model". Further pyrosequencing to analyse methylation patterns may address this theory. Furthermore, upregulation of IGF-II mRNA, induced by manipulation of the metabolic environment, was not translated into IGF-II peptide. This may be due to the downregulation or an absence of IGF-II mRNA binding proteins (IMPs) or translational repression by miRNAs. Further studies to assess the expression of IMPs and/or candidate miRNAs would address these issues.

In conclusion, chapter 3 has shown that disturbances of the metabolic environment (to mimic those of an inflammatory and/or hyperglycaemic physiological state) disrupts IGF-II/H19 imprinting status in PCa, *in vitro*.

CHAPTER 4: LOSS OF IMPRINTING IN IGF-II/H19 IN PCA, *in vivo*

4.1 Introduction

Novel findings in chapter 3 demonstrated that epigenetic disruption in the form of imprinting loss, to IGF/H19, was induced under inflammatory conditions and that surprisingly, this was not reflected by an increase in IGF-II peptide.

Loss of imprinting in PCa was first reported in 1995 (Jarrard, Bussemakers *et al*. 1995), where biallelic expression of IGF-II was found in both cancerous and the associated normal peripheral tissue of prostate tumours. Findings published in 2011 (Bhusari, Yang *et al*. 2011) showed similar findings, with LOI in IGF-II to occur in both tumour-adjacent and 10mm distal tissue, with the tumour focus presenting with MOI. These findings suggested that a field defect had occurred within the region of the prostate.

Since Jarrad *et al*.'s findings in 1995, more studies have focused on the mechanistic causes of imprinting disruption to IGF-II/H19; in 2009, Paradowska *et al*. (Paradowska, Fenic *et al*. 2009) compared the number of epigenetic alterations within the CTCF binding domain in two cohorts of prostate tissue: one classified as presenting with benign prostate hyperplasia (BPH), and the other cancerous. The BPH samples showed over 80% methylation of CpG islands within CTCF; in cancerous tissue, this was found to be 41%. More recently, in 2017, Schagdarsurengin *et al*. (Schagdarsurengin, Lammert *et al*. 2017), identified an additional mechanism for aberrant IGF-II expression. Aside from disrupted methylation at the ICR, it was shown that hypomethylation at DMR0 and decreased expression of IGF-II were associated with PCa and benign prostate hyperplasia. In 2018 (Kuffer, Gutting *et al*. 2018) a report focused on promoter methylation as a factor contributing to IGF-II transcription (Kuffer, Gutting *et al*. 2018). IGF-II mRNA and peptide levels were decreased in 80% of PCa tissue compared to non-neoplastic adjacent prostate and were independent of LOI status. IGF-II expression in both tumour and adjacent tissue depended on usage of the IGF-II promoters P3 and P4; decreased IGF-II expression in tumour tissue was strongly related to hypermethylation of these

two promoters. The cause of hyper-methylation in this cohort was attributed to cumulative DNA damage, due to aging.

This chapter focused on assessing imprinting status of IGF/H19 and levels of IGF-II peptide in prostate tissue, to establish whether correlations in expression of IGF-II/H19 and abundance of IGF-II were similar to those identified *in vitro*.

4.2 Hypothesis

Disrupted imprinting of IGF-II/H19 occurs in prostate tissue, and this is reflected by altered mRNA expression and IGF-II peptide levels.

4.3 Aims

- Assess and quantify IGF-II/H19 imprinting status.
- Investigate the effects of IGF-II/H19 imprinting upon IGF-II / H19 mRNA.
- Explore the effects of IGF-II/H19 imprinting upon IGF-II peptide levels and localisation.

4.3 Materials & Methods

4.3.1 Evaluation of methods, optimisation, and troubleshooting.

For both cohorts, FFPE prostate tissue was used as the source of RNA. Issues can arise with recovery of genetic material from FFPE tissue, due to degradation by the embedding process, humidity and/or temperature, or limited availability of sample. Such degradation leads to poor quality of RNA and/or low yield. Where RNA yields are low, usual quantification methods – such as PCR and qPCR (used in chapter 3) may not be sensitive enough to quantify such small amounts of genetic material. To overcome such issues, digital droplet PCR (ddPCR) was developed. ddPCR was first used in 1992 (Sykes, Neoh *et al*. 1992) as a method of quantifying low copy numbers of target genes. The underlying mechanism of ddPCR resembles traditional end-point PCR, with the exception that a droplet-generation oil is added to the reaction mix. This mixture is placed in a droplet generator, where the oil is mixed with the PCR reagents. Each oil droplet captures and contains all the components of a standard PCR reaction, with each droplet acting like a PCR micro-reactor (Quan, Sauzade *et al*. 2018). The resulting product is then placed in a reader which uses fluorescence to detect amplicons.

To optimize the detection of total IGF-II and H19 transcript expression with ddPCR, an annealing temperature gradient test was performed using total RNA derived from the PC3 PCa cell line.

At 55°C, annealing temperature for ddPCR reactions total IGF-II and H19 amplicon-containing droplets showed the best separation between positive and negative clusters. To assess relative expression, the ratio of IGF-II/H19 concentration to the internal/housekeeping control G2 / M phase-specific E3 ubiquitin-protein ligase (G2E3) concentration was used.

Optimization of the IHC staining with the IGF-II antibody was conducted in-house by a third party, prior to use in my study for FFPE sample.

4.3.2 Prostate tissue.

Name of study	Tissue format	Origin
Study 2536: Assessment of metabolic biomarkers in archival formalin fixed paraffin embedded (FFPE) sections from prostate tissue. REC ref: 15/WM/0449. **Herein referred to as "Cohort 1".**	FFPE	Radical prostatectomy
Prostate Cancer Evidence of Exercise and Nutrition Trial: nutritional and physical activity interventions for men with localised PCa – feasibility study. REC ref: 14/SW/0056. **Herein referred to as "PrEvENT cohort".**	FFPE	Radical prostatectomy

Prostate tissue from the above clinical cohorts was used to study IGF-II imprinting status, IGF-II / H19 mRNA quantification and IGF-II peptide levels and localisation. Informed consent was obtained from all subjects involved in the studies.

4.3.3 Isolation of RNA

RNA was isolated using the FFPE extraction protocol, as described in 2.3.

4.3.4 Preparation of cDNA

RNA was converted to cDNA as described in 2.2.

4.3.5 Pyrosequencing

Pyrosequencing for imprinted allele expression (PIE) was conducted as described in 2.9.

4.3.6 Digital droplet PCR (ddPCR)

ddPCR was conducted as outlined in 2.8.

4.3.7 Immunohistochemistry

Slides were prepared and stained for IGF-II as described in 2.10. They were subsequently scored using an adapted version of the Allred system, as described in 2.10.3

4.3.8 Use of cBioPortal for Cancer Genomics.

The cBio Cancer Genomics Portal (Cerami, Gao *et al*. 2012) and (Gao, Aksoy *et al*. 2013) was used to explore co-expression of IGF-II and H19 mRNA; one representative Cancer Genome Atlas cohort was selected from the list of breast and PCa studies. Each cohort was assessed for availability of IGF-II and H19 mRNA co-expression data, which had been gathered using the Illumina HiSeq sequencing system.

4.3.9 Statistical analysis

A two-tailed *t* test was used for *in vivo* data, to compare the differences between two groups. For correlation analyses, the Pearson correlation co-efficient was calculated, with results being expressed as an R value. *P* values less than 0.05 were deemed statistically significant, with the following denotations: * $p = 0.05$, ** $p = 0.01$ and *** $p \leq .001$. Analyses were conducted using the IBM SPSS Version 24 Statistics software package.

4.3 Results

4.3.1.1 Genotyping of cohort 1 using pyrosequencing.

Genotyping of Cohort 1 was conducted. Tissue was typed as either 'MOI' (maintained imprinting) or 'LOI' (loss of imprinting). Of 13 paired patient samples, 1 presented with no change of MOI status (in the benign sample compared to its malignant counterpart), 2 presented with a change in status from MOI to LOI, 7 presented with a change in status from LOI to MOI and 3 presented with no change of LOI status (figure 4.3.1.1).

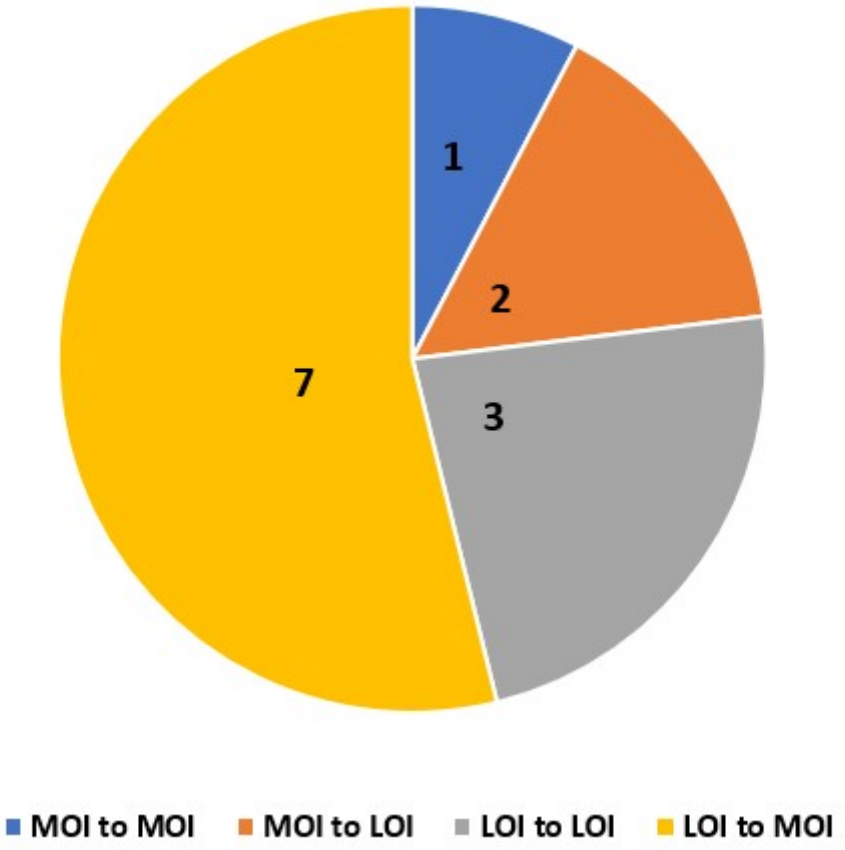

Figure 4.3.3.1: Genotyping of cohort 1 using pyrosequencing. Of 13 patients, 1 presented with no change of MOI status (in the benign sample compared to its malignant counterpart), 2 presented with a change in status from MOI to LOI, 7 presented with a change in status from LOI to MOI and 3 presented with no change of LOI status (n=13).

4.3.1.2 IGF-II imprinting percentages of Cohort 1

Of 13 patient paired samples, the group containing 3 paired samples - with LOI in both benign and malignant tissues - showed no significant changes in imprinting percentages; the group containing 7 paired samples - with MOI in malignant compared with LOI in the benign tissue - showed a significant increase ($p \leq .001$) in imprinting percentage (figure 4.3.1.2).

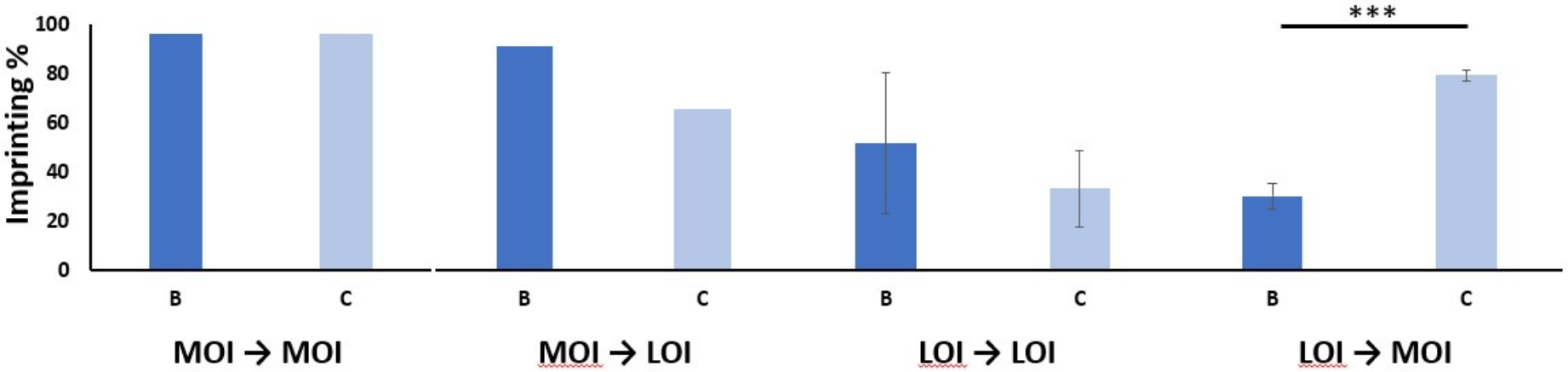

Figure 4.3.1.2: IGF-II imprinting percentages of Cohort 1. The groups containing 1 paired sample set (MOI to MOI) and 2 paired sample sets (MOI to LOI) were not subject to statistical analysis due to group size. The group containing 3 paired samples, with LOI in both benign and malignant tissues, showed no significant changes in imprinting percentages. The group containing 7 paired samples, with MOI in malignant compared with LOI in the benign tissue showed a significant increase ($p \leq .001$) in imprinting percentage (n=13).

4.3.1.3 Imprinting percentage related to IGF-II mRNA expression in Cohort 1.

In benign and malignant tissue there were no significant correlations between imprinting percentage and IGF-II mRNA expression (figure A and B).

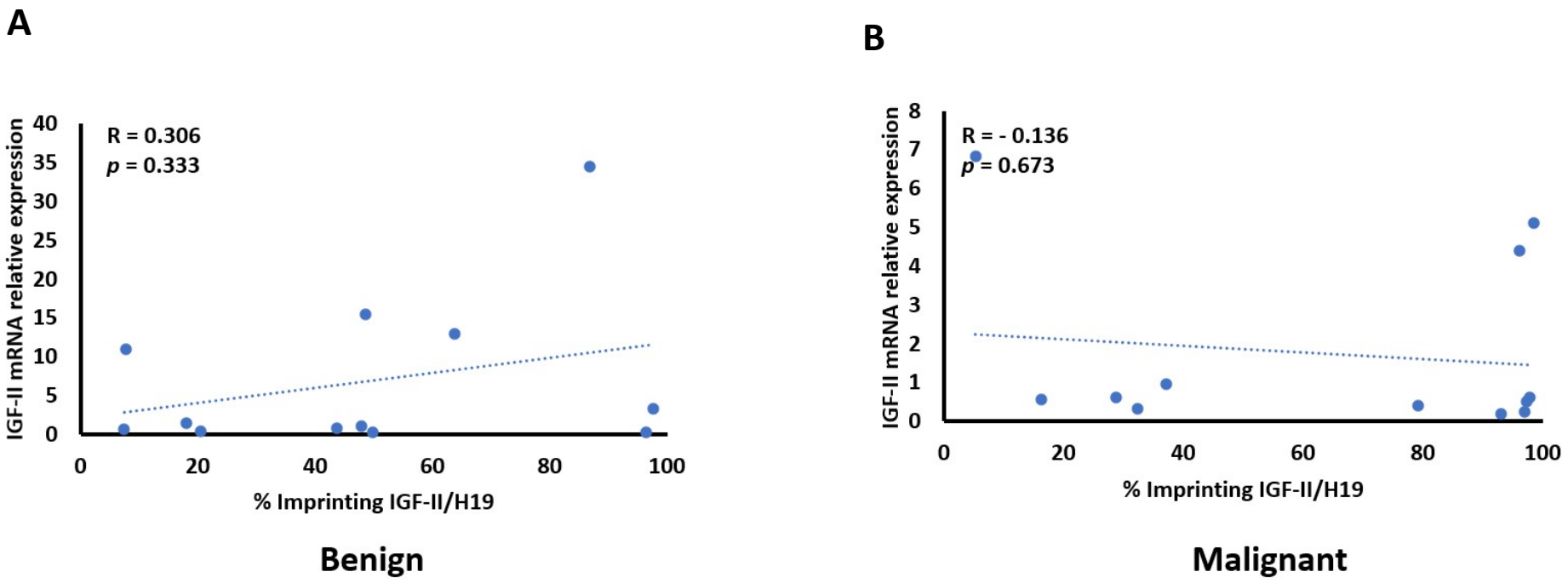

Figure 4.3.1.3: IGF-II mRNA expression related to imprinting percentage in Cohort 1. In benign (A) and malignant (B) tissue there were no significant correlations between imprinting percentage and IGF-II mRNA expression (n=13).

4.3.1.4 IGF-II peptide levels of Cohort 1.

Figure A shows IHC scores of 13 paired samples from cohort 1. There was no significant difference in IGF-II peptide scores between benign and malignant prostate tissue, overall. The groups containing 1 paired sample set (MOI to MOI) and 2 paired sample sets (MOI to LOI) were not subject to statistical analysis due to group size.

There was no significant difference in the sample group that showed no change in LOI status. In the group showing a change from LOI in benign tissue to MOI in malignant tissue, IGF-II peptide was significantly higher (p = 0.017) in the malignant group. The cytoplasmic staining patterns are shown by micrographs depicted in figure B. (n=13)

A

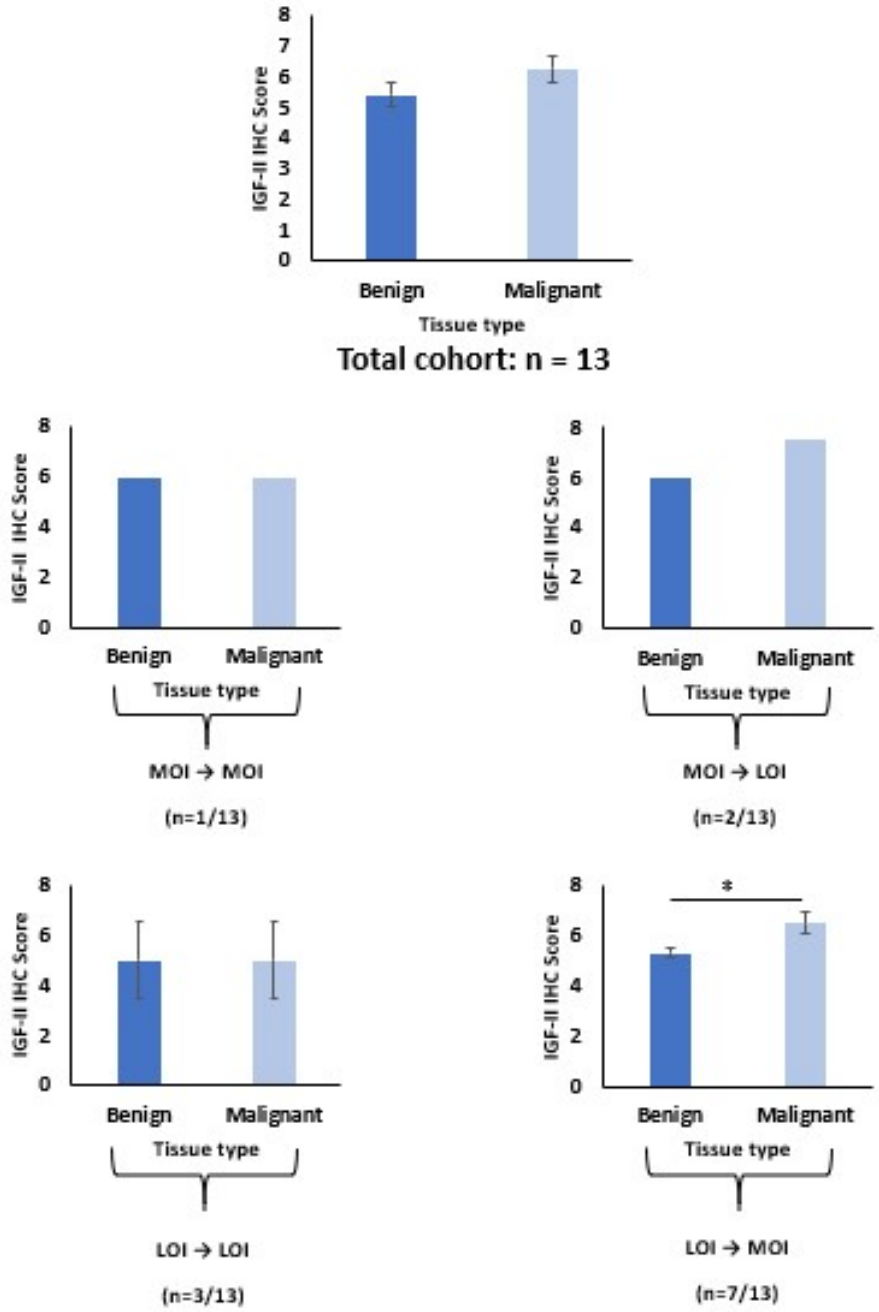

Figure 4.3.1.4.A: **IGF-II peptide levels of Cohort 1.** There was no significant difference in IGF-II peptide scores between benign and malignant prostate tissue, overall. The groups containing 1 paired sample set (MOI to MOI) and 2 paired sample sets (MOI to LOI) were not subject to statistical analysis due to sample numbers. There was no significant difference in the sample group that showed no change in LOI status. In the group showing a change from LOI in benign tissue to MOI in malignant tissue, IGF-II peptide was significantly higher (p = 0.017) in the malignant group (n=13).

B

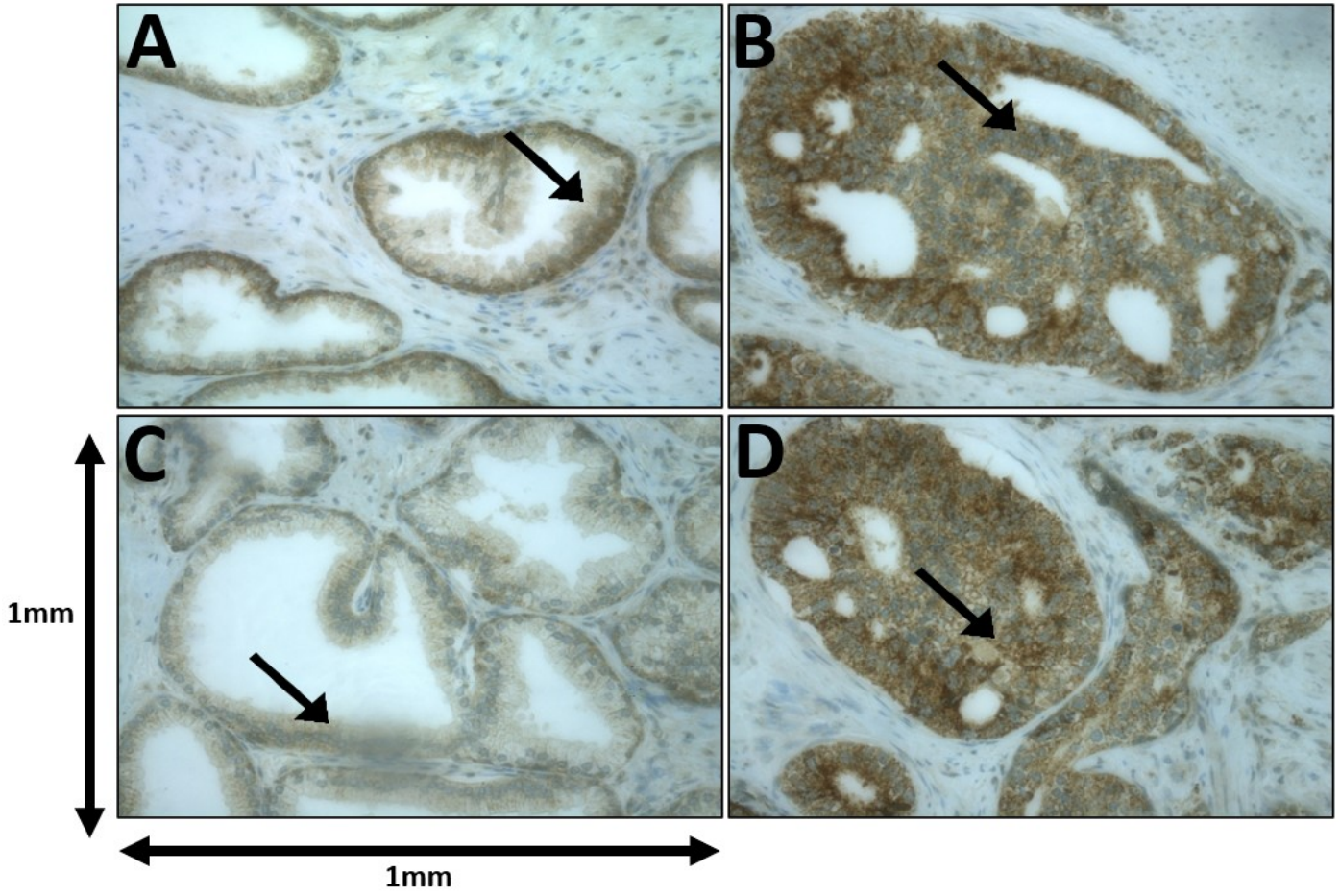

Figure 4.3.1.4.B: Patterns of IGF-II cytoplasmic IHC staining in paired tissue samples from 2 patients in Cohort 1. Benign tissue is shown in image A and C; malignant tissue is shown in image B and D. Arrows indicate strong cytoplasmic staining, observed in both benign and malignant tissues (A & B respectively), and weak staining (C & D, respectively). Scale is 1x1 mm, at 40x magnification.

4.3.1.5 IGF-II peptide related to imprinting percentage in Cohort 1.

The relationship between peptide and imprinting percentage is depicted by figure 4.3.1.4. There was a non-significant, positive (p = 0.889; R = 0.043) correlation between IGF-II peptide expression and imprinting percentage in benign tissue (figure A). In malignant tissue (figure B), there was a non-significant positive correlation (p = 0.402; R = 0.254) between IGF-II peptide expression and imprinting percentage (n = 13).

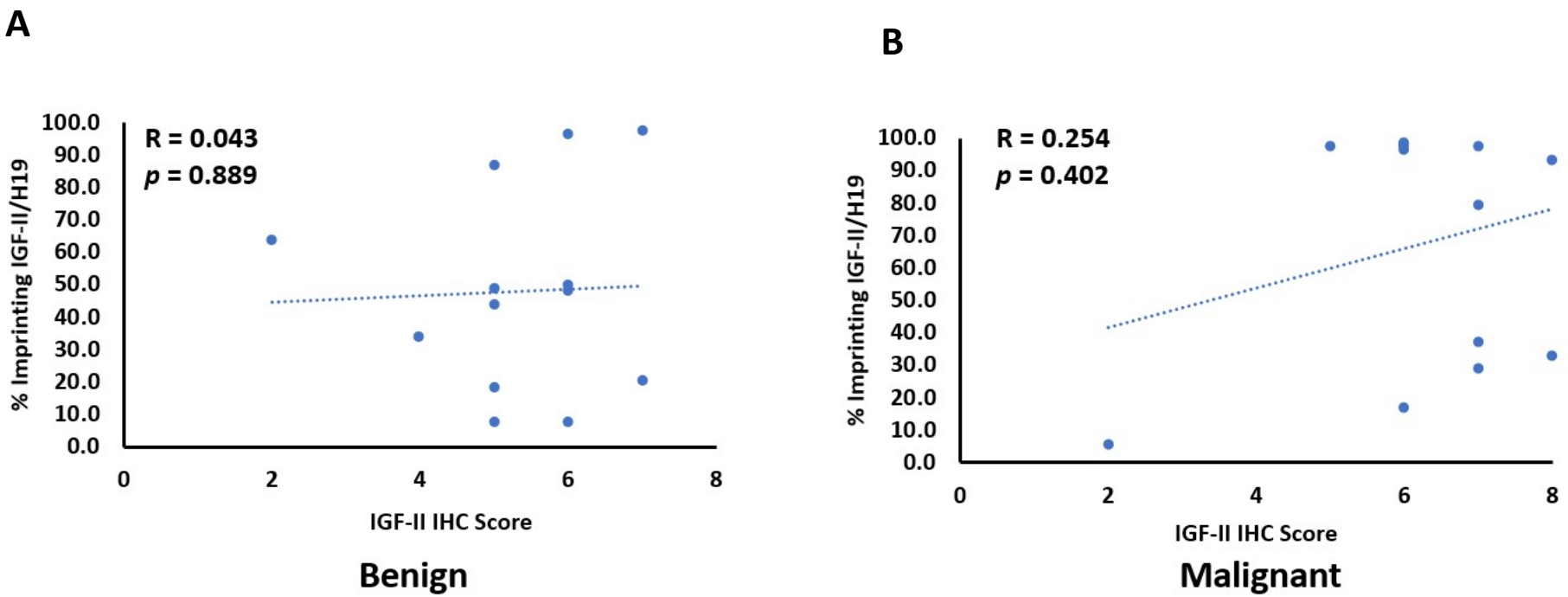

Figure 4.3.1.5: IGF-II peptide expression related to imprinting percentage in Cohort 1. There was a non-significant, positive (p = 0.889; R = 0.043) correlation between IGF-II peptide expression and imprinting percentage in benign (**A**) tissue. In malignant tissue (**B**), there was a non-significant positive correlation (p = 0.402; R = 0.254) between IGF-II peptide expression and imprinting percentage (n = 13).

4.3.1.6 IGF-II peptide related to IGF-II mRNA, in Cohort 1.

In benign tissue there was a non-significant (p = 0.16) negative correlation (R = - 0.427) between IGF-II peptide and mRNA expression (figure A). In malignant tissue there was a significant (p = 0.007) negative correlation (R = - 0.73) between IGF-II peptide and mRNA expression (figure B). (n=13)

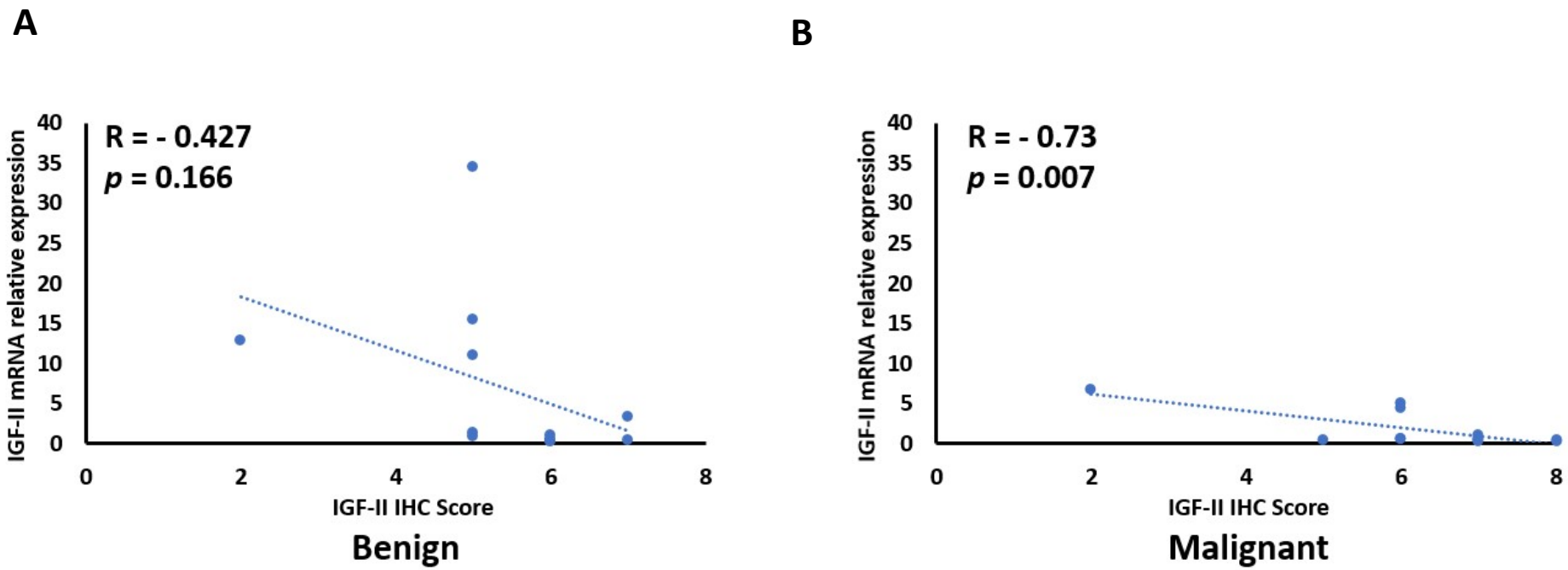

Figure 4.3.1.6: IGF-II peptide expression related to IGF-II mRNA in Cohort 1. In benign tissue there was a non-significant (p = 0.166) negative correlation (R = - 0.427) between IGF-II peptide and mRNA expression (**A**). In malignant tissue there was a significant (p = 0.007) negative correlation (R = - 0.73) between IGF-II peptide and mRNA expression (**B**) (n=13).

4.3.2.1 Genotyping of PrEvENT cohort using pyrosequencing.

Figure 4.3.2.1 depicts the total cohort with proportional representation of each tissue pairing; out of 84 patients 64 presented with no change of MOI status (in the benign sample compared to its cancer counterpart), 6 presented with a change in status from MOI to LOI, 7 presented with a change in status from LOI to MOI and 7 presented with no change of LOI status (n=84).

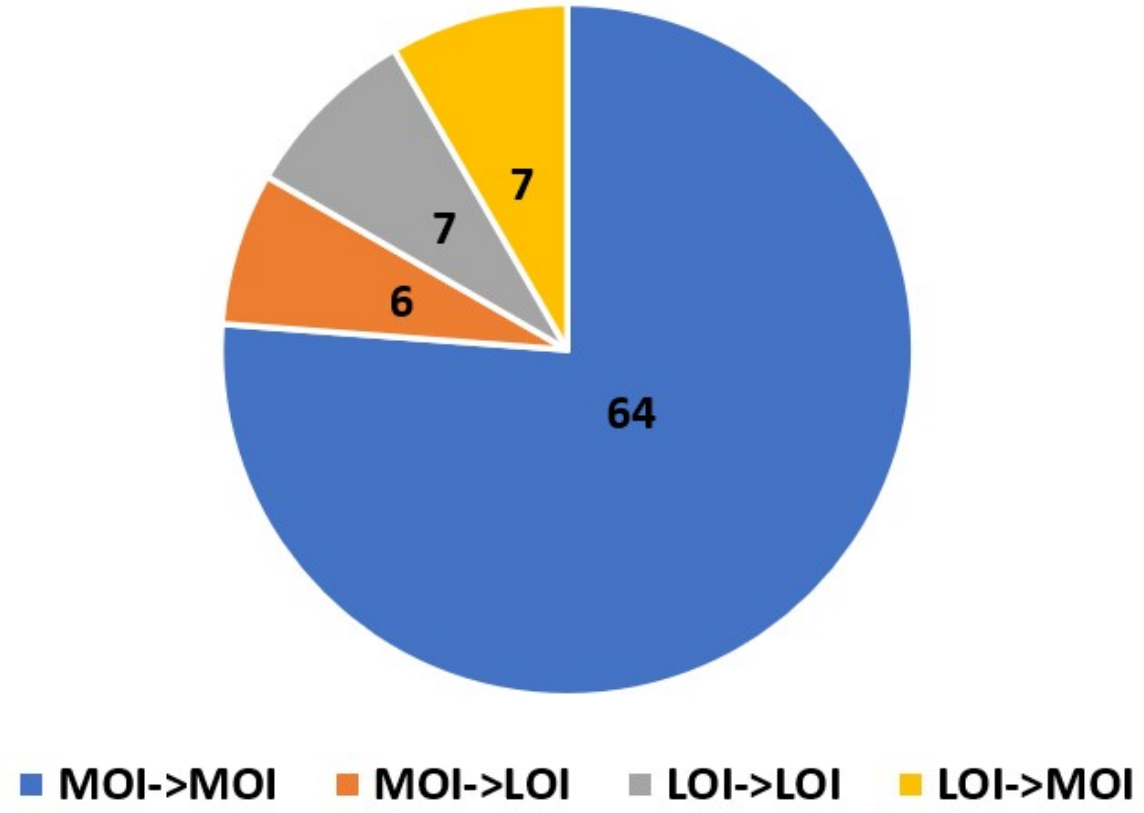

Figure 4.3.2.1: Genotyping of PrEvENT cohort samples using pyrosequencing. 84 patients from the PrEvENT cohort had representative paired samples of benign and malignant tissue; out of 84 patients 64 presented with no change of MOI status (in the benign sample compared to its cancer counterpart), 6 presented with a change in status from MOI to LOI, 7 presented with a change in status from LOI to MOI and 7 presented with no change of LOI status (n=84).

4.3.2.2 IGF-II imprinting percentages of PrEvENT cohort.

Figure 4.3.2.2 shows the percentage imprinting within each genotype grouping. The group containing the 6 paired samples, with LOI in cancer compared with MOI in the benign tissue, showed a significant decrease ($p \leq .001$) in imprinting percentage. The group containing the 7 paired samples, with MOI in cancer compared with LOI in the benign tissue showed a significant increase ($p \leq .001$) in imprinting percentage. (n=84)

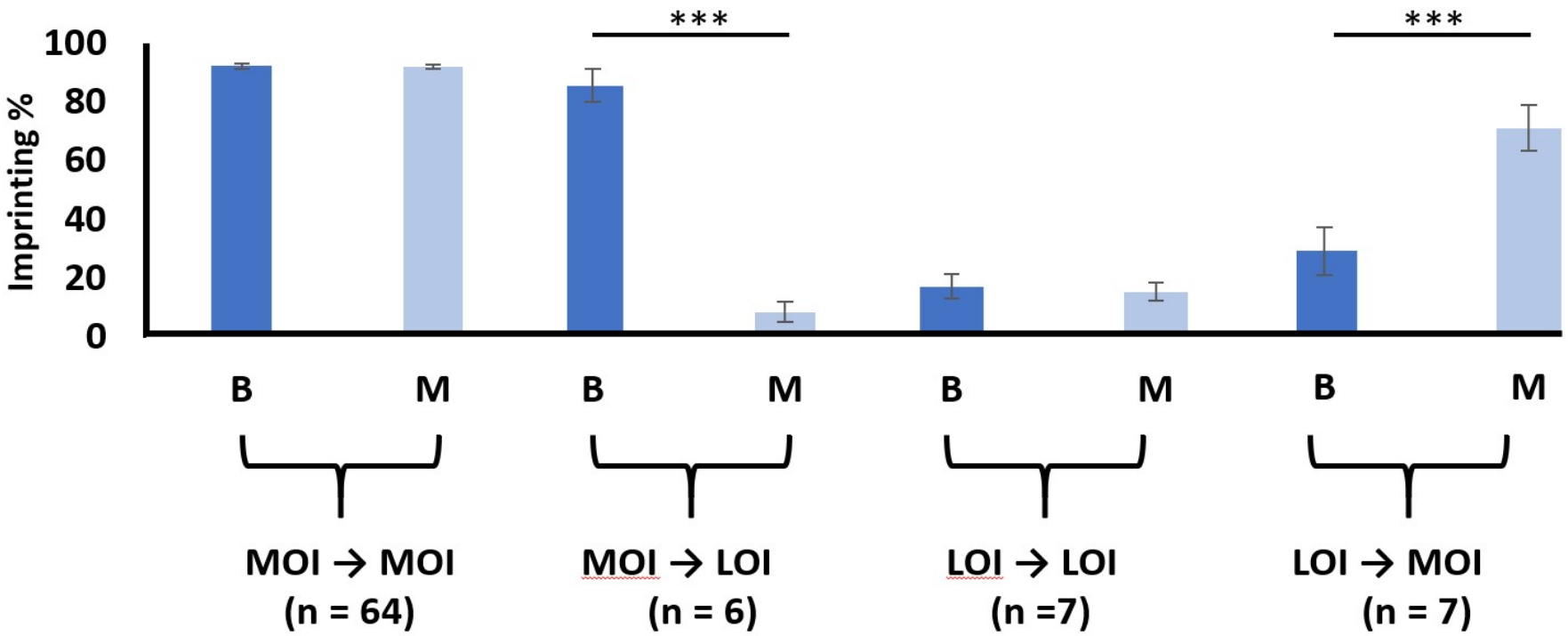

Figure 4.3.2.2: Imprinting percentages of PrEvENT cohort, using pyrosequencing. The group containing the 6 paired samples, with LOI in cancer compared with MOI in the benign tissue, showed a significant decrease ($p \leq .001$) in imprinting percentage. The group containing the 7 paired samples, with MOI in cancer compared with LOI in the benign tissue showed a significant increase ($p \leq .001$) in imprinting percentage. (n=84)

4.3.2.3 Imprinting percentage related to IGF-II mRNA expression in the PrEvENT cohort.

In benign tissue there was a significant (p = 0.002) positive correlation (R = 0.326) between imprinting percentage and IGF-II mRNA expression (figure A). In malignant tissue, there was a significant (p = 0.035) positive correlation (R = 0.224) between imprinting percentage and IGF-II mRNA expression (figure B). (n=89)

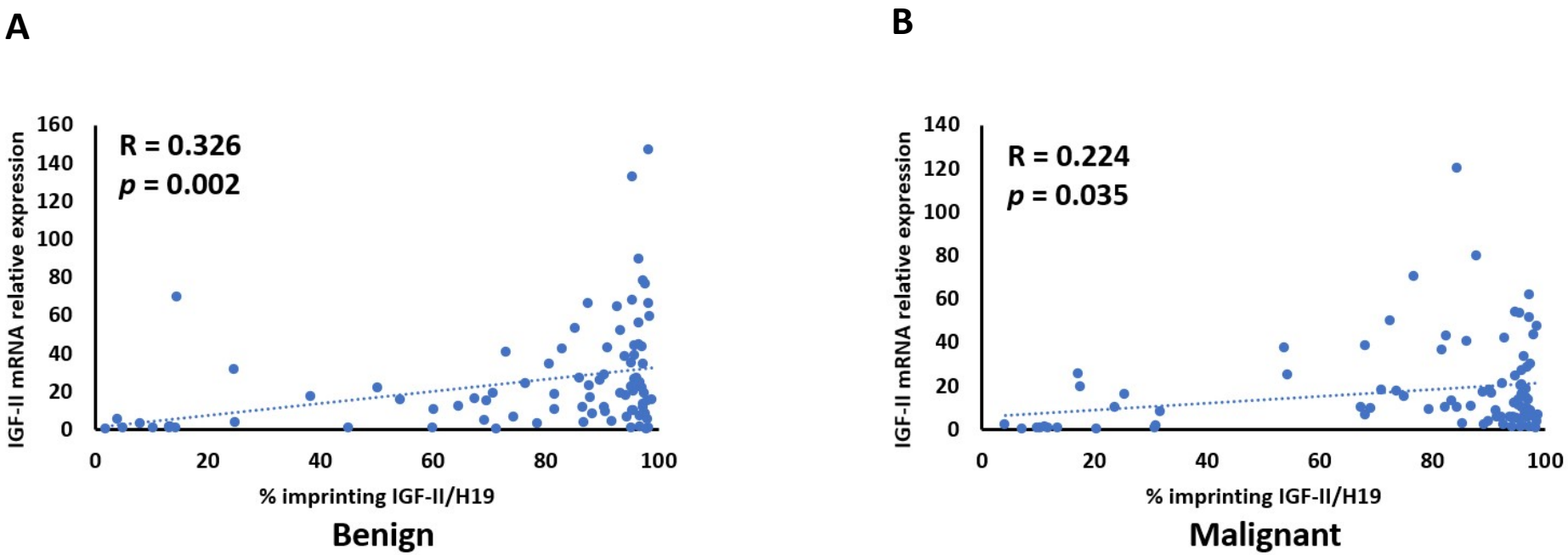

Figure 4.3.2.3: Imprinting percentage related to IGF-II mRNA expression in the PrEvENT cohort. In benign tissue there was a significant (p = 0.002) positive correlation (R = 0.326) between imprinting percentage and IGF-II mRNA expression (**A**). In malignant tissue, there was a significant (p = 0.035) positive correlation between imprinting percentage and IGF-II mRNA expression (**B**). (n=89)

4.3.2.4 Imprinting percentage related to H19 mRNA expression in the PrEvENT cohort.

In benign tissue there was a non-significant (p = 0.852) negative correlation (R = - 0.021) between imprinting percentage and H19 mRNA expression (figure A). In malignant tissue, there was a significant (p = 0.044) positive (R = 0.214) correlation between imprinting percentage and IGF-II mRNA expression (figure B). (n=89)

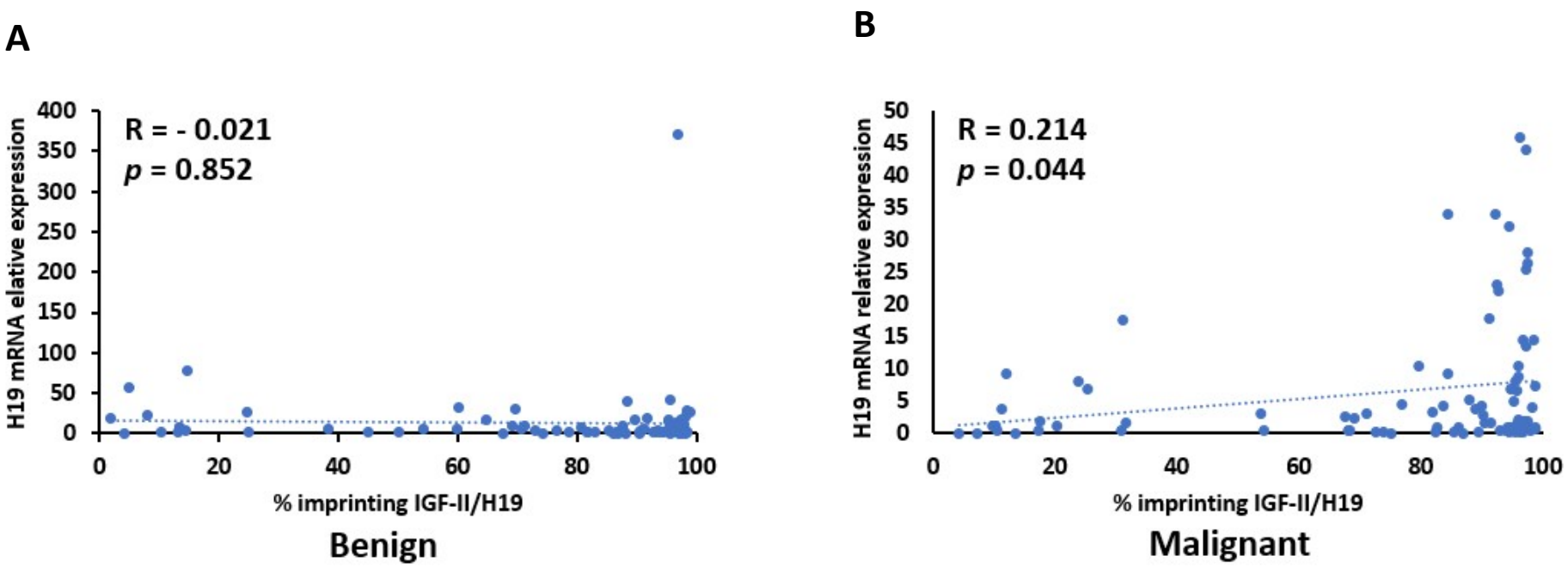

Figure 4.3.2.4: Imprinting percentage related to H19 mRNA expression in the PrEvENT cohort. In benign tissue there was a non-significant (p = 0.852) negative correlation (R = - 0.021) between imprinting percentage and H19 mRNA expression (**A**). In malignant tissue, there was a significant (p = 0.044) positive (R = 0.214) correlation between imprinting percentage and IGF-II mRNA expression (**B**) (n=89).

4.3.2.5 Co-expression of IGF-II and H19 mRNA in the PrEvENT cohort.

There was no difference in absolute expression of IGF-II or H19 between benign and malignant tissue. However, we did observe a positive correlation between IGF-II and H19 expression; with a significant positive correlation (Pearson: R = 0.28, $p = 0.01$) in the benign tissue (figure A) and a stronger positive correlation in malignant prostate tissue (R = 0.67, $p \leq .001$) (figure B) (n=97).

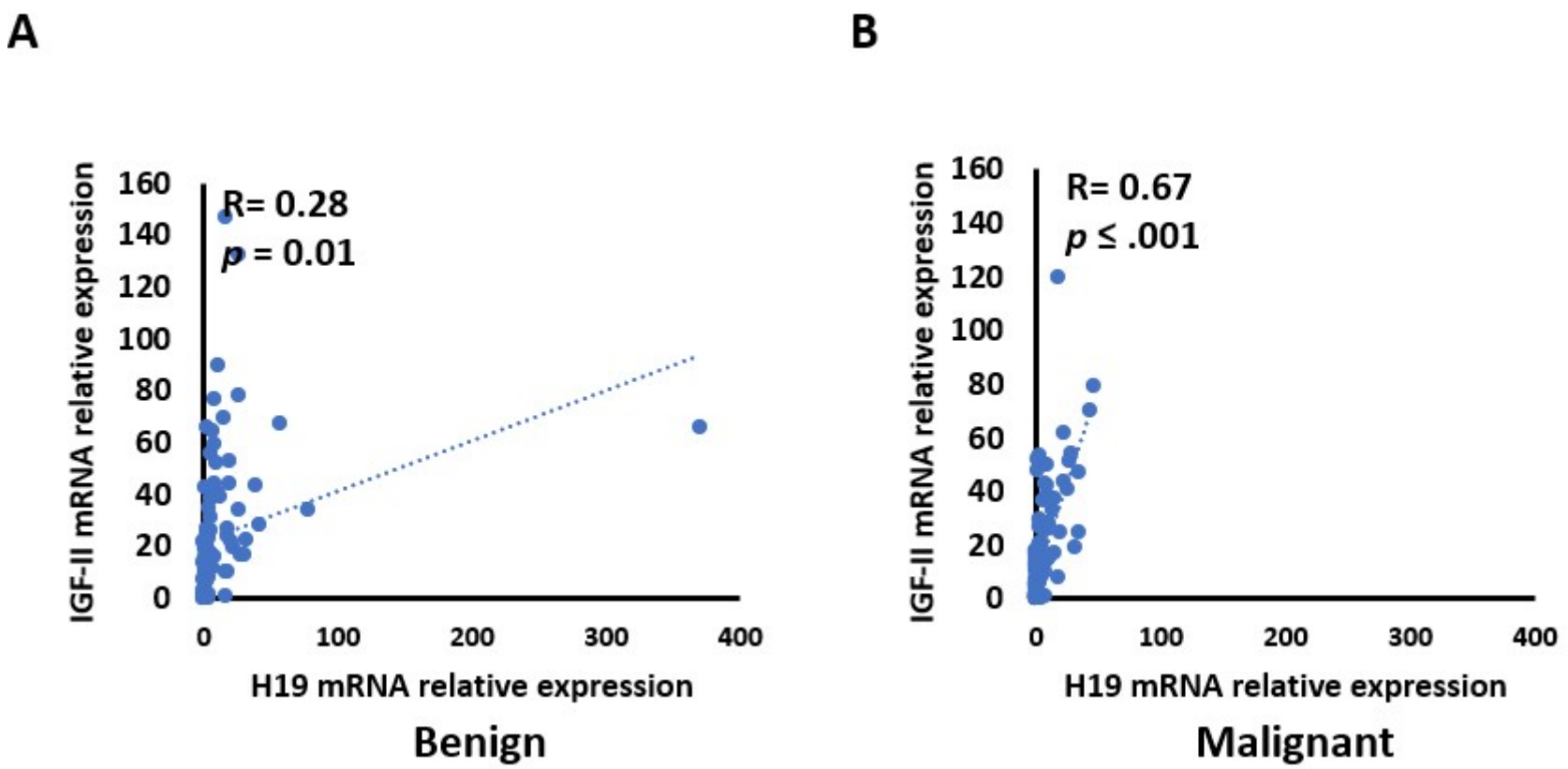

Figure 4.3.2.5 Co-expression of IGF-II and H19 mRNA is positively correlated in the PrEveNT cohort. There was no difference in absolute expression of IGF-II or H19 between benign and malignant tissue. However, there was a positive correlation between IGF-II and H19 expression; with a significant positive correlation (Pearson: R = 0.28, $p = 0.01$) in the benign tissue (**A**) and a stronger positive correlation in malignant prostate tissue (R = 0.67, $p \leq .001$) (**B**) (n=97).

4.3.2.6 Metabric data from The Cancer Genome Atlas (TCGA).

After quantifying IGF-II and H19 mRNA expression in the PrEvENT cohort, the cBioPortal for Cancer Genomics website was accessed to assess whether co-expression of IGF-II and H19 mRNA existed, in a larger PCa cohort, as well as another hormone-responsive cancer type: breast.

In the prostate cohort - provided by the Cancer Genome Atlas (TCGA) – a strong positive correlation (Pearson: 0.6) was seen in the co-expression of H19 and IGF-II ($p \leq .001$) with 489 patients (figure A). Similarly, in the TCGA breast cancer cohort (figure B), a strong positive correlation (Pearson: 0.64) was also seen in the co-expression of H19 and IGF-II ($p \leq .001$) with 994 patients.

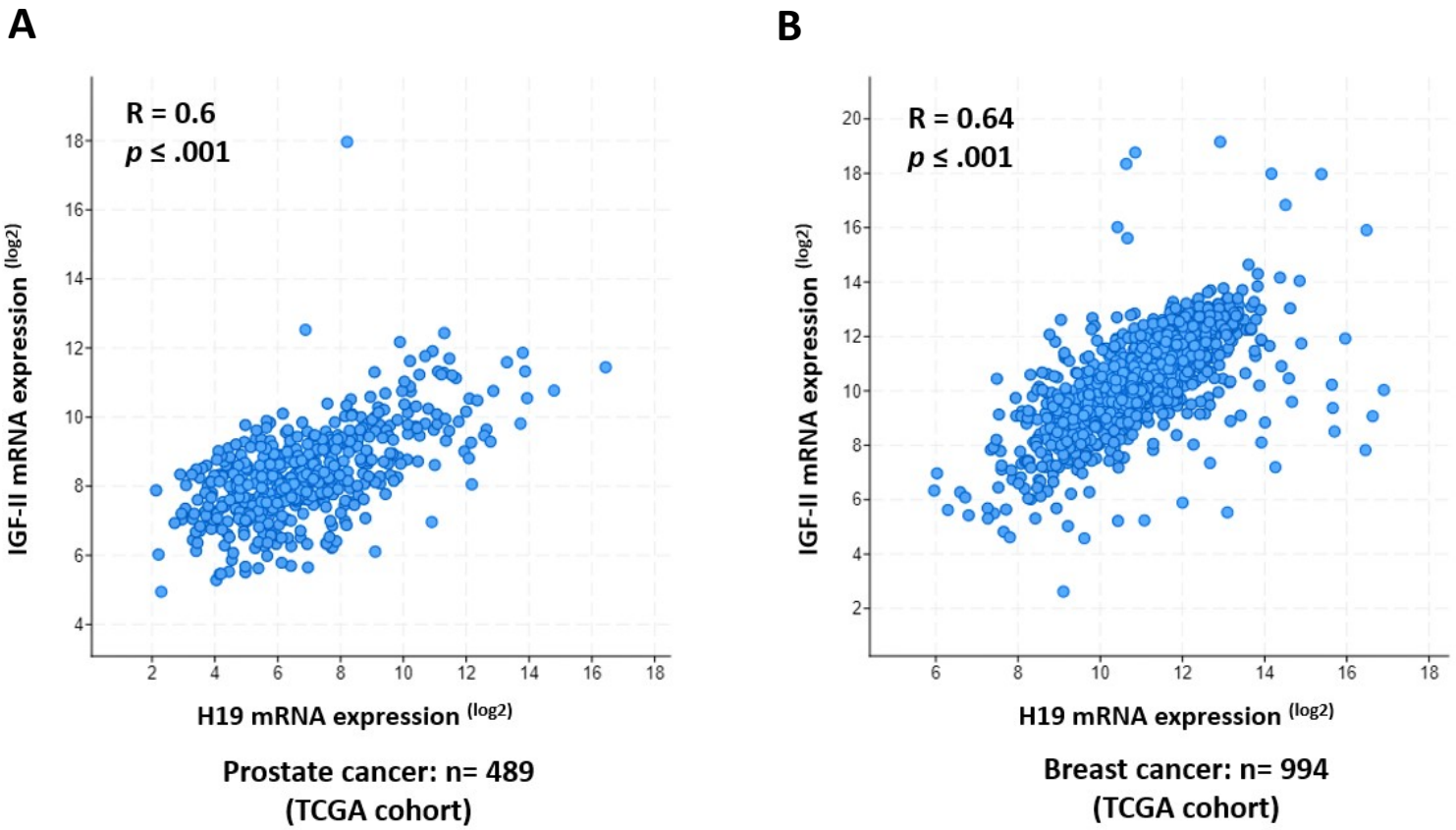

Figure 4.3.2.6: Metabric data from The Cancer Genome Atlas (TCGA). In the prostate cohort (**A**) - provided by the Cancer Genome Atlas (TCGA) – a strong positive correlation (Pearson: 0.6) was seen in the co-expression of H19 and IGF-II ($p \leq .001$) with 489 patients. Similarly, in the TCGA breast cancer cohort (**B**), a strong positive correlation (Pearson: 0.64) was also seen in the co-expression of H19 and IGF-II ($p \leq .001$) with 994 patients.

4.3.2.7 IGF-II peptide localisation in PrEvENT cohort samples.

IHC scores of 73 paired samples from the PrEvENT cohort were divided into benign and malignant categories. The 2 groups were then compared. Overall, there was no significant difference in staining scores between malignant and benign tissue (figure A). The staining patterns are shown by micrographs depicted in figure B**.** (n=73)

A

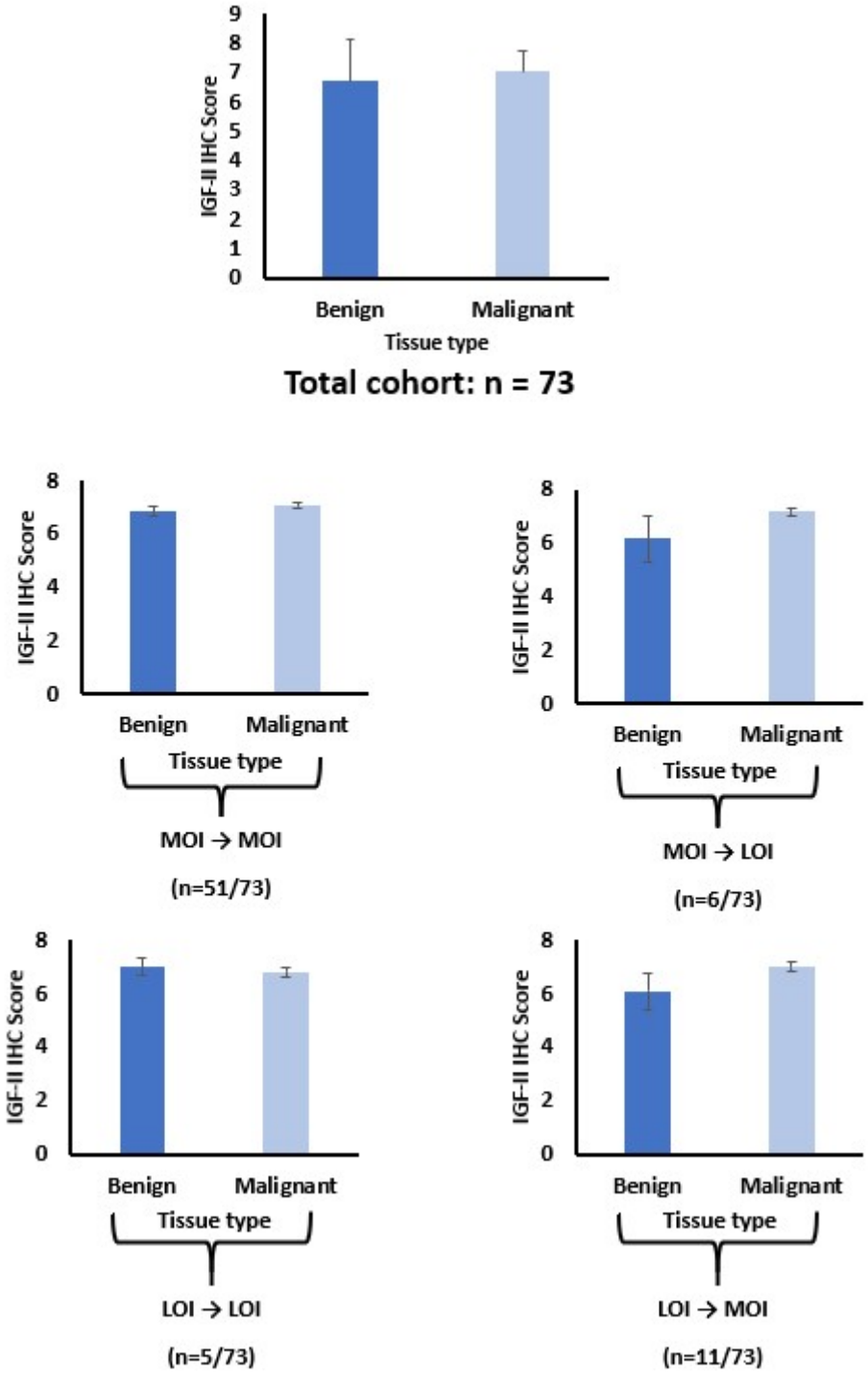

Figure 4.3.2.7.A: **IGF-II peptide levels in PrEvENT cohort samples.**

There were no significant differences in IGF-II peptide scores between benign and malignant prostate tissue overall, or in any of the genotyped sub-groups. (n=73)

B

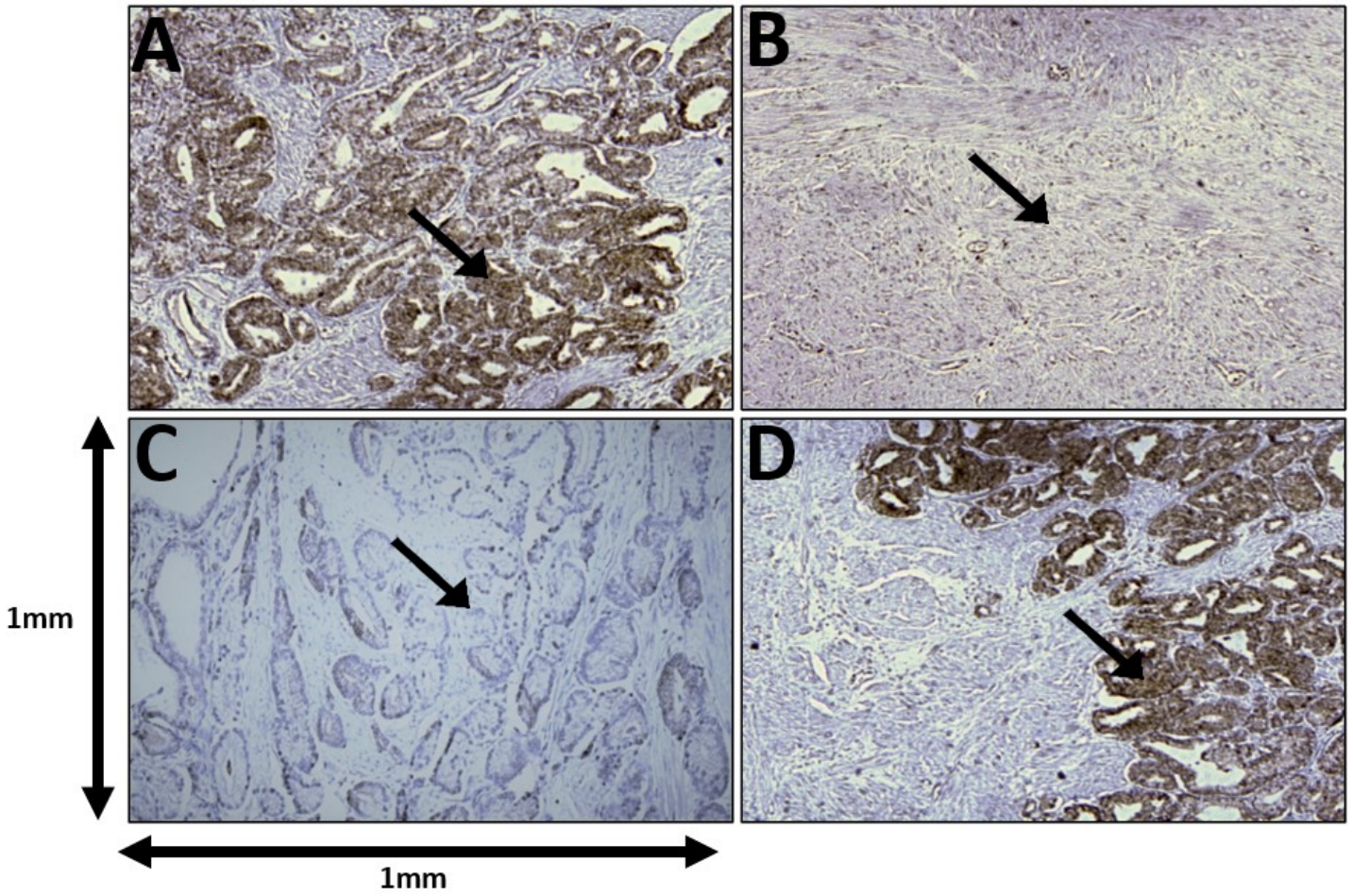

Figure 4.3.2.7.B: Patterns of IGF-II cytoplasmic IHC staining in paired tissue samples from 2 patients from the PrEvENT cohort. Arrows indicate strong IGF-II cytoplasmic staining in both benign (A) and malignant (D) tissue, and weak staining in benign (C) and malignant tissue (B). Scale is 1x1 mm, at 20x magnification.

4.3.2.8 IGF-II peptide related to imprinting percentage in the PrEvENT cohort.

The relationship between peptide and imprinting percentage is depicted by figure 4.3.2.6. There was a non-significant, positive (p = 0.152; R = 0.180) correlation between IGF-II peptide expression and imprinting percentage in benign (figure A) tissue. In malignant tissue (figure B), there was a non-significant positive correlation (p = 0.805; R = 0.031) between IGF-II peptide expression and imprinting percentage. (n = 65)

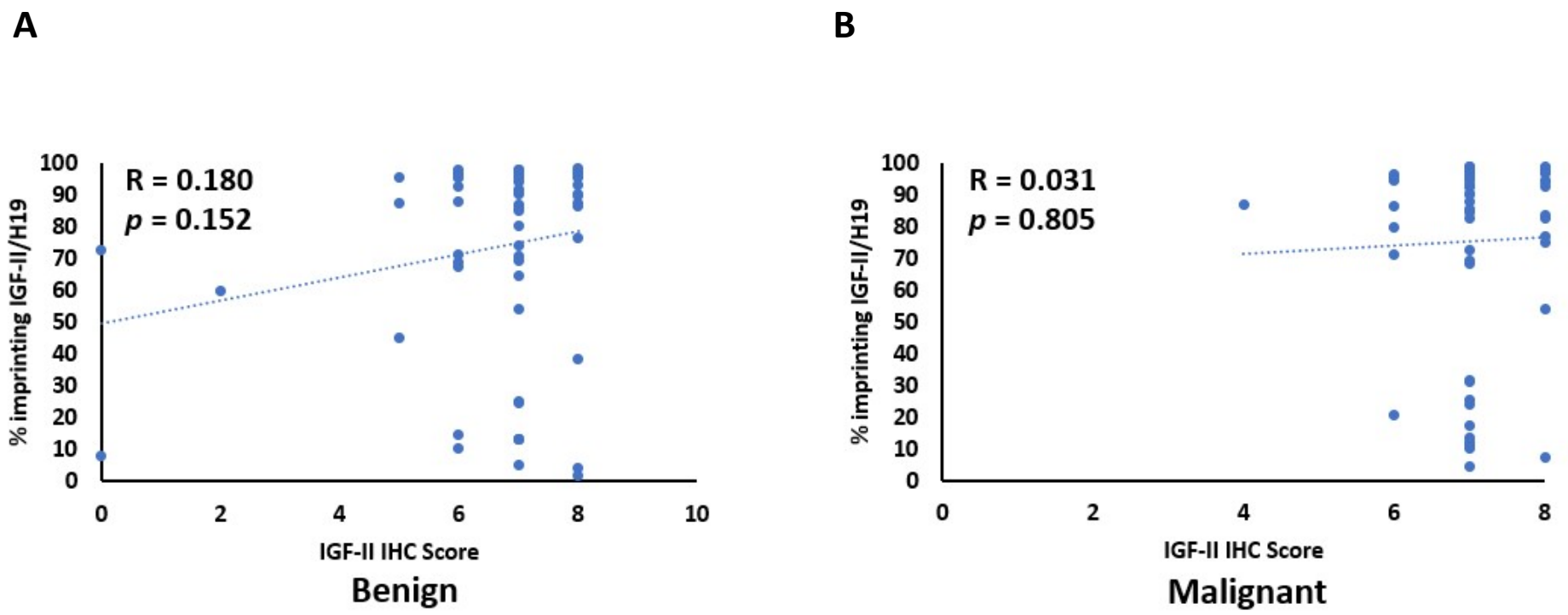

Figure 4.3.2.8: IGF-II peptide levels related to imprinting percentage in the PrEvENT cohort. There was a non-significant, positive (p = 0.152; R = 0.180) correlation between IGF-II peptide expression and imprinting percentage in benign (**A**) tissue. In malignant tissue (**B**), there was a non-significant positive correlation (p = 0.805; R = 0.031) between IGF-II peptide expression and imprinting percentage. (n = 65)

4.3.2.9 IGF-II peptide related to IGF-II mRNA, in the PrEvENT cohort.

In benign tissue there was a non-significant (p = 0.867) negative correlation (R = - 0.021) between IGF-II peptide and mRNA expression (figure A). In malignant tissue there was a non-significant (p = 0.628) positive correlation (R = 0.058) between IGF-II peptide and mRNA expression (figure B). (n=73)

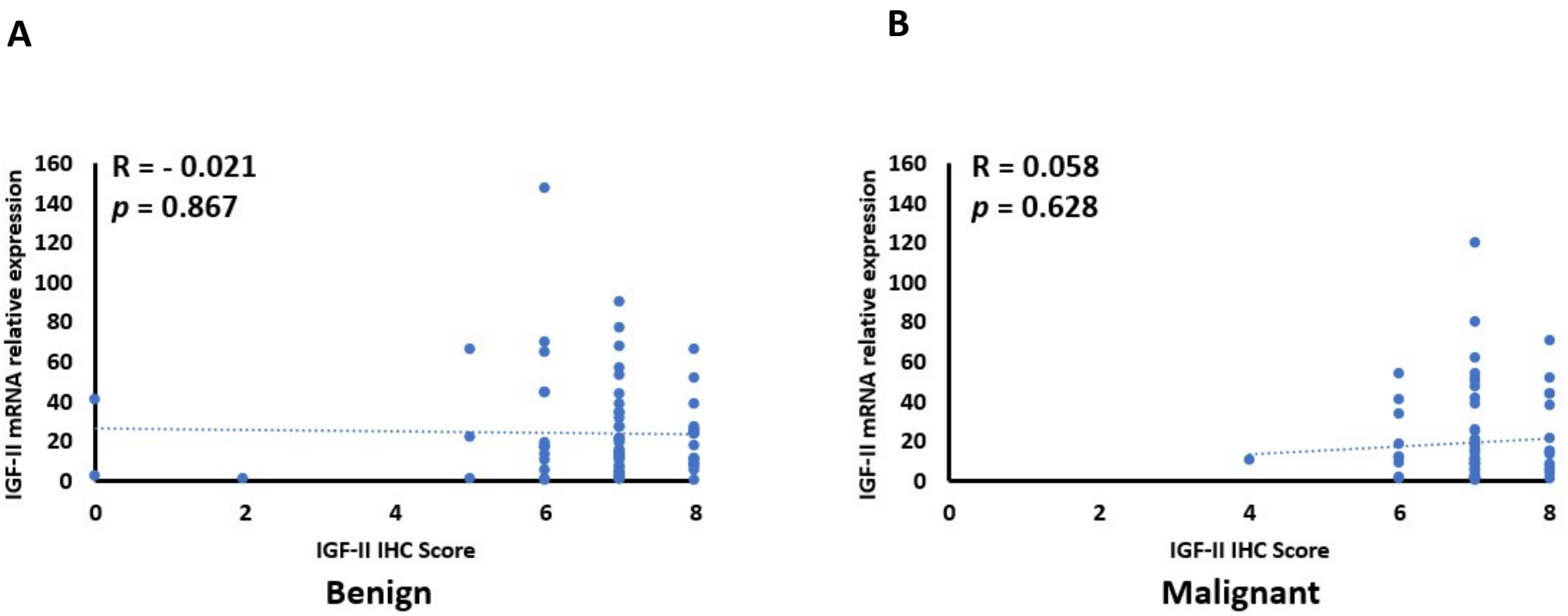

Figure 4.3.2.9: IGF-II peptide levels related to IGF-II mRNA, in the PrEvENT cohort. In benign tissue there was a non-significant (p = 0.867) negative correlation (R = - 0.021) between IGF-II peptide and mRNA expression (**A**). In malignant tissue there was a non-significant (p = 0.628) positive correlation (R = 0.058) between IGF-II peptide and mRNA expression (**B**). (n=73)

4.4 Discussion

This chapter has shown data describing the effects of IGF-II/H19 imprinting status and how this impacts upon IGF-II & H19 mRNA, and the abundance and localisation of IGF-II peptide *in vivo*, using prostate tissue from two clinical cohorts: Cohort 1 and the PrEvENT cohort.

In Cohort 1, which was composed of 12 paired benign and malignant specimens, approximately 60% of the paired benign and malignant specimens – 7 out of 12 - showed a change of imprinting status from LOI to MOI. This was marked by a significant increase in imprinting percentage, in the malignant tissue compared with the benign. The same sub-group from Cohort 1 also exhibited a significant difference in peptide expression, whereby the malignant tissue expressed a higher amount of IGF-II compared to the benign counterparts, despite retaining imprinting status. Comparing IGF-II peptide with its pre-cursor mRNA in the benign tissue from Cohort 1 yielded no significant findings. In the PrEvENT cohort, most matched benign and malignant specimens showed no change in imprinting status, with MOI being most prevalent in both tissue types. Conversely, in malignant tissue there was a strong negative correlation between the two; peptide increased as mRNA decreased.

Imprinting results from Cohort 1 correlated with those published by Bhusari *et al*. (Bhusari, Yang *et al*. 2011) 10 years ago. In that study it was shown that in 18 prostate tissue samples, taken from both the tumour, and 2- and 10mm away from tumour foci, LOI was found to occur at all three sites. The IGF-II/H19 LOI found in benign tissues, both adjacent to and distant from the tumour, are demonstrative of an epigenetic field defect. Conversely, the PrEvENT data disagreed with Bhusari *et al*.'s findings; that LOI is more frequent in prostates associated with cancer (Bhusari, Yang *et al*. 2011). It may be suggested, therefore, that imprinting data may vary with to cohort size.

The epigenetic field defect is known to be caused by methylation at specific CpG sites within genes and has been documented in other cancer types; a study conducted in 2005 (Dammann, Strunnikova *et al*. 2005) identified the presence of hypermethylated CpG sites within the gene promoters of tissue inhibitor of metalloproteinases 4 (TIMP4) and sex determining region Y-box 18 (SOX18), derived from histologically normal lung tissue taken from patients with lung cancer. Hypermethylation had led to inactivation of TIMP4 and SOX18 – both of which play crucial roles in tumour suppression and metastasis (Higashijima and Kanki 2020; Raeeszadeh-Sarmazdeh, Do *et al*. 2020). Occurrence of the epigenetic field defect has also been recorded in gastric (Takamaru, Yamamoto *et al*. 2012) and colorectal (Chen, Xu *et al*. 2018) cancer, where hypermethylation of the cell growth-inhibitory Ras-specific guanin nucleotide-release factor 1 (RASGRF1) gene was found in both benign and malignant tissue from afflicted patients.

Loss of imprinting in IGF-II / is also found in normal tissue and not just malignant, where frequently imprinting status does not relate to expression levels. For example, 22% of normal infants have IGF-II LOI with no changes in expression levels in the majority. It may be suggested that imprinting is only one factor in regulating expression and may not be that important in human tissues; IGF-II and H19 share a common enhancer 30kb downstream from H19 (Verona and Bartolomei 2004) that could be a more important determinant of expression of both, rather than imprinting controls.

Chapter three's *in vitro* findings demonstrated that imprinting percentage did not affect secreted IGF-II peptide; this was also true of both *in vivo* cohorts. These findings did not change when comparing benign with malignant tissue in both cohorts. These findings did not concur with published literature where aberrant imprinting has been shown to increase IGF-II peptide (Cui 2007; Belharazem, Kirchner *et al*. 2012). It may be hypothesised that these *in vivo* findings, of both cohorts, were limited by size; a larger cohort may reduce standard error, resulting in a significant result, thus concurring with those shown by Belharazem *et al* and Cui.

With regards to co-expression of IGF-II and H19 mRNA in the PrEvENT cohort, the positive correlation was in benign tissue. The stronger positive correlation—seen in malignant tissue—concurred with that of the larger TGCA prostate and breast cancer cohorts. A similar relationship was seen between imprinting percentage and mRNA; significant positive correlations between the two in both tissue types. These were also matched by a significant positive correlation with H19, but only in malignant tissue. This was unexpected, as chapter three's *in vitro* results found that loss of imprinting led to increased mRNA, due to partial expression of the maternal allele. It may be suggested that, due to the heterogeneity of clinical tissues and, in particular FFPE specimens, the extracted RNA is not necessarily a true representation of the whole sample; the slices taken with the microtome provide a 'snapshot' of tumour at a particular point. This differs greatly from cell line studies, which involves extraction from and analysis of a unicellular culture.

The main discovery of this clinical study was that there was no measurable change in IGF-II peptide, irrespective of IGF-II / H19 mRNA. This was also true of the *in vitro* cell line experiments documented in chapter three. Quantification of IGF-II peptide from the clinical cohorts differed from that of the *in vitro* experiments in that it was tissue based and not secreted. Circulating IGF-II peptide is unstable and may be susceptible to degradation (Bergman, Halje *et al*. 2013). To combat this, it binds with specific binding proteins—insulin-like growth factor binding proteins (IGFBPs). There are six IGFBPs: IGFBP1-6 and they bind to IGF-I and -II with high affinity (Yu and Rohan 2000). More specifically, IGFBP2 binds to IGF-II with very high affinity (Yamanaka, Wilson *et al*. 1997). Therefore, the inconsistency of IGF-II staining is likely due to the presence of peptide bound to IGFBP-2. Different associations have been reported between IGF-II LOI, mRNA and peptide levels and this reflects the limited number of studies and the use of diverse methodologies and assays. For example, one report in men with PCa found no relationship between IGF-II LOI status in circulating blood and serum IGF-II levels, whereas a relationship between the two existed in men without PCa (Belharazem, Kirchner *et al*. 2012). In contrast, IGF-II peptide was increased in triple-negative breast tumours with LOI

(Radhakrishnan, Hernandez *et al*. 2015) and a relationship between IGF-II levels in blood was found with LOI in gastric cancers (Zuo, Yan *et al*. 2011).

4.5 Conclusion

In conclusion, it may be stated that imprinting status induces changes in expression of IGF-II/H19 mRNA; changes in IGF-II mRNA do not appear to affect peptide levels. This suggests alternative mechanisms, other than imprinting, may be involved with mRNA to peptide translation.

CHAPTER 5: LOSS OF IMPRINTING IN IGF-II/H19 IN COLORECTAL CANCER, *in vitro*

5.1 Introduction

In the UK, there are around 40,000 new colorectal cancer diagnoses each year (Cancerresearchuk.org, 2020[3]). In 2018, there were almost 2 million diagnoses, globally, making it the fourth most common type of cancer (Bray, Ferlay *et al*. 2018). Several risk factors are known to contribute to disease susceptibility. These factors can be divided into two category types: modifiable and non-modifiable. Modifiable risk factors include diet, obesity, and smoking (Yuan, Deng *et al*. 2021), whilst non-modifiable risk factors include heritability (Uson, Riegert-Johnson *et al*. 2021) and familial history (Daca Alvarez, Quintana *et al*. 2021) and inflammatory bowel diseases (Onfroy-Roy, Hamel *et al*. 2021).

Non-modifiable risk factors may be treatable but, ultimately, cannot be eliminated. This is not the case with modifiable risk factors; through lifestyle changes, these can be addressed to lessen CRC disease susceptibility. This chapter will focus on two key modifiable risk factors: diet and obesity.

A healthy, balanced diet should provide adequate amount of dietary fibre required by our bodies. Extensive research has been conducted upon the protective effects of fibre against colorectal cancer. Fibre increases the transit rate of waste in the bowel, reducing the length of time of which gut mucosa is exposed to carcinogenic substances contained in faecal matter. Rapid transit time is also accompanied by bacterial fermentation processes, which results in the release of substances, such as sodium butyrate and propionate, which inhibit proliferation and facilitate apoptosis (Baena and Salinas 2015). Conversely, low fibre diets – typically those associated with a high consumption of processed foods -slow the transit time of waste in the gut, which leads to low-grade inflammation (Viennois, Merlin *et al*. 2017).

The combined effects of a low fibre diet and a sedentary lifestyle has led to an obesity epidemic, with a quarter of UK adults falling into the category of clinical obesity (Capehorn, Haslam *et al*. 2016). Many studies have highlighted the relationship between obesity and CRC risk (Jochem and Leitzmann 2016; Dong, Zhou *et al*. 2017; Motawi, Shaker *et al*. 2017; Ye, Xi *et al*. 2020), with one of

the underlying causes thought to be an increase in the synthesis of inflammatory cytokines by adipose tissue (Iyengar, Gucalp *et al*. 2016).

The progression to obesity is often accompanied by the development of type 2 diabetes (T2D). It is thought that the elevated synthesis of inflammatory cytokines by increased amounts of adipose tissue disrupts cellular responses to insulin, leading to insulin resistance. This results in increased levels of glucose in the blood (hyperglycaemia) (Diabetes.co.uk, 2019).

Insulin-like growth factor II (IGF-II) is a growth factor expressed in high quantities during early embryonic development (Liu, Greenberg *et al*. 1989). Expression continues throughout adulthood, with the liver being the primary site of synthesis (Baxter, Holman *et al*. 1995). IGF-II plays a critical role in a number of cellular events, including proliferation and survival (Resnicoff, Abraham *et al*. 1995).

The IGF-II/H19 gene is located on the short arm of chromosome 11p.15.5 (Brissenden, Ullrich *et al*. 1984); 128 kb downstream from IGF-II is a long non-coding RNA, H19, which is linked to IGF-II by an imprinting control region (ICR) (Rotwein 2018). IGF-II was the first gene identified to be 'imprinted' (Ogawa, Eccles *et al*. 1993). Since its discovery in Wilms tumour in 1993, IGF-II/H19 loss of imprinting (LOI) has been reported in many solid tumours, including colorectal, where it was first identified in 1996 (Kinouchi, Hiwatashi *et al*. 1996). In 2000 (Takano, Shiota *et al*. 2000), expression of IGF-II mRNA was found to be upregulated in malignant colorectal tissue, compared to benign; LOI was attributed to be the cause. In 2002, a report identified a link between LOI and hypomethylation of IGF-II/H19; these findings contradicted the widely-accepted enhancer-competition model of imprinting, where hypermethylation of the ICR or binding of CTCF is identified as the cause of relaxed imprinting (Cui, Onyango *et al*. 2002).

Chapter three's findings showed that artificially induced metabolic disturbances, designed to mimic an inflammatory state, can disrupt imprinting status of IGF-II/H19 in PCa. This chapter will aim to prove the same hypothesis, using colorectal cancer cell lines; cells will be exposed to glucose and

TNFα, as before, but will extend further to include the addition of the glucose-sensitising drug metformin, and the dietary fibre by-product sodium butyrate. The inclusion of metformin will elucidate whether its glycaemic activity will affect imprinting status after cellular exposure to elevated glucose conditions. Additionally, metformin is the first line of treatment for T2D; it suppresses glucose production by the liver and increases glucose uptake by skeletal muscle (Kaneto, Kimura *et al*. 2021). Furthermore, oral administration of metformin has been shown to elicit its therapeutic action through the gut, where gastrointestinal mucosal concentrations are up to 300 times higher compared to that in circulating blood plasma (Jones and Molloy 2020). Sodium butyrate (NaB) possesses anti-inflammatory properties, is produced in the gut by bacterial fermentation of dietary fibre and is a metabolite of colonic epithelial cells, which are essential for water and salt absorption (Bedford and Gong 2018). Moreover, NaB is an epigenetic regulator, behaving as an histone deacetylase inhibitor to regulate gene expression (Steliou, Boosalis *et al*. 2012) and has also been shown to induce LOI in IGF-II/H19 in human and mouse fibroblasts (Hu, Oruganti *et al*. 1998; Pedone, Pikaart *et al*. 1999) and bovine kidney cells (Shin, Li *et al*. 2013).

5.2 Hypothesis and Aims.

Hypothesis:

Metabolic disturbances in the growth environment will disrupt imprinting status of the IGF-II/H19 gene, in colorectal cancer, *in vitro*.

Aims.

Investigate the effects of manipulating the metabolic environment to mimic those of an inflammatory state *in vitro*, in colorectal cancer cell lines on a) the imprinting status of IGF-II/H19, and b) the imprinting behaviour of IGF-II/H19.

5.3. Materials & Methods

5.3.1 Method selection and troubleshooting.

The HCT116 cell line was new to the laboratory. Experiments were initially conducted in McCoy's 5A medium, which is specified by the American Type Culture Collection (ATCC) – the commercial source of the cell line. McCoy's 5A medium (M5M) contains a glucose concentration of 3,000 mg/L, which equates to approximately 17 mM/L and this is the only one available. To be able to perform the glucose experiments, HCT116 cells were cultured in high (25mM) and normal (5mM) glucose Dulbecco's Modified Eagle's Medium (DMEM).

Whilst conducting initial qPCR experiments, there were general inconsistencies with the GAPDH ct values which caused large error bars in the data (figures 5.4.2.1, 5.4.3.1 and 5.4.41). Following a literature search, the internal control genes beta-actin and Tata box binding protein (TBP) were tested for suitability. TBP provided more consistent ct values with each qPCR run and, therefore, was selected place of GAPDH.

In chapter 3, RFLP analysis was used to visualise allelic expression after dosing with glucose and TNFα. This was subsequently followed by pyrosequencing for imprinted allele expression (PIE). Whilst RFLP provided a result that could be visualised as bands on a gel, it was unable to show any fine nuances pertaining to imprinting percentage; band pattern intensity varied from gel to gel and was only successful in providing a binary result. Hence, in this chapter, pyrosequencing only was used to provide accurate and definitive assessment of allelic expression and imprinting percentages in the cells, following exposure to glucose, TNFα, NaB and metformin.

A literature search on studies that had previously used metformin and butyrate *in vitro* was conducted to ascertain appropriate concentrations and time points (Hu, Oruganti *et al*. 1998; Chen, Shieh *et al*. 2013; Erices, Bravo *et al*. 2013; Shin, Li *et al*. 2013; Ko, Choi *et al*. 2016).

5.3.2 Culturing of immortalised colorectal cancer cell lines.

Colorectal cell lines HT29, CaCO2, HCT116, HCT115, H747, SW480 and SW620 were used in this study. They were sourced and cultured as described in 2.1.3

5.3.3 Isolation of nucleic acids

DNA and RNA were isolated from cells as outlined in 2.2. Extracts were quantified, "cleaned" and stored as described in 2.1.

5.3.4 Preparation of cDNA.

RNA was converted to cDNA as explained in 2.2.

5.3.5 Genotyping of cell lines by RFLP analysis.

DNA and cDNA were genotyped using the SNP at rs680 (APA1) in exon 7 of IF-II, as described in 2.5.

5.3.6 Dosing with glucose.

Cells were seeded and cultured for 24 hours as outlined in 2.1. After this time, media was exchanged for a serum free version, each containing a different level of glucose as described in 2.1. At 6-, 24- and 48-hour time points, flasks were removed and processed for cDNA as shown in 2.2. Experiments were repeated three times.

5.3.7 Dosing with TNFα.

Two sets of TNFα dosing experiments were conducted: one using McCoys 5A Medium (M5M), and the second using Dulbecco's Modified Eagle's Medium (DMEM).

Cells were seeded and cultured for 24 hours as outlined in 2.X.X. After this time, growth media was replaced with serum free. At 6-, 24- and 48-hour time points, flasks were removed and processed for cDNA as shown in 2.2. Experiments were repeated three times.

5.3.8 Dosing with sodium butyrate (NaB).

Two sets of NaB dosing experiments were conducted: one using M5M, and the second using DMEM. M5M. Cells were seeded and cultured for 24 hours as outlined in 2.1. After this time, growth media was replaced with serum free. At 6-, 24- and 48-hour time points, flasks were removed and processed for cDNA as shown in 2.2. Experiments were repeated three times.

5.3.9 Dosing with metformin.

Two sets of metformin dosing experiments were conducted: one using M5M, and the second using DMEM. Cells were seeded and cultured for 24 hours as outlined in 2.1. After this time, growth media was replaced with serum free. At 6-, 24- and 48-hour time points, flasks were removed and processed for cDNA as shown in 2.2. Experiments were repeated three times.

5.3.10 Quantitative PCR (qPCR)

For dosing experiments conducted in M5M, qPCR was performed as described in 2.6, using GAPDH as an internal control; those conducted in DMEM used TBP as an internal control. Relative expression was calculated using the Pfaffl method (as outlined in 2.6).

5.3.11 Pyrosequencing.

Pyrosequencing for imprinted allele expression (PIE) was conducted as described in 2.9.

5.3.12 Statistical analysis.

Experiments were conducted in triplicate. Analysis of variance (ANOVA) was performed followed by a least significant (LSD) post-hoc test. Analyses were conducted using IBM SPSS statistics 24 software (IBM Corporation, version 24.X.X). P values less than 0.05 were considered statistically significant, with the following denotations: * $p \leq 0.05$, ** $p \leq 0.01$ and *** $p \leq .001$.

5.4 Results

5.4.1.1 Identification of colorectal cell line suitability for dosing experiments.

To investigate the effects of metabolic conditions on LOI of IGF-II, a suitable colorectal cell line needed to be determined. DNA was extracted (as described in 2.X) from 7 immortalised colorectal cancer cell lines: CaCO2, HT29, HCT115, HCT116, SW480, SW620 and H747. These were genotyped using RFLP digestion at the APA1 restriction site: rs680 (as described in 2.X). The HT29, HCT116 and H747 cell lines were found to be heterozygous, presenting with 2 bands of sizes 292- and 229bp, respectively (figure 3.4.1.1). These cell lines were classified as informative and would be suitable for further assessment of imprinting status. Cell lines CaCO2, HCT115, SW480 and SW620 were found to be homozygous for the SNP at rs680 resulting in a single and pattern and, as such, were deemed non-informative.

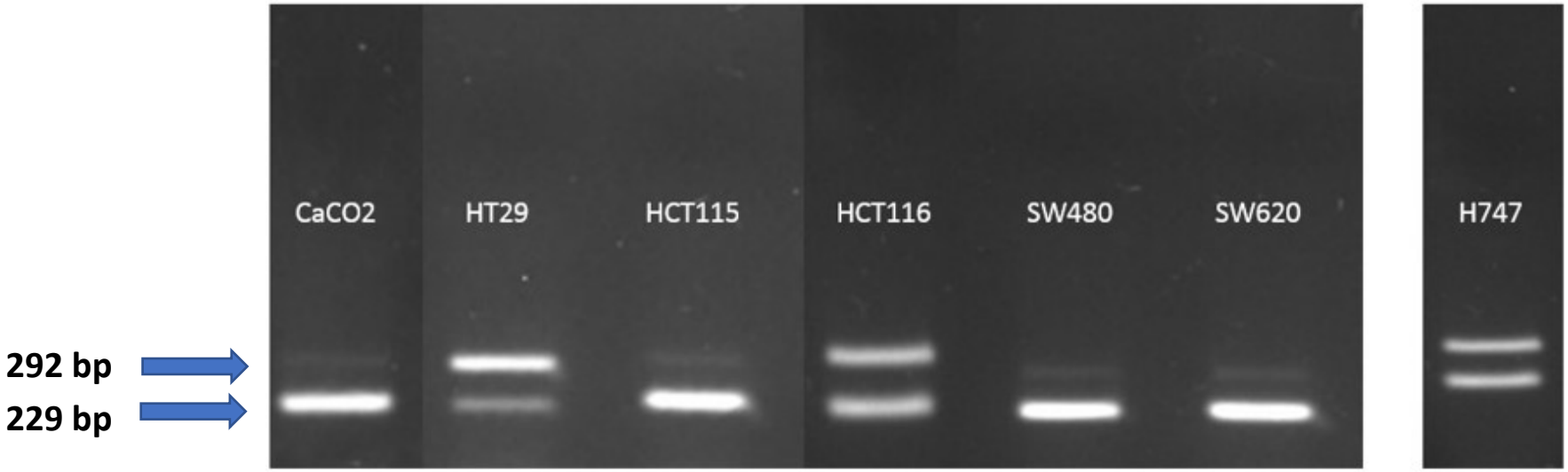

Figure 5.4.1.1: Genotyping of colorectal cancer cell lines using APA1 RFLP. Cell lines HT29, HCT116 and H747 were found to be heterozygous, presenting with 2 bands of sizes 292- and 229 bp respectively. These cell lines were classified as informative and would be suitable for further assessment of imprinting status. Cell lines Caco2, HCT115, SW480 and SW620 were found to be homozygous for the SNP at rs680, resulting in a single band pattern and, as such, were deemed non-informative. (This is a representative gel of experiments repeated three times)

5.4.1.2 Confirmation of IGF-II/H19 imprinting status of HT29, HCT116 and H747.

The HT29 and H747 cell lines expressed two bands of sizes 292 and 229 bp, confirming bi-allelic expression of IGF-II/H19 and therefore, loss of imprinting (LOI). The HCT116 cell line, produced a single band, sized 292bp, indicating mono-allelic expression and therefore, maintenance of imprinting status (MOI). Because of its MOI status, HCT116 was a suitable cell line for assessing the induction of LOI.

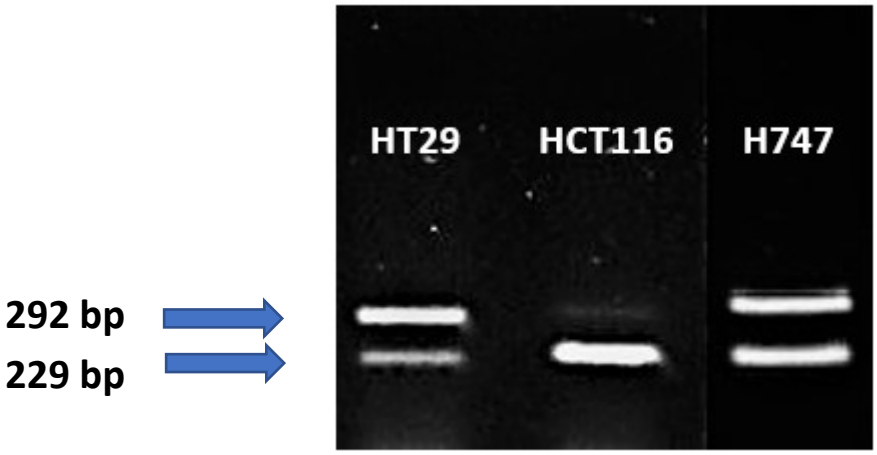

5.4.1.2 Confirmation of IGF-II/H19 imprinting status of HT29, HCT116 and H747. The HT29 and H747 cell lines expressed two bands of sizes 292- and 229 bp, confirming bi-allelic expression of IGF-II/H19 and therefore, loss of imprinting (LOI). The HCT116 cell line, produced a single band, sized 292bp, indicating mono-allelic expression and therefore, maintenance of imprinting status (MOI). (This is a representative gel of experiments repeated three times)

5.4.2.1 The effects of metformin on the levels of IGF-II and H19 mRNA in HCT116 cells cultured in M5M (17mM/L glucose), using GAPDH as an internal control.

After 24 hours, there were no significant differences in IGF-II mRNA relative expression after dosing with 2.5-, 5- or 10mM metformin, when compared with the untreated control; this was also true after 48 hours exposure (figure A). Similarly, after 24- and 48 hours, there were no significant differences in H19 mRNA relative expression after dosing with 2.5-, 5- or 10mM metformin, when compared with the untreated control (figure B).

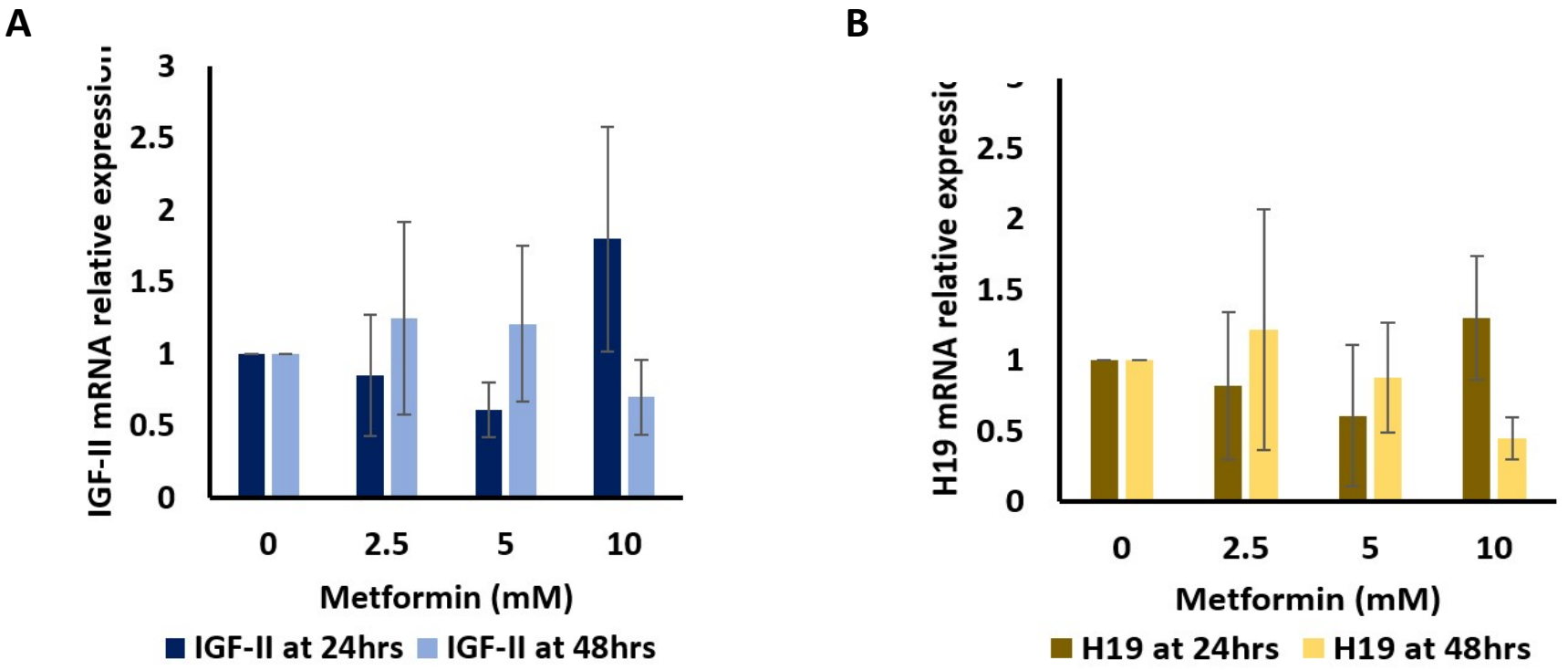

Figure 5.4.2.1: The effects of metformin on the expression of IGF-II and H19 mRNA in HCT116 cells cultured in M5M (17mM/L glucose), using GAPDH as an internal control. After 24 hours, there were no significant differences in IGF-II mRNA relative expression after dosing with 2.5-, 5- or 10mM metformin, when compared with the untreated control; this was also true after 48 hours exposure (**A**). After 24 hours, there were no significant differences in H19 mRNA relative expression after dosing with 2.5-, 5- or 10mM metformin, when compared with the untreated control; this was also true after 48 hours exposure (**B**). (This is a representative data set of experiments repeated three times)

5.4.2.2 The effects of metformin on the levels of IGF-II and H19 mRNA in HCT116 cells cultured in normal (5mM) and high (25mM) glucose media, using TBP as an internal control.

After treatment with 10- and 5mM metformin, there was a significant increase in IGF-II and H19 mRNA relative expression, when cultured in 5mM glucose DMEM (p = 0.008 and 0.025 respectively) (figure A). After treatment with 10mM metformin, there was a significant increase in H19 mRNA relative expression, when cultured in 25mM glucose media ($p \leq .001$) (figure B).

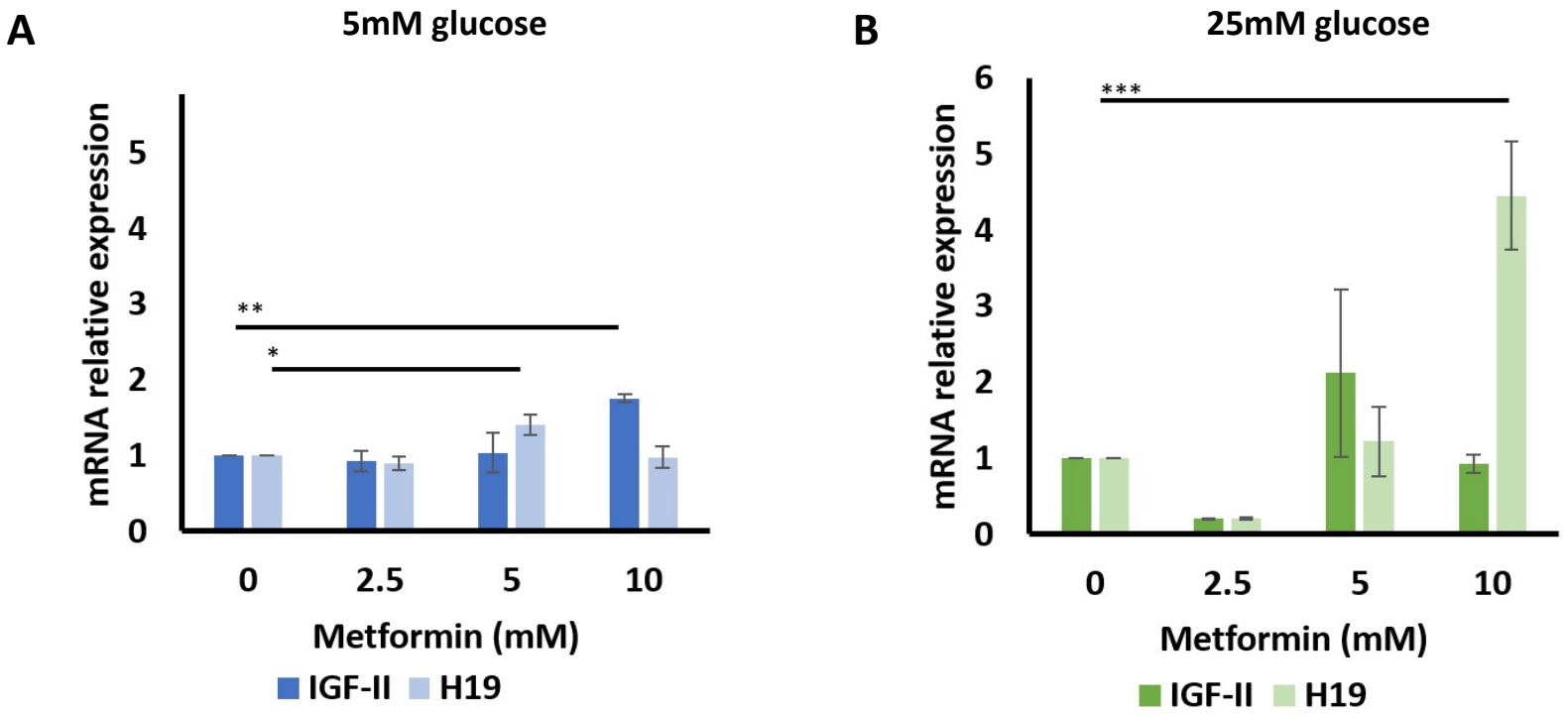

Figure 5.4.2.2: The effects of metformin on IGF-II and H19 mRNA expression in cells cultured in normal (5mM) and high (25mM) glucose media, using TBP as an internal control. After treatment with 10- and 5mM metformin, there was a significant increase in IGF-II or H19 mRNA relative expression, when cultured in 5mM glucose DMEM (p = 0.008 and 0.025 respectively) (**A**). After treatment with 10mM metformin, there was a significant increase in H19 mRNA relative expression, when cultured in 25mM glucose media ($p \leq .001$) (**B**); there were no significant changes in IGF-II mRNA. (This is a representative data set of experiments repeated three times)

5.4.3.1 The effects of NaB on the levels IGF-II and H19 mRNA on HCT116 cells cultured in M5M (17mM/L glucose), using GAPDH as an internal control.

After 24- and 48 hours, there was a significant increase in IGF-II mRNA relative expression in cells dosed with 10- and 5mM NaB respectively, when compared with the untreated control (p = 0.033 and 0.011 respectively) (figure. A). After 24 hours, there were no significant differences in H19 mRNA relative expression after dosing with 2.5-, 5- or 10mM metformin, when compared with the untreated control; this was also true after 48 hours exposure (figure B).

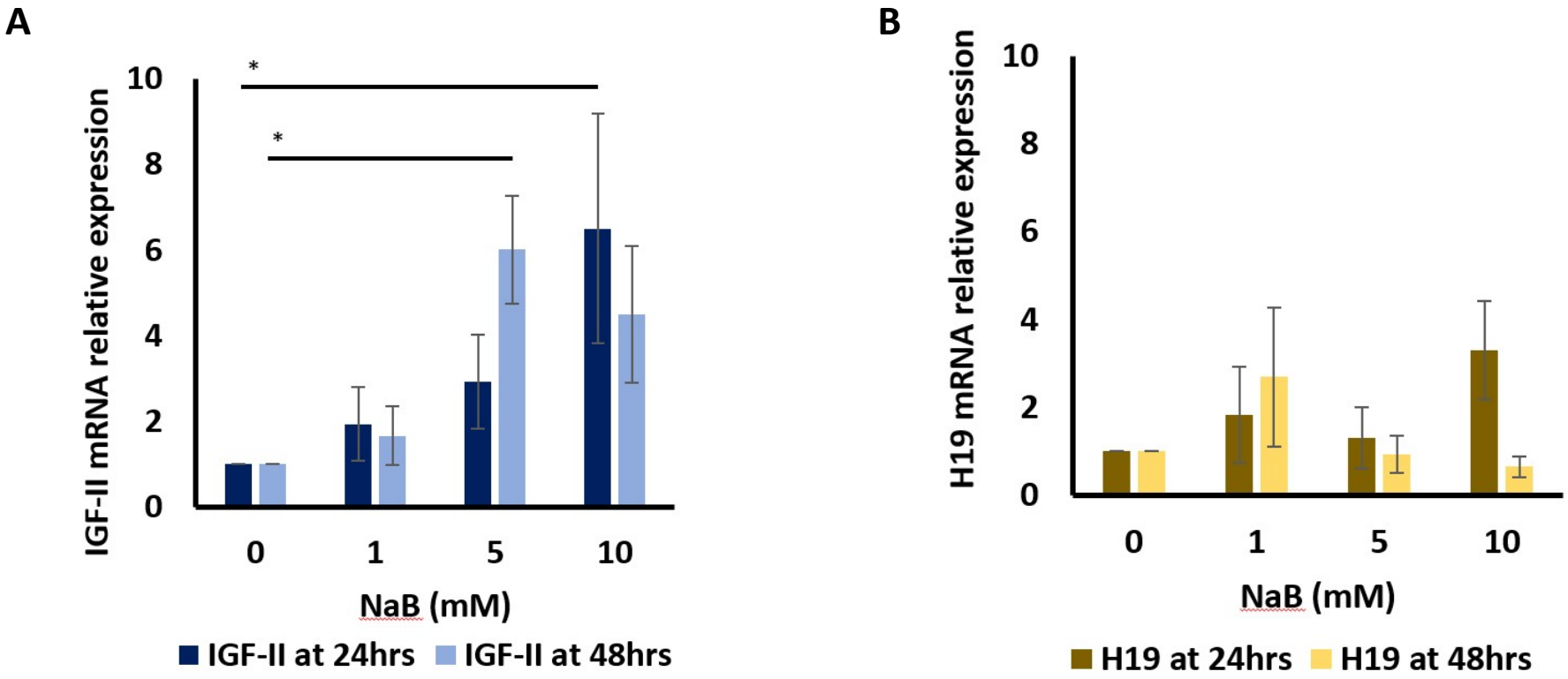

Figure 5.4.3.1: The effects of NaB on IGF-II and H19 mRNA on HCT116 cells cultured in M5M (17mM/L glucose), using GAPDH as an internal control.

After 24- and 48 hours, there was a significant increase in IGF-II mRNA relative expression in cells dosed with 10- and 5mM NaB respectively, when compared with the untreated control (p = 0.033 and 0.011 respectively) (**A**). After 24 hours, there were no significant differences in H19 mRNA relative expression after dosing with 2.5-, 5- or 10mM metformin, when compared with the untreated control; this was also true after 48 hours exposure (**B**). (This is a representative data set of experiments repeated three times)

5.4.3.2 The effects of NaB on the levels IGF-II and H19 mRNA expression in cells cultured in normal (5mM) and high (25mM) glucose media, using TBP as an internal control.

After treatment with 5- and 10mM NaB, there was a significant increase in IGF-II a mRNA relative expression, when cultured in 5mM glucose media (p = 0.005 and ≤ .001 respectively) (figure A). After treatment with 1-, 5- and 10mM NaB, there was a significant increase in H19 mRNA relative expression, when cultured in 5mM glucose media (p = 0.021, 0.018 and 0.050 respectively) (figure A). After treatment with 1-, 5- and 10mM NaB, there was a significant increase in IGF-II mRNA relative expression, when cultured in 25mM glucose media (p = 0.031, 0.007 and ≤ .001 respectively) (figure B). After treatment with 1-, 5- and 10mM NaB, there was a significant increase in H19 mRNA relative expression, when cultured in 25mM glucose media (p ≤ .001, = 0.044 and 0.002 respectively) (figure B).

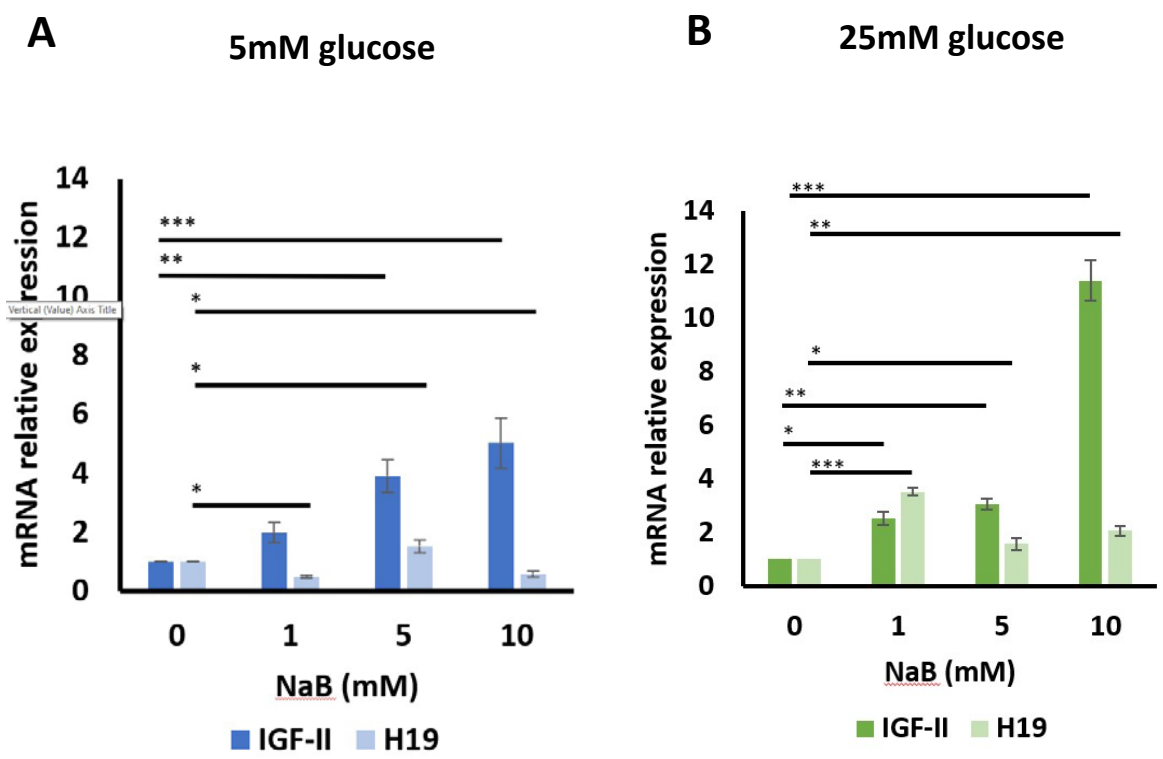

Figure 5.4.3.2: The effects of NaB on IGF-II and H19 mRNA expression in cells cultured in normal (5mM) and high (25mM) glucose media, using TBP as an internal control. After treatment with 5- and 10mM NaB, there was a significant increase in IGF-II mRNA relative expression, when cultured in 5mM glucose DMEM (p = 0.005 and ≤ .001 respectively) (**A**). After treatment with 1-, 5- and 10mM NaB, there was a significant increase in H19 mRNA relative expression, when cultured in 5mM glucose media (p = 0.021, 0.018 and 0.050 respectively) (**A**). After treatment with 1-, 5- and 10mM NaB, there was a significant increase in IGF-II mRNA relative expression, when cultured in 25mM glucose media (p = 0.031, 0.007 and ≤ .001 respectively) (**B**). After treatment with 1-, 5- and 10mM NaB, there was a significant increase in H19 mRNA relative expression, when cultured in 25mM glucose media (p ≤ .001, = 0.044 and 0.002 respectively (**B**). (This is a representative data set of experiments repeated three times)

5.4.4.1 The effects of TNFα on the levels IGF-II and H19 mRNA on HCT116 cells cultured in M5M (17mM/L glucose), using GAPDH as an internal control.

After 24 hours, there were no significant differences in IGF-II (figure A) or H19 (figure B) mRNA relative expression after dosing with 1-, 5- or 10ng/ml TNFα, when compared with the untreated control; this was also true after 48 hours exposure.

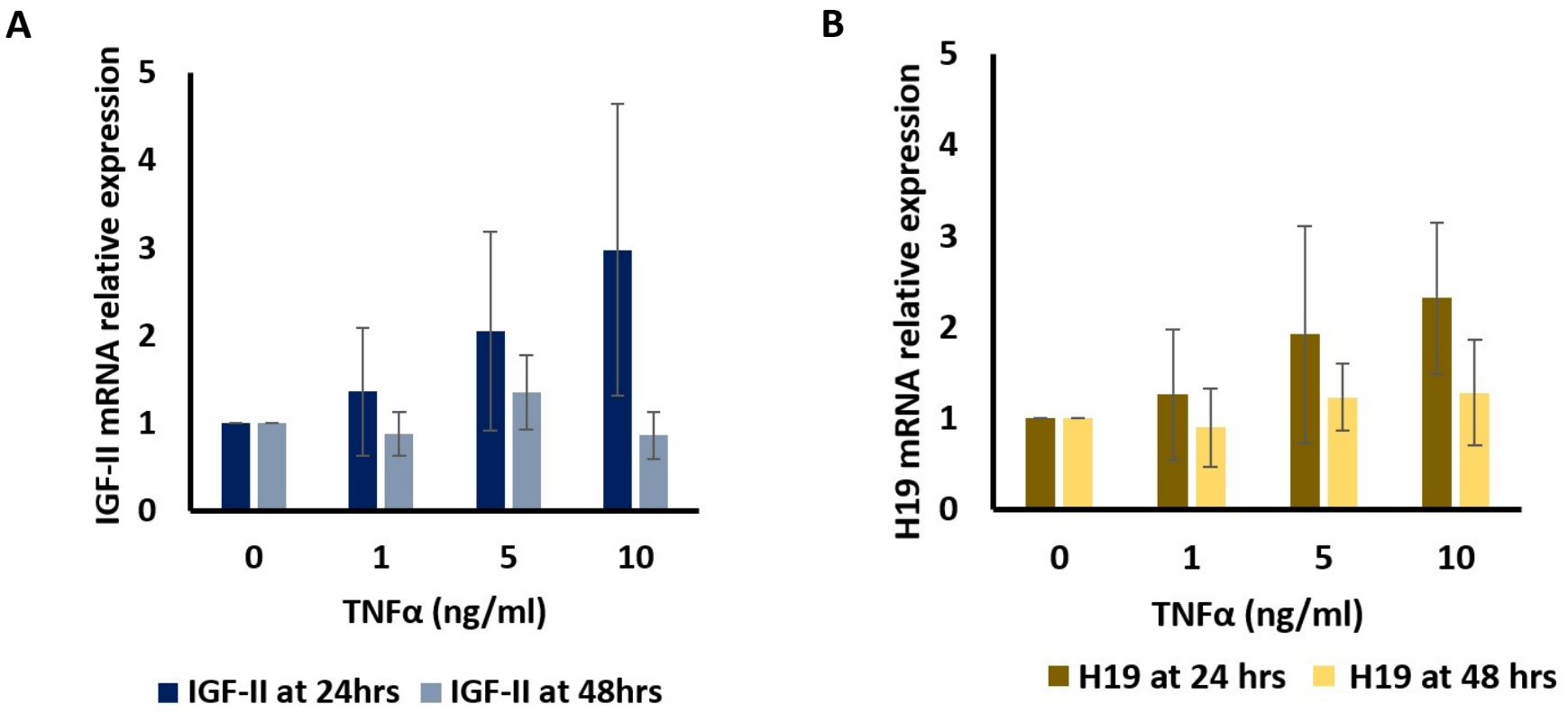

Figure 5.4.4.1: The effects of tumour necrosis factor alpha (TNFα) on IGF-II and H19 mRNA on HCT116 cells cultured in M5M (17mM/L glucose), using GAPDH as an internal control. After 24 hours, there were no significant differences in IGF-II (**A**) or H19 (**B**) mRNA relative expression after dosing with 1-, 5- or 10ng/ml TNFα, when compared with the untreated control; this was also true after 48 hours exposure. (This is a representative data set of experiments repeated three times)

5.4.4.2 The effects of TNFα on the levels IGF-II and H19 mRNA expression in cells cultured in normal (5mM) and high (25mM) glucose media, using TBP as an internal control.

After treatment with 1- and 5 ng/ml TNFα, there was a significant increase in IGF-II mRNA relative expression, when cultured in 5mM glucose media (p = 0.004 and 0.002 respectively) (figure A). After treatment with 1- and 10ng/ml TNFα, there was a significant increase in H19 mRNA relative expression, when cultured in 5mM glucose media ($p \leq .001$ and .001 respectively) (figure A). After treatment with 5- and 10 ng/ml TNFα, there was a significant increase in IGF-II mRNA relative expression, when cultured in 25mM glucose media (p = 0.002 and 0.004 respectively) compared with the control (figure B). After treatment with 1 ng/ml TNFα, there was a significant increase in H19 mRNA relative expression, when cultured in 25mM glucose media, compared to the control (p = 0.027) (figure B).

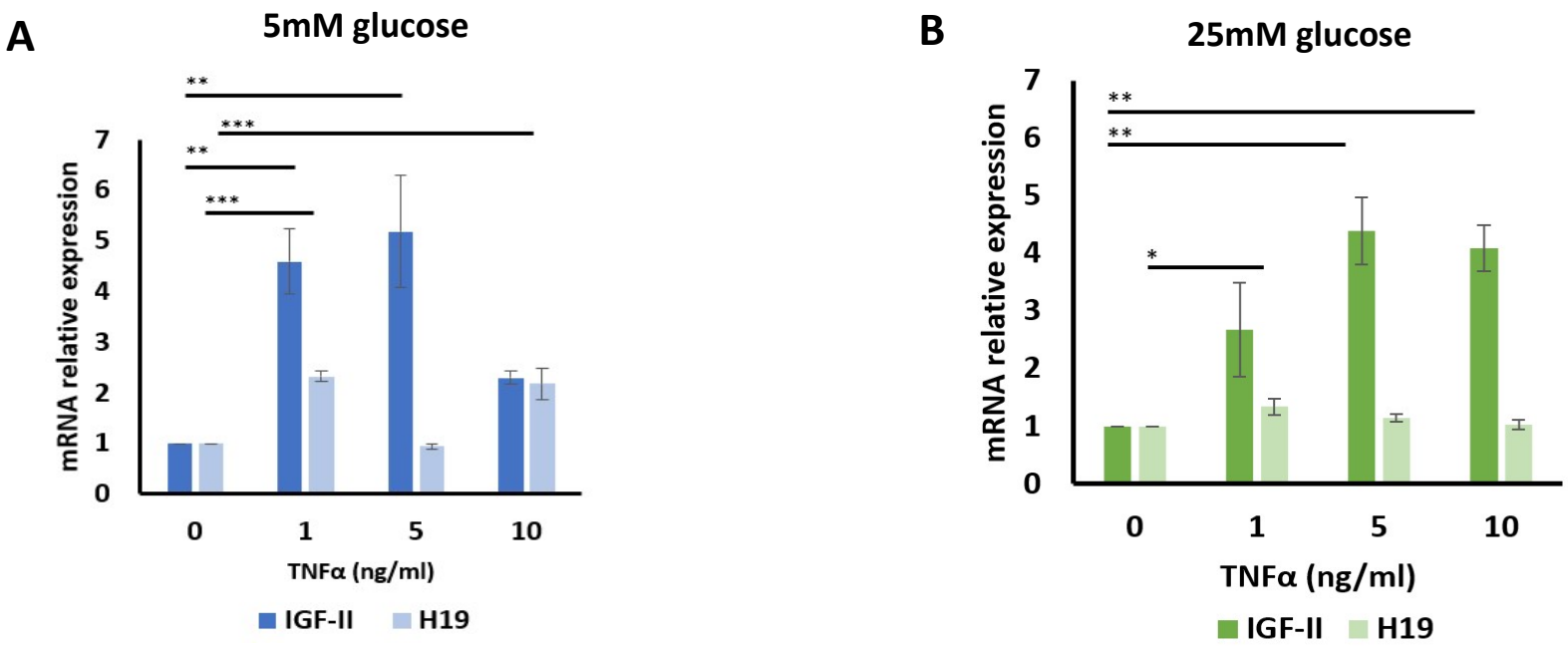

Figure 5.4.4.2: The effects of TNFα on IGF-II and H19 mRNA expression in cells cultured in normal (5mM) and high (25mM) glucose media, using TBP as an internal control. After treatment with 1- and 5 ng/ml TNFα, there was a significant increase in IGF-II mRNA relative expression, when cultured in 5mM glucose media (p = 0.004 and 0.002 respectively) (**A**). After treatment with 1- and 10ng/ml TNFα, there was a significant increase in H19 mRNA relative expression, when cultured in 5mM glucose media ($p \leq .001$ and .001 respectively) (**A**). After treatment with 5- and 10 ng/ml TNFα, there was a significant increase in IGF-II mRNA relative expression, when cultured in 25mM glucose media (p = 0.002 and 0.004 respectively) compared with the control (**B**). After treatment with 1 ng/ml TNFα, there was a significant increase in H19 mRNA relative expression, when cultured in 25mM glucose media, compared to the control (p = 0.027) (**B**). (This is a representative data set of experiments repeated three times)

5.4.5.1 The effects of altered levels of glucose on the levels IGF-II and H19 mRNA expression, using TBP as an internal control.

After 48 hours, there was a significant increase in IGF-II mRNA in cells cultured in 9- and 25mM glucose (p = 0.017 and 0.020 respectively), when compared with the control (5mM glucose) (figure A). After 6 hours there was a significant increase in H19 mRNA in cells cultured in 9- and 25mM glucose ($p \leq .001$ and .001 respectively), when compared with the control (5mM glucose) (figure B).

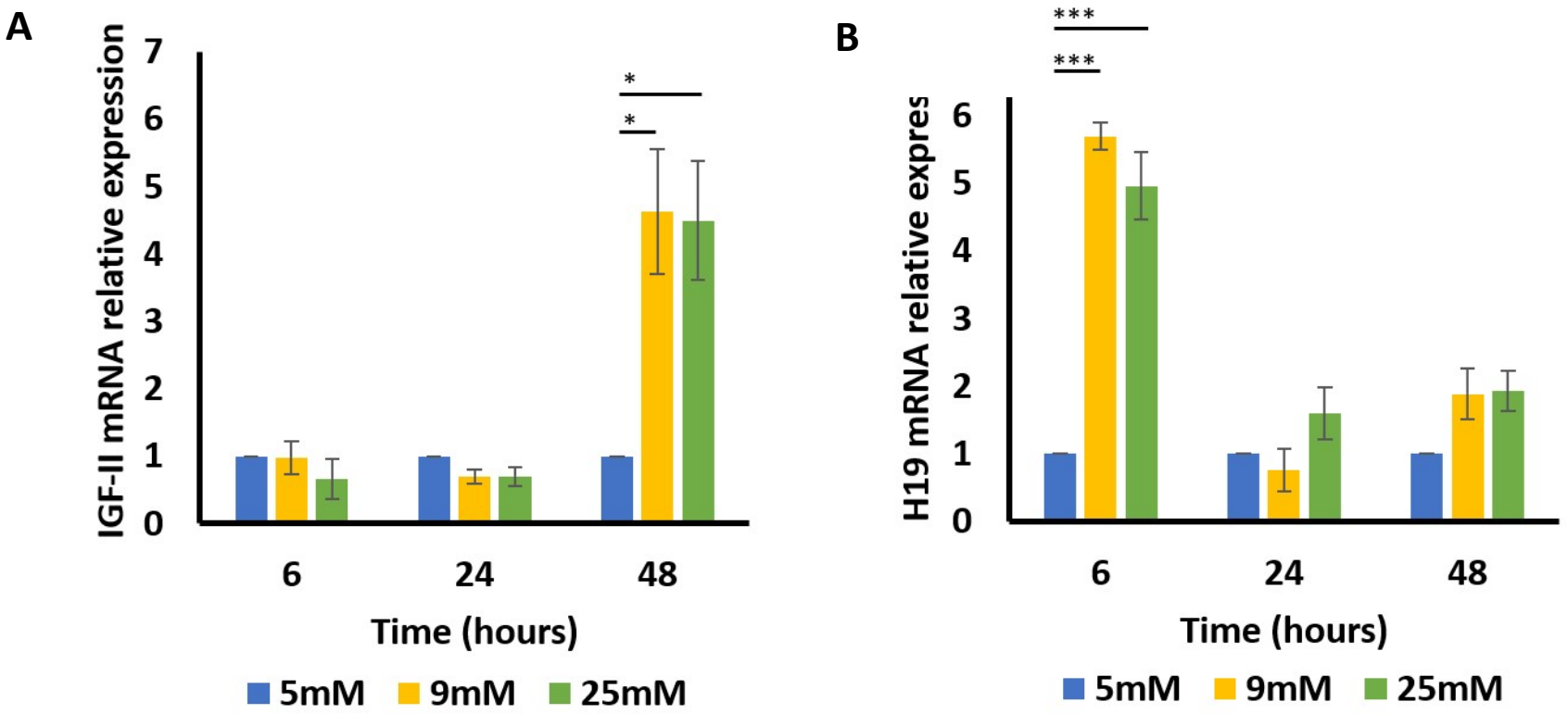

Figure 5.4.5.1: The effects of altered levels of glucose on IGF-II and H19 mRNA expression, using TBP as an internal control.

After 48 hours, there was a significant increase in IGF-II mRNA in cells cultured in 9- and 25mM glucose (p = 0.017 and 0.020 respectively), when compared with the control (5mM glucose) (**A**). After 6 hours there was a significant increase in H19 mRNA in cells cultured in 9- and 25mM glucose ($p \leq .001$ and .001 respectively), when compared with the control (5mM glucose) (**B**). (This is a representative data set of experiments repeated three times)

5.4.6.1 The effects of metformin on IGF-II/H19 imprinting percentage, in cells cultured in normal (5mM) and high glucose media.

Cells cultured in 5mM glucose and dosed with 1-, 5- and 10mM metformin showed no significant changes to imprinting percentage (figure A), when compared with the untreated control. Cells cultured in 25mM glucose and dosed with 5mM metformin showed a significant increase in imprinting percentage ($p \leq .001$), when compared with the untreated control (figure B).

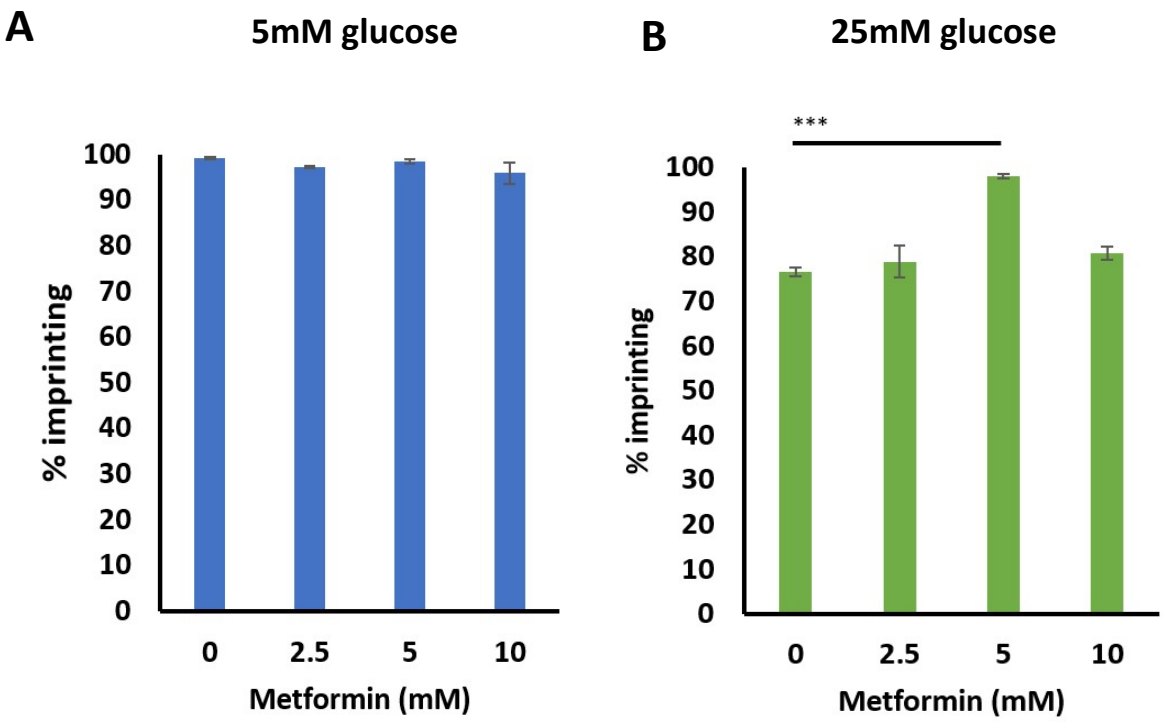

Figure 5.4.6.1 The effects of metformin on IGF-II/H19 imprinting percentage, in cells cultured in normal (5mM) and high (25mM) glucose media. Cells cultured in 5mM glucose and dosed with 1-, 5- and 10mM metformin showed no significant changes to imprinting percentage (**A**), when compared with the untreated control. Cells cultured in 25mM glucose and dosed with 5mM metformin showed a significant increase in imprinting percentage ($p \leq .001$), when compared with the untreated control (**B**). (This is a representative data set of experiments repeated three times)

5.4.6.2 The effects of sodium butyrate (NaB) on IGF-II/H19 imprinting percentage, in cells cultured in normal (5mM) and high glucose media.

Cells treated with 5- and 10mM NaB and cultured in 5mM glucose media showed significant decreases in imprinting percentage ($p \leq .001$ and .001 respectively), compared with the control (figure A). Cells treated with 10mM NaB and cultured in 25mM glucose media showed a significant decrease in imprinting percentage ($p \leq .001$), compared with the control (figure B).

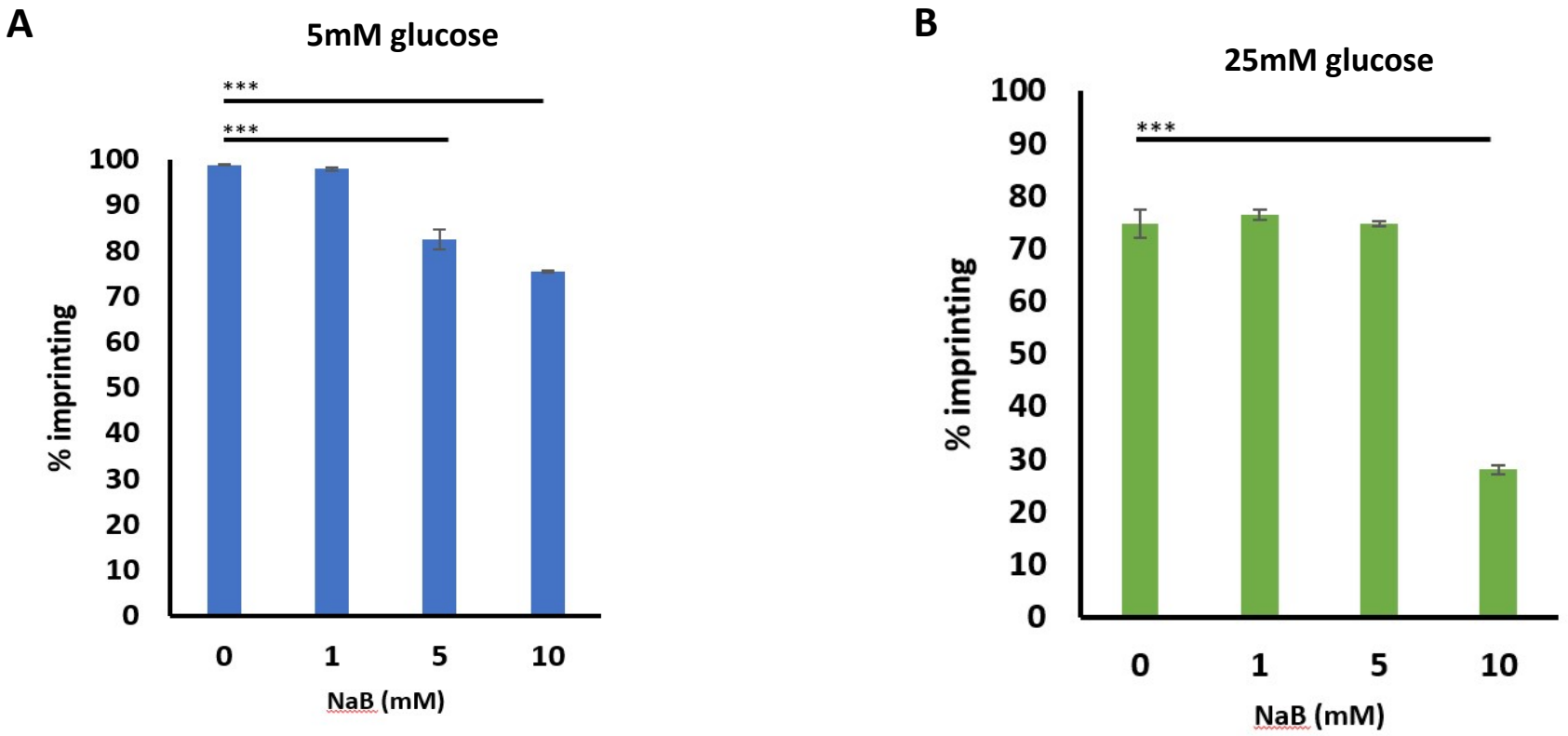

Figure 5.4.6.2 The effects of NaB on IGF-II/H19 imprinting percentage in cells cultured in normal (5mM) and high (25mM) glucose media. Cells treated with 5- and 10mM NaB and cultured in 5mM glucose DMEM showed significant decreases in imprinting percentage ($p \leq .001$ and .001 respectively), compared with the control (**A**). Cells treated with 10mM NaB and cultured in 25mM glucose DMEM showed a significant decrease in imprinting percentage ($p \leq .001$), compared with the control (**B**). (This is a representative data set of experiments repeated three times)

5.4.6.3 The effects of TNFα on IGF-II/H19 imprinting percentage, in cells cultured in normal (5mM) and high (25mM) glucose media.

Cells treated with 5- and 10ng/ml TNFα and cultured in 5mM glucose media showed significant decreases in imprinting percentage ($p \leq .001$ and .001 respectively), compared with the control (figure A). Cells treated with 1-, 5- and 10ng/ml TNFα and cultured in 25mM glucose media showed a significant decrease in imprinting percentage ($p \leq .001$, < .001 and .001 respectively), when compared with the control (figure B).

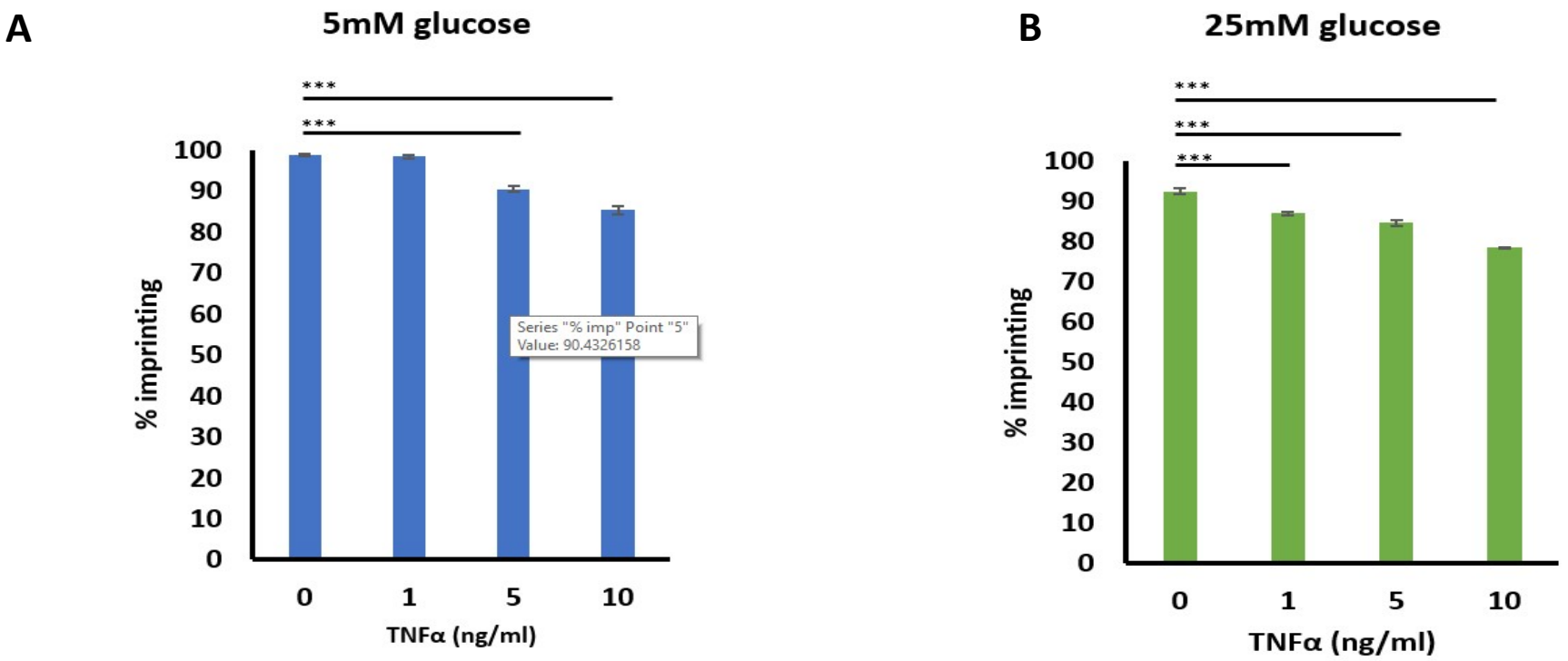

Figure 5.4.6.3: The effects of TNFα on IGF-II/H19 imprinting percentage, in cells cultured in normal (5mM) and high (25mM) glucose media. Cells treated with 5- and 10ng/ml TNFα and cultured in 5mM glucose media showed significant decreases in imprinting percentage ($p \leq .001$ and .001 respectively), compared with the control (**A**). Cells treated with 1-, 5- and 10ng/ml TNFα and cultured in 25mM glucose media showed a significant decrease in imprinting percentage ($p \leq .001$, .001 and .001 respectively), when compared with the control (**B**). (This is a representative data set of experiments repeated three times)

5.4.6.4 IGF-II/H19 imprinting percentage after treatment with glucose.

After 24 hours, cells cultured in 25mM glucose showed a significant decrease in imprinting percentage ($p \leq .001$), when compared with the control (5mM glucose); after 48 hours, cells cultured in 9- and 25mM glucose showed significant decreases in imprinting percentage ($p \leq 0.001$ and = 0.013, respectively) when compared with the control (5mM glucose) (figure 5.4.6.4).

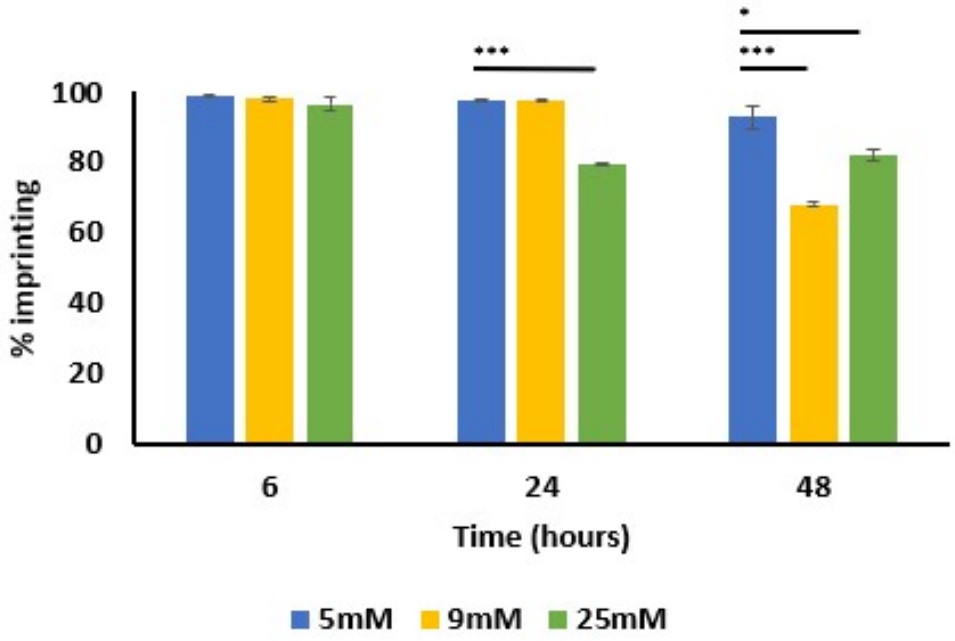

Figure 5.4.6.4: IGF-II/H19 imprinting percentage after treatment with altered glucose levels. After 24 hours, cells cultured in 25mM glucose showed a significant decrease in imprinting percentage ($p \leq .001$), when compared with the control (5mM glucose); after 48 hours, cells cultured in 9- and 25mM glucose showed significant decreases in imprinting percentage ($p \leq 0.001$ and = 0.013, respectively) when compared with the control (5mM glucose).

5.5 Discussion

Loss of imprinting in the IGF-II/H19 gene is a common feature of many different cancer types; its occurrence in colorectal cancer tissue was first identified in 1998 (Cui, Horon *et al*. 1998)

This chapter explored whether manipulation of the metabolic environment can influence LOI in IGF-II/H19. As in chapter 3, an inflammatory environment was mimicked through the addition of an inflammatory cytokine (TNFα) and inducing hyperglycaemia (increasing glucose). The addition of these two additives was originally designed to replicate the physiological conditions typically associated with T2D. Two further exposures were included: metformin and sodium butyrate. For individuals with T2D, metformin is the first line of treatment; it suppresses glucose production by the liver and increases glucose uptake by skeletal muscle (Kaneto, Kimura *et al*. 2021). Furthermore, oral administration of metformin has been shown to elicit its therapeutic action through the gut, where gastrointestinal mucosal concentrations have been found to be up to 300 times higher compared to that in circulating blood plasma (Jones and Molloy 2020). Sodium butyrate (NaB) is a short-chain fatty acid, with anti-inflammatory properties, produced in the gut by bacterial fermentation of dietary fibre; it is a metabolite of colonic epithelial cells, which are essential for water and salt absorption (Bedford and Gong 2018). Moreover, NaB is an epigenetic regulator, behaving as an histone deacetylase inhibitor to regulate gene expression (Steliou, Boosalis *et al*. 2012). In addition, NaB has also been shown to induce LOI in IGF-II/H19 (Hu, Oruganti *et al*. 1998; Shin, Li *et al*. 2013), which seems to be contradictive; that a substance known to have anti-proliferative effects should induce a phenomenon typically associated with carcinogenesis.

Cells cultured in 9- and 25mM glucose media showed significant decreases in imprinting percentage, after 48 hours, when compared with the control. These decreases were matched with increased expression of IGF-II mRNA, suggesting that high glucose levels (above 5mM) are sufficient to induce partial loss of imprinting, resulting in biallelic expression of IGF-II. Conversely, there were significant increases in H19 mRNA after 6 hours, in cells cultured in 9- and 25mM glucose DMEM.

Having established that high glucose is able to disrupt allelic and IGF-II mRNA expression, the next stage was to examine whether metformin may counteract this disruption. There were no significant changes to imprinting percentage in cells cultured in normal glucose media, regardless of metformin dosage. However, cells cultured in high glucose media and treated with 5mM metformin showed a significant increase in imprinting percentage, when compared to the control. This demonstrated that metformin was able to effectively reverse LOI, in a hyperglycaemic environment. Interestingly, this increase in imprinting percentage, was not matched by decreased IGF-II expression under high glucose conditions. Moreover, the addition of 10mM metformin was sufficient to significantly increase IGF-II mRNA expression in normal glucose media. Interestingly, H19 mRNA expression significantly increased under both normal and high glucose conditions, when treated with 5- and 10mM metformin, respectively. Whilst these changes were not quantifiable, in terms of imprinting, the metformin may have epigenetically affected transcription, independent of the imprint control region. Other studies have also shown metformin to exert an epigenetic effect upon gene expression, largely through its ability to activate 5' adenosine monophosphate-activated protein kinase (AMPK) (Bridgeman, Ellison *et al*. 2018); the mechanistic actions of metformin take place in the mitochondria – the key site of adenosine triphosphate (ATP) synthesis; once inside, metformin suppresses ATP synthesis, resulting in a build-up of adenosine monophosphate (AMP) and adenosine diphosphate (ADP). An accumulation of AMP and ADP activates AMPK, which behaves like a cellular energy sensor (Rena, Hardie *et al*. 2017). In the liver, AMPK phosphorylates and inactivates glycogen synthase, inhibiting glucose production (Bultot, Guigas *et al*. 2012). Metformin also enhances insulin sensitivity in peripheral tissues, by enhancing insulin receptor tyrosine kinase activity (Giannarelli, Aragona *et al*. 2003). In 2017, Marin *et al* showed activated AMPK, through treatment with metformin, phosphorylated three key proteins implicated in nucleosome modelling. These proteins triggered the transcription of genes involved in mitochondrial biogenesis in human umbilical vein endothelial cells (Marin, Gongol *et al*. 2017). In 2018, Wu *et al* identified the tumour suppressor, Ten-eleven translocation dioxygenase 2 (TET2), to be a substrate of AMPK; it was shown that in high

glucose, AMPK is impeded from phosphorylating TET2, resulting in its destabilisation. TET2 has a regulatory effect upon DNA methylation; destabilised TET2 is unable to act as a tumour suppressor by regulating DNA methylation. Metformin was shown to stabilise AMPK's effect upon TET2, thus maintaining its regulatory effect upon DNA methylation. The stabilising behaviour exerted upon nucleosome modelling and DNA methylation by metformin may aid in the explanation for the observed effects upon imprinting in IGF-II/H19.

The addition of 5- and 10mM NaB was able to significantly decrease imprinting percentage, in cells cultured in normal glucose media. This was coupled with significant increases in IGF-II and H19 mRNA expression. Likewise, after the addition of 10mM NaB in high glucose media, imprinting percentage significantly decreased and IGF-II and H19 mRNA significantly increased. These findings correlate with published evidence, which has shown NaB to affect allelic expression of IGF-II (Hu, Oruganti *et al*. 1998). In the context of these findings, it is likely that NaB, in combination with high glucose, is exerting its epigenetic effects in two ways, as shown by figure 5.5. Normal imprinting status of IGF-II/H19 is associated with acetylated histone proteins and methylation at the ICR; this results in IGF-II expression and silencing of H19 on the paternal allele. The maternal allele has acetylated histone proteins in H19 and CTCF bound at the ICR; this results in silenced IGF-II and transcribed H19. The proposed mechanism by which NaB, and high glucose are exerting their effects is shown by the second image; NaB inhibits the histone deacetylation, whilst glucose displaces CTCF from the ICR. This results in biallelic expression of IGF-II and H19. This suggested mechanism is a combination of the enhancer competition model, proposed by Moutlton *et al* and Steenman *et al* (Moulton, Crenshaw *et al*. 1994; Steenman, Rainier *et al*. 1994), and histone acetylation for imprinting of IGF-II, by Hu *et al* (Hu, Oruganti *et al*. 1998).

After treating with 5- and 10 ng/ml TNFα, cells cultured in normal and high glucose media all showed significant decreases in imprinting percentage, with the inclusion of those treated with

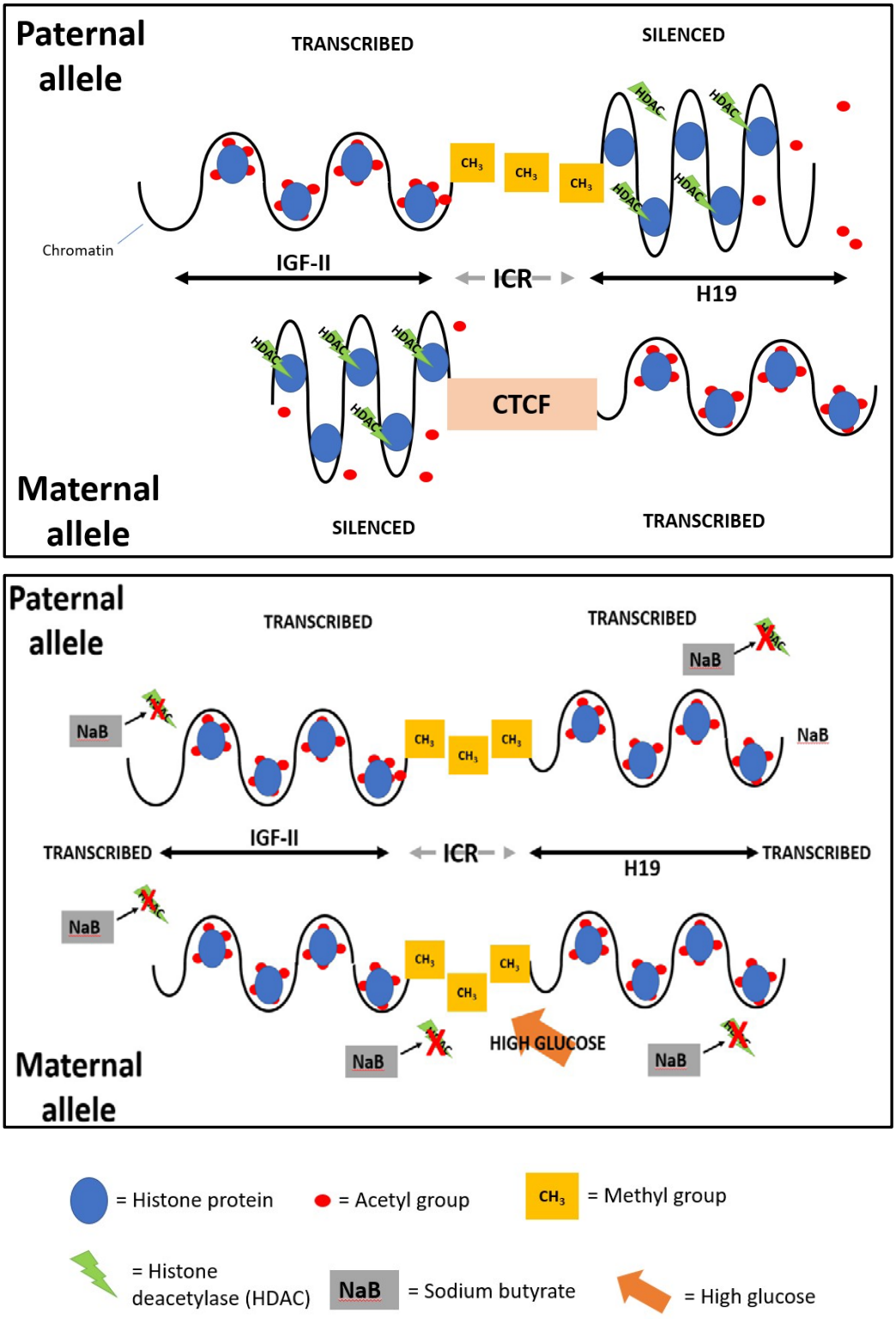

Figure 5.5: Proposed epigenetic mechanisms of NaB and high glucose: Normal imprinting status (**top**) and the proposed mechanism by which NaB and high glucose are exerting their effects **(bottom**).

(adapted from Hu, Oruganti *et al*. 1998; Reik and Murrell 2000)

1ng/ml in high glucose media – which also showed a decrease. These decreases in imprinting percentage were coupled with increases in IGF-II and H19 mRNA expression, in both normal and high glucose media. These results resemble findings in chapter 3, where the addition of TNFα significantly decreased imprinting percentage. However, decreased imprinting percentage equated to increased H19 *and* IGF-II mRNA in both normal and high glucose media, and not just IGF-II - in normal glucose media - and H19 – in high glucose media, which was true of chapter 3's findings. These findings may differ due to variations in prostate and colorectal cell morphology, whereby membrane structure could differ greatly. For example, glucose transport is facilitated by glucose transporters (Navale and Paranjape 2016). Due to increased exposure to glucose and nutrients in the colon, it may be that the HCT116 cell line, derived from the colon / large intestine, may have a higher expression of transporters on its cell membrane compared with those in the prostate (i.e., PC3 cells).

The addition of TNFα in normal glucose media was sufficient to elicit a reduction in imprinting percentage and an increase in mRNA, suggesting a gradual introduction of allelic expression by the silenced maternal allele and, therefore, a loss of imprinting. Clarification of whether TNFα may have affected the methylation patterns in and around the IGF-II/H19 locus, could potentially be investigated by methylation analysis using pyrosequencing. Methylated sites within a gene contain a high expression of CpG islands, whereby a cytosine will be followed by a guanine base. It is at these locations where methylation occurs. The IGF-II/H19 gene has a specific methylation pattern, ensuring epigenetic control of its expression. Conducting a bisulphite conversion of the DNA strand will convert unmethylated cytosine bases to uracil; methylated cytosines remain unchanged. Subsequent pyrosequencing of the bisulphite converted strand will show where these changes have occurred, by emitting a light signal.

5.6 Conclusion

Data in this chapter has demonstrated that under inflammatory conditions, *in vitro*, it is possible to induce loss of imprinting in the IGF-II/H19 gene in colorectal cancer. The underlying cause of this occurrence may be attributed to one, or a combination, of two mechanisms:

1) Displacement of the ICR-bound CTCF transcription factor, by hypermethylation, leading to biallelic expression of IGF-II and H19.
2) Inhibition of histone deacetylation, resulting in relaxation of chromatin leading to biallelic expression of IGF-II and H19.

CHAPTER 6: LOSS OF IMPRINTING IN IGF-II/H19 IN COLORECTAL CANCER, *in vivo*

6.1 Introduction

Colorectal cancer is the fourth most frequently diagnosed cancer type, with incidence rising annually in first world countries (Rawla, Sunkara *et al*. 2019). Several risk factors are known to increase disease susceptibility. These include poor dietary habits (Baena and Salinas 2015; Viennois, Merlin *et al*. 2017; Hullings, Sinha *et al*. 2020), type 2 diabetes (T2D) (Cheng, Chang *et al*. 2021; Joseph, Li *et al*. 2021), inflammatory bowel disease (Hanahan and Weinberg 2011; Jellema, van Tulder *et al*. 2011; Ullman and Itzkowitz 2011), obesity and low physical activity (Capehorn, Haslam *et al*. 2016; Jochem and Leitzmann 2016), heritable gene mutations (Huang, Bian *et al*. 2021; Uson Junior, Riegert-Johnson *et al*. 2021) and familial history (Henrikson, Webber *et al*. 2015).

The association of obesity and T2D with colorectal cancer has been the topic of numerous studies (Voutsadakis 2017; Cirillo, Catellani *et al*. 2019; Croft, Reed *et al*. 2019). It is understood that adipose tissue secretes over 20 different growth hormones and cytokines (Ahima and Osei 2008). Therefore, excessive adipose tissue will produce larger quantities of these molecules, leading to disruption of the cellular milieu (Booth, Magnuson *et al*. 2015). Obesity also increases the risk of developing T2D (Garg, Maurer *et al*. 2014), the key symptom of which is an abnormally elevated amount of glucose in the blood - also known as hyperglycaemia (Chen, Nooromid *et al*. 2019). As glucose is the primary source of energy for cells, an increase in its supply will cause an increase in cellular activities (Chang and Yang 2016).

Insulin-like growth factor II (IGF-II) is a growth factor expressed in high quantities during early foetal development (Liu, Greenberg *et al*. 1989).Expression of IGF-II continues throughout adult life, with the liver being the primary source of its production (Baxter, Holman *et al*. 1995) . IGF-II has been shown to play an essential role in numerous cellular events, including growth, proliferation, migration and survival (Resnicoff, Abraham *et al*. 1995). Within the IGF-II gene locus lies a long non-coding RNA (lnRNA) called H19, which is not translated into peptide (Brannan, Dees *et al*. 1990). As with IGF-II, H19 is also primarily expressed during foetal development (Milligan, Antoine *et al*. 2000),

but becomes active in tumour development (Raveh, Matouk *et al*. 2015). Therefore, the IGF-II/H19 gene has been described as “oncofoetal” in behaviour.

IGF-II/H19 was the first gene identified to be ‘imprinted’, in humans (Ogawa, Eccles *et al*. 1993): a heritable epigenetic event whereby, through changes to the DNA structure (such as methylation or histone modification) one parental copy is silenced or imprinted (Park, Mitra *et al*. 2017). The loss of this natural silencing phenomenon (loss of imprinting – LOI) has been identified across a number of cancers, including prostate (Damaschke, Yang *et al*. 2017), breast (Mishima, Kagara *et al*. 2016), colorectal (Belharazem, Magdeburg *et al*. 2016) and lung (Zhang, Wu *et al*. 2014).

The occurrence of IGF-II/H19 imprinting loss in colorectal cancer was first identified in 1996 (Kinouchi, Hiwatashi *et al*. 1996), whereby loss of imprinting was detected in both benign and malignant colorectal tissue. This was further confirmed two years later (1998), where LOI was also found in benign tissue taken from colorectal cancer patients (Cui, Horon *et al*. 1998). Furthermore, in 1999 (Yun, Soejima *et al*. 1999), LOI was confirmed to be coupled with biallelic expression of IGF-II/H19 in colorectal cancer.

In 1998, Kawamoto *et al* (Kawamoto, Onodera *et al*. 1998) demonstrated IGF-II expression to be a useful prognostic tool in patients with colorectal cancer; an increase in IGF-II correlated with tumour progression and patient survival. This was further confirmed by another study in 1999 (Xu, Liu *et al*. 1999).

6.2. Hypothesis and Aims.

Hypothesis:

Imprinting status of the IGF-II/H19 gene is disrupted in colorectal cancer and will affect mRNA expression and/or peptide levels.

Aims.

Using a clinical cohort of colorectal tissue, the aims for this study were to:

1) Analyse imprinting status and subsequent expression of IGF and H19 mRNA.
2) Explore the impact of imprinting upon IGF-II peptide expression.
3) Establish whether there are correlations between IGF/H19 mRNA, imprinting percentage and IGF-II peptide with disease severity.

6.3. Materials & Methods

6.3.1 Method selection, optimisation, and troubleshooting.

Collection of colorectal tissue for the Colorectal Cancer Metabolic Study (CRCM) took place between November 2014 and May 2017, primarily by a single surgeon. The total cohort comprises 94 patients, of which 69 specimens could be located. 6 of the 69 had been prescribed metformin for T2D. With such a small sub-set of patients, the whole cohort was assessed, disregarding metformin status. However, this is an ongoing study; it is hoped that more patients taking metformin will be collected, to allow for further analysis on the impact of metformin on IGF-II/H19 imprinting. Additionally, several cohort specimens were excluded due to the tissue being harvested from non-cancer related surgeries. Table 6.3.1 outlines the tissue types, surgical origins for samples in the CRCM cohort.

Number of patients	**Surgery type**	**Included / excluded in cohort imprinting analysis**
60 (54 with representative benign and malignant specimens)	Removal of malignancy	Included
3	IBD- related	Excluded
5	Polyp removal	Excluded
1	Appendectomy	Excluded
25	Unable to locate	Excluded

Table 6.3.1: Tissues included in the CRCM cohort. Samples taken from malignancy-related surgeries were included in the Metformin cohort for imprinting analysis; all others were excluded.

This study employed the automated KingFisher™ technique of RNA extraction. As this method was new to the laboratory, some optimisation was required. The extraction kit protocol specifies the minimum amount of tissue required is 20mg. Availability of some samples exceeded this quantity and, as such, were used to test the RNA extraction protocol program. Preliminary tests showed RNA yield to be low (under 10ng/µl), when eluted in 100µl of elution buffer. By reducing the elution volume from 100 µl to 30µl, the yield increased, giving a more concentrated volume of sample.

6.3.2 Colorectal tissue.

Fresh frozen and FFPE colorectal tissue from the CRCM cohort was used to study IGF-II / H19 imprinting status, mRNA, and IGF-II peptide expression as described in 6.3.1.

6.3.3 Isolation of RNA

RNA was extracted from fresh tissue using the KingFisher™ Automated Extraction system, as described in 2.4.

6.3.4 Preparation of cDNA

RNA was concerted to cDNA as outlined in 2.2.

6.3.5 Pyrosequencing

Pyrosequencing for imprinted allele expression (PIE) was conducted as described in 2.9.

6.3.6 Digital droplet PCR (ddPCR)

ddPCR was conducted as outlined in 2.8.

6.3.7 Immunohistochemistry

Slides were prepared and stained for IGF-II as described in 2.10. They were subsequently scored using an adapted version of the Allred system, as described in 2.10.3.

6.3.8 Use of cBioportal for Cancer Genomics

The cBio Cancer Genomics Portal (Cerami, Gao *et al*. 2012) and (Gao, Aksoy *et al*. 2013) was used to explore co-expression of IGF-II and H19 mRNA; one representative Cancer Genome Atlas cohort was selected from the list of colorectal studies. Each cohort was assessed for availability of IGF-II and H19 mRNA co-expression data, which had been gathered using the Illumina HiSeq sequencing system.

6.3.9 Use of the NHS patient records system: Sunquest Integrated Clinical Environment (ICE)

Disease staging details and metformin status were obtained from the North Bristol Trust NHS patient records system, Sunquest Integrated Clinical Environment (ICE).

6.3.10 Statistical analysis.

A two-tailed *t* test was used to compare the differences between benign/malignant paired groups of data. For correlation analyses, the Pearson correlation co-efficient was calculated, with results being expressed as an R value. The mean was used as representative data from each group, with SEM calculated. *P* values less than 0.05 were deemed statistically significant, with the following denotations: * $p \leq 0.05$, ** $p \leq 0.01$ and *** $p \leq .001$. Analyses were conducted using the IBM SPSS Version 24 Statistics software package.

6.4 Results

6.4.1.1 Imprinting status of CRCM cohort samples using pyrosequencing.

Tissue was typed as either ‘MOI’ (maintained imprinting) or ‘LOI’ (loss of imprinting) (figure 6.4.1.1). Of 58 paired patient samples, 25 presented with no change of MOI status (in the benign sample compared to its malignant counterpart), 15 presented with a change in status from MOI to LOI, 13 presented with a change in status from LOI to MOI and 5 presented with no change of LOI status.

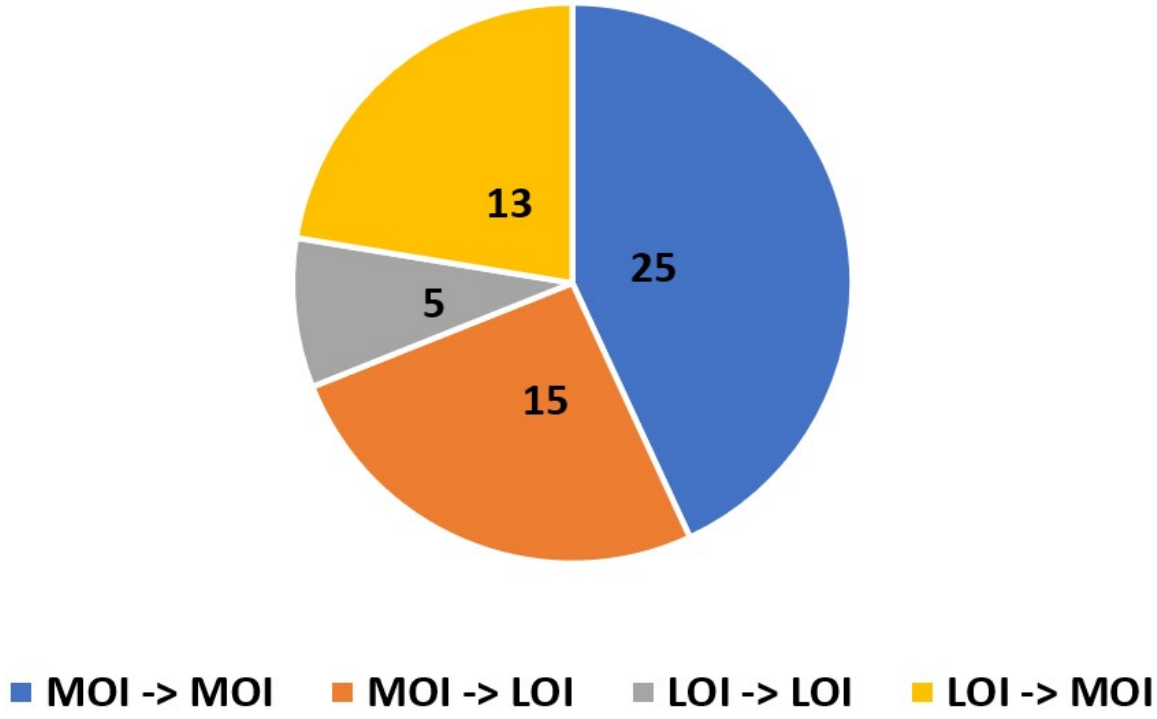

Figure 6.4.1.1: Imprinting status of the CRCM cohort using pyrosequencing. Tissue was typed as either 'MOI' (maintained imprinting) or 'LOI' (loss of imprinting). Of 58 paired patient samples, 25 presented with no change of MOI status (in the benign sample compared to its malignant counterpart), 15 presented with a change in status from MOI to LOI, 13 presented with a change in status from LOI to MOI and 5 presented with no change of LOI status (n=58).

6.4.1.2 Imprinting percentage of the CRCM cohort samples, using pyrosequencing.

Figure 6.4.1.2 shows the percentage imprinting within each genotype grouping. The group containing the 15 paired samples, with LOI in cancer compared with MOI in the benign tissue, showed a significant decrease ($p \leq .001$) in imprinting percentage. The group containing the 13 paired samples, with MOI in cancer compared with LOI in the benign tissue showed a significant increase ($p \leq .001$) in imprinting percentage (n=58).

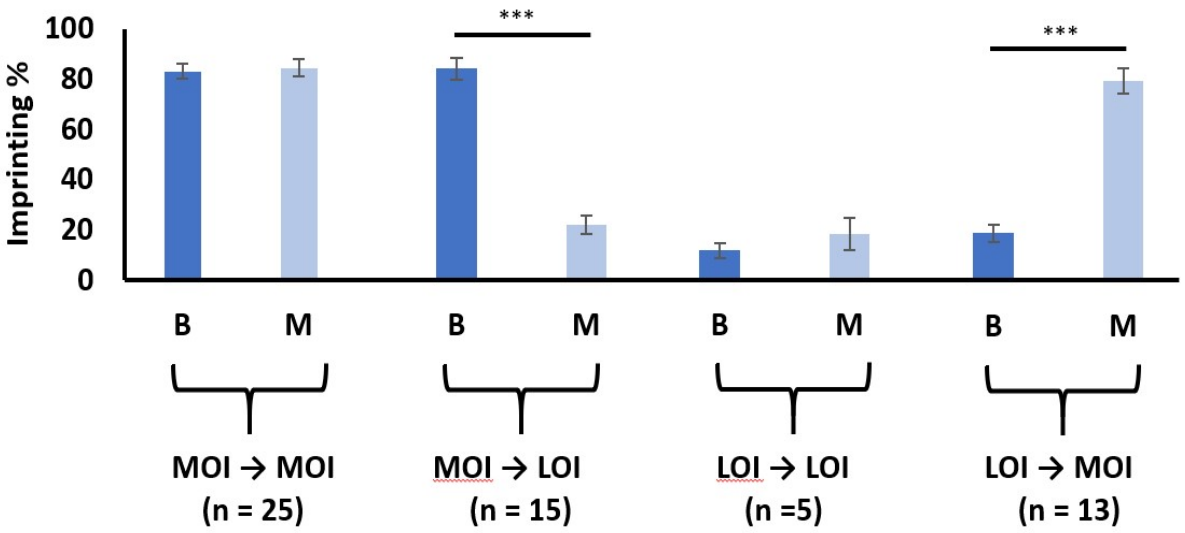

Figure 6.4.1.2: Imprinting percentage of the CRCM cohort using pyrosequencing. The group containing the 15 paired samples, with LOI in cancer compared with MOI in the benign tissue, showed a significant decrease ($p \leq .001$) in imprinting percentage. The group containing the 13 paired samples, with MOI in cancer compared with LOI in the benign tissue showed a significant increase ($p \leq .001$) in imprinting percentage (n=58).

6.4.1.3 Imprinting percentage related to IGF-II mRNA expression in the CRCM cohort.

There were non-significant positive correlations between imprinting percentage and IGF-II mRNA relative expression in benign (p = 0.718; R = 0.046) (figure A) and malignant (p = 0.992; R = 0.001) (figure B) tissue.

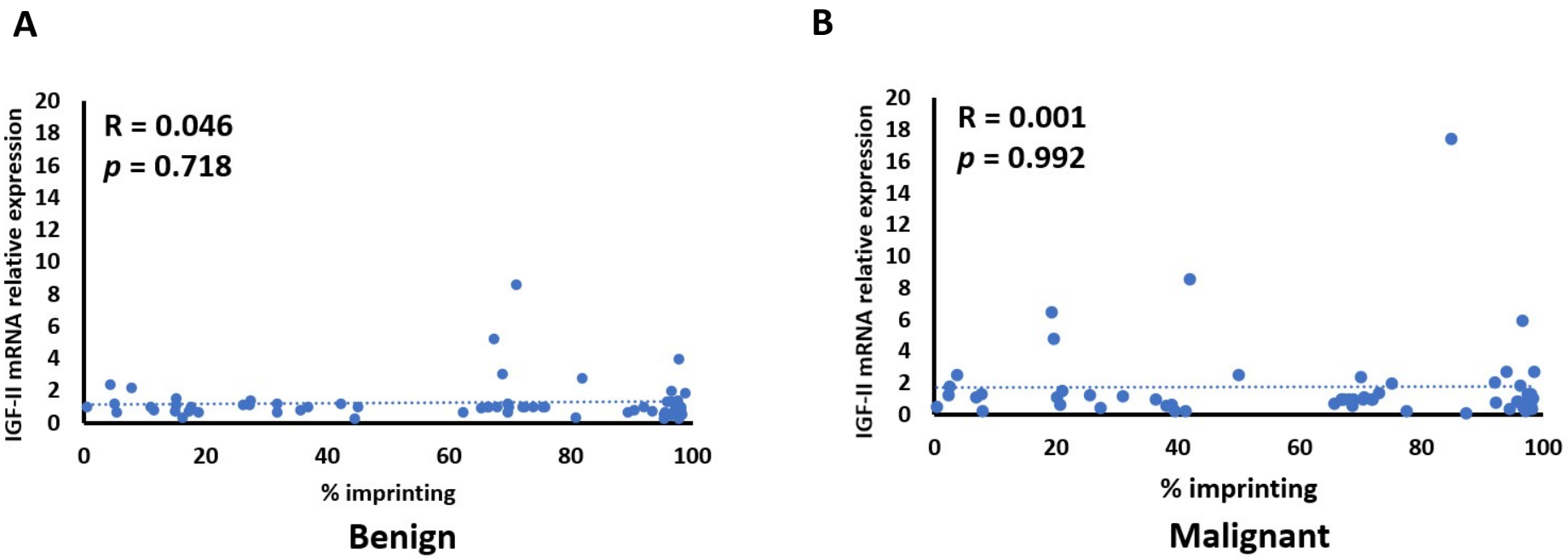

Figure 6.4.1.3 Imprinting percentage related to IGF-II mRNA expression in the CRCM cohort. There were non-significant positive correlations between imprinting percentage and IGF-II mRNA relative expression in benign (p = 0.718; R = 0.046) (**A**) and malignant (p = 0.992; R = 0.001) (**B**) tissue (n=58).

6.4.1.4 Imprinting percentage related to H19 mRNA expression in the CRCM cohort.

There were non-significant positive correlations between imprinting percentage and H19 mRNA relative expression in benign (p = 0.970; R = 0.005) (figure A) and malignant (p = 0.549; R = 0.082) (figure B) tissue.

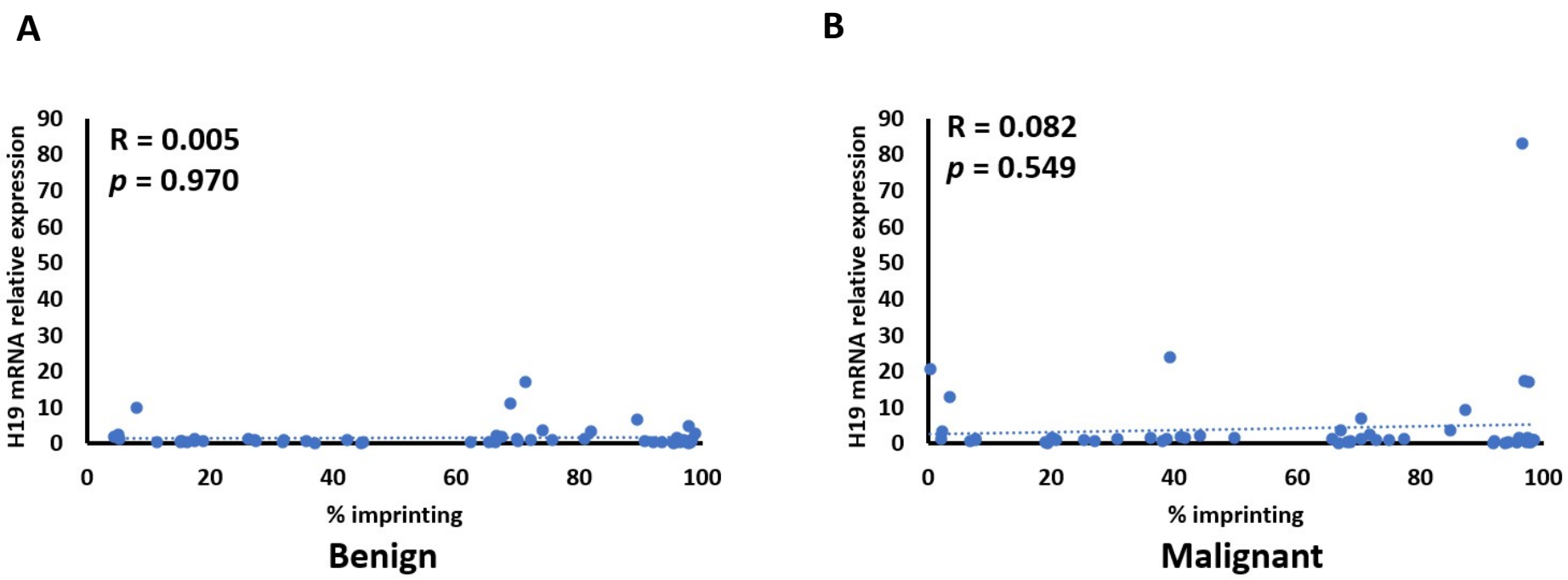

Figure 6.4.1.4 Imprinting percentage related to H19 mRNA expression in the CRCM cohort. There were non-significant positive correlations between imprinting percentage and H19 mRNA relative expression in benign (p = 0.970; R = 0.005) (**A**) and malignant (p = 0.549; R = 0.082) (**B**) tissue (n=58).

6.4.2.1 Co-expression of IGF-II and H19 in the CRCM cohort.

In benign colorectal tissue, there was a significant positive ($p \leq .001$; R = 0.750) correlation between co-expression of IGF-II and H19 mRNA (figure A). This was also true of malignant colorectal tissue, with the correlation being slightly weaker ($p = 0.015$; R = 0.317) (figure B).

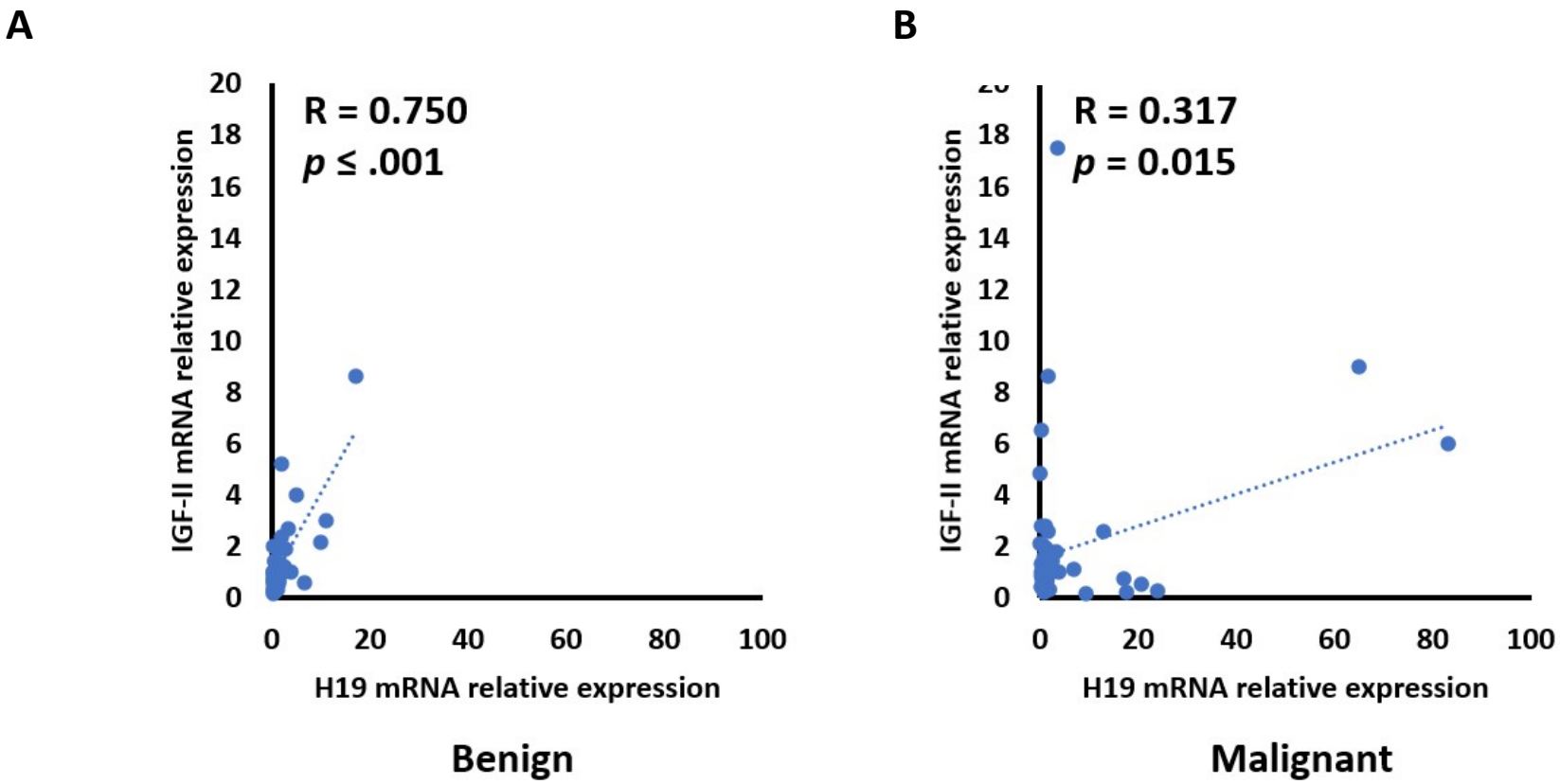

Figure 6.4.2.1: Co-expression of IGF-II and H19 in the CRCM cohort. In benign colorectal tissue, there was a significant positive ($p \leq .001$; R = 0.750) correlation between co-expression of IGF-II and H19 mRNA (**A**). This was also true of malignant colorectal tissue, with the correlation being slightly weaker ($p = 0.015$; R = 0.317) (**B**) (n=58).

6.4.2.2 Analysis of Metabric data from The Cancer Genome Atlas (TCGA).

After quantifying IGF-II and H19 mRNA expression in the CRCM cohort, the cBioPortal for Cancer Genomics website was accessed to assess whether there was a correlation between co-expression of IGF-II and H19 mRNA, in a larger colorectal cancer cohort. In the cohort, provided by the Cancer Genome Atlas (TCGA), a significant positive correlation ($p \leq .001$; R = 0.33) was seen between the co-expression of H19 and IGF-II mRNA in 592 patients (figure 6.4.2.2).

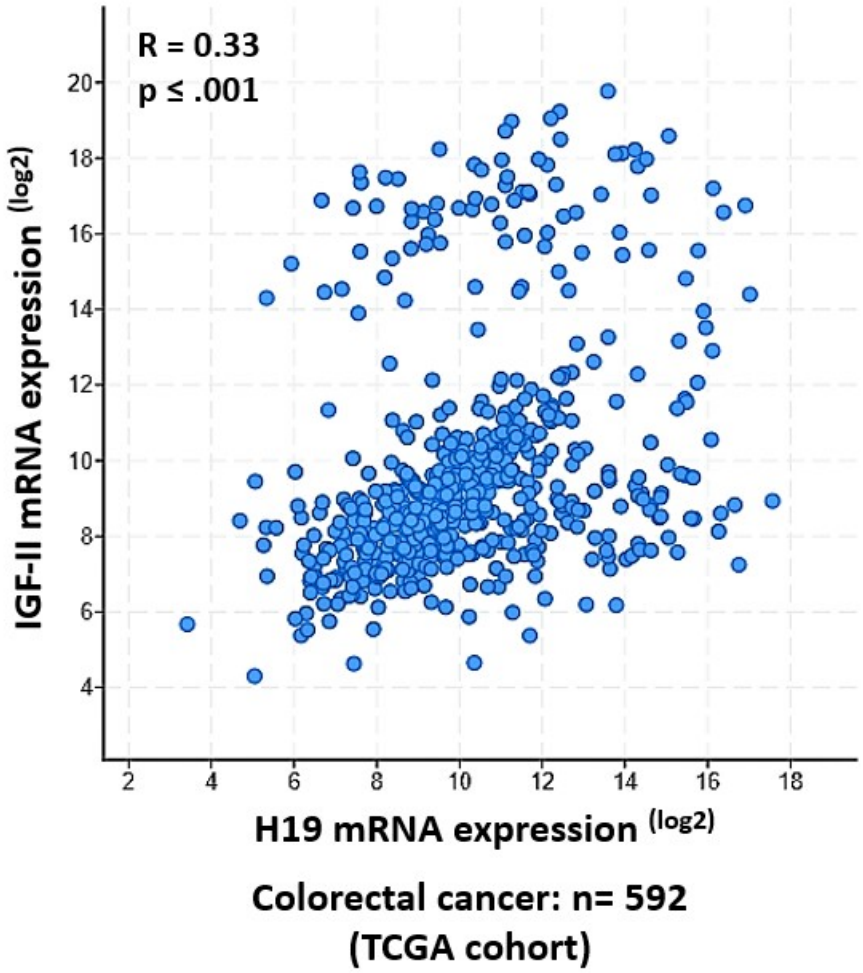

Figure 6.4.2.2: Analysis of Metabric data from The Cancer Genome Atlas (TCGA). In the TCGA cohort, a significant positive correlation ($p \leq .001$; R = 0.33) was seen between the co-expression of H19 and IGF-II mRNA in 592 patients.

6.4.3.1 IGF-II peptide levels and localisation in the CRCM cohort samples

Having analysed imprinting status and percentage, the tissue specimens were assessed for abundance of IGF-II peptide. Figure A shows IHC scores for 54, out of 58, paired samples from samples of the CRCM cohort. There was no significant difference in IGF-II peptide scores between benign and malignant colorectal tissue, overall.

In the group showing no change from MOI in benign tissue to MOI in malignant tissue, IGF-II peptide was significantly higher (p = 0.040) in the malignant group. There were no significant differences in the sample groups that showed a change from MOI to LOI, LOI to LOI or LOI to MOI status.

Representative staining patterns are shown by micrographs depicted in figure B.

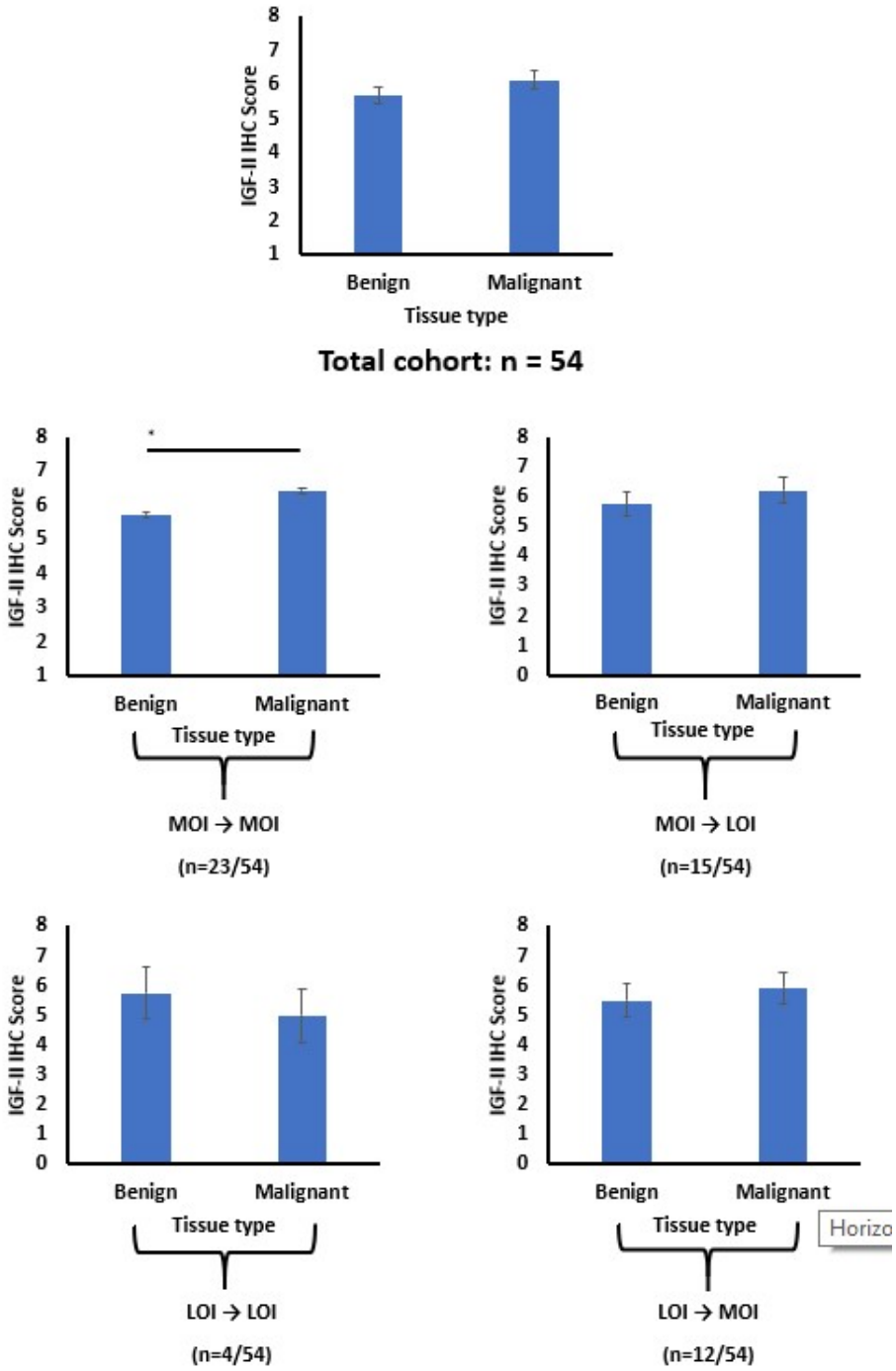

Figure 6.4.3.1.A: IHC scores of 54 paired samples from the CRCM cohort. There was no significant difference in IGF-II peptide scores between benign and malignant colorectal tissue, overall. In the group showing no change, from MOI in benign tissue to MOI in malignant tissue, IGF-II peptide was significantly higher (p = 0.040) in the malignant group. There were no significant differences in the sample groups that showed a change from MOI to LOI, LOI to LOI or LOI to MOI status.

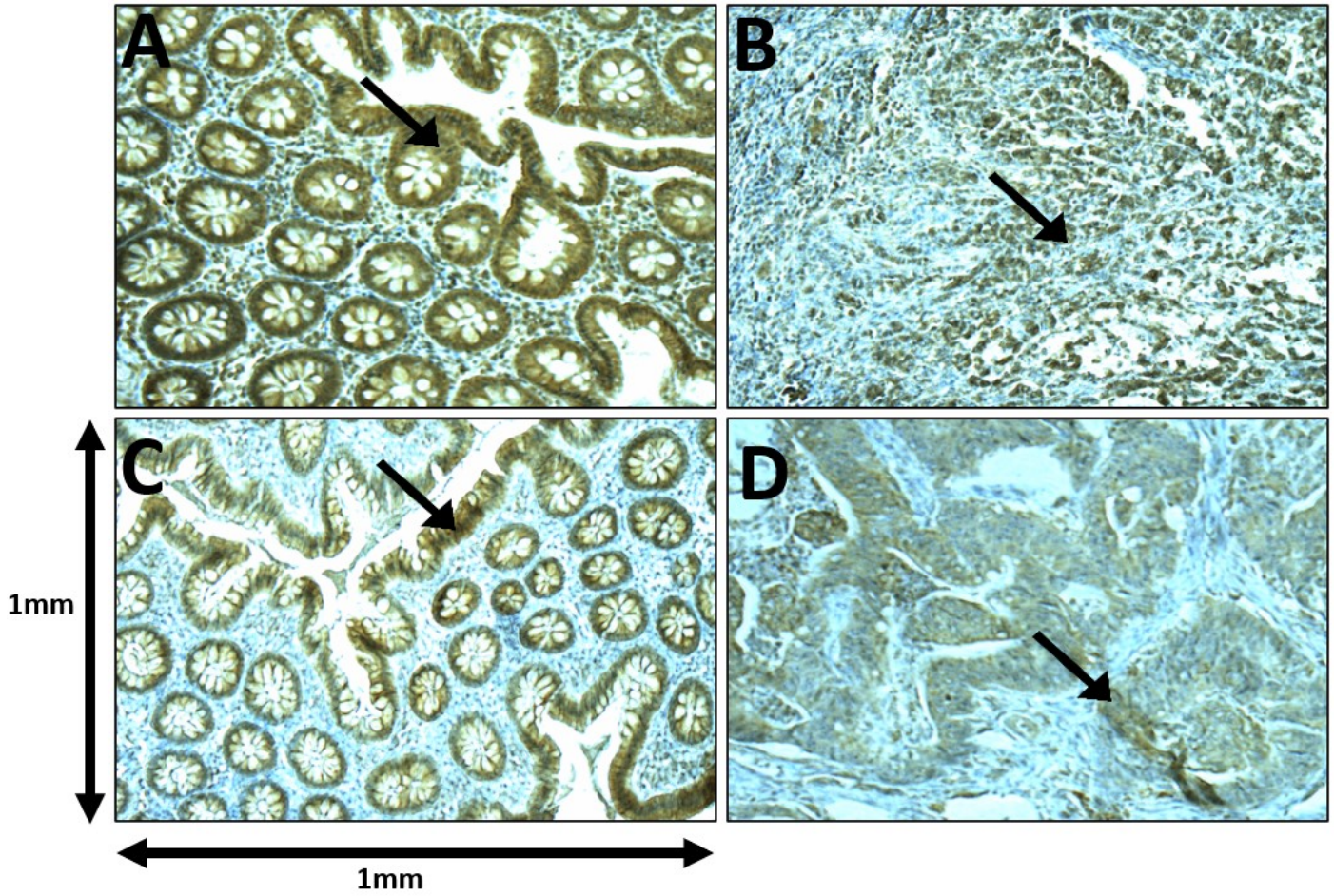

Figure 6.4.3.1.B: Benign and malignant paired colorectal cancer tissue samples from 2 patients of the CRCM cohort. Benign tissue is shown in images A and C; malignant tissue is shown in images B and D. Arrows indicate areas of strong, dark brown cytoplasmic staining, observed in both benign and malignant tissues. Scale is 1x1 mm, at 20x magnification.

6.4.3.2 IGF-II peptide levels related to imprinting percentage in the CRCM cohort.

To assess whether there was an association between IGF-II peptide expression and imprinting percentage in the CRCM cohort, a Pearson correlation coefficient was calculated. There was a non-significant, positive correlation (p = 0.095; R = 0.010) between IGF-II peptide expression and imprinting percentage in benign colorectal tissue (figure A). In malignant colorectal tissue (figure B), there was a non-significant positive correlation (p = 0.059; R = 0.259) between IGF-II peptide expression and imprinting percentage.

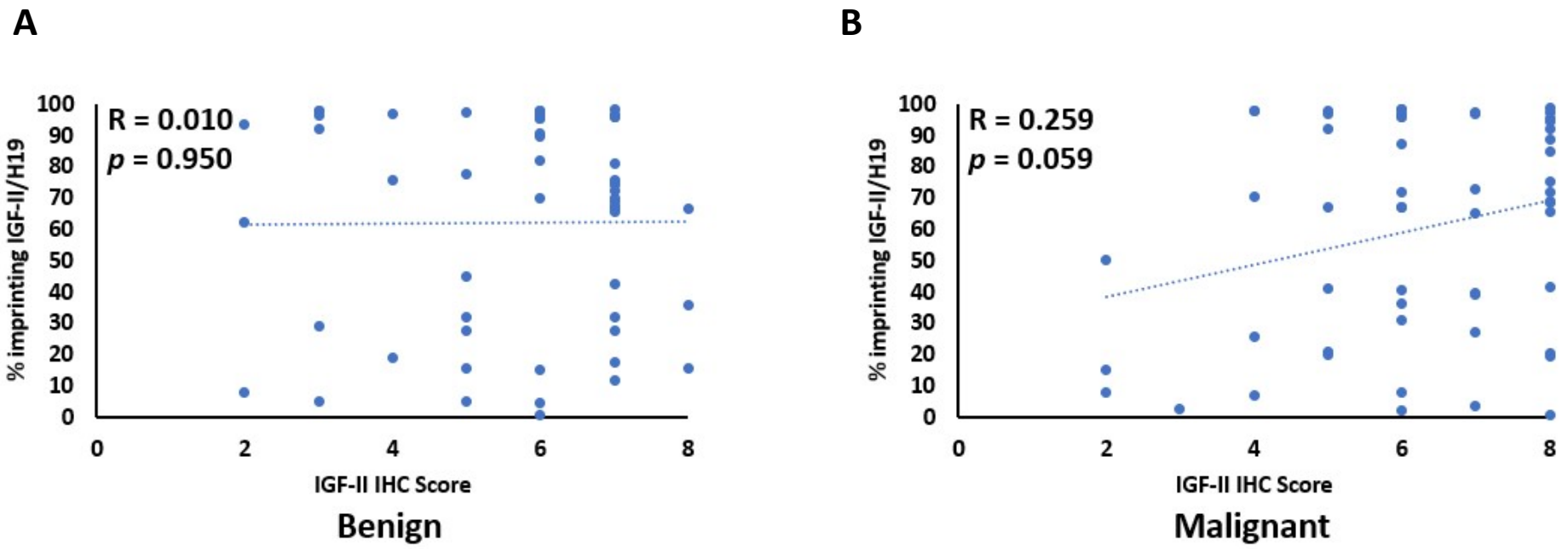

Figure 6.4.3.2: IGF-II peptide expression related to imprinting percentage in the CRCM cohort. There was a non-significant, positive (p = 0.095; R = 0.010) correlation between IGF-II peptide levels and imprinting percentage in benign (**A**) tissue. In (**B**) malignant tissue, there was a non-significant positive correlation (p = 0.059; R = 0.259) between IGF-II peptide expression and imprinting percentage (n = 54).

6.4.3.3 IGF-II peptide levels related to IGF-II mRNA, in the CRCM cohort.

To assess whether there was an association between IGF-II peptide and IGF-II mRNA expression in the CRCM cohort, a Pearson correlation coefficient was calculated. In benign colorectal tissue there was a non-significant negative correlation (p = 0.950; R = - 0.019) between IGF-II peptide and mRNA expression (figure A). In malignant colorectal tissue there was a non-significant positive correlation (p = 0.146; R = 0.213) between IGF-II peptide and mRNA expression (figure B).

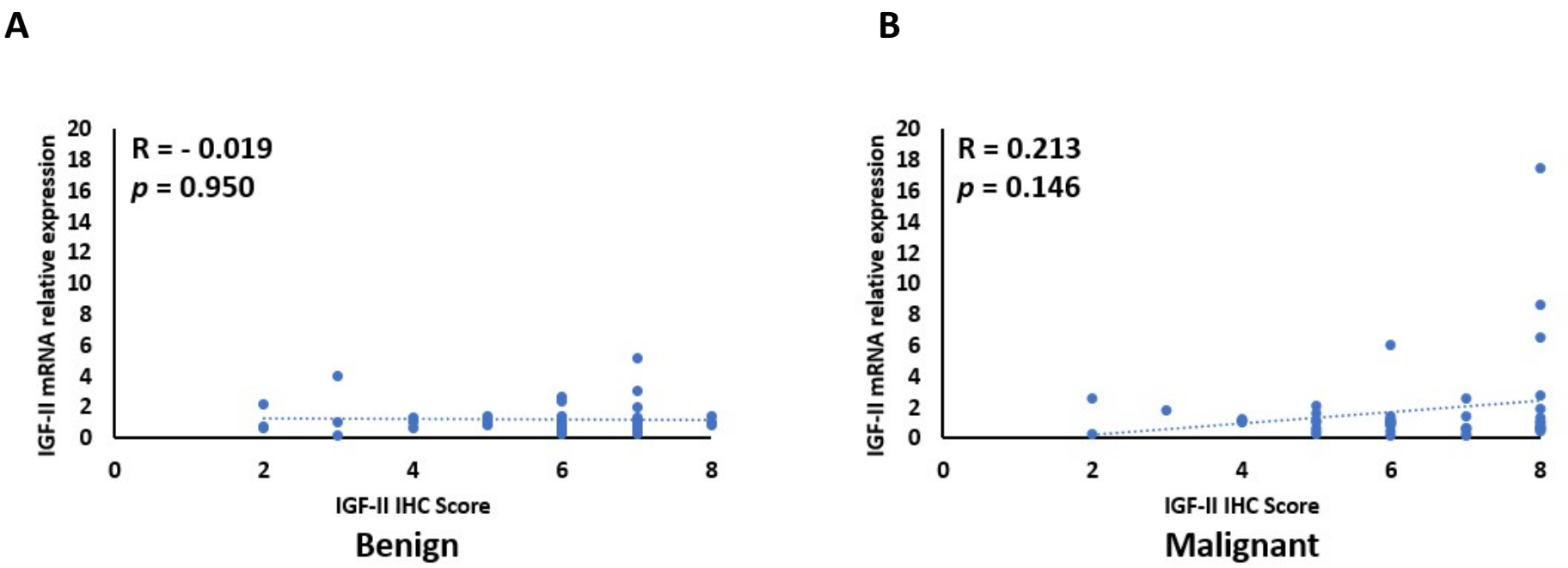

Figure 6.4.3.3 IGF-II peptide levels related to IGF-II mRNA, in the CRCM cohort. In benign colorectal tissue there was a non-significant negative correlation (*p* = 0.950; R = - 0.019) between IGF-II peptide and mRNA expression (**A**). In malignant colorectal tissue there was a non-significant positive correlation (*p* = 0.146; R = 0.213) between IGF-II peptide and mRNA expression (**B**).

6.4.4.1 Disease staging related to imprinting percentage.

Disease staging was classified using the TNM system (Bowelcanceruk.org.uk., 2019[2]). This data was accessed through the Sunquest Integrated Clinical Environment (ICE) patient records system. Disease staging was defined as below.

T stage	Tumour location
1	Tumour is small and localised to the inner layer of the bowel
2	Tumour has invaded the muscle layer of the bowel wall
3	Tumour has invaded the outer layer of the bowel wall
4	Tumour has grown through the outer lining of the bowel wall

To ascertain whether there was a correlation between disease staging and imprinting percentage, a Pearson correlation coefficient was calculated. There was a non-significant negative correlation (p = 0.101; R = - 0.161) between disease stage and imprinting percentage (figure 6.4.4.1.).

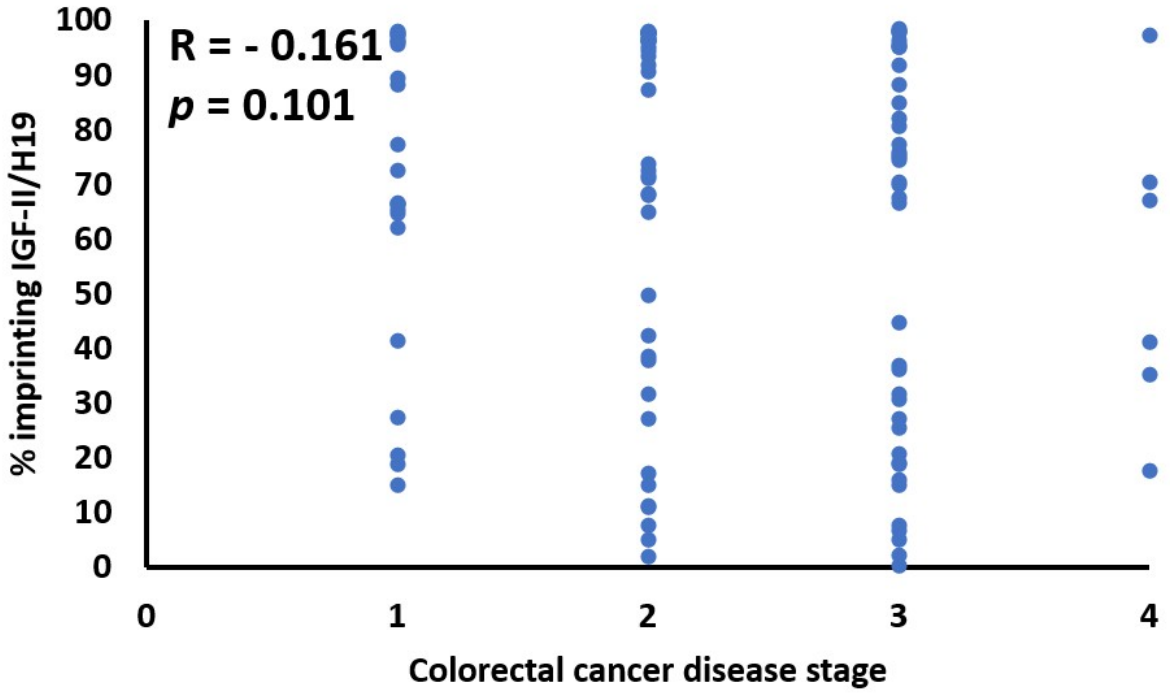

Figure 6.4.4.1: Disease staging related to imprinting percentage. There was a non-significant negative correlation (p = 0.101; R = -0.161) between disease stage and imprinting percentage.

6.4.4.2 Disease staging related to IGF-II peptide.

There was a non-significant positive correlation (p = 0.697; R = 0.039) between disease stage and IGF-II peptide (figure 6.4.4.2).

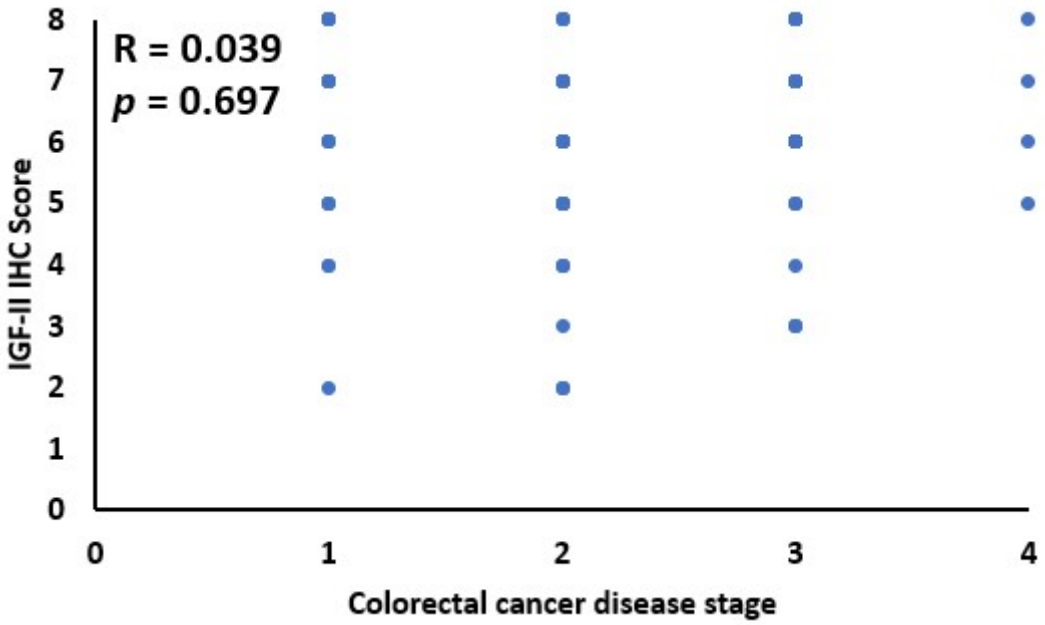

Figure 6.4.4.2: Disease staging related to IGF-II peptide. There was a non-significant positive correlation (p = 0.697; R = 0.039) between disease stage and IGF-II peptide.

6.4.4.3 Disease staging related to IGF-II mRNA relative expression.

There was a non-significant positive correlation (p = 0.798; R = 0.024) between disease stage and IGF-II peptide (figure 6.4.4.3).

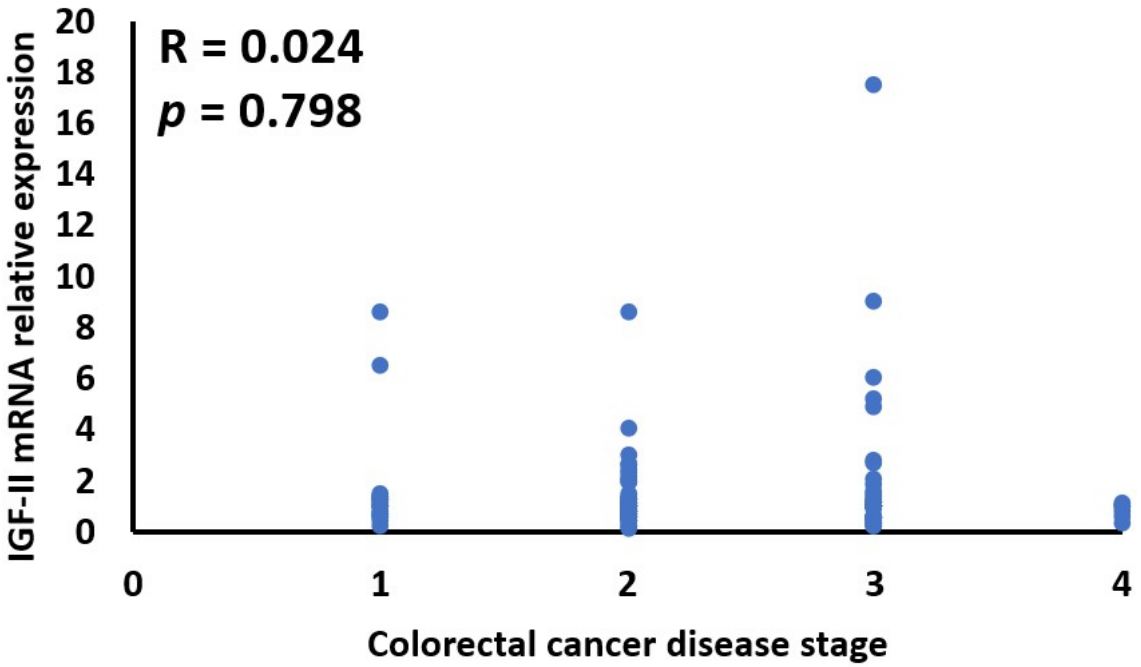

Figure 6.4.4.3: Disease staging related to IGF-II mRNA expression. There was a non-significant positive correlation (p = 0.798; R = 0.024) between disease stage and IGF-II peptide.

6.5 Discussion.

This study has explored the effects of IGF-II/H19 imprinting upon mRNA, peptide, and disease staging in a colorectal clinical cohort.

Initial genotyping of matched benign and malignant CRC tissue specimens revealed most samples exhibited no change in maintenance of imprinting status. These findings concur with those of Kinouchi *et al*, where MOI was found in 8 out of 13 cancer patient tissue samples, and LOI in 5. Moreover, 3 of the 5 patients with LOI presented with biallelic expression of IGF-II in the normal mucosa (Kinouchi, Hiwatashi *et al*. 1996). Conversely, Cui *et al* showed LOI to occur in 12 out 27 patient cases of cancer, with 11 of those 12 showing LOI in normal mucosa; the imprinting status in 15 out of 27 cases was not discussed (Cui, Horon *et al*. 1998). Elsewhere, Nakagawa *et al* showed LOI to have occurred in 17 out of 20 CRC patient samples, with LOI occurring in the normal mucosa of 13 (Nakagawa, Chadwick *et al*. 2001). It is likely that findings described in this chapter may be limited by cohort size. Alternatively, if samples were to be grouped purely by imprinting status and not tissue type, 32% presented with LOI. This *is* comparable with those findings by Cui *et al.* (Cui, Horon *et al*. 1998; Cui, Cruz-Correa *et al*. 2003).

Subsequent analysis of genotyped samples revealed significant decreases in imprinting percentage in specimens presenting with LOI, in both benign and malignant tissues. In terms of allelic expression, the imprinting percentage value was devised to equate as a quantifiable measure of this occurrence; where biallelic expression increases, imprinting percentage decreases and vice versa. These data – increased biallelic expression in tissues with LOI - concurs with initial findings by Weksberg *et al*. (Weksberg, Shen *et al*. 1993) who demonstrated LOI in IGF-II to be synonymous with biallelic expression in patients with Beckwith-Wiedemann syndrome. Subsequent studies in the cancer field, such as those in hepatoblastoma (Davies 1993), neuroblastoma (Wada, Seeger *et al*. 1995),

colorectal (Kinouchi, Hiwatashi *et al*. 1996) and breast (Wu, Squire *et al*. 1997) cancer further confirmed these findings.

Investigation of co-expression of IGF and H19 mRNA revealed positive correlations in both benign and malignant colorectal tissue. This was further confirmed by a comparative analysis with a larger colorectal cancer cohort, accessed through the cBioPortal Cancer Genomics database. Data included in the Cancer Genomics database does not specify imprinting status of included samples. Moreover, approximately two-thirds of the CRCM cohort retained imprinting status. Therefore, it may be deduced that aberrant expression of IGF-II and H19 is occurring through other means, in addition to LOI. Other causes of increased IGF-II mRNA expression include reactivation of promoter 3 (Brouwer-Visser and Huang 2015), loss of suppression (Lu, Cai *et al*. 2019) and increased copy number (Weischenfeldt, Dubash *et al*. 2017). Causes of aberrant H19 expression include loss of suppression (Liang, Zou *et al*. 2017) and upregulation of CTCF (Lai, Li *et al*. 2020). Co-expression of IGF-II and H19 was further explored in other cancer types, using the cBioPortal database; significant positive correlations were also seen in liver hepatocellular carcinoma ($p \leq .001$; R = 0.51; n=366), stomach adenocarcinoma ($p \leq .001$; R = 0.55; n=412), bladder cancer ($p \leq .001$; R = 0.36; n=407), head and neck squamous cell carcinoma ($p \leq .001$; R = 0.17; n=515) and pancreatic adenocarcinoma ($p \leq .001$; R = 0.42; n=96).

Analysis of IGF-II peptide levels showed no significant differences between benign and malignant colorectal tissue, overall. Due to the short half life of unbound IGF-II (Guler, Zapf *et al*. 1989; Allard and Duan 2018), it will bind with a binding protein, to form a stabilised complex (Yamanaka, Wilson *et al*. 1997). IGF-II primarily binds with IGFBP2, but can also bind IGFBP3 (Ismayilnajadteymurabadi and Konukoglu 2018). The limitation of the IGF-II IHC stain is that it does not differentiate between IGF binding protein type. Whilst IGF-II tissue-based evidence is limited, there have been some serum-based findings which may be offer some explanation for the CRCM IGF-II peptide data;

Renehan *et al* showed elevated serum levels of both IGF-II and IGFBP2 in patients with colorectal cancer (Renehan, Jones *et al*. 2000), as did Liou *et al* (Liou, Shun *et al*. 2010) . Conversely, increased circulatory IGF-II peptide has been linked with elevated IGFBP3 in two studies (Probst-Hensch, Yuan *et al*. 2001; Murphy, Knuppel *et al*. 2020). Moreover, Yamamoto *et al* suggested IGFBP-3 as an effective predictor of disease prognosis, with overexpression being linked with poor 5-year survival (Yamamoto, Oshima *et al*. 2017).

The absence of a significant correlation between IGF-II peptide and IGF-II/H19 mRNA expression was unexpected, as the links between CRC and IGF-II peptide have been described (Matuschek, Rudoy *et al*. 2011; see review by Kasprzak and Adamek 2019). Whilst the correlation was non-significant, it's likely that a larger cohort may have strengthened the P value (Thiese, Ronna *et al*. 2016). A recent publication described lnc91H to play an influential role in IGF-II peptide levels in colorectal cancer; lncRNA 91H is an antisense transcript of H19. Upregulation of 91H is associated with poor prognostic outcome in colorectal cancer (Deng, He *et al*. 2014; Gao, Liu *et al*. 2018). A recent study found 91H to be instrumental in the regulation of IGF-II expression by interacting with IGFBP-2 (Gao, Liu *et al*. 2020). In the context of the CRCM data, 91H may have regulated expression of IGF-II by regulating expression of IGFBP2, keeping both IGF-II mRNA and peptide in balance with one another.

Examining the potential link between disease staging and IGF-II imprinting revealed a non-significant, negative correlation: as imprinting decreases, disease stage increases. Again, with the correlation being non-significant, a larger cohort could have strengthened the P value (Thiese, Ronna *et al*. 2016). The presence of a negative correlation concurs with findings shown by other studies, where loss of imprinting was shown to be to be associated with disease progression in other cancer types; in leukaemia, upregulation of H19 caused by disrupted imprinting, correlated with poor prognosis (Zhang, Zhou *et al*. 2018). Cheng *et al* (Chen, Zhu *et al*. 2017) showed overexpression of

H19, through disrupted imprinting, to be linked with disease metastasis and poor prognosis in colorectal cancer.

Exploring the link between tissue-based IGF-II peptide levels in and disease staging showed a non-significant positive correlation. Once more, these results may be attributed to cohort size since positive correlations have been shown elsewhere; elevated expression of tissue-based IGF-II peptide has been linked with poor prognostic outcome in ovarian cancer (Dong, Li *et al*. 2015). In 2017, Unger *et al* (Unger, Kramer *et al*. 2017) established that CRC cell stroma-derived IGF-II drove cancer progression.

Whilst there were no significant findings between IGF-II mRNA and disease staging in this study, a study published in 2016 (Ye, Song *et al*. 2016) identified an IGF-II mRNA binding protein, IMP2, as not only being upregulated in CRC, but also behaving as an enhancer of cancer cell proliferation. Increased expression of IMP2 has also been linked to disease staging and prognosis in oesophageal cancer (Barghash, Golob-Schwarzl *et al*. 2016). Quantification of IMP2 may serve to clarify the underlying reason behind an absence of correlative findings between IGF-II peptide, imprinting and mRNA; IMP2 is a post-transcriptional modulator. It binds with IGF-II mRNA transcripts to form stable RBP complexes, which play an intermediary role in the peptide translation process (Oleynikov and Singer 2003; Huang, Zhang *et al*. 2018).

6.6 Conclusion

Despite results in this chapter being largely non-significant, positive correlations were seen between imprinting percentage and IGF-II mRNA, H19 mRNA and IGF-II peptide and a negative correlation was also observed between imprinting percentage and disease staging. A significant positive correlation was seen between co-expression of IGF-II and H19 mRNA.

CHAPTER 7: FINAL DISCUSSION & FUTURE WORK

7.1 Final discussion.

Current evidence linking metabolism to imprinting loss is limited; many studies have highlighted the relationship between T2D/obesity ("diabesity") and IGF-II/H19, or DNA methylation through meta-analyses, but appear to have neglected how "diabesity" exerts its metabolic disturbance specifically upon loss of imprinting of IGF-II/H19. This thesis has aimed to address this gap in knowledge by investigating the effects of "diabesity" on IGF-II/H19 imprinting status at the molecular level, through simulating an environment, akin to that associated with T2D and/or obesity, *in vitro* and quantifying of imprinting percentage, IGF-II and H19 mRNA and IGF-II peptide levels. Further comparisons of *in vitro* data with *in vivo* tissue samples provided an insight into the mechanistic behaviour of imprinting in two different cancer types. This was achieved with access to PCa and CRC tissue collected for two clinical studies; between 2008 and 2015, over 100 PCa patient samples were collected for the PrEvENT study, whilst CRC tissue from more than 60 patients was collected for the Metformin study, between 2014 and 2017. Through comparison of data sets, it became apparent that disruption of IGF-II/H19 imprinting, *in vitro,* shares some similarities with that *in vivo*; moreover, the mechanics of imprinting appear to differ between PCa and CRC tissue.

Aberrant expression of IGF-II was first explored in the paediatric cancer, Wilms tumour; elevated amounts of IGF-II mRNA were first explored in 1985 (Reeve, Eccles *et al*. 1985), with the subsequent cause identified as being loss of imprinting, in 1993 (Ogawa, Eccles *et al*. 1993). The effect of imprinting loss of IGF-II upon H19 was explored a year later (Steenman, Rainier *et al*. 1994), where it was found to have caused down regulation of H19, due to altered methylation patterns. Since these discoveries, loss of imprinting of IGF-II has been identified in other cancer types, such as lung (Skinner, Vollmer *et al*. 1990), breast (Ali, Lidereau *et al*. 1987), prostate (Jarrard, Bussemakers *et al*. 1995) and colorectal (Kinouchi, Hiwatashi *et al*. 1996). This thesis has focused on IGF-II/ H19 imprinting loss in PCa and CRC.

Although loss of imprinting in IGF-II / H19 has been recorded in PCa (Jarrard, Bussemakers *et al*. 1995) and colorectal (Kinouchi, Hiwatashi *et al*. 1996) cancer, little evidence is available regarding the cause of such events. Relaxation of imprinting is thought to occur from disrupted methylation patterns across the gene locus at one or more of the differentially methylated regions (DMRs) (Schagdarsurengin, Lammert *et al*. 2017; Kuffer, Gutting *et al*. 2018). Imprinting of IGF / H19 is a heritable epigenetic trait, but what causes sporadic imprinting loss in some cancers? Known causes of epigenetic alterations include dietary intake, viral and bacterial infection, physical fitness and environmental pollution (Bayarsaihan 2011).

Diet and body mass index (BMI) are two intertwined elements that are known to be implicated in PCa and CRC risk (Alsheridah and Akhtar 2018; Fujita, Hayashi *et al*. 2019); a diet high in processed foods, partnered with low/limited physical activity, contributes to increased adiposity and/or obesity (Poti, Braga *et al*. 2017). Increased adiposity associated with obesity will result in increased secretion of growth factors and cytokines, which may disrupt the delicate balance of the cellular milieu (Lengyel, Makowski *et al*. 2018). Another complication of obesity is type 2 diabetes (T2D) (Wang, McPherson *et al*. 2011; Huang, Liu *et al*. 2018); a chronic condition characterised by an excess of glucose in the blood, which is also known as hyperglycaemia (NHS.uk, 2018). First line treatment for T2D is metformin, a glucose-sensitising drug that exerts its effects by decreasing hepatic glucose output, and increasing absorption by peripheral tissues (Kaneto, Kimura *et al*. 2021). Moreover, cancer incidence amongst metformin-prescribed individuals with T2D is lower than those receiving other types of diabetic medication (Decensi, Puntoni *et al*. 2010; Franciosi, Lucisano *et al*. 2013; Kim, Lee *et al*. 2018). Coupled with elevated amounts of adipocytokines, hyperglycaemia results in a physiological inflammatory state (Karczewski, Sledzinska *et al*. 2018). As epigenetic modifications occur as a result of chronic inflammation (Shanmugam and Sethi 2013), the effects of simulating elements of an inflammatory state on the imprinting status of IGF-II / H19 in PCa and CRC was addressed in chapters 3 and 5.

In PCa, *in vitro* findings showed that glucose levels above the physiologically normal range – 5mM/L (4- to 5.9 mM/L for an adult – according to NICE guidelines, The National Institute for Health and Care Excellence, 2012) were sufficient to induce partial loss of imprinting. This caused an increase in IGF-II mRNA and a reciprocal decrease in H19 mRNA after 48 hours. This partial loss of imprinting was marked by the gradual introduction of biallelic expression of IGF-II, with both parental copies being either partially or completely expressed. In CRC, a significant increase in IGF-II mRNA by cells cultured glucose media containing >5mM/L was similarly observed. However, this was not associated with a reciprocal decrease in H19; an initial increase in H19 was observed at an early stage (6 hours), which dropped back to control levels after 24 hours. These data suggest that glucose may be exerting its effects differently according to cell type. Because of its large molecular weight and polar charge, glucose is unable to pass through cell membranes by straightforward diffusion. Instead, passage is facilitated by glucose transporters (GLUTs) (Navale and Paranjape 2016). At the cellular level, transport of glucose across the membrane of a PCa cell may differ to that of a CRC cell; PC3 cells might have a comparatively low number or fewer types of glucose transporter, which may explain how glucose was able to exert a response after prolonged exposure. Whilst PC3 cells are derived from the prostate, the HCT116 cell line is derived from the colon / large intestine. The initial increase in H19 seen after 6 hours, by HCT116 cells, may be due to rapid transport of glucose across the cell membrane by either a greater transporter number and/or variety. A literature search of the potential differences between PCa and CRC cells was conducted; Gonzalez-Menendez *et al* demonstrated overexpression of GLUT1 in PCa protects cells from glucose deprivation-induced oxidative stress (Gonzalez-Menendez, Hevia *et al*. 2018), whilst Shao *et al* demonstrated that silencing GLUT1 reduces glucose uptake (Shao, Yu *et al*. 2020). Expression of GLUT1 is also upregulated in high-risk PCa (Meziou, Ringuette Goulet *et al*. 2020). However, upregulation of GLUT1 has also been shown in CRC (Yang, Wen *et al*. 2017; Ancey, Contat *et al*. 2018). Aberrant expression of GLUT3 has also been seen in CRC; Yes-associated protein (YAP) has been shown to promote

expression of GLUT3, causing enhanced cellular proliferation and migration in CRC cell lines HCT116 and CaCo2, as well as in tissue (Jiang, Zhang *et al*. 2021); Yang *et al* showed high mobility group protein A1 (HMGA1) to upregulate GLUT3 in CRC, which enhanced metastatic behaviour of cancer cells (Yang, Guo *et al*. 2020). It may be suggested, therefore, that a combination of differential GLUT expression and type could be potential causes behind the discordant findings between the two cell lines.

High glucose levels have also been shown to cause epigenetic disruption to the structure of chromatin by activating signalling pathways associated with the regulation of epigenetic factors connected with DNA methylation, histone modifications and microRNAs, resulting in aberrant gene expression (Villeneuve, Reddy *et al*. 2011). For example, in human pancreatic islet cells, high glucose has been shown to epigenetically alter the gene expression of those involved in insulin secretion, *in vitro*; human pancreatic islets were shown to express aberrant levels of glycine receptor alpha-1 (GLRA1), rat sarcoma-related dexamethasone induced-1 (RASD1), solute carrier organic anion transporter family-5 (SLCO5A1) and cholinergic receptor nicotinic alpha 5 subunit (CHRNA5) as a result of disrupted methylation patterns, induced by high glucose media (Hall, Dekker Nitert *et al*. 2018). Similarly, exposure to high glucose has been shown to cause disrupted histone deacetylase inhibition and histone methyltransferase expression in kidney cells, resembling those seen in diabetic nephropathy (Fuhrmann, Lindner *et al*. 2021). High glucose has also been shown to induce apoptosis of chondrocytes (cartilage cells) by epigenetically activating caspase-3 (Hua, Wang *et al*. 2020).

In PCa, at the mRNA level, glucose appears to exert its effect by inducing upregulation of IGF-II and downregulation of H19 mRNA, after 48 hours. At the same time point, in CRC, only IGF-II is upregulated. Applying the previously posited 'Enhancer Competition Model' (Nordin, Bergman *et al*. 2014) to these findings, it could be suggested that high glucose levels cause disruption of IGF-II / H19

imprinting status by displacing ICR-bound CTCF on the maternal allele, to permit transcription of IGF-II and block transcription of H19. This theory would serve to address the events of those seen in PCa; imprinting percentage decreased and biallelic expression of IGF-II was observed. However, the same expression pattern of mRNA by the colorectal cells was not seen. In 2010 (Cheng, Idrees *et al*. 2010) posited an alternative mechanism for IGF-II/H19 imprinting loss in CRC; through methylation analysis it was shown that LOI correlated with hypomethylation of the DMRs in both IGF-II and H19. It was also demonstrated that IGF-II promoter hypomethylation induced loss of imprinting, and aberrant methylation of IGF-II or H19 correlated with increased expression of IGF-II. These findings were further confirmed two years later by Tian *et al*, where hypermethylation of CTCF was four-times higher in CRC tissue with MOI status compared to those with LOI (Tian, Tang *et al*. 2012). The alternative imprinting scenarios, posited by Cheng *et al* and Tian *et al* may serve to address the discordant expression patterns of H19 observed between the two cancer types (i.e., PC3 and HCT116).

Aside from imprinting loss, upregulation of IGF-II in also occurs through reactivation of its promoter, P3 (Brouwer-Visser and Huang 2015; Kasprzak and Adamek 2019), although other mechanisms have been identified – such as chromosomal gains at 11p15.5 (Rogers, Kalter *et al*. 2016) and enhancer hijacking (Weischenfeldt, Dubash *et al*. 2017) (the recruitment of ectopic gene enhancers to enable transcription (Helmsauer, Valieva *et al*. 2020). P3 is oncofoetal and is activated by the E2F transcription factor (E2F3) (Lui and Baron 2013). Interestingly, as with IGF-II, E2F3 has been shown to be upregulated in a number of cancer types including bladder (Bellmunt 2018), breast (Liu, Bi *et al*. 2018), prostate (Liang, Hu *et al*. 2020; Hu, Lou *et al*. 2021) and colorectal (Chang, Yue *et al*. 2015; Wu, Sheng *et al*. 2018) . Moreover, also like IGF-II, the E2F3 gene is subject to epigenetic regulation (Feng, Peng *et al*. 2018; Ramos-Lopez, Riezu-Boj *et al*. 2019; Xu, Li *et al*. 2020).

As with the effects of glucose, treatment with the inflammatory cytokine, TNF-alpha, also elicited different responses in each cell line; in PCa, it significantly increased expression of IGF-II mRNA but

had no effect on H19. Conversely, in CRC it increased levels of both IGF-II and H19 mRNA. TNF-alpha is a pro-inflammatory cytokine involved in wide range of cellular processes, such as proliferation, differentiation and apoptosis (Wang and Lin 2008). In obese individuals and those with T2D, TNF-alpha levels have been shown to be higher than those of healthy persons (Hotamisligil, Shargill *et al*. 1993; Ibfelt, Fischer *et al*. 2014). Moreover, TNF-alpha has been shown to impact the effects of glucose by contributing to insulin resistance through down regulation of GLUT4 (Hauner, Petruschke *et al*. 1995; Kaddai, Jager *et al*. 2009; Zhao, Liu *et al*. 2021). However, IGF-II and H19 mRNA expression were affected in both cell lines, in normal glucose conditions. Assuming TNF-alpha affected glucose uptake, a state of oxidative stress caused by glucose deprivation, may have arisen (Spitz, Sim *et al*. 2000; Simons, Mattson *et al*. 2009). Oxidative stress creates reactive oxygen species (ROS), also known as free radicals; these molecules cause disruption to the regulation of specific genes and pathways, resulting in aberrant expression and signalling (Allen and Tresini 2000); TNF-alpha-induced oxidative stress may account for the aberrant expression of IGF-II and H19 mRNA expression in normal glucose conditions. The discordant findings between the two cell types may again be attributed to differential expression of GLUT proteins, either through cell membrane morphology or inhibited GLUT expression by TNF-alpha (Hauner, Petruschke *et al*. 1995).

In PCa, loss of imprinting status – induced independently by high glucose, TNF-alpha, or in combination - resulted in increased IGF-II mRNA expression. Unexpectedly, these increases in mRNA were untranslated into peptide. In the context of these findings, it may be suggested that an absence or insufficient amount of post-transcriptional modification proteins - such as IGF-II mRNA binding proteins (IMPs) - may offer a potential explanation as to why the increased IGF-II mRNA was not converted into protein; IMPs bind to IGF-II mRNA transcripts to form stable protein complexes, called ribonucleoprotein particles or RNPs (Oleynikov and Singer 2003). They also act as post-transcriptional modulators, regulating expression of IGF-II mRNA transcripts that are vital for cellular growth and proliferation (Huang, Zhang *et al*. 2018). There are three classes of IMP: IMP1-3 (Dai, Ji *et*

al. 2017). However, available evidence pertaining to IMP expression in cancer is associated with increased synthesis; upregulation of IMP1 has been shown in CRC (Andres, Williams *et al*. 2019), melanoma (Kim, Havighurst *et al*. 2018); upregulation of IMP2 has been observed in hepatocellular carcinoma (Xing, Li *et al*. 2019) and pancreatic (Dahlem, Barghash *et al*. 2019) and breast (McMullen, Gonzalez *et al*. 2018) cancer, whilst overexpression of IMP3 has been seen in rectal (Bevanda Glibo, Bevanda *et al*. 2021) and lung (Xueqing, Jun *et al*. 2020) cancers, and in melanoma (Ramirez-Moreno, Lozano-Lozano *et al*. 2020). It may be suggested that epigenetic disruption, induced by high glucose and/or TNF-alpha, has occurred at other gene loci across the PC3 genome, in addition to the observed loss of imprinting of IGF-II/H19. Further exploration into the expression of these proteins may address why increased IGF-II mRNA did not result in increased levels of IGF-II peptide. Alternatively, the increased expression of IGF-II mRNA may still not be high enough impact protein expression.

Due to restricted access to laboratory facilities, because of the recent pandemic, there was insufficient time to address whether increased IGF-II mRNA culminated in increased peptide, in CRC.

Sodium butyrate (NaB) is a short-chain fatty acid, with anti-inflammatory properties, produced in the gut by bacterial fermentation of dietary fibre; it is a metabolite of colonic epithelial cells, which is essential for water and salt absorption (Bedford and Gong 2018). Moreover, NaB is an epigenetic regulator, behaving as an histone deacetylase inhibitor to regulate gene expression (Steliou, Boosalis *et al*. 2012). NaB has also been shown to affect imprinting status of IGF-II/H19; in 1998 (Hu, Oruganti *et al*. 1998), building on the basis of heritable epigenetic patterns of histone acetylation, Hu *et al* showed that treating with NaB induced loss of imprinting of IGF-II. This is consistent with the data described in chapter 5, where treating with high dose sodium butyrate induced a significant decrease in imprinting percentage, with subsequent increases in the expression of IGF-II and H19 mRNA. Therefore, it may be inferred that increased expression of both gene components is demonstrative of biallelic expression, through imprinting loss. The suggested mechanistic action of

IGF-II/H19 imprinting loss by butyrate has been described in depth by Shin *et al.* (Shin, Li *et al*. 2013), where using ChIP analysis, activation of IGF-II/H19 was shown to be through HDAC inhibitory activity. Disruption of imprinting by butyrate, outlined in chapter 5, may have been further enhanced by culturing in a high glucose environment; disruption to imprinting may have been caused by disturbances to both epigenetic patterns of histone acetylation and methylation. For example, in 2008, El-Osta *et al* showed that exposure to high glucose epigenetically altered p65 gene transcription in human aortic endothelial cells, by disrupting methylation patterns (El-Osta, Brasacchio *et al*. 2008) and Yun *et al* showed upregulation of TNF-alpha in human monocytes, induced by high glucose, could be reversed by curcumin though inhibition of histone acetylase (Yun, Jialal *et al*. 2011).

Metformin is a glucose-sensitising drug, and is the first line of treatment for type 2 diabetes (Pernicova and Korbonits 2014). It inhibits glucose production by the liver (Bultot, Guigas *et al*. 2012) and enhances cellular insulin sensitivity in peripheral tissues (Giannarelli, Aragona *et al*. 2003). Over the past decade, metformin has been the focus of many epidemiological studies due to its anti-cancer effects (Zhang, Zheng *et al*. 2011; Zhang, Gao *et al*. 2013; Wang, Lai *et al*. 2014; Meng, Song *et al*. 2017; Yao, Liu *et al*. 2019; Chen, Liao *et al*. 2020); the key outcome of each study being that cancer incidence, amongst the metformin-prescribed diabetic populace, was lower compared to those receiving other or no diabetic treatment. The effects of metformin upon IGF-II and H19 have been documented in other cancer types; in breast cancer, metformin has been shown to act as an epigenetic regulator by increasing methylation and reducing H19 expression (Zhong, Men *et al*. 2017). In adrenocortical carcinoma, metformin has been shown to downregulate IGF-II (Poli, Cantini *et al*. 2016).

In the context of this thesis, results in chapter 5 demonstrated that high dose metformin increased imprinting in cells cultured in high glucose (25mM/L) media. This was accompanied by a significant increase in H19 mRNA expression. Whilst no apparent effects to imprinting percentage were noted in low glucose media, a significant increase in IGF-II and H19 mRNA was recorded. These findings disagree with those published by Yan *et al.* (Yan, Zhou *et al*. 2015), where metformin was shown to down-regulate H19 by DNA methylation, in ovarian cancer. Further confirmation of this inhibitory action upon H19 by metformin was also shown by Zhong *et al*. (Zhong, Men *et al*. 2017), in endometrial cancer. Data shown here suggests that, whilst metformin serves to reverse glucose-induced imprinting loss, there are other pathways involved causing the upregulation of H19 and, to a lesser extent, IGF-II.

A study published in 2018 (Geng, Bu *et al*. 2018) detailed the impact of an inflammatory environment upon H19; using tissue from patients with ulcerative colitis (a form of IBD), it was noted that levels of H19 were higher compared with healthy individuals. A screen of inflammatory cytokines identified interleukin 22 (IL22) as the cause of this upregulation. Aberrant expression of H19 in bile duct cancer was also shown by Wang *et al*. (Wang, Ye *et al*. 2016), where cultured cells subjected to oxidative stress and inflammatory cytokines were shown to upregulate H19.

From these data it is apparent that the mechanism by which metformin exerts its effect on imprinting of IGF-II/H19 remains unclear. The origin of the cell line may be relevant; absorption of metformin occurs mainly in the upper small intestine (Foretz, Guigas *et al*. 2019). Experiments shown in chapter 5, were conducted using the HCT-116 cell line; a cell line whose origin is defined as being “colorectal” (ATCC.org, 2016). As the location of cell source is not specified, it may be that absorption of metformin may have been negligible due to HCT-116 originating in the large intestine. Therefore, any effects of note may have been due to the high glucose culture media and not the drug.

The artificially created inflammatory conditions, in vitro, were greatly condensed. They were designed to mimic the effects of a hyperglycaemic and/or an increased pro-inflammatory cytokine environment in a set time frame. *In vivo*, it is likely that any epigenetic effects caused by chronic exposure to such conditions would occur over a longer period of time.

Following investigations into the *in vitro* effects of disturbances to imprinting, parallel *in vivo* comparisons were explored. Genotyping benign and malignant tissue pairs in the prostate and colorectal cohorts showed several similarities; most genotyped benign-malignant pairs showed no change in maintenance of imprinting status. Genotyping was determined by the Qiagen Pyrosequencing SNP Analysis programme, whereby LOI is deemed to have occurred in samples with A/G expression ratios of 1:3 or 3:1. These figures are used for threshold purposes, and do not include samples where small amounts of imprinting loss may have occurred. For example, an A/G expression ratio of 80:20 may be genotyped as "MOI", but some biallelic expression has still occurred. In both cohorts, no single sample exhibited an imprinting percentage of 99% >. Most MOI samples possessed between 80 and 94% imprinting. An absence of 99% > imprinting maintenance or loss may be explained by the heterogeneous nature of tumour tissue; tumour tissue is composed of different subpopulations, each with different genotypes and phenotypes that exhibit varied behaviours (Fisher, Pusztai *et al*. 2013). Additionally, the absence of imprinting percentage being 99% >, in benign and malignant tissue, is suggestive of the epigenetic field defect. The epigenetic field defect is a phenomenon that affects tissue, causing it to become pre-cancerous; such tissues look histologically normal under high magnification, but they tend to exhibit elevated numbers of epigenetic alterations – such as aberrant patterns of DNA methylation or histone acetylation (Bernstein, Nfonsam *et al*. 2013).

Another similarity between the prostate and colorectal cohort was the existence of a significant positive correlation between IGF-II and H19 mRNA expression. These correlations were further confirmed by comparisons with larger tissue cohorts, using the cBioPortal Cancer Genomics database. The link between these sets of data is that, whilst LOI has occurred in a small subgroup of

samples, the same co-expressive relationship exists between IGF-II and H19 mRNA. Additionally, in samples of the CGA cohorts, imprinting status is not specified. These patterns suggest that imprinting loss is not the sole cause of increased IGF-II and H19 expression in prostate and CRC. A review published in 2015 (Brouwer-Visser and Huang 2015) cited several mechanisms known to disrupt IGF-II expression, including gene amplification, regulation by micro RNAs, transcription factors, increased membranous receptor number, IGFBPs and IMPs.

Similar patterns of co-expression were also observed in lung and thyroid cancer (figure 7.1). Identical findings pertaining to peptide expression link *in vivo* data from chapters 4 and 6. This offers some insight into the behaviour of translated IGF-II. Analysis of IGF-II peptide expression showed no significant differences between benign and malignant tissue in both cancer cohorts. Due to the short half-life of unbound circulating IGF-II, its binding to IGFBP2 will form a stabilised complex (Yamanaka, Wilson *et al*. 1997). Therefore, the observed IHC staining may have been due to the presence of this complex, localised to tissue.

7.1

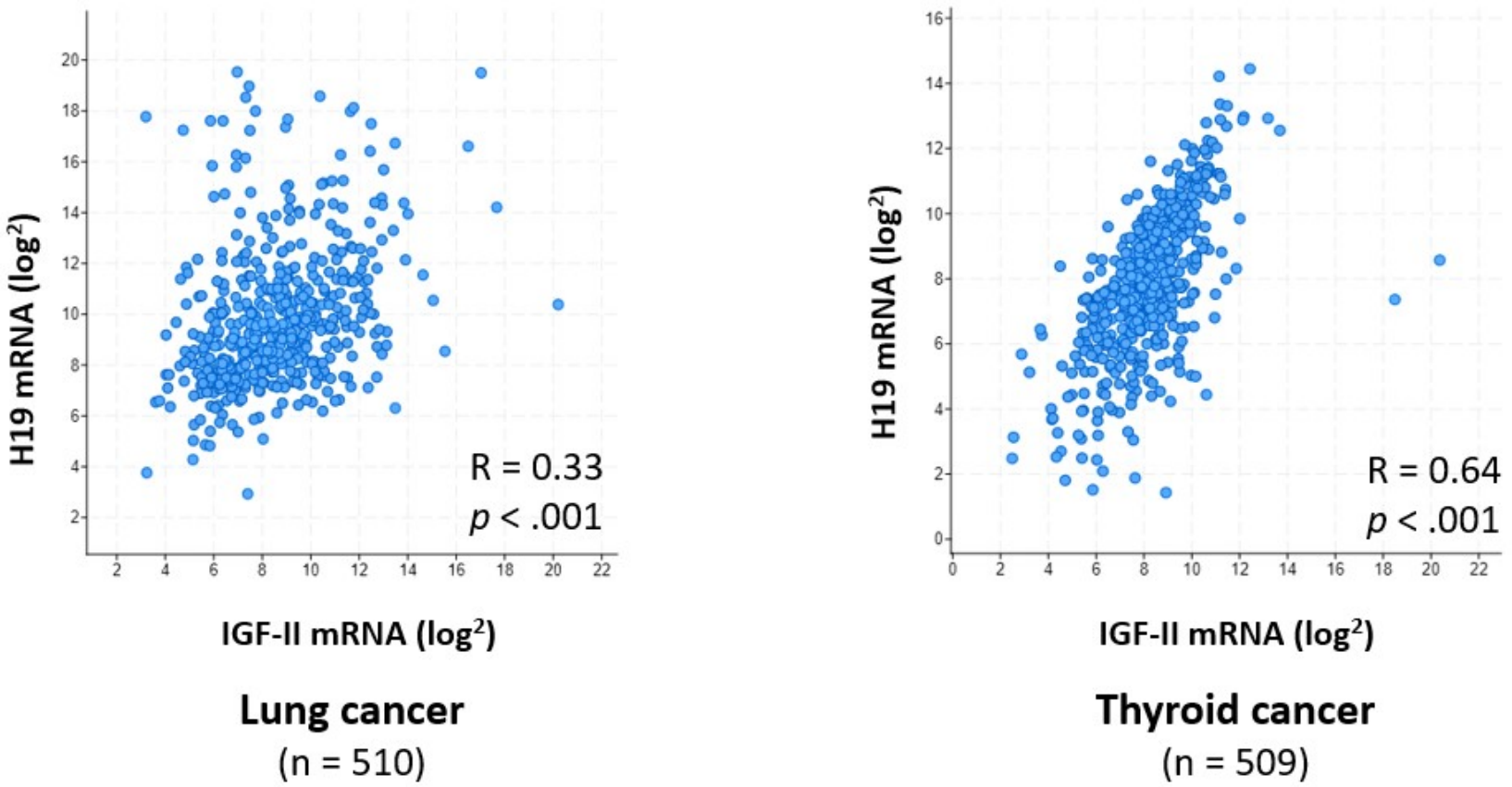

Figure 7.1: Co-expression of IGF-II and H19 mRNA in lung and thyroid cancer.

Data obtained from cBioPortal.org.

Findings shown by this thesis have demonstrated, for the first time, the effects of a disturbed metabolic environment upon the epigenetic regulation of a key growth factor, IGF-II, and its embedded lncRNA, H19, in prostate and CRC cell lines *in vitro*. Without diminishing these findings, it may be worth considering that there are limitations of working with immortalised cell lines, *in vitro*. For example, over-passaging of cells may lead to changes in genotype and phenotype, causing increased likelihood of heterogeneity in a culture, as a specific time point (Kaur and Dufour 2012). To circumvent this issue, it is essential to compare findings with those observed at passage 1. Additionally, cultured cells can be prone to contamination by mycoplasma and other micro-organisms, which can cause false / untrue results (Lorsch, Collins et al. 2014). Fortunately, the laboratory in which these experiments were conducted routinely checks for such events.
Such limitations highlight the importance of using animal models, such as mouse and zebrafish.

IGF-II/H19 has been investigated as a potential therapeutic target in the treatment of many cancer types, varying from immune-stimulating therapies to receptor agonists; De Giovanni *et al* vaccinated mice with electroporated DNA plasmids to elicit an immune response against IGF-II, which successfully reduced metastatic rhabdomyosarcoma growth (De Giovanni, Nanni *et al*. 2019); Mutanabe *et al* identified the ability of IGF-II to bind IGF-IR as a mechanism of chemotherapy-resistance to the tyrosinase inhibitor, Osimertinib, in lung cancer (Manabe, Yasuda *et al*. 2020).
In 2018, Mutgan *et al* reviewed a number of studies focused on targeting the proteins involved in the communication between cancer cells and stroma, in pancreatic cancer (Mutgan, Besikcioglu *et al*. 2018); Tian *et al* documented the inhibitory effect of dietary turmeric upon IGF-II signalling in bladder cancer (Tian, Zhao *et al*. 2017) and in 2017, Tarnowski *et al* highlighted the inhibitory effects of plant-derived picropodophyllin upon IGF-II in rhabdomyosarcoma *in vitro* and *in vivo* (Tarnowski, Tkacz *et al*. 2017). However, if it is possible to decrease the likelihood of developing such illnesses, through modifications to lifestyle, this may be preferable by both doctors and patients. Reduction of

BMI is one such modification; a GWAS conducted in 2014 highlighted the link between increased BMI and methylation (Dick, Nelson *et al*. 2014). In 2017 Bollepalli *et al* showed that short and long-term weight loss affected DNA methylation and subsequent transcription patterns in healthy individuals (Bollepalli, Kaye *et al*. 2018). More recently, Keller *et al* published findings linking weight loss to DNA methylation signatures in blood (Keller, Yaskolka Meir *et al*. 2020).

By decreasing adiposity and blood sugar levels, internal physiological environments will become less hospitable for epigenetic disruption to occur: "prevention is better than cure" Desiderius Erasmus, (1466–1536).

7.2 Thesis Summary.

Hypothesis:

Metabolic disturbances epigenetically disrupt imprinting status in the IGF-II/H19 gene, in prostate and colorectal cancer.

In vitro: An inflammatory state will disrupt imprinting status of IGF-II/H19, resulting in aberrant mRNA expression. These disruptions do not appear to impact IGF-II peptide, in prostate cancer.

In vivo: Disrupted imprinting of IGF-II/H19 caused aberrant expression of IGF-II and H19 mRNA in colorectal and prostate cancer. These changes were not reflected by peptide levels.

7.3 Future work

In vitro* & *in vivo.

- Loss of imprinting in IGF-II/H19 was seen in PCa and CRC, both *in vitro* and *in vivo*. To determine the mechanism by which LOI occurred, methylation analysis by pyrosequencing would serve to address the sites of aberrant methylation. The IGF-II/H19 gene has a specific methylation pattern spread across three differentially methylated regions (DMRs), which ensures epigenetic control of its expression. Methylation affects specific DNA sequence sites known as CpG islands; regions of DNA code that deviate from standard genomic sequences whereby sequences are GC-rich (Deaton and Bird 2011). Conducting a bisulphite conversion of the DNA strand will convert unmethylated cytosine bases to uracil; methylated cytosines remain unchanged. Subsequent pyrosequencing of the bisulphite converted strand will show where these changes have occurred, by emitting a light signal.

In vitro

- Conducting RIA analysis of secreted IGF-II peptide by the PCa cell line, PC3, highlighted the translatory effects of imprinting. This assay needs to be repeated for the CRC HCT116 dosing experiments also, to ascertain whether disrupted imprinting status affects peptide synthesis.

- The dietary effects of butyrate have been shown to be beneficial by acting as an anti-inflammatory agent in the bowel (Chen and Vitetta 2018), yet its effects upon imprinting of IGF-II/H19 seem counter-intuitive. Quantifying peptide as a result of butyrate induced LOI may provide some insight into its epigenetic effects.

- Exposure to high levels of glucose and/or TNFα disrupt imprinting, affecting mRNA expression. Thus far the cause of an absence in a translatory response remains unaddressed. Recreating the experiments for the purposes of quantifying IMPs, by qPCR and/or western

blot, may serve to proffer an explanation of why upregulated mRNA is not translated into protein.

- Two key microRNAs, miR-483 and miR-675, are embedded within the IGF-II/H19. The IGF-II-embedded miR-483 has been shown to enhance transcription of IGF-II from P3 (Liu, Roth *et al*. 2013) in Wilms tumour (Liu, Roth *et al*. 2013), colorectal cancer (Yong, Law *et al*. 2013) and hepatocellular carcinoma (Shen, Wang *et al*. 2013), whilst increased expression of miR-675 has been seen in gastric (Yan, Zhang *et al*. 2017), lung (Zheng, Wu *et al*. 2019) and breast (Muller, Oliveira-Ferrer *et al*. 2019) cancer. Quantifying expression of these miRNAs using ddPCR may provide some further insight into the link between imprinting loss and the effects upon miRNA expression.

- Analysis of GLUT expression, through Western blot or qPCR, may address the issue of whether the effects of glucose upon expression of IGF-II and H19 were cell type specific. It would also establish whether TNF-alpha has an inhibitory effect upon GLUT expression.

- Conducting a glucose-uptake assay may serve to address the issue of any potential differences between cell-surface GLUT expression across each cell line.

- Having shown metformin to increase IGF-II/H19 imprinting percentage in the CRC cell line, HCT-116, in high glucose conditions, a comparative dosing experiment using PC3 cells would address the issue whether metformin affects imprinting status of IGF-II/H19 in PCa.

- Were any of these dosing experiments to be recreated, it would be prudent to explore whether any of the treatment reagents were exerting cytotoxic effects. Quantifying cytotoxicity would address whether the measured levels of mRNA are a true representation

of cellular response, as cell number would affect the quantities of measurable mRNA. A trypan blue cell count or Muse Cell Analyser assay would address this issue.

In vivo.

- In both the prostate and CRC cohorts, there were no significant differences in peptide expression between benign and malignant tissue. Additionally, imprinting status did not appear to affect peptide expression. Assessing the expression of IGFBPs may provide some insight into IGF-II peptide binding behaviour and whether there is a preferential binding protein in each cancer type.
- After tissue collection has concluded for the CRCM Study, a more in-depth analysis should be conducted upon cohort members receiving metformin for treatment of T2D, and its effects upon IGF-II/H19 imprinting. This study would address whether IGF-II/H19 imprinting behaviour, in relation to metformin, is the same *in vivo* as it is *in vitro.*

REFERENCES

Adesunloye, B. A. (2021). "Mechanistic Insights into the Link between Obesity and Prostate Cancer." Int J Mol Sci **22**(8).

Ahearn, T. U., S. Peisch, A. Pettersson, E. M. Ebot, C. K. Zhou, R. E. Graff, J. A. Sinnott, L. Fazli, G. L. Judson, T. A. Bismar, J. R. Rider, T. Gerke, J. M. Chan, M. Fiorentino, R. Flavin, H. D. Sesso, S. Finn, E. L. Giovannucci, M. Gleave, M. Loda, Z. Li, M. Pollak, L. A. Mucci and P. Transdisciplinary Prostate Cancer (2018). "Expression of IGF/insulin receptor in prostate cancer tissue and progression to lethal disease." Carcinogenesis **39**(12): 1431-1437.

Ahima, R. S. and S. Y. Osei (2008). "Adipokines in obesity." Front Horm Res **36**: 182-197.

Ali, I. U., R. Lidereau, C. Theillet and R. Callahan (1987). "Reduction to homozygosity of genes on chromosome 11 in human breast neoplasia." Science **238**(4824): 185-188.

Allard, J. B. and C. Duan (2018). "IGF-Binding Proteins: Why Do They Exist and Why Are There So Many?" Front Endocrinol (Lausanne) **9**: 117.

Allen, R. G. and M. Tresini (2000). "Oxidative stress and gene regulation." Free Radic Biol Med **28**(3): 463-499.

Allott, E. H. and S. D. Hursting (2015). "Obesity and cancer: mechanistic insights from transdisciplinary studies." Endocr Relat Cancer **22**(6): R365-386.

Alsheridah, N. and S. Akhtar (2018). "Diet, obesity and colorectal carcinoma risk: results from a national cancer registry-based middle-eastern study." BMC Cancer **18**(1): 1227.

Ambros, V. (2001). "microRNAs: tiny regulators with great potential." Cell **107**(7): 823-826.

Ancey, P. B., C. Contat and E. Meylan (2018). "Glucose transporters in cancer - from tumor cells to the tumor microenvironment." FEBS J **285**(16): 2926-2943.

Andres, S. F., K. N. Williams, J. B. Plesset, J. J. Headd, R. Mizuno, P. Chatterji, A. A. Lento, A. J. Klein-Szanto, R. Mick, K. E. Hamilton and A. K. Rustgi (2019). "IMP1 3' UTR shortening enhances metastatic burden in colorectal cancer." Carcinogenesis **40**(4): 569-579.

Arcidiacono, B., S. Iiritano, A. Nocera, K. Possidente, M. T. Nevolo, V. Ventura, D. Foti, E. Chiefari and A. Brunetti (2012). "Insulin resistance and cancer risk: an overview of the pathogenetic mechanisms." Exp Diabetes Res **2012**: 789174.

Aref-Eshghi, E., S. Biswas, C. Chen, B. Sadikovic and S. Chakrabarti (2020). "Glucose-induced, duration-dependent genome-wide DNA methylation changes in human endothelial cells." Am J Physiol Cell Physiol **319**(2): C268-C276.

Bach, L. A. (2017). "IGF binding proteins." Journal of Molecular Endocrinology: JME-17-0254.

Baena, R. and P. Salinas (2015). "Diet and colorectal cancer." Maturitas **80**(3): 258-264.

Bandi, P., A. K. Minihan, R. L. Siegel, F. Islami, N. Nargis, A. Jemal and S. A. Fedewa (2021). "Updated Review of Major Cancer Risk Factors and Screening Test Use in the United States in 2018 and 2019, with a Focus on Smoking Cessation." Cancer Epidemiol Biomarkers Prev.

Banting, F. G. and C. H. Best (1922). Pancreatic extracts. Toronto, The University Library: pub. by the librarian.

Banting, F. G., C. H. Best, J. B. Collip, W. R. Campbell and A. A. Fletcher (1922). "Pancreatic Extracts in the Treatment of Diabetes Mellitus." Can Med Assoc J **12**(3): 141-146.

Baral, K. and P. Rotwein (2019). "The insulin-like growth factor 2 gene in mammals: Organizational complexity within a conserved locus." PLoS One **14**(6): e0219155.

Barentsz, J. O., J. Richenberg, R. Clements, P. Choyke, S. Verma, G. Villeirs, O. Rouviere, V. Logager, J. J. Futterer and R. European Society of Urogenital (2012). "ESUR prostate MR guidelines 2012." Eur Radiol **22**(4): 746-757.

Barghash, A., N. Golob-Schwarzl, V. Helms, J. Haybaeck and S. M. Kessler (2016). "Elevated expression of the IGF2 mRNA binding protein 2 (IGF2BP2/IMP2) is linked to short survival and metastasis in esophageal adenocarcinoma." Oncotarget **7**(31): 49743-49750.

Barletta, J. M., S. Rainier and A. P. Feinberg (1997). "Reversal of loss of imprinting in tumor cells by 5-aza-2'-deoxycytidine." Cancer Res **57**(1): 48-50.

Bartolomei, M. S., A. L. Webber, M. E. Brunkow and S. M. Tilghman (1993). "Epigenetic mechanisms underlying the imprinting of the mouse H19 gene." Genes Dev **7**(9): 1663-1673.
Baxter, R. C. (1994). "Insulin-like growth factor binding proteins in the human circulation: a review." Horm Res **42**(4-5): 140-144.
Baxter, R. C., S. R. Holman, A. Corbould, S. Stranks, P. J. Ho and W. Braund (1995). "Regulation of the insulin-like growth factors and their binding proteins by glucocorticoid and growth hormone in nonislet cell tumor hypoglycemia." J Clin Endocrinol Metab **80**(9): 2700-2708.
Bayarsaihan, D. (2011). "Epigenetic mechanisms in inflammation." J Dent Res **90**(1): 9-17.
Bedford, A. and J. Gong (2018). "Implications of butyrate and its derivatives for gut health and animal production." Anim Nutr **4**(2): 151-159.
Belfiore, A. (2007). "The role of insulin receptor isoforms and hybrid insulin/IGF-I receptors in human cancer." Curr Pharm Des **13**(7): 671-686.
Belharazem, D., M. Kirchner, F. Geissler, P. Bugert, M. Spahn, B. Kneitz, H. Riedmiller, C. Sauer, S. Kuffer, L. Trojan, C. Bolenz, M. S. Michel, A. Marx and P. Strobel (2012). "Relaxed imprinting of IGF2 in peripheral blood cells of patients with a history of prostate cancer." Endocr Connect **1**(2): 87-94.
Belharazem, D., J. Magdeburg, A. K. Berton, L. Beissbarth, C. Sauer, C. Sticht, A. Marx, R. Hofheinz, S. Post, P. Kienle and P. Strobel (2016). "Carcinoma of the colon and rectum with deregulation of insulin-like growth factor 2 signaling: clinical and molecular implications." J Gastroenterol **51**(10): 971-984.
Bell, G. I., R. L. Pictet, W. J. Rutter, B. Cordell, E. Tischer and H. M. Goodman (1980). "Sequence of the human insulin gene." Nature **284**(5751): 26-32.
Bell, K. J., C. Del Mar, G. Wright, J. Dickinson and P. Glasziou (2015). "Prevalence of incidental prostate cancer: A systematic review of autopsy studies." Int J Cancer **137**(7): 1749-1757.
Bellmunt, J. (2018). "Stem-Like Signature Predicting Disease Progression in Early Stage Bladder Cancer. The Role of E2F3 and SOX4." Biomedicines **6**(3).
Belobrajdic, D. P., J. Frystyk, N. Jeyaratnaganthan, U. Espelund, A. Flyvbjerg, P. M. Clifton and M. Noakes (2010). "Moderate energy restriction-induced weight loss affects circulating IGF levels independent of dietary composition." Eur J Endocrinol **162**(6): 1075-1082.
Benafif, S. and R. Eeles (2016). "Genetic predisposition to prostate cancer." Br Med Bull **120**(1): 75-89.
Bergman, D., M. Halje, M. Nordin and W. Engstrom (2013). "Insulin-like growth factor 2 in development and disease: a mini-review." Gerontology **59**(3): 240-249.
Bernstein, C., V. Nfonsam, A. R. Prasad and H. Bernstein (2013). "Epigenetic field defects in progression to cancer." World J Gastrointest Oncol **5**(3): 43-49.
Bevanda Glibo, D., D. Bevanda, K. Vukojevic and S. Tomic (2021). "IMP3 protein is an independent prognostic factor of clinical stage II rectal cancer." Sci Rep **11**(1): 10844.
Bhusari, S., B. Yang, J. Kueck, W. Huang and D. F. Jarrard (2011). "Insulin-like growth factor-2 (IGF2) loss of imprinting marks a field defect within human prostates containing cancer." Prostate **71**(15): 1621-1630.
Biernacka, K. M., C. C. Uzoh, L. Zeng, R. A. Persad, A. Bahl, D. Gillatt, C. M. Perks and J. M. Holly (2013). "Hyperglycaemia-induced chemoresistance of prostate cancer cells due to IGFBP2." Endocr Relat Cancer **20**(5): 741-751.
Bleach, R., M. Sherlock, M. W. O'Reilly and M. McIlroy (2021). "Growth Hormone/Insulin Growth Factor Axis in Sex Steroid Associated Disorders and Related Cancers." Front Cell Dev Biol **9**: 630503.
Blum, W. F., K. Albertsson-Wikland, S. Rosberg and M. B. Ranke (1993). "Serum levels of insulin-like growth factor I (IGF-I) and IGF binding protein 3 reflect spontaneous growth hormone secretion." J Clin Endocrinol Metab **76**(6): 1610-1616.
Blyth, A. J., N. S. Kirk and B. E. Forbes (2020). "Understanding IGF-II Action through Insights into Receptor Binding and Activation." Cells **9**(10).
Boguszewski, C. L., M. C. Boguszewski and J. J. Kopchick (2016). "Growth hormone, insulin-like growth factor system and carcinogenesis." Endokrynol Pol **67**(4): 414-426.

Boissonnas, C. C., H. E. Abdalaoui, V. Haelewyn, P. Fauque, J. M. Dupont, I. Gut, D. Vaiman, P. Jouannet, J. Tost and H. Jammes (2010). "Specific epigenetic alterations of IGF2-H19 locus in spermatozoa from infertile men." Eur J Hum Genet **18**(1): 73-80.
Bollepalli, S., S. Kaye, S. Heinonen, J. Kaprio, A. Rissanen, K. A. Virtanen, K. H. Pietilainen and M. Ollikainen (2018). "Subcutaneous adipose tissue gene expression and DNA methylation respond to both short- and long-term weight loss." Int J Obes (Lond) **42**(3): 412-423.
Booth, A., A. Magnuson, J. Fouts and M. Foster (2015). "Adipose tissue, obesity and adipokines: role in cancer promotion." Horm Mol Biol Clin Investig **21**(1): 57-74.
Bowers, L. W., E. L. Rossi, C. H. O'Flanagan, L. A. deGraffenried and S. D. Hursting (2015). "The Role of the Insulin/IGF System in Cancer: Lessons Learned from Clinical Trials and the Energy Balance-Cancer Link." Front Endocrinol (Lausanne) **6**: 77.
Brandao, A., P. Paulo and M. R. Teixeira (2020). "Hereditary Predisposition to Prostate Cancer: From Genetics to Clinical Implications." Int J Mol Sci **21**(14).
Brannan, C. I., E. C. Dees, R. S. Ingram and S. M. Tilghman (1990). "The product of the H19 gene may function as an RNA." Mol Cell Biol **10**(1): 28-36.
Bray, F., J. Ferlay, I. Soerjomataram, R. L. Siegel, L. A. Torre and A. Jemal (2018). "Global cancer statistics 2018: GLOBOCAN estimates of incidence and mortality worldwide for 36 cancers in 185 countries." CA Cancer J Clin **68**(6): 394-424.
Bridgeman, S. C., G. C. Ellison, P. E. Melton, P. Newsholme and C. D. S. Mamotte (2018). "Epigenetic effects of metformin: From molecular mechanisms to clinical implications." Diabetes Obes Metab **20**(7): 1553-1562.
Brissenden, J. E., A. Ullrich and U. Francke (1984). "Human chromosomal mapping of genes for insulin-like growth factors I and II and epidermal growth factor." Nature **310**(5980): 781-784.
Brouwer-Visser, J. and G. S. Huang (2015). "IGF2 signaling and regulation in cancer." Cytokine Growth Factor Rev **26**(3): 371-377.
Brown, J. C., T. L. Carson, H. J. Thompson and T. Agurs-Collins (2021). "The Triple Health Threat of Diabetes, Obesity, and Cancer-Epidemiology, Disparities, Mechanisms, and Interventions." Obesity (Silver Spring) **29**(6): 954-959.
Buchanan, C. M., A. R. Phillips and G. J. Cooper (2001). "Preptin derived from proinsulin-like growth factor II (proIGF-II) is secreted from pancreatic islet beta-cells and enhances insulin secretion." Biochem J **360**(Pt 2): 431-439.
Bultot, L., B. Guigas, A. Von Wilamowitz-Moellendorff, L. Maisin, D. Vertommen, N. Hussain, M. Beullens, J. J. Guinovart, M. Foretz, B. Viollet, K. Sakamoto, L. Hue and M. H. Rider (2012). "AMP-activated protein kinase phosphorylates and inactivates liver glycogen synthase." Biochem J **443**(1): 193-203.
Burisch, J. and P. Munkholm (2015). "The epidemiology of inflammatory bowel disease." Scand J Gastroenterol **50**(8): 942-951.
Capehorn, M. S., D. W. Haslam and R. Welbourn (2016). "Obesity Treatment in the UK Health System." Curr Obes Rep **5**(3): 320-326.
Cerami, E., J. Gao, U. Dogrusoz, B. E. Gross, S. O. Sumer, B. A. Aksoy, A. Jacobsen, C. J. Byrne, M. L. Heuer, E. Larsson, Y. Antipin, B. Reva, A. P. Goldberg, C. Sander and N. Schultz (2012). "The cBio cancer genomics portal: an open platform for exploring multidimensional cancer genomics data." Cancer Discov **2**(5): 401-404.
Chang, S. C. and W. V. Yang (2016). "Hyperglycemia, tumorigenesis, and chronic inflammation." Crit Rev Oncol Hematol **108**: 146-153.
Chang, S. W., J. Yue, B. C. Wang and X. L. Zhang (2015). "miR-503 inhibits cell proliferation and induces apoptosis in colorectal cancer cells by targeting E2F3." Int J Clin Exp Pathol **8**(10): 12853-12860.
Chao, W. and P. A. D'Amore (2008). "IGF2: epigenetic regulation and role in development and disease." Cytokine Growth Factor Rev **19**(2): 111-120.

Chen, E. B., M. J. Nooromid, I. B. Helenowski, N. J. Soper and A. L. Halverson (2019). "The relationship of preoperative versus postoperative hyperglycemia on clinical outcomes after elective colorectal surgery." Surgery **166**(4): 655-662.
Chen, H., Z. Xu, B. Yang, X. Zhou and H. Kong (2018). "RASGRF1 Hypermethylation, a Putative Biomarker of Colorectal Cancer." Ann Clin Lab Sci **48**(1): 3-10.
Chen, H. P., J. J. Shieh, C. C. Chang, T. T. Chen, J. T. Lin, M. S. Wu, J. H. Lin and C. Y. Wu (2013). "Metformin decreases hepatocellular carcinoma risk in a dose-dependent manner: population-based and in vitro studies." Gut **62**(4): 606-615.
Chen, J. and L. Vitetta (2018). "Inflammation-Modulating Effect of Butyrate in the Prevention of Colon Cancer by Dietary Fiber." Clin Colorectal Cancer **17**(3): e541-e544.
Chen, L., F. Liao, Z. Jiang, C. Zhang, Z. Wang, P. Luo, Q. Jiang, J. Wu, Q. Wang, M. Luo, X. Li, Y. Leng, L. Ma, G. Shen, Z. Chen, Y. Wang, X. Tan, Y. Gan, D. Liu, Y. Liu and C. Shi (2020). "Metformin mitigates gastrointestinal radiotoxicity and radiosensitises P53 mutation colorectal tumours via optimising autophagy." Br J Pharmacol **177**(17): 3991-4006.
Chen, S. W., J. Zhu, J. Ma, J. L. Zhang, S. Zuo, G. W. Chen, X. Wang, Y. S. Pan, Y. C. Liu and P. Y. Wang (2017). "Overexpression of long non-coding RNA H19 is associated with unfavorable prognosis in patients with colorectal cancer and increased proliferation and migration in colon cancer cells." Oncol Lett **14**(2): 2446-2452.
Cheng, H. C., T. K. Chang, W. C. Su, H. L. Tsai and J. Y. Wang (2021). "Narrative review of the influence of diabetes mellitus and hyperglycemia on colorectal cancer risk and oncological outcomes." Transl Oncol **14**(7): 101089.
Cheng, Y. W., K. Idrees, R. Shattock, S. A. Khan, Z. Zeng, C. W. Brennan, P. Paty and F. Barany (2010). "Loss of imprinting and marked gene elevation are 2 forms of aberrant IGF2 expression in colorectal cancer." Int J Cancer **127**(3): 568-577.
Christiansen, J., A. M. Kolte, T. Hansen and F. C. Nielsen (2009). "IGF2 mRNA-binding protein 2: biological function and putative role in type 2 diabetes." J Mol Endocrinol **43**(5): 187-195.
Cirillo, F., C. Catellani, C. Sartori, P. Lazzeroni, S. Amarri and M. E. Street (2019). "Obesity, Insulin Resistance, and Colorectal Cancer: Could miRNA Dysregulation Play A Role?" Int J Mol Sci **20**(12).
Corona, G., E. Baldi and M. Maggi (2011). "Androgen regulation of prostate cancer: where are we now?" J Endocrinol Invest **34**(3): 232-243.
Crocker, K. C., A. Domingo-Relloso, K. Haack, A. M. Fretts, W. Y. Tang, M. Herreros, M. Tellez-Plaza, M. Daniele Fallin, S. A. Cole and A. Navas-Acien (2020). "DNA methylation and adiposity phenotypes: an epigenome-wide association study among adults in the Strong Heart Study." Int J Obes (Lond) **44**(11): 2313-2322.
Croft, B., M. Reed, C. Patrick, N. Kovacevich and I. A. Voutsadakis (2019). "Diabetes, Obesity, and the Metabolic Syndrome as Prognostic Factors in Stages I to III Colorectal Cancer Patients." J Gastrointest Cancer **50**(2): 221-229.
Cui, H. (2007). "Loss of imprinting of IGF2 as an epigenetic marker for the risk of human cancer." Dis Markers **23**(1-2): 105-112.
Cui, H., M. Cruz-Correa, F. M. Giardiello, D. F. Hutcheon, D. R. Kafonek, S. Brandenburg, Y. Wu, X. He, N. R. Powe and A. P. Feinberg (2003). "Loss of IGF2 imprinting: a potential marker of colorectal cancer risk." Science **299**(5613): 1753-1755.
Cui, H., I. L. Horon, R. Ohlsson, S. R. Hamilton and A. P. Feinberg (1998). "Loss of imprinting in normal tissue of colorectal cancer patients with microsatellite instability." Nat Med **4**(11): 1276-1280.
Cui, H., P. Onyango, S. Brandenburg, Y. Wu, C. L. Hsieh and A. P. Feinberg (2002). "Loss of imprinting in colorectal cancer linked to hypomethylation of H19 and IGF2." Cancer Res **62**(22): 6442-6446.
Czech, M. P. (2017). "Insulin action and resistance in obesity and type 2 diabetes." Nat Med **23**(7): 804-814.
Daca Alvarez, M., I. Quintana, M. Terradas, P. Mur, F. Balaguer and L. Valle (2021). "The Inherited and Familial Component of Early-Onset Colorectal Cancer." Cells **10**(3).

Dahlem, C., A. Barghash, P. Puchas, J. Haybaeck and S. M. Kessler (2019). "The Insulin-Like Growth Factor 2 mRNA Binding Protein IMP2/IGF2BP2 is Overexpressed and Correlates with Poor Survival in Pancreatic Cancer." Int J Mol Sci **20**(13).
Dai, N. (2020). "The Diverse Functions of IMP2/IGF2BP2 in Metabolism." Trends Endocrinol Metab **31**(9): 670-679.
Dai, N., J. Christiansen, F. C. Nielsen and J. Avruch (2013). "mTOR complex 2 phosphorylates IMP1 cotranslationally to promote IGF2 production and the proliferation of mouse embryonic fibroblasts." Genes Dev **27**(3): 301-312.
Dai, N., F. Ji, J. Wright, L. Minichiello, R. Sadreyev and J. Avruch (2017). "IGF2 mRNA binding protein-2 is a tumor promoter that drives cancer proliferation through its client mRNAs IGF2 and HMGA1." Elife **6**.
Dai, N., J. Rapley, M. Angel, M. F. Yanik, M. D. Blower and J. Avruch (2011). "mTOR phosphorylates IMP2 to promote IGF2 mRNA translation by internal ribosomal entry." Genes Dev **25**(11): 1159-1172.
Damaschke, N. A., B. Yang, S. Bhusari, M. Avilla, W. Zhong, M. L. Blute, Jr., W. Huang and D. F. Jarrard (2017). "Loss of Igf2 Gene Imprinting in Murine Prostate Promotes Widespread Neoplastic Growth." Cancer Res **77**(19): 5236-5247.
Damaschke, N. A., B. Yang, S. Bhusari, J. P. Svaren and D. F. Jarrard (2013). "Epigenetic susceptibility factors for prostate cancer with aging." Prostate **73**(16): 1721-1730.
Dammann, R., M. Strunnikova, U. Schagdarsurengin, M. Rastetter, M. Papritz, U. E. Hattenhorst, H. S. Hofmann, R. E. Silber, S. Burdach and G. Hansen (2005). "CpG island methylation and expression of tumour-associated genes in lung carcinoma." Eur J Cancer **41**(8): 1223-1236.
Davies, S. M. (1993). "Maintenance of genomic imprinting at the IGF2 locus in hepatoblastoma." Cancer Res **53**(20): 4781-4783.
De Giovanni, C., P. Nanni, L. Landuzzi, M. L. Ianzano, G. Nicoletti, S. Croci, A. Palladini and P. L. Lollini (2019). "Immune targeting of autocrine IGF2 hampers rhabdomyosarcoma growth and metastasis." BMC Cancer **19**(1): 126.
De Meyts, P. and J. Whittaker (2002). "Structural biology of insulin and IGF1 receptors: implications for drug design." Nat Rev Drug Discov **1**(10): 769-783.
de Pagter-Holthuizen, P., J. W. Hoppener, M. Jansen, A. H. Geurts van Kessel, G. J. van Ommen and J. S. Sussenbach (1985). "Chromosomal localization and preliminary characterization of the human gene encoding insulin-like growth factor II." Hum Genet **69**(2): 170-173.
de Rooij, M., E. H. Hamoen, J. J. Futterer, J. O. Barentsz and M. M. Rovers (2014). "Accuracy of multiparametric MRI for prostate cancer detection: a meta-analysis." AJR Am J Roentgenol **202**(2): 343-351.
De Vroede, M. A., M. M. Rechler, S. P. Nissley, H. Ogawa, S. Joshi, G. T. Burke and P. G. Katsoyannis (1986). "Mitogenic activity and receptor reactivity of hybrid molecules containing portions of the insulin-like growth factor I (IGF-I), IGF-II, and insulin molecules." Diabetes **35**(3): 355-361.
Dean, S. J., C. M. Perks, J. M. Holly, N. Bhoo-Pathy, L. M. Looi, N. A. Mohammed, K. S. Mun, S. H. Teo, M. O. Koobotse, C. H. Yip and A. Rhodes (2014). "Loss of PTEN expression is associated with IGFBP2 expression, younger age, and late stage in triple-negative breast cancer." Am J Clin Pathol **141**(3): 323-333.
Deaton, A. M. and A. Bird (2011). "CpG islands and the regulation of transcription." Genes Dev **25**(10): 1010-1022.
Decensi, A., M. Puntoni, P. Goodwin, M. Cazzaniga, A. Gennari, B. Bonanni and S. Gandini (2010). "Metformin and cancer risk in diabetic patients: a systematic review and meta-analysis." Cancer Prev Res (Phila) **3**(11): 1451-1461.
DeChiara, T. M., E. J. Robertson and A. Efstratiadis (1991). "Parental imprinting of the mouse insulin-like growth factor II gene." Cell **64**(4): 849-859.
Demetriou, C., S. Abu-Amero, A. C. Thomas, M. Ishida, R. Aggarwal, L. Al-Olabi, L. J. Leon, J. L. Stafford, A. Syngelaki, D. Peebles, K. H. Nicolaides, L. Regan, P. Stanier and G. E. Moore (2014).

"Paternally expressed, imprinted insulin-like growth factor-2 in chorionic villi correlates significantly with birth weight." PLoS One **9**(1): e85454.
Deng, K., H. Wang, X. Guo and J. Xia (2016). "The cross talk between long, non-coding RNAs and microRNAs in gastric cancer." Acta Biochim Biophys Sin (Shanghai) **48**(2): 111-116.
Deng, Q., B. He, T. Gao, Y. Pan, H. Sun, Y. Xu, R. Li, H. Ying, F. Wang, X. Liu, J. Chen and S. Wang (2014). "Up-regulation of 91H promotes tumor metastasis and predicts poor prognosis for patients with colorectal cancer." PLoS One **9**(7): e103022.
Dess, R. T., H. E. Hartman, B. A. Mahal, P. D. Soni, W. C. Jackson, M. R. Cooperberg, C. L. Amling, W. J. Aronson, C. J. Kane, M. K. Terris, Z. S. Zumsteg, S. Butler, J. R. Osborne, T. M. Morgan, R. Mehra, S. S. Salami, A. U. Kishan, C. Wang, E. M. Schaeffer, M. Roach, 3rd, T. M. Pisansky, W. U. Shipley, S. J. Freedland, H. M. Sandler, S. Halabi, F. Y. Feng, J. J. Dignam, P. L. Nguyen, M. J. Schipper and D. E. Spratt (2019). "Association of Black Race With Prostate Cancer-Specific and Other-Cause Mortality." JAMA Oncol **5**(7): 975-983.
Dey, B. K., K. Pfeifer and A. Dutta (2014). "The H19 long noncoding RNA gives rise to microRNAs miR-675-3p and miR-675-5p to promote skeletal muscle differentiation and regeneration." Genes Dev **28**(5): 491-501.
Diabetes Genetics Initiative of Broad Institute of, H., L. U. Mit, R. Novartis Institutes of BioMedical, R. Saxena, B. F. Voight, V. Lyssenko, N. P. Burtt, P. I. de Bakker, H. Chen, J. J. Roix, S. Kathiresan, J. N. Hirschhorn, M. J. Daly, T. E. Hughes, L. Groop, D. Altshuler, P. Almgren, J. C. Florez, J. Meyer, K. Ardlie, K. Bengtsson Bostrom, B. Isomaa, G. Lettre, U. Lindblad, H. N. Lyon, O. Melander, C. Newton-Cheh, P. Nilsson, M. Orho-Melander, L. Rastam, E. K. Speliotes, M. R. Taskinen, T. Tuomi, C. Guiducci, A. Berglund, J. Carlson, L. Gianniny, R. Hackett, L. Hall, J. Holmkvist, E. Laurila, M. Sjogren, M. Sterner, A. Surti, M. Svensson, M. Svensson, R. Tewhey, B. Blumenstiel, M. Parkin, M. Defelice, R. Barry, W. Brodeur, J. Camarata, N. Chia, M. Fava, J. Gibbons, B. Handsaker, C. Healy, K. Nguyen, C. Gates, C. Sougnez, D. Gage, M. Nizzari, S. B. Gabriel, G. W. Chirn, Q. Ma, H. Parikh, D. Richardson, D. Ricke and S. Purcell (2007). "Genome-wide association analysis identifies loci for type 2 diabetes and triglyceride levels." Science **316**(5829): 1331-1336.
Dick, K. J., C. P. Nelson, L. Tsaprouni, J. K. Sandling, D. Aissi, S. Wahl, E. Meduri, P. E. Morange, F. Gagnon, H. Grallert, M. Waldenberger, A. Peters, J. Erdmann, C. Hengstenberg, F. Cambien, A. H. Goodall, W. H. Ouwehand, H. Schunkert, J. R. Thompson, T. D. Spector, C. Gieger, D. A. Tregouet, P. Deloukas and N. J. Samani (2014). "DNA methylation and body-mass index: a genome-wide analysis." Lancet **383**(9933): 1990-1998.
Ding, H. and T. Wu (2018). "Insulin-Like Growth Factor Binding Proteins in Autoimmune Diseases." Front Endocrinol (Lausanne) **9**: 499.
Dobosy, J. R., V. X. Fu, J. A. Desotelle, R. Srinivasan, M. L. Kenowski, N. Almassi, R. Weindruch, J. Svaren and D. F. Jarrard (2008). "A methyl-deficient diet modifies histone methylation and alters Igf2 and H19 repression in the prostate." Prostate **68**(11): 1187-1195.
Dong, Y., J. Li, F. Han, H. Chen, X. Zhao, Q. Qin, R. Shi and J. Liu (2015). "High IGF2 expression is associated with poor clinical outcome in human ovarian cancer." Oncol Rep **34**(2): 936-942.
Dong, Y., J. Zhou, Y. Zhu, L. Luo, T. He, H. Hu, H. Liu, Y. Zhang, D. Luo, S. Xu, L. Xu, J. Liu, J. Zhang and Z. Teng (2017). "Abdominal obesity and colorectal cancer risk: systematic review and meta-analysis of prospective studies." Biosci Rep **37**(6).
Doucrasy, S., J. Coll, M. Barrois, A. Joubel, S. Prost, C. Dozier, D. Stehelin and G. Riou (1993). "Expression of the human fetal bac h19 gene in invasive cancers." Int J Oncol **2**(5): 753-758.
Du, J., H.-R. Shi, F. Ren, J.-L. Wang, Q.-H. Wu, X. Li and R.-T. Zhang (2017). "Inhibition of the IGF signaling pathway reverses cisplatin resistance in ovarian cancer cells." BMC Cancer: 851: 851-811.
Eggermann, K., J. Bliek, F. Brioude, E. Algar, K. Buiting, S. Russo, Z. Tumer, D. Monk, G. Moore, T. Antoniadi, F. Macdonald, I. Netchine, P. Lombardi, L. Soellner, M. Begemann, D. Prawitt, E. R. Maher, M. Mannens, A. Riccio, R. Weksberg, P. Lapunzina, K. Gronskov, D. J. Mackay and T. Eggermann (2016). "EMQN best practice guidelines for the molecular genetic testing and reporting of

chromosome 11p15 imprinting disorders: Silver-Russell and Beckwith-Wiedemann syndrome." Eur J Hum Genet **24**(10): 1377-1387.
El-Osta, A., D. Brasacchio, D. Yao, A. Pocai, P. L. Jones, R. G. Roeder, M. E. Cooper and M. Brownlee (2008). "Transient high glucose causes persistent epigenetic changes and altered gene expression during subsequent normoglycemia." J Exp Med **205**(10): 2409-2417.
Engstrom, W., A. Shokrai, K. Otte, M. Granerus, A. Gessbo, P. Bierke, A. Madej, M. Sjolund and A. Ward (1998). "Transcriptional regulation and biological significance of the insulin like growth factor II gene." Cell Prolif **31**(5-6): 173-189.
Epstein, J. I., L. Egevad, M. B. Amin, B. Delahunt, J. R. Srigley, P. A. Humphrey and C. Grading (2016). "The 2014 International Society of Urological Pathology (ISUP) Consensus Conference on Gleason Grading of Prostatic Carcinoma: Definition of Grading Patterns and Proposal for a New Grading System." Am J Surg Pathol **40**(2): 244-252.
Erices, R., M. L. Bravo, P. Gonzalez, B. Oliva, D. Racordon, M. Garrido, C. Ibanez, S. Kato, J. Branes, J. Pizarro, M. I. Barriga, A. Barra, E. Bravo, C. Alonso, E. Bustamente, M. A. Cuello and G. I. Owen (2013). "Metformin, at concentrations corresponding to the treatment of diabetes, potentiates the cytotoxic effects of carboplatin in cultures of ovarian cancer cells." Reprod Sci **20**(12): 1433-1446.
Fawzy, I. O., M. T. Hamza, K. A. Hosny, G. Esmat and A. I. Abdelaziz (2016). "Abrogating the interplay between IGF2BP1, 2 and 3 and IGF1R by let-7i arrests hepatocellular carcinoma growth." Growth Factors **34**(1-2): 42-50.
Feng, Z., C. Peng, D. Li, D. Zhang, X. Li, F. Cui, Y. Chen and Q. He (2018). "E2F3 promotes cancer growth and is overexpressed through copy number variation in human melanoma." Onco Targets Ther **11**: 5303-5313.
Fernandez, C. J., A. S. George, N. A. Subrahmanyan and J. M. Pappachan (2021). "Epidemiological link between obesity, type 2 diabetes mellitus and cancer." World J Methodol **11**(3): 23-45.
Firth, S. M. and R. C. Baxter (2002). "Cellular actions of the insulin-like growth factor binding proteins." Endocr Rev **23**(6): 824-854.
Fisher, R., L. Pusztai and C. Swanton (2013). "Cancer heterogeneity: implications for targeted therapeutics." Br J Cancer **108**(3): 479-485.
Foretz, M., B. Guigas and B. Viollet (2019). "Understanding the glucoregulatory mechanisms of metformin in type 2 diabetes mellitus." Nat Rev Endocrinol **15**(10): 569-589.
Franciosi, M., G. Lucisano, E. Lapice, G. F. Strippoli, F. Pellegrini and A. Nicolucci (2013). "Metformin therapy and risk of cancer in patients with type 2 diabetes: systematic review." PLoS One **8**(8): e71583.
Frasca, F., G. Pandini, P. Scalia, L. Sciacca, R. Mineo, A. Costantino, I. D. Goldfine, A. Belfiore and R. Vigneri (1999). "Insulin receptor isoform A, a newly recognized, high-affinity insulin-like growth factor II receptor in fetal and cancer cells." Mol Cell Biol **19**(5): 3278-3288.
Fu, V. X., J. R. Dobosy, J. A. Desotelle, N. Almassi, J. A. Ewald, R. Srinivasan, M. Berres, J. Svaren, R. Weindruch and D. F. Jarrard (2008). "Aging and cancer-related loss of insulin-like growth factor 2 imprinting in the mouse and human prostate." Cancer Res **68**(16): 6797-6802.
Fu, V. X., S. R. Schwarze, M. L. Kenowski, S. Leblanc, J. Svaren and D. F. Jarrard (2004). "A loss of insulin-like growth factor-2 imprinting is modulated by CCCTC-binding factor down-regulation at senescence in human epithelial cells." J Biol Chem **279**(50): 52218-52226.
Fuhrmann, L., S. Lindner, A. T. Hauser, C. Hose, O. Kretz, C. D. Cohen, M. T. Lindenmeyer, W. Sippl, M. Jung, T. B. Huber and N. Wanner (2021). "Effects of Environmental Conditions on Nephron Number: Modeling Maternal Disease and Epigenetic Regulation in Renal Development." Int J Mol Sci **22**(8).
Fujita, K., T. Hayashi, M. Matsushita, M. Uemura and N. Nonomura (2019). "Obesity, Inflammation, and Prostate Cancer." J Clin Med **8**(2).
Gabory, A., M. A. Ripoche, T. Yoshimizu and L. Dandolo (2006). "The H19 gene: regulation and function of a non-coding RNA." Cytogenet Genome Res **113**(1-4): 188-193.

Gao, J., B. A. Aksoy, U. Dogrusoz, G. Dresdner, B. Gross, S. O. Sumer, Y. Sun, A. Jacobsen, R. Sinha, E. Larsson, E. Cerami, C. Sander and N. Schultz (2013). "Integrative analysis of complex cancer genomics and clinical profiles using the cBioPortal." Sci Signal **6**(269): pl1.
Gao, T., X. Liu, B. He, Z. Nie, C. Zhu, P. Zhang and S. Wang (2018). "Exosomal lncRNA 91H is associated with poor development in colorectal cancer by modifying HNRNPK expression." Cancer Cell Int **18**: 11.
Gao, T., X. Liu, B. He, Y. Pan and S. Wang (2020). "IGF2 loss of imprinting enhances colorectal cancer stem cells pluripotency by promoting tumor autophagy." Aging (Albany NY) **12**(21): 21236-21252.
Gao, T., X. Liu, B. He, Y. Pan and S. Wang (2020). "Long non-coding RNA 91H regulates IGF2 expression by interacting with IGF2BP2 and promotes tumorigenesis in colorectal cancer." Artif Cells Nanomed Biotechnol **48**(1): 664-671.
Garg, S. K., H. Maurer, K. Reed and R. Selagamsetty (2014). "Diabetes and cancer: two diseases with obesity as a common risk factor." Diabetes Obes Metab **16**(2): 97-110.
Geng, H., H. F. Bu, F. Liu, L. Wu, K. Pfeifer, P. M. Chou, X. Wang, J. Sun, L. Lu, A. Pandey, M. S. Bartolomei, I. G. De Plaen, P. Wang, J. Yu, J. Qian and X. D. Tan (2018). "In Inflamed Intestinal Tissues and Epithelial Cells, Interleukin 22 Signaling Increases Expression of H19 Long Noncoding RNA, Which Promotes Mucosal Regeneration." Gastroenterology **155**(1): 144-155.
Giannarelli, R., M. Aragona, A. Coppelli and S. Del Prato (2003). "Reducing insulin resistance with metformin: the evidence today." Diabetes Metab **29**(4 Pt 2): 6S28-35.
Giri, V. N. and J. L. Beebe-Dimmer (2016). "Familial prostate cancer." Semin Oncol **43**(5): 560-565.
Glass, M., P. Michl and A. S. Huttelmaier (2020). "RNA Binding Proteins as Drivers and Therapeutic Target Candidates in Pancreatic Ductal Adenocarcinoma." Int J Mol Sci **21**(11).
Gleason, D. F. (1966). "Classification of prostatic carcinomas." Cancer Chemother Rep **50**(3): 125-128.
Gleason, D. F., G. T. Mellinger and G. Veterans Administration Cooperative Urological Research (2017). "Prediction of Prognosis for Prostatic Adenocarcinoma by Combined Histological Grading and Clinical Staging." J Urol **197**(2S): S134-S139.
Goldgar, D. E., D. F. Easton, L. A. Cannon-Albright and M. H. Skolnick (1994). "Systematic population-based assessment of cancer risk in first-degree relatives of cancer probands." J Natl Cancer Inst **86**(21): 1600-1608.
Gomes, M. V., M. R. Soares, A. Pasqualim-Neto, C. R. Marcondes, R. B. Lobo and E. S. Ramos (2005). "Association between birth weight, body mass index and IGF2/ApaI polymorphism." Growth Horm IGF Res **15**(5): 360-362.
Gonzalez-Menendez, P., D. Hevia, R. Alonso-Arias, A. Alvarez-Artime, A. Rodriguez-Garcia, S. Kinet, I. Gonzalez-Pola, N. Taylor, J. C. Mayo and R. M. Sainz (2018). "GLUT1 protects prostate cancer cells from glucose deprivation-induced oxidative stress." Redox Biol **17**: 112-127.
Goto, A., T. Yamaji, N. Sawada, Y. Momozawa, Y. Kamatani, M. Kubo, T. Shimazu, M. Inoue, M. Noda, S. Tsugane and M. Iwasaki (2020). "Diabetes and cancer risk: A Mendelian randomization study." Int J Cancer **146**(3): 712-719.
Gu, W., Z. Katz, B. Wu, H. Y. Park, D. Li, S. Lin, A. L. Wells and R. H. Singer (2012). "Regulation of local expression of cell adhesion and motility-related mRNAs in breast cancer cells by IMP1/ZBP1." J Cell Sci **125**(Pt 1): 81-91.
Guler, H. P., J. Zapf, C. Schmid and E. R. Froesch (1989). "Insulin-like growth factors I and II in healthy man. Estimations of half-lives and production rates." Acta Endocrinol (Copenh) **121**(6): 753-758.
Gutierrez-Salmeron, M., S. R. Lucena, A. Chocarro-Calvo, J. M. Garcia-Martinez, R. M. Martin Orozco and C. Garcia-Jimenez (2021). "Metabolic and hormonal remodeling of colorectal cancer cell signalling by diabetes." Endocr Relat Cancer **28**(6): R191-R206.
Gutschner, T., M. Hammerle, N. Pazaitis, N. Bley, E. Fiskin, H. Uckelmann, A. Heim, M. Grobeta, N. Hofmann, R. Geffers, B. Skawran, T. Longerich, K. Breuhahn, P. Schirmacher, B. Muhleck, S. Huttelmaier and S. Diederichs (2014). "Insulin-like growth factor 2 mRNA-binding protein 1

(IGF2BP1) is an important protumorigenic factor in hepatocellular carcinoma." Hepatology **59**(5): 1900-1911.
Hall, E., M. Dekker Nitert, P. Volkov, S. Malmgren, H. Mulder, K. Bacos and C. Ling (2018). "The effects of high glucose exposure on global gene expression and DNA methylation in human pancreatic islets." Mol Cell Endocrinol **472**: 57-67.
Hanahan, D. and R. A. Weinberg (2011). "Hallmarks of cancer: the next generation." Cell **144**(5): 646-674.
Hauner, H., T. Petruschke, M. Russ, K. Rohrig and J. Eckel (1995). "Effects of tumour necrosis factor alpha (TNF alpha) on glucose transport and lipid metabolism of newly-differentiated human fat cells in cell culture." Diabetologia **38**(7): 764-771.
Helmsauer, K., M. E. Valieva, S. Ali, R. Chamorro Gonzalez, R. Schopflin, C. Roefzaad, Y. Bei, H. Dorado Garcia, E. Rodriguez-Fos, M. Puiggros, K. Kasack, K. Haase, C. Keskeny, C. Y. Chen, L. P. Kuschel, P. Euskirchen, V. Heinrich, M. I. Robson, C. Rosswog, J. Toedling, A. Szymansky, F. Hertwig, M. Fischer, D. Torrents, A. Eggert, J. H. Schulte, S. Mundlos, A. G. Henssen and R. P. Koche (2020). "Enhancer hijacking determines extrachromosomal circular MYCN amplicon architecture in neuroblastoma." Nat Commun **11**(1): 5823.
Henrikson, N. B., E. M. Webber, K. A. Goddard, A. Scrol, M. Piper, M. S. Williams, D. T. Zallen, N. Calonge, T. G. Ganiats, A. C. Janssens, A. Zauber, I. Lansdorp-Vogelaar, M. van Ballegooijen and E. P. Whitlock (2015). "Family history and the natural history of colorectal cancer: systematic review." Genet Med **17**(9): 702-712.
Hidaka, H., K. Higashimoto, S. Aoki, H. Mishima, C. Hayashida, T. Maeda, Y. Koga, H. Yatsuki, K. Joh, H. Noshiro, R. Iwakiri, A. Kawaguchi, K. I. Yoshiura, K. Fujimoto and H. Soejima (2018). "Comprehensive methylation analysis of imprinting-associated differentially methylated regions in colorectal cancer." Clin Epigenetics **10**(1): 150.
Higashijima, Y. and Y. Kanki (2020). "Molecular mechanistic insights: The emerging role of SOXF transcription factors in tumorigenesis and development." Semin Cancer Biol **67**(Pt 1): 39-48.
Hotamisligil, G. S., N. S. Shargill and B. M. Spiegelman (1993). "Adipose expression of tumor necrosis factor-alpha: direct role in obesity-linked insulin resistance." Science **259**(5091): 87-91.
Hsu, K. F., M. R. Shen, Y. F. Huang, Y. M. Cheng, S. H. Lin, N. H. Chow, S. W. Cheng, C. Y. Chou and C. L. Ho (2015). "Overexpression of the RNA-binding proteins Lin28B and IGF2BP3 (IMP3) is associated with chemoresistance and poor disease outcome in ovarian cancer." Br J Cancer **113**(3): 414-424.
Hu, J. F., H. Oruganti, T. H. Vu and A. R. Hoffman (1998). "The role of histone acetylation in the allelic expression of the imprinted human insulin-like growth factor II gene." Biochem Biophys Res Commun **251**(2): 403-408.
Hu, Y. M., X. L. Lou, B. Z. Liu, L. Sun, S. Wan, L. Wu, X. Zhao, Q. Zhou, M. M. Sun, K. Tao, Y. S. Zhang and S. L. Wang (2021). "TGF-beta1-regulated miR-3691-3p targets E2F3 and PRDM1 to inhibit prostate cancer progression." Asian J Androl **23**(2): 188-196.
Hua, L., F. Q. Wang, H. W. Du, J. Fan, Y. F. Wang, L. Q. Wang and X. W. Shi (2020). "Upregulation of caspase-3 by high glucose in chondrocyte involves the cytoskeleton aggregation." Eur Rev Med Pharmacol Sci **24**(11): 5925-5932.
Huang, W., J. Bian, X. Qian, L. Shao, H. Li, L. Zhang and L. Wang (2021). "Case Report: Coinheritance of Germline Mutations in APC and BRCA1 in Colorectal Cancer." Front Oncol **11**: 658389.
Huang, X., G. Liu, J. Guo and Z. Su (2018). "The PI3K/AKT pathway in obesity and type 2 diabetes." Int J Biol Sci **14**(11): 1483-1496.
Huang, X., H. Zhang, X. Guo, Z. Zhu, H. Cai and X. Kong (2018). "Insulin-like growth factor 2 mRNA-binding protein 1 (IGF2BP1) in cancer." J Hematol Oncol **11**(1): 88.
Hughes, J., M. Surakhy, S. Can, M. Ducker, N. Davies, F. Szele, C. Buhnemann, E. Carter, R. Trikin, M. P. Crump, S. Frago and A. B. Hassan (2019). "Maternal transmission of an Igf2r domain 11: IGF2 binding mutant allele (Igf2r(I1565A)) results in partial lethality, overgrowth and intestinal adenoma progression." Sci Rep **9**(1): 11388.

Hullings, A. G., R. Sinha, L. M. Liao, N. D. Freedman, B. I. Graubard and E. Loftfield (2020). "Whole grain and dietary fiber intake and risk of colorectal cancer in the NIH-AARP Diet and Health Study cohort." Am J Clin Nutr **112**(3): 603-612.
Ianza, A., M. Sirico, O. Bernocchi and D. Generali (2021). "Role of the IGF-1 Axis in Overcoming Resistance in Breast Cancer." Front Cell Dev Biol **9**: 641449.
Ibfelt, T., C. P. Fischer, P. Plomgaard, G. van Hall and B. K. Pedersen (2014). "The acute effects of low-dose TNF-alpha on glucose metabolism and beta-cell function in humans." Mediators Inflamm **2014**: 295478.
Iida, Y., M. P. Salomon, K. Hata, K. Tran, S. Ohe, C. F. Griffiths, S. C. Hsu, N. Nelson and D. S. B. Hoon (2018). "Predominance of triple wild-type and IGF2R mutations in mucosal melanomas." BMC Cancer **18**(1): 1054.
Ismayilnajadteymurabadi, H. and D. Konukoglu (2018). "The relationship between IGF-2, IGFBP-2, and IGFBP-3 levels in patients suffering from pre-diabetes." J Biol Regul Homeost Agents **32**(1): 63-68.
Ito, Y., T. Koessler, A. E. Ibrahim, S. Rai, S. L. Vowler, S. Abu-Amero, A. L. Silva, A. T. Maia, J. E. Huddleston, S. Uribe-Lewis, K. Woodfine, M. Jagodic, R. Nativio, A. Dunning, G. Moore, E. Klenova, S. Bingham, P. D. Pharoah, J. D. Brenton, S. Beck, M. S. Sandhu and A. Murrell (2008). "Somatically acquired hypomethylation of IGF2 in breast and colorectal cancer." Hum Mol Genet **17**(17): 2633-2643.
Iwakawa, H. O. and Y. Tomari (2015). "The Functions of MicroRNAs: mRNA Decay and Translational Repression." Trends Cell Biol **25**(11): 651-665.
Iyengar, N. M., A. Gucalp, A. J. Dannenberg and C. A. Hudis (2016). "Obesity and Cancer Mechanisms: Tumor Microenvironment and Inflammation." J Clin Oncol **34**(35): 4270-4276.
Jaenisch, R. and A. Bird (2003). "Epigenetic regulation of gene expression: how the genome integrates intrinsic and environmental signals." Nat Genet **33 Suppl**: 245-254.
Jarrard, D. F., M. J. Bussemakers, G. S. Bova and W. B. Isaacs (1995). "Regional loss of imprinting of the insulin-like growth factor II gene occurs in human prostate tissues." Clin Cancer Res **1**(12): 1471-1478.
Jellema, P., M. W. van Tulder, H. E. van der Horst, J. Florie, C. J. Mulder and D. A. van der Windt (2011). "Inflammatory bowel disease: a systematic review on the value of diagnostic testing in primary care." Colorectal Dis **13**(3): 239-254.
Jeziorska, D. M., R. J. S. Murray, M. De Gobbi, R. Gaentzsch, D. Garrick, H. Ayyub, T. Chen, E. Li, J. Telenius, M. Lynch, B. Graham, A. J. H. Smith, J. N. Lund, J. R. Hughes, D. R. Higgs and C. Tufarelli (2017). "DNA methylation of intragenic CpG islands depends on their transcriptional activity during differentiation and disease." Proc Natl Acad Sci U S A **114**(36): E7526-E7535.
Jiang, C. and B. F. Pugh (2009). "Nucleosome positioning and gene regulation: advances through genomics." Nat Rev Genet **10**(3): 161-172.
Jiang, L., J. Zhang, Q. Xu, B. Wang, Y. Yao, L. Sun, X. Wang, D. Zhou, L. Gao, S. Song and X. Zhu (2021). "YAP promotes the proliferation and migration of colorectal cancer cells through the Glut3/AMPK signaling pathway." Oncol Lett **21**(4): 312.
Jochem, C. and M. Leitzmann (2016). "Obesity and Colorectal Cancer." Recent Results Cancer Res **208**: 17-41.
Jones, A. L. and F. Chinegwundoh (2014). "Update on prostate cancer in black men within the UK." Ecancermedicalscience **8**: 455.
Jones, G. R. and M. P. Molloy (2020). "Metformin, Microbiome and Protection Against Colorectal Cancer." Dig Dis Sci.
Joseph, D. F., E. Li, S. L. Stanley Iii, Y. C. Zhu, X. N. Li, J. Yang, L. F. Ottaviano, J. C. Bucobo, J. M. Buscaglia, J. D. Miller, R. Veluvolu, M. Follen and E. B. Grossman (2021). "Impact of type 2 diabetes on adenoma detection in screening colonoscopies performed in disparate populations." World J Clin Cases **9**(11): 2433-2445.

Kaddai, V., J. Jager, T. Gonzalez, R. Najem-Lendom, S. Bonnafous, A. Tran, Y. Le Marchand-Brustel, P. Gual, J. F. Tanti and M. Cormont (2009). "Involvement of TNF-alpha in abnormal adipocyte and muscle sortilin expression in obese mice and humans." Diabetologia **52**(5): 932-940.
Kahn, B. B. and J. S. Flier (2000). "Obesity and insulin resistance." J Clin Invest **106**(4): 473-481.
Kandilya, D., S. Shyamasundar, D. K. Singh, A. Banik, M. P. Hande, W. Stunkel, Y. S. Chong and S. T. Dheen (2020). "High glucose alters the DNA methylation pattern of neurodevelopment associated genes in human neural progenitor cells in vitro." Sci Rep **10**(1): 15676.
Kaneto, H., T. Kimura, A. Obata, M. Shimoda and K. Kaku (2021). "Multifaceted Mechanisms of Action of Metformin Which Have Been Unraveled One after Another in the Long History." Int J Mol Sci **22**(5).
Karczewski, J., E. Sledzinska, A. Baturo, I. Jonczyk, A. Maleszko, P. Samborski, B. Begier-Krasinska and A. Dobrowolska (2018). "Obesity and inflammation." Eur Cytokine Netw **29**(3): 83-94.
Kasprzak, A. and A. Adamek (2019). "Insulin-Like Growth Factor 2 (IGF2) Signaling in Colorectal Cancer-From Basic Research to Potential Clinical Applications." Int J Mol Sci **20**(19).
Kasprzak, A., W. Kwasniewski, A. Adamek and A. Gozdzicka-Jozefiak (2017). "Insulin-like growth factor (IGF) axis in cancerogenesis." Mutat Res Rev Mutat Res **772**: 78-104.
Kaur, G. and J. M. Dufour (2012). "Cell lines: Valuable tools or useless artifacts." Spermatogenesis **2**(1): 1-5.
Kawamoto, K., H. Onodera, S. Kondo, S. Kan, D. Ikeuchi, S. Maetani and M. Imamura (1998). "Expression of insulin-like growth factor-2 can predict the prognosis of human colorectal cancer patients: correlation with tumor progression, proliferative activity and survival." Oncology **55**(3): 242-248.
Keller, M., A. Yaskolka Meir, S. H. Bernhart, Y. Gepner, I. Shelef, D. Schwarzfuchs, G. Tsaban, H. Zelicha, L. Hopp, L. Muller, K. Rohde, Y. Bottcher, P. F. Stadler, M. Stumvoll, M. Bluher, P. Kovacs and I. Shai (2020). "DNA methylation signature in blood mirrors successful weight-loss during lifestyle interventions: the CENTRAL trial." Genome Med **12**(1): 97.
Keniry, A., D. Oxley, P. Monnier, M. Kyba, L. Dandolo, G. Smits and W. Reik (2012). "The H19 lincRNA is a developmental reservoir of miR-675 that suppresses growth and Igf1r." Nat Cell Biol **14**(7): 659-665.
Kern, P. A., S. Ranganathan, C. Li, L. Wood and G. Ranganathan (2001). "Adipose tissue tumor necrosis factor and interleukin-6 expression in human obesity and insulin resistance." Am J Physiol Endocrinol Metab **280**(5): E745-751.
Khaodhiar, L., K. C. McCowen and G. L. Blackburn (1999). "Obesity and its comorbid conditions." Clin Cornerstone **2**(3): 17-31.
Kim, H. J., S. Lee, K. H. Chun, J. Y. Jeon, S. J. Han, D. J. Kim, Y. S. Kim, J. T. Woo, M. S. Nam, S. H. Baik, K. J. Ahn and K. W. Lee (2018). "Metformin reduces the risk of cancer in patients with type 2 diabetes: An analysis based on the Korean National Diabetes Program Cohort." Medicine (Baltimore) **97**(8): e0036.
Kim, M., K. Jung, I. S. Kim, I. S. Lee, Y. Ko, J. E. Shin and K. I. Park (2018). "TNF-alpha induces human neural progenitor cell survival after oxygen-glucose deprivation by activating the NF-kappaB pathway." Exp Mol Med **50**(4): 1-14.
Kim, T., T. Havighurst, K. Kim, M. Albertini, Y. G. Xu and V. S. Spiegelman (2018). "Targeting insulin-like growth factor 2 mRNA-binding protein 1 (IGF2BP1) in metastatic melanoma to increase efficacy of BRAF(V600E) inhibitors." Mol Carcinog **57**(5): 678-683.
Kinouchi, Y., N. Hiwatashi, S. Higashioka, F. Nagashima, M. Chida and T. Toyota (1996). "Relaxation of imprinting of the insulin-like growth factor II gene in colorectal cancer." Cancer Lett **107**(1): 105-108.
Knuppel, A., G. K. Fensom, E. L. Watts, M. J. Gunter, N. Murphy, K. Papier, A. Perez-Cornago, J. A. Schmidt, K. Smith Byrne, R. C. Travis and T. J. Key (2020). "Circulating Insulin-like Growth Factor-I Concentrations and Risk of 30 Cancers: Prospective Analyses in UK Biobank." Cancer Res **80**(18): 4014-4021.

Ko, Y., A. Choi, M. Lee and J. A. Lee (2016). "Metformin displays in vitro and in vivo antitumor effect against osteosarcoma." Korean J Pediatr **59**(9): 374-380.
Kobel, M., D. Weidensdorfer, C. Reinke, M. Lederer, W. D. Schmitt, K. Zeng, C. Thomssen, S. Hauptmann and S. Huttelmaier (2007). "Expression of the RNA-binding protein IMP1 correlates with poor prognosis in ovarian carcinoma." Oncogene **26**(54): 7584-7589.
Kobel, M., H. Xu, P. A. Bourne, B. O. Spaulding, M. Shih Ie, T. L. Mao, R. A. Soslow, C. A. Ewanowich, S. E. Kalloger, E. Mehl, C. H. Lee, D. Huntsman and C. B. Gilks (2009). "IGF2BP3 (IMP3) expression is a marker of unfavorable prognosis in ovarian carcinoma of clear cell subtype." Mod Pathol **22**(3): 469-475.
Kondo, M., H. Suzuki, R. Ueda, H. Osada, K. Takagi, T. Takahashi and T. Takahashi (1995). "Frequent loss of imprinting of the H19 gene is often associated with its overexpression in human lung cancers." Oncogene **10**(6): 1193-1198.
Kornfeld, S. (1992). "Structure and function of the mannose 6-phosphate/insulinlike growth factor II receptors." Annu Rev Biochem **61**: 307-330.
Kuffer, S., T. Gutting, D. Belharazem, C. Sauer, M. S. Michel, A. Marx, L. Trojan and P. Strobel (2018). "Insulin-like growth factor 2 expression in prostate cancer is regulated by promoter-specific methylation." Mol Oncol **12**(2): 256-266.
Kumar, A., P. Singh, A. Pandey and S. B. Gosipatala (2020). "IGFBP3 gene promoter methylation analysis and its association with clinicopathological characteristics of colorectal carcinoma." Mol Biol Rep **47**(9): 6919-6927.
Lagos-Quintana, M., R. Rauhut, W. Lendeckel and T. Tuschl (2001). "Identification of novel genes coding for small expressed RNAs." Science **294**(5543): 853-858.
Lai, Q., Q. Li, C. He, Y. Fang, S. Lin, J. Cai, J. Ding, Q. Zhong, Y. Zhang, C. Wu, X. Wang, J. He, Y. Liu, Q. Yan, A. Li and S. Liu (2020). "CTCF promotes colorectal cancer cell proliferation and chemotherapy resistance to 5-FU via the P53-Hedgehog axis." Aging (Albany NY) **12**(16): 16270-16293.
Laron, Z. (2001). "Insulin-like growth factor 1 (IGF-1): a growth hormone." Mol Pathol **54**(5): 311-316.
Lauby-Secretan, B., C. Scoccianti, D. Loomis, Y. Grosse, F. Bianchini, K. Straif and G. International Agency for Research on Cancer Handbook Working (2016). "Body Fatness and Cancer--Viewpoint of the IARC Working Group." N Engl J Med **375**(8): 794-798.
Lengyel, E., L. Makowski, J. DiGiovanni and M. G. Kolonin (2018). "Cancer as a Matter of Fat: The Crosstalk between Adipose Tissue and Tumors." Trends Cancer **4**(5): 374-384.
Lewitt, M. S., H. Saunders, J. L. Phuyal and R. C. Baxter (1994). "Complex formation by human insulin-like growth factor-binding protein-3 and human acid-labile subunit in growth hormone-deficient rats." Endocrinology **134**(6): 2404-2409.
Li, L., B.-F. Chen and W.-Y. Chan (2015). "An Epigenetic Regulator: Methyl-CpG-Binding Domain Protein 1 (MBD1)." International Journal of Molecular Sciences(16): 5125-5140.
Liang, W., Y. Zou, F. Qin, J. Chen, J. Xu, S. Huang, J. Chen and S. Dai (2017). "sTLR4/MD-2 complex inhibits colorectal cancer migration and invasiveness in vitro and in vivo by lncRNA H19 down-regulation." Acta Biochim Biophys Sin (Shanghai) **49**(11): 1035-1041.
Liang, X., K. Hu, D. Li, Y. Wang, M. Liu, X. Wang, W. Zhu, X. Wang, Z. Yang and J. Lu (2020). "Identification of Core Genes and Potential Drugs for Castration-Resistant Prostate Cancer Based on Bioinformatics Analysis." DNA Cell Biol **39**(5): 836-847.
Liao, L. M., J. N. Hofmann, E. Cho, M. N. Pollak, W. H. Chow and M. P. Purdue (2017). "Circulating levels of obesity-related markers and risk of renal cell carcinoma in the PLCO cancer screening trial." Cancer Causes & Control **28**(7): 801-807.
Lifshitz, K., Y. Ber and D. Margel (2021). "Role of Metabolic Syndrome in Prostate Cancer Development." Eur Urol Focus.
Liou, J. M., C. T. Shun, J. T. Liang, H. M. Chiu, M. J. Chen, C. C. Chen, H. P. Wang, M. S. Wu and J. T. Lin (2010). "Plasma insulin-like growth factor-binding protein-2 levels as diagnostic and prognostic biomarker of colorectal cancer." J Clin Endocrinol Metab **95**(4): 1717-1725.

Liu, L., S. Greenberg, S. M. Russell and C. S. Nicoll (1989). "Effects of insulin-like growth factors I and II on growth and differentiation of transplanted rat embryos and fetal tissues." Endocrinology **124**(6): 3077-3082.
Liu, M., A. Roth, M. Yu, R. Morris, F. Bersani, M. N. Rivera, J. Lu, T. Shioda, S. Vasudevan, S. Ramaswamy, S. Maheswaran, S. Diederichs and D. A. Haber (2013). "The IGF2 intronic miR-483 selectively enhances transcription from IGF2 fetal promoters and enhances tumorigenesis." Genes Dev **27**(23): 2543-2548.
Liu, S. B., L. B. Zhou, H. F. Wang, G. Li, Q. P. Xie and B. Hu (2020). "Loss of IGF2R indicates a poor prognosis and promotes cell proliferation and tumorigenesis in bladder cancer via AKT signaling pathway." Neoplasma **67**(1): 129-136.
Liu, W., Y. Li, B. Wang, L. Dai, W. Qian and J. Y. Zhang (2015). "Autoimmune Response to IGF2 mRNA-Binding Protein 2 (IMP2/p62) in Breast Cancer." Scand J Immunol **81**(6): 502-507.
Liu, W., Z. Li, W. Xu, Q. Wang and S. Yang (2013). "Humoral autoimmune response to IGF2 mRNA-binding protein (IMP2/p62) and its tissue-specific expression in colon cancer." Scand J Immunol **77**(4): 255-260.
Liu, X. Z., L. Pedersen and N. Halberg (2021). "Cellular mechanisms linking cancers to obesity." Cell Stress **5**(5): 55-72.
Liu, Y., C. Yu, Y. Wu, X. Sun, Q. Su, C. You and H. Xin (2017). "CD44(+) fibroblasts increases breast cancer cell survival and drug resistance via IGF2BP3-CD44-IGF2 signalling." J Cell Mol Med **21**(9): 1979-1988.
Liu, Z. L., X. W. Bi, P. P. Liu, D. X. Lei, Y. Wang, Z. M. Li, W. Q. Jiang and Y. Xia (2018). "Expressions and prognostic values of the E2F transcription factors in human breast carcinoma." Cancer Manag Res **10**: 3521-3532.
Livingstone, C. and A. Borai (2014). "Insulin-like growth factor-II: its role in metabolic and endocrine disease." Clin Endocrinol (Oxf) **80**(6): 773-781.
Locatelli, V. and V. E. Bianchi (2014). "Effect of GH/IGF-1 on Bone Metabolism and Osteoporsosis." Int J Endocrinol **2014**: 235060.
Lorente-Sorolla, C., A. Garcia-Gomez, F. Catala-Moll, V. Toledano, L. Ciudad, J. Avendano-Ortiz, C. Maroun-Eid, A. Martin-Quiros, M. Martinez-Gallo, A. Ruiz-Sanmartin, A. G. Del Campo, R. Ferrer-Roca, J. C. Ruiz-Rodriguez, D. Alvarez-Errico, E. Lopez-Collazo and E. Ballestar (2019). "Inflammatory cytokines and organ dysfunction associate with the aberrant DNA methylome of monocytes in sepsis." Genome Med **11**(1): 66.
Lorsch, J. R., F. S. Collins and J. Lippincott-Schwartz (2014). "Cell Biology. Fixing problems with cell lines." Science **346**(6216): 1452-1453.
Lu, L., M. Cai, M. Peng, F. Wang and X. Zhai (2019). "miR-491-5p functions as a tumor suppressor by targeting IGF2 in colorectal cancer." Cancer Manag Res **11**: 1805-1816.
Lui, J. C. and J. Baron (2013). "Evidence that Igf2 down-regulation in postnatal tissues and up-regulation in malignancies is driven by transcription factor E2f3." Proc Natl Acad Sci U S A **110**(15): 6181-6186.
Manabe, T., H. Yasuda, H. Terai, H. Kagiwada, J. Hamamoto, T. Ebisudani, K. Kobayashi, K. Masuzawa, S. Ikemura, I. Kawada, Y. Hayashi, K. Fukui, K. Horimoto, K. Fukunaga and K. Soejima (2020). "IGF2 Autocrine-Mediated IGF1R Activation Is a Clinically Relevant Mechanism of Osimertinib Resistance in Lung Cancer." Mol Cancer Res **18**(4): 549-559.
Mancarella, C., G. Caldoni, I. Ribolsi, A. Parra, M. C. Manara, A. M. Mercurio, A. Morrione and K. Scotlandi (2020). "Insulin-Like Growth Factor 2 mRNA-Binding Protein 3 Modulates Aggressiveness of Ewing Sarcoma by Regulating the CD164-CXCR4 Axis." Front Oncol **10**: 994.
Mancarella, C., A. Morrione and K. Scotlandi (2021). "Novel Regulators of the IGF System in Cancer." Biomolecules **11**(2).
Mantzoros, C. S., A. Tzonou, L. B. Signorello, M. Stampfer, D. Trichopoulos and H. O. Adami (1997). "Insulin-like growth factor 1 in relation to prostate cancer and benign prostatic hyperplasia." Br J Cancer **76**(9): 1115-1118.

Marin, T. L., B. Gongol, F. Zhang, M. Martin, D. A. Johnson, H. Xiao, Y. Wang, S. Subramaniam, S. Chien and J. Y. Shyy (2017). "AMPK promotes mitochondrial biogenesis and function by phosphorylating the epigenetic factors DNMT1, RBBP7, and HAT1." Sci Signal **10**(464).
Marshall, R. N., L. E. Underwood, S. J. Voina, D. B. Foushee and J. J. Van Wyk (1974). "Characterization of the insulin and somatomedin-C receptors in human placental cell membranes." J Clin Endocrinol Metab **39**(2): 283-292.
Massague, J. and M. P. Czech (1982). The subunit structures of two distinct receptors for insulin-like growth factors I and II and their relationship to the insulin receptor. Journal of Biological Chemistry**:** 5038-5045.
Massague, J., P. F. Pilch and M. P. Czech (1980). "Electrophoretic resolution of three major insulin receptor structures with unique subunit stoichiometries." Proc Natl Acad Sci U S A **77**(12): 7137-7141.
Matuschek, C., M. Rudoy, M. Peiper, P. A. Gerber, N. P. Hoff, B. A. Buhren, B. Flehmig, W. Budach, W. T. Knoefel, H. Bojar, H. B. Prisack, G. Steinbach, V. Shukla, A. Schwarz, K. Kammers, A. Erhardt, A. Scherer, E. Bolke and M. Schauer (2011). "Do insulin-like growth factor associated proteins qualify as a tumor marker? Results of a prospective study in 163 cancer patients." Eur J Med Res **16**(10): 451-456.
McGrath, J. and D. Solter (1984). "Completion of mouse embryogenesis requires both the maternal and paternal genomes." Cell **37**(1): 179-183.
McMullen, E. R., M. E. Gonzalez, S. L. Skala, M. Tran, D. Thomas, S. I. Djomehri, B. Burman, K. M. Kidwell and C. G. Kleer (2018). "CCN6 regulates IGF2BP2 and HMGA2 signaling in metaplastic carcinomas of the breast." Breast Cancer Res Treat **172**(3): 577-586.
Meinsma, D., P. E. Holthuizen, J. L. Van den Brande and J. S. Sussenbach (1991). "Specific endonucleolytic cleavage of IGF-II mRNAs." Biochem Biophys Res Commun **179**(3): 1509-1516.
Meng, F., L. Song and W. Wang (2017). "Metformin Improves Overall Survival of Colorectal Cancer Patients with Diabetes: A Meta-Analysis." J Diabetes Res **2017**: 5063239.
Messina, C., C. Cattrini, D. Soldato, G. Vallome, O. Caffo, E. Castro, D. Olmos, F. Boccardo and E. Zanardi (2020). "BRCA Mutations in Prostate Cancer: Prognostic and Predictive Implications." J Oncol **2020**: 4986365.
Meziou, S., C. Ringuette Goulet, H. Hovington, V. Lefebvre, E. Lavallee, M. Bergeron, H. Brisson, A. Champagne, B. Neveu, D. Lacombe, J. M. Beauregard, F. A. Buteau, J. Riopel and F. Pouliot (2020). "GLUT1 expression in high-risk prostate cancer: correlation with (18)F-FDG-PET/CT and clinical outcome." Prostate Cancer Prostatic Dis **23**(3): 441-448.
Miles, F. L., P. J. Goodman, C. Tangen, K. C. Torkko, J. M. Schenk, X. Song, M. Pollak, I. M. Thompson and M. L. Neuhouser (2017). "Interactions of the Insulin-Like Growth Factor Axis and Vitamin D in Prostate Cancer Risk in the Prostate Cancer Prevention Trial." Nutrients **9**(4): E378.
Milligan, L., E. Antoine, C. Bisbal, M. Weber, C. Brunel, T. Forne and G. Cathala (2000). "H19 gene expression is up-regulated exclusively by stabilization of the RNA during muscle cell differentiation." Oncogene **19**(50): 5810-5816.
Mishima, C., N. Kagara, T. Tanei, Y. Naoi, M. Shimoda, A. Shimomura, K. Shimazu, S. J. Kim and S. Noguchi (2016). "Loss of imprinting of IGF2 in fibroadenomas and phyllodes tumors of the breast." Oncol Rep **35**(3): 1511-1518.
Mohan, S. and D. J. Baylink (2002). "IGF-binding proteins are multifunctional and act via IGF-dependent and -independent mechanisms." J Endocrinol **175**(1): 19-31.
Molnar, K., A. Meszaros, C. Fazakas, M. Kozma, F. Gyori, Z. Reisz, L. Tiszlavicz, A. E. Farkas, A. Nyul-Toth, J. Hasko, I. A. Krizbai and I. Wilhelm (2020). "Pericyte-secreted IGF2 promotes breast cancer brain metastasis formation." Mol Oncol **14**(9): 2040-2057.
Morimoto-Kamata, R. and S. Yui (2017). "Insulin-like growth factor-1 signaling is responsible for cathepsin G-induced aggregation of breast cancer MCF-7 cells." Cancer Science **108** (8): 1574-1583.
Motawi, T. K., O. G. Shaker, M. F. Ismail and N. H. Sayed (2017). "Peroxisome Proliferator-Activated Receptor Gamma in Obesity and Colorectal Cancer: the Role of Epigenetics." Sci Rep **7**(1): 10714.

Moulton, T., T. Crenshaw, Y. Hao, J. Moosikasuwan, N. Lin, F. Dembitzer, T. Hensle, L. Weiss, L. McMorrow, T. Loew, W. Kraus, W. Gerald and B. Tycko (1994). "Epigenetic lesions at the H19 locus in Wilms' tumour patients." Nat Genet **7**(3): 440-447.
Mountziaris, P. M., S. N. Tzouanas and A. G. Mikos (2010). "Dose effect of tumor necrosis factor-alpha on in vitro osteogenic differentiation of mesenchymal stem cells on biodegradable polymeric microfiber scaffolds." Biomaterials **31**(7): 1666-1675.
Muller, V., L. Oliveira-Ferrer, B. Steinbach, K. Pantel and H. Schwarzenbach (2019). "Interplay of lncRNA H19/miR-675 and lncRNA NEAT1/miR-204 in breast cancer." Mol Oncol **13**(5): 1137-1149.
Murphy, N., A. Knuppel, N. Papadimitriou, R. M. Martin, K. K. Tsilidis, K. Smith-Byrne, G. Fensom, A. Perez-Cornago, R. C. Travis, T. J. Key and M. J. Gunter (2020). "Insulin-like growth factor-1, insulin-like growth factor-binding protein-3, and breast cancer risk: observational and Mendelian randomization analyses with approximately 430 000 women." Ann Oncol **31**(5): 641-649.
Mutgan, A. C., H. E. Besikcioglu, S. Wang, H. Friess, G. O. Ceyhan and I. E. Demir (2018). "Insulin/IGF-driven cancer cell-stroma crosstalk as a novel therapeutic target in pancreatic cancer." Mol Cancer **17**(1): 66.
Mutskov, V. and G. Felsenfeld (2009). "The human insulin gene is part of a large open chromatin domain specific for human islets." Proc Natl Acad Sci U S A **106**(41): 17419-17424.
Nakagawa, H., R. B. Chadwick, P. Peltomaki, C. Plass, Y. Nakamura and A. de La Chapelle (2001). "Loss of imprinting of the insulin-like growth factor II gene occurs by biallelic methylation in a core region of H19-associated CTCF-binding sites in colorectal cancer." Proc Natl Acad Sci U S A **98**(2): 591-596.
Navale, A. M. and A. N. Paranjape (2016). "Glucose transporters: physiological and pathological roles." Biophys Rev **8**(1): 5-9.
Nielsen, J., J. Christiansen, J. Lykke-Andersen, A. H. Johnsen, U. M. Wewer and F. C. Nielsen (1999). "A family of insulin-like growth factor II mRNA-binding proteins represses translation in late development." Mol Cell Biol **19**(2): 1262-1270.
Nordin, M., D. Bergman, M. Halje, W. Engstrom and A. Ward (2014). "Epigenetic regulation of the Igf2/H19 gene cluster." Cell Prolif **47**(3): 189-199.
Nwokafor, C. U., R. S. Sellers and R. H. Singer (2016). "IMP1, an mRNA binding protein that reduces the metastatic potential of breast cancer in a mouse model." Oncotarget **7**(45): 72662-72671.
O'Dell, S. D., G. J. Miller, J. A. Cooper, P. C. Hindmarsh, P. J. Pringle, H. Ford, S. E. Humphries and I. N. Day (1997). "Apal polymorphism in insulin-like growth factor II (IGF2) gene and weight in middle-aged males." Int J Obes Relat Metab Disord **21**(9): 822-825.
Ogawa, O., M. R. Eccles, J. Szeto, L. A. McNoe, K. Yun, M. A. Maw, P. J. Smith and A. E. Reeve (1993). "Relaxation of insulin-like growth factor II gene imprinting implicated in Wilms' tumour." Nature **362**(6422): 749-751.
Oleynikov, Y. and R. H. Singer (2003). "Real-time visualization of ZBP1 association with beta-actin mRNA during transcription and localization." Curr Biol **13**(3): 199-207.
Oliva, C. R., B. Halloran, A. B. Hjelmeland, A. Vazquez, S. M. Bailey, J. N. Sarkaria and C. E. Griguer (2018). "IGFBP6 controls the expansion of chemoresistant glioblastoma through paracrine IGF2/IGF-1R signaling." Cell Commun Signal **16**(1): 61.
Onfroy-Roy, L., D. Hamel, L. Malaquin and A. Ferrand (2021). "Colon Fibroblasts and Inflammation: Sparring Partners in Colorectal Cancer Initiation?" Cancers (Basel) **13**(8).
Ong, X. R. S., D. Bagguley, J. W. Yaxley, A. A. Azad, D. G. Murphy and N. Lawrentschuk (2020). "Understanding the diagnosis of prostate cancer." Med J Aust **213**(9): 424-429.
Osher, E. and V. M. Macaulay (2019). "Therapeutic Targeting of the IGF Axis." Cells **8**(8).
Owerbach, D., G. I. Bell, W. J. Rutter, J. A. Brown and T. B. Shows (1981). "The insulin gene is located on the short arm of chromosome 11 in humans." Diabetes **30**(3): 267-270.
Pachnis, V., A. Belayew and S. M. Tilghman (1984). "Locus unlinked to alpha-fetoprotein under the control of the murine raf and Rif genes." Proc Natl Acad Sci U S A **81**(17): 5523-5527.

Paradowska, A., I. Fenic, L. Konrad, K. Sturm, F. Wagenlehner, W. Weidner and K. Steger (2009). "Aberrant epigenetic modifications in the CTCF binding domain of the IGF2/H19 gene in prostate cancer compared with benign prostate hyperplasia." Int J Oncol **35**(1): 87-96.
Park, K. S., A. Mitra, B. Rahat, K. Kim and K. Pfeifer (2017). "Loss of imprinting mutations define both distinct and overlapping roles for misexpression of IGF2 and of H19 lncRNA." Nucleic Acids Res **45**(22): 12766-12779.
Pedone, P. V., M. J. Pikaart, F. Cerrato, M. Vernucci, P. Ungaro, C. B. Bruni and A. Riccio (1999). "Role of histone acetylation and DNA methylation in the maintenance of the imprinted expression of the H19 and Igf2 genes." FEBS Lett **458**(1): 45-50.
Pernicova, I. and M. Korbonits (2014). "Metformin--mode of action and clinical implications for diabetes and cancer." Nat Rev Endocrinol **10**(3): 143-156.
Pfaffl, M. W. (2001). "A new mathematical model for relative quantification in real-time RT-PCR." Nucleic Acids Research: 2002-2007.
Philippou, A., M. Maridaki, S. Pneumaticos and M. Koutsilieris (2014). "The complexity of the IGF1 gene splicing, posttranslational modification and bioactivity." Mol Med **20**: 202-214.
Pilie, P. G., V. N. Giri and K. A. Cooney (2016). "HOXB13 and other high penetrant genes for prostate cancer." Asian J Androl **18**(4): 530-532.
Pinzon-Cortes, J. A., A. Perna-Chaux, N. S. Rojas-Villamizar, A. Diaz-Basabe, D. C. Polania-Villanueva, M. F. Jacome, C. O. Mendivil, H. Groot and V. Lopez-Segura (2017). "Effect of diabetes status and hyperglycemia on global DNA methylation and hydroxymethylation." Endocr Connect **6**(8): 708-725.
Poli, G., G. Cantini, R. Armignacco, R. Fucci, R. Santi, L. Canu, G. Nesi, M. Mannelli and M. Luconi (2016). "Metformin as a new anti-cancer drug in adrenocortical carcinoma." Oncotarget **7**(31): 49636-49648.
Poti, J. M., B. Braga and B. Qin (2017). "Ultra-processed Food Intake and Obesity: What Really Matters for Health-Processing or Nutrient Content?" Curr Obes Rep **6**(4): 420-431.
Probst-Hensch, N. M., J. M. Yuan, F. Z. Stanczyk, Y. T. Gao, R. K. Ross and M. C. Yu (2001). "IGF-1, IGF-2 and IGFBP-3 in prediagnostic serum: association with colorectal cancer in a cohort of Chinese men in Shanghai." Br J Cancer **85**(11): 1695-1699.
Quail, D. F. and A. J. Dannenberg (2019). "The obese adipose tissue microenvironment in cancer development and progression." Nat Rev Endocrinol **15**(3): 139-154.
Quan, P. L., M. Sauzade and E. Brouzes (2018). "dPCR: A Technology Review." Sensors (Basel) **18**(4).
Radhakrishnan, V. K., L. C. Hernandez, K. Anderson, Q. Tan, M. De Leon and D. D. De Leon (2015). "Expression of Intratumoral IGF-II Is Regulated by the Gene Imprinting Status in Triple Negative Breast Cancer from Vietnamese Patients." Int J Endocrinol **2015**: 401851.
Raeeszadeh-Sarmazdeh, M., L. D. Do and B. G. Hritz (2020). "Metalloproteinases and Their Inhibitors: Potential for the Development of New Therapeutics." Cells **9**(5).
Rainier, S., C. J. Dobry and A. P. Feinberg (1995). "Loss of imprinting in hepatoblastoma." Cancer Res **55**(9): 1836-1838.
Rajaram, S., D. J. Baylink and S. Mohan (1997). "Insulin-like growth factor-binding proteins in serum and other biological fluids: regulation and functions." Endocr Rev **18**(6): 801-831.
Ramirez-Moreno, E., M. Lozano-Lozano, F. O'Valle Ravassa, C. Ramirez-Tortosa and R. Ruiz-Villaverde (2020). "Expression of IMP3 in a retrospective cohort of melanomas with selective lymph node biopsy." Dermatol Ther **33**(6): e14413.
Ramos-Lopez, O., J. I. Riezu-Boj, F. I. Milagro, J. Alfredo Martinez and M. Project (2019). "Association of Methylation Signatures at Hepatocellular Carcinoma Pathway Genes with Adiposity and Insulin Resistance Phenotypes." Nutr Cancer **71**(5): 840-851.
Raveh, E., I. J. Matouk, M. Gilon and A. Hochberg (2015). "The H19 Long non-coding RNA in cancer initiation, progression and metastasis - a proposed unifying theory." Mol Cancer **14**: 184.
Rawla, P., T. Sunkara and A. Barsouk (2019). "Epidemiology of colorectal cancer: incidence, mortality, survival, and risk factors." Prz Gastroenterol **14**(2): 89-103.

Reaven, G. M. (1995). "Pathophysiology of insulin resistance in human disease." Physiol Rev **75**(3): 473-486.
Reaven, G. M. (2005). "The insulin resistance syndrome: definition and dietary approaches to treatment." Annu Rev Nutr **25**: 391-406.
Rebbeck, T. R. (2017). "Prostate Cancer Genetics: Variation by Race, Ethnicity, and Geography." Semin Radiat Oncol **27**(1): 3-10.
Rebbeck, T. R. (2018). "Prostate Cancer Disparities by Race and Ethnicity: From Nucleotide to Neighborhood." Cold Spring Harb Perspect Med **8**(9).
Rebello, R. J., C. Oing, K. E. Knudsen, S. Loeb, D. C. Johnson, R. E. Reiter, S. Gillessen, T. Van der Kwast and R. G. Bristow (2021). "Prostate cancer." Nat Rev Dis Primers **7**(1): 9.
Reeve, A. E., M. R. Eccles, R. J. Wilkins, G. I. Bell and L. J. Millow (1985). "Expression of insulin-like growth factor-II transcripts in Wilms' tumour." Nature **317**(6034): 258-260.
Reik, W. and A. Murrell (2000). "Genomic imprinting. Silence across the border." Nature **405**(6785): 408-409.
Rena, G., D. G. Hardie and E. R. Pearson (2017). "The mechanisms of action of metformin." Diabetologia **60**(9): 1577-1585.
Renehan, A. G., J. Jones, C. S. Potten, S. M. Shalet and S. T. O'Dwyer (2000). "Elevated serum insulin-like growth factor (IGF)-II and IGF binding protein-2 in patients with colorectal cancer." Br J Cancer **83**(10): 1344-1350.
Resnicoff, M., D. Abraham, W. Yutanawiboonchai, H. L. Rotman, J. Kajstura, R. Rubin, P. Zoltick and R. Baserga (1995). "The insulin-like growth factor I receptor protects tumor cells from apoptosis in vivo." Cancer Res **55**(11): 2463-2469.
Rinderknecht, E. and R. E. Humbel (1976). Amino-terminal sequences of two polypeptides from human serum with nonsuppressible insulin-like and cell-growth-promoting activities: Evidence for structural homology with insulin B chain. Proceedings of the National Academy of Sciences of the United States of America**:** 4379-4381.
Rogers, M. A., V. Kalter, M. Strowitzki, M. Schneider and P. Lichter (2016). "IGF2 knockdown in two colorectal cancer cell lines decreases survival, adhesion and modulates survival-associated genes." Tumour Biol **37**(9): 12485-12495.
Rosenfeld, L. (2002). "Insulin: discovery and controversy." Clin Chem **48**(12): 2270-2288.
Rotwein, P. (2018). "The insulin-like growth factor 2 gene and locus in nonmammalian vertebrates: Organizational simplicity with duplication but limited divergence in fish." J Biol Chem **293**(41): 15912-15932.
Sakatani, T., A. Kaneda, C. A. Iacobuzio-Donahue, M. G. Carter, S. de Boom Witzel, H. Okano, M. S. Ko, R. Ohlsson, D. L. Longo and A. P. Feinberg (2005). "Loss of imprinting of Igf2 alters intestinal maturation and tumorigenesis in mice." Science **307**(5717): 1976-1978.
Salmon, W. D., Jr. and W. H. Daughaday (1957). "A hormonally controlled serum factor which stimulates sulfate incorporation by cartilage in vitro." J Lab Clin Med **49**(6): 825-836.
Samblas, M., F. I. Milagro and A. Martinez (2019). "DNA methylation markers in obesity, metabolic syndrome, and weight loss." Epigenetics **14**(5): 421-444.
Sanger, F. and H. Tuppy (1951). "The amino-acid sequence in the phenylalanyl chain of insulin. I. The identification of lower peptides from partial hydrolysates." Biochem J **49**(4): 463-481.
Sara, V. R., K. Hall, H. Von Holtz, R. Humbel, B. Sjogren and L. Wetterberg (1982). "Evidence for the presence of specific receptors for insulin-like growth factors 1 (IGE-1) and 2 (IGF-2) and insulin throughout the adult human brain." Neurosci Lett **34**(1): 39-44.
Schaeffer, D. F., D. R. Owen, H. J. Lim, A. K. Buczkowski, S. W. Chung, C. H. Scudamore, D. G. Huntsman, S. S. Ng and D. A. Owen (2010). "Insulin-like growth factor 2 mRNA binding protein 3 (IGF2BP3) overexpression in pancreatic ductal adenocarcinoma correlates with poor survival." BMC Cancer **10**: 59.

Schaeffer, V., K. M. Hansen, D. R. Morris, R. C. LeBoeuf and C. K. Abrass (2012). "RNA-binding protein IGF2BP2/IMP2 is required for laminin-beta2 mRNA translation and is modulated by glucose concentration." Am J Physiol Renal Physiol **303**(1): F75-82.
Schagdarsurengin, U., A. Lammert, N. Schunk, D. Sheridan, S. Gattenloehner, K. Steger, F. Wagenlehner and T. Dansranjavin (2017). "Impairment of IGF2 gene expression in prostate cancer is triggered by epigenetic dysregulation of IGF2-DMR0 and its interaction with KLF4." Cell Commun Signal **15**(1): 40.
Schoen, R. E., C. M. Tangen, L. H. Kuller, G. L. Burke, M. Cushman, R. P. Tracy, A. Dobs and P. J. Savage (1999). "Increased blood glucose and insulin, body size, and incident colorectal cancer." J Natl Cancer Inst **91**(13): 1147-1154.
Scott, L. J., K. L. Mohlke, L. L. Bonnycastle, C. J. Willer, Y. Li, W. L. Duren, M. R. Erdos, H. M. Stringham, P. S. Chines, A. U. Jackson, L. Prokunina-Olsson, C. J. Ding, A. J. Swift, N. Narisu, T. Hu, R. Pruim, R. Xiao, X. Y. Li, K. N. Conneely, N. L. Riebow, A. G. Sprau, M. Tong, P. P. White, K. N. Hetrick, M. W. Barnhart, C. W. Bark, J. L. Goldstein, L. Watkins, F. Xiang, J. Saramies, T. A. Buchanan, R. M. Watanabe, T. T. Valle, L. Kinnunen, G. R. Abecasis, E. W. Pugh, K. F. Doheny, R. N. Bergman, J. Tuomilehto, F. S. Collins and M. Boehnke (2007). "A genome-wide association study of type 2 diabetes in Finns detects multiple susceptibility variants." Science **316**(5829): 1341-1345.
Sedhom, R. and E. S. Antonarakis (2019). "Clinical implications of mismatch repair deficiency in prostate cancer." Future Oncol **15**(20): 2395-2411.
Shaalan, Y. M., H. Handoussa, R. A. Youness, R. A. Assal, A. H. El-Khatib, M. W. Linscheid, H. M. El Tayebi and A. I. Abdelaziz (2018). "Destabilizing the interplay between miR-1275 and IGF2BPs by Tamarix articulata and quercetin in hepatocellular carcinoma." Nat Prod Res **32**(18): 2217-2220.
Shanmugam, M. K. and G. Sethi (2013). "Role of epigenetics in inflammation-associated diseases." Subcell Biochem **61**: 627-657.
Shao, M., Z. Yu and J. Zou (2020). "LncRNA-SNHG16 Silencing Inhibits Prostate Carcinoma Cell Growth, Downregulate GLUT1 Expression and Reduce Glucose Uptake." Cancer Manag Res **12**: 1751-1757.
Shen, J., A. Wang, Q. Wang, I. Gurvich, A. B. Siegel, H. Remotti and R. M. Santella (2013). "Exploration of genome-wide circulating microRNA in hepatocellular carcinoma: MiR-483-5p as a potential biomarker." Cancer Epidemiol Biomarkers Prev **22**(12): 2364-2373.
Shin, J. H., R. W. Li, Y. Gao, D. M. Bickhart, G. E. Liu, W. Li, S. Wu and C. J. Li (2013). "Butyrate Induced IGF2 Activation Correlated with Distinct Chromatin Signatures Due to Histone Modification." Gene Regul Syst Bio **7**: 57-70.
Siegel, R. L., K. D. Miller and A. Jemal (2016). "Cancer statistics, 2016." CA Cancer J Clin **66**(1): 7-30.
Simons, A. L., D. M. Mattson, K. Dornfeld and D. R. Spitz (2009). "Glucose deprivation-induced metabolic oxidative stress and cancer therapy." J Cancer Res Ther **5 Suppl 1**: S2-6.
Skinner, M. A., R. Vollmer, G. Huper, P. Abbott and J. D. Iglehart (1990). "Loss of heterozygosity for genes on 11p and the clinical course of patients with lung carcinoma." Cancer Res **50**(8): 2303-2306.
Soravia, C., B. Bapat and Z. Cohen (1997). "Familial adenomatous polyposis (FAP) and hereditary nonpolyposis colorectal cancer (HNPCC): a review of clinical, genetic and therapeutic aspects." Schweiz Med Wochenschr **127**(16): 682-690.
Spitz, D. R., J. E. Sim, L. A. Ridnour, S. S. Galoforo and Y. J. Lee (2000). "Glucose deprivation-induced oxidative stress in human tumor cells. A fundamental defect in metabolism?" Ann N Y Acad Sci **899**: 349-362.
Srivastava, S. P. and J. E. Goodwin (2020). "Cancer Biology and Prevention in Diabetes." Cells **9**(6).
Steenman, M. J., S. Rainier, C. J. Dobry, P. Grundy, I. L. Horon and A. P. Feinberg (1994). "Loss of imprinting of IGF2 is linked to reduced expression and abnormal methylation of H19 in Wilms' tumour." Nat Genet **7**(3): 433-439.
Steiger, P. and H. C. Thoeny (2016). "Prostate MRI based on PI-RADS version 2: how we review and report." Cancer Imaging **16**: 9.

Steliou, K., M. S. Boosalis, S. P. Perrine, J. Sangerman and D. V. Faller (2012). "Butyrate histone deacetylase inhibitors." Biores Open Access **1**(4): 192-198.
Surani, M. A., S. C. Barton and M. L. Norris (1984). "Development of reconstituted mouse eggs suggests imprinting of the genome during gametogenesis." Nature **308**(5959): 548-550.
Sykes, P. J., S. H. Neoh, M. J. Brisco, E. Hughes, J. Condon and A. A. Morley (1992). "Quantitation of targets for PCR by use of limiting dilution." Biotechniques **13**(3): 444-449.
Taitt, H. E. (2018). "Global Trends and Prostate Cancer: A Review of Incidence, Detection, and Mortality as Influenced by Race, Ethnicity, and Geographic Location." Am J Mens Health **12**(6): 1807-1823.
Takamaru, H., E. Yamamoto, H. Suzuki, M. Nojima, R. Maruyama, H. O. Yamano, K. Yoshikawa, T. Kimura, T. Harada, M. Ashida, R. Suzuki, H. Yamamoto, M. Kai, T. Tokino, T. Sugai, K. Imai, M. Toyota and Y. Shinomura (2012). "Aberrant methylation of RASGRF1 is associated with an epigenetic field defect and increased risk of gastric cancer." Cancer Prev Res (Phila) **5**(10): 1203-1212.
Takano, Y., G. Shiota and H. Kawasaki (2000). "Analysis of genomic imprinting of insulin-like growth factor 2 in colorectal cancer." Oncology **59**(3): 210-216.
Tang, Z., D. Gillatt, E. Rowe, A. Koupparis, J. M. P. Holly and C. M. Perks (2019). "IGFBP-2 acts as a tumour suppressor and plays a role in determining chemosensitivity in bladder cancer cells." Oncotarget **10**(66): 7043-7057.
Taniguchi, T., M. J. Sullivan, O. Ogawa and A. E. Reeve (1995). "Epigenetic changes encompassing the IGF2/H19 locus associated with relaxation of IGF2 imprinting and silencing of H19 in Wilms tumor." Proc Natl Acad Sci U S A **92**(6): 2159-2163.
Tarnowski, M., M. Tkacz, K. Zgutka, J. Bujak, P. Kopytko and A. Pawlik (2017). "Picropodophyllin (PPP) is a potent rhabdomyosarcoma growth inhibitor both in vitro and in vivo." BMC Cancer **17**(1): 532.
Theis, D. R. Z. and M. White (2021). "Is Obesity Policy in England Fit for Purpose? Analysis of Government Strategies and Policies, 1992-2020." Milbank Q **99**(1): 126-170.
Thiese, M. S., B. Ronna and U. Ott (2016). "P value interpretations and considerations." J Thorac Dis **8**(9): E928-E931.
Thomson, A., M. Li, J. Grummet and S. Sengupta (2020). "Transperineal prostate biopsy: a review of technique." Transl Androl Urol **9**(6): 3009-3017.
Tian, B., Y. Zhao, T. Liang, X. Ye, Z. Li, D. Yan, Q. Fu and Y. Li (2017). "Curcumin inhibits urothelial tumor development by suppressing IGF2 and IGF2-mediated PI3K/AKT/mTOR signaling pathway." J Drug Target **25**(7): 626-636.
Tian, F., Z. Tang, G. Song, Y. Pan, B. He, Q. Bao and S. Wang (2012). "Loss of imprinting of IGF2 correlates with hypomethylation of the H19 differentially methylated region in the tumor tissue of colorectal cancer patients." Mol Med Rep **5**(6): 1536-1540.
Tsekrekos, A., A. Lovece, D. Chrysikos, N. Ndegwa, D. Schizas, K. Kumagai and I. Rouvelas (2021). "Impact of obesity on the outcomes after gastrectomy for gastric cancer: A meta-analysis." Asian J Surg.
Ullman, T. A. and S. H. Itzkowitz (2011). "Intestinal inflammation and cancer." Gastroenterology **140**(6): 1807-1816.
Um, C. Y., V. Fedirko, W. D. Flanders, C. Hoflich, E. Wirthgen and R. M. Bostick (2017). "Circulating insulin-like growth factor-related biomarkers: Correlates and responses to calcium supplementation in colorectal adenoma patients." Molecular Carcinogenesis **56**(9): 2127-2134.
Unger, C., N. Kramer, D. Unterleuthner, M. Scherzer, A. Burian, A. Rudisch, M. Stadler, M. Schlederer, D. Lenhardt, A. Riedl, S. Walter, A. Wernitznig, L. Kenner, M. Hengstschlager, J. Schuler, W. Sommergruber and H. Dolznig (2017). "Stromal-derived IGF2 promotes colon cancer progression via paracrine and autocrine mechanisms." Oncogene **36**(38): 5341-5355.
Uson Junior, P. L. S., D. Riegert-Johnson, L. Boardman, J. Kisiel, L. Mountjoy, N. Patel, B. Lizaola-Mayo, M. J. Borad, D. Ahn, M. B. Sonbol, J. Jones, J. A. Leighton, S. Gurudu, H. Singh, M. Klint, K. L. Kunze, M. A. Golafshar, E. D. Esplin, R. L. Nussbaum, A. K. Stewart, T. Bekaii-Saab and N. J. Samadder

(2021). "Germline cancer susceptibility gene testing in unselected patients with colorectal adenocarcinoma: A multi-center prospective study." Clin Gastroenterol Hepatol.
Uson, P. L. S., Jr., D. Riegert-Johnson, L. Boardman, J. Kisiel, L. Mountjoy, N. Patel, B. Lizaola-Mayo, M. J. Borad, D. Ahn, M. B. Sonbol, J. Jones, J. A. Leighton, S. Gurudu, H. Singh, M. Klint, K. L. Kunze, M. A. Golafshar, E. D. Esplin, R. L. Nussbaum, A. K. Stewart, T. Bekaii-Saab and N. Jewel Samadder (2021). "Germline Cancer Susceptibility Gene Testing in Unselected Patients With Colorectal Adenocarcinoma: A Multicenter Prospective Study." Clin Gastroenterol Hepatol.
van Dijk, M. A., F. M. van Schaik, H. J. Bootsma, P. Holthuizen and J. S. Sussenbach (1991). "Initial characterization of the four promoters of the human insulin-like growth factor II gene." Mol Cell Endocrinol **81**(1-3): 81-94.
Verona, R. I. and M. S. Bartolomei (2004). "Role of H19 3' sequences in controlling H19 and Igf2 imprinting and expression." Genomics **84**(1): 59-68.
Verschoor, C. P., L. M. McEwen, V. Kohli, C. Wolfson, D. M. Bowdish, P. Raina, M. S. Kobor and C. Balion (2017). "The relation between DNA methylation patterns and serum cytokine levels in community-dwelling adults: a preliminary study." BMC Genet **18**(1): 57.
Viennois, E., D. Merlin, A. T. Gewirtz and B. Chassaing (2017). "Dietary Emulsifier-Induced Low-Grade Inflammation Promotes Colon Carcinogenesis." Cancer Res **77**(1): 27-40.
Villeneuve, L. M., M. A. Reddy and R. Natarajan (2011). "Epigenetics: deciphering its role in diabetes and its chronic complications." Clin Exp Pharmacol Physiol **38**(7): 451-459.
Vinciguerra, M., A. Musaro and N. Rosenthal (2010). "Regulation of muscle atrophy in aging and disease." Adv Exp Med Biol **694**: 211-233.
Volkmar, M., S. Dedeurwaerder, D. A. Cunha, M. N. Ndlovu, M. Defrance, R. Deplus, E. Calonne, U. Volkmar, M. Igoillo-Esteve, N. Naamane, S. Del Guerra, M. Masini, M. Bugliani, P. Marchetti, M. Cnop, D. L. Eizirik and F. Fuks (2012). "DNA methylation profiling identifies epigenetic dysregulation in pancreatic islets from type 2 diabetic patients." EMBO J **31**(6): 1405-1426.
Voutsadakis, I. A. (2017). "Obesity and diabetes as prognostic factors in patients with colorectal cancer." Diabetes Metab Syndr **11 Suppl 1**: S109-S114.
Vu, T. H., C. Yballe, S. Boonyanit and A. R. Hoffman (1995). "Insulin-like growth factor II in uterine smooth-muscle tumors: maintenance of genomic imprinting in leiomyomata and loss of imprinting in leiomyosarcomata." J Clin Endocrinol Metab **80**(5): 1670-1676.
Wada, M., R. C. Seeger, H. Mizoguchi and H. P. Koeffler (1995). "Maintenance of normal imprinting of H19 and IGF2 genes in neuroblastoma." Cancer Res **55**(15): 3386-3388.
Wang, B. J., L. Wang, S. Y. Yang and Z. J. Liu (2015). "Expression and clinical significance of IMP3 in microdissected premalignant and malignant pancreatic lesions." Clin Transl Oncol **17**(3): 215-222.
Wang, H., C. Tang, M. Na, W. Ma, Z. Jiang, Y. Gu, G. Ma, H. Ge, H. Shen and Z. Lin (2017). "miR-422a Inhibits Glioma Proliferation and Invasion by Targeting IGF1 and IGF1R." Oncology Research **25**(2): 187-194.
Wang, J., X. Wang, T. Chen, L. Jiang and Q. Yang (2017). "Huaier Extract Inhibits Breast Cancer Progression Through a LncRNA-H19/MiR-675-5p Pathway." Cell Physiol Biochem **44**(2): 581-593.
Wang, L., A. Aireti, A. Aihaiti and K. Li (2019). "Expression of microRNA-150 and its Target Gene IGF2BP1 in Human Osteosarcoma and their Clinical Implications." Pathol Oncol Res **25**(2): 527-533.
Wang, Q., S. B. Tang, X. B. Song, T. F. Deng, T. T. Zhang, S. Yin, S. M. Luo, W. Shen, C. L. Zhang and Z. J. Ge (2018). "High-glucose concentrations change DNA methylation levels in human IVM oocytes." Hum Reprod **33**(3): 474-481.
Wang, R. J., J. W. Li, B. H. Bao, H. C. Wu, Z. H. Du, J. L. Su, M. H. Zhang and H. Q. Liang (2015). "MicroRNA-873 (miRNA-873) inhibits glioblastoma tumorigenesis and metastasis by suppressing the expression of IGF2BP1." J Biol Chem **290**(14): 8938-8948.
Wang, W. T., H. Ye, P. P. Wei, B. W. Han, B. He, Z. H. Chen and Y. Q. Chen (2016). "LncRNAs H19 and HULC, activated by oxidative stress, promote cell migration and invasion in cholangiocarcinoma through a ceRNA manner." J Hematol Oncol **9**(1): 117.

Wang, X. and Y. Lin (2008). "Tumor necrosis factor and cancer, buddies or foes?" Acta Pharmacol Sin **29**(11): 1275-1288.
Wang, Y., R. G. MacDonald, G. Thinakaran and S. Kar (2017). "Insulin-Like Growth Factor-II/Cation-Independent Mannose 6-Phosphate Receptor in Neurodegenerative Diseases." Mol Neurobiol **54**(4): 2636-2658.
Wang, Y. C., K. McPherson, T. Marsh, S. L. Gortmaker and M. Brown (2011). "Health and economic burden of the projected obesity trends in the USA and the UK." Lancet **378**(9793): 815-825.
Wang, Z., S. T. Lai, L. Xie, J. D. Zhao, N. Y. Ma, J. Zhu, Z. G. Ren and G. L. Jiang (2014). "Metformin is associated with reduced risk of pancreatic cancer in patients with type 2 diabetes mellitus: a systematic review and meta-analysis." Diabetes Res Clin Pract **106**(1): 19-26.
Weinlich, S., S. Huttelmaier, A. Schierhorn, S. E. Behrens, A. Ostareck-Lederer and D. H. Ostareck (2009). "IGF2BP1 enhances HCV IRES-mediated translation initiation via the 3'UTR." RNA **15**(8): 1528-1542.
Weischenfeldt, J., T. Dubash, A. P. Drainas, B. R. Mardin, Y. Chen, A. M. Stutz, S. M. Waszak, G. Bosco, A. R. Halvorsen, B. Raeder, T. Efthymiopoulos, S. Erkek, C. Siegl, H. Brenner, O. T. Brustugun, S. M. Dieter, P. A. Northcott, I. Petersen, S. M. Pfister, M. Schneider, S. K. Solberg, E. Thunissen, W. Weichert, T. Zichner, R. Thomas, M. Peifer, A. Helland, C. R. Ball, M. Jechlinger, R. Sotillo, H. Glimm and J. O. Korbel (2017). "Pan-cancer analysis of somatic copy-number alterations implicates IRS4 and IGF2 in enhancer hijacking." Nat Genet **49**(1): 65-74.
Weksberg, R., D. R. Shen, Y. L. Fei, Q. L. Song and J. Squire (1993). "Disruption of insulin-like growth factor 2 imprinting in Beckwith-Wiedemann syndrome." Nat Genet **5**(2): 143-150.
Wellcome Trust Case Control, C. (2007). "Genome-wide association study of 14,000 cases of seven common diseases and 3,000 shared controls." Nature **447**(7145): 661-678.
Wrigley, S., D. Arafa and D. Tropea (2017). "Insulin-Like Growth Factor 1: At the Crossroads of Brain Development and Aging." Front Cell Neurosci **11**: 14.
Wu, H. K., J. A. Squire, C. G. Catzavelos and R. Weksberg (1997). "Relaxation of imprinting of human insulin-like growth factor II gene, IGF2, in sporadic breast carcinomas." Biochem Biophys Res Commun **235**(1): 123-129.
Wu, Q. B., X. Sheng, N. Zhang, M. W. Yang and F. Wang (2018). "Role of microRNAs in the resistance of colorectal cancer to chemoradiotherapy." Mol Clin Oncol **8**(4): 523-527.
Xing, M., P. Li, X. Wang, J. Li, J. Shi, J. Qin, X. Zhang, Y. Ma, G. Francia and J. Y. Zhang (2019). "Overexpression of p62/IMP2 can Promote Cell Migration in Hepatocellular Carcinoma via Activation of the Wnt/beta-Catenin Pathway." Cancers (Basel) **12**(1).
Xu, T., H. T. Li, J. Wei, M. Li, T. C. Hsieh, Y. T. Lu, R. Lakshminarasimhan, R. Xu, E. Hodara, G. Morrison, H. Gujar, S. K. Rhie, K. Siegmund, G. Liang and A. Goldkorn (2020). "Epigenetic plasticity potentiates a rapid cyclical shift to and from an aggressive cancer phenotype." Int J Cancer **146**(11): 3065-3076.
Xu, X., Y. Yu, K. Zong, P. Lv and Y. Gu (2019). "Up-regulation of IGF2BP2 by multiple mechanisms in pancreatic cancer promotes cancer proliferation by activating the PI3K/Akt signaling pathway." J Exp Clin Cancer Res **38**(1): 497.
Xu, Z., F. Liu, X. Qi and J. Li (1999). "[Relationship between insulin-like growth factor II and prognosis of colorectal cancer]." Zhonghua Wai Ke Za Zhi **37**(12): 718-720, 743.
Xueqing, H., Z. Jun, J. Yueqiang, L. Xin, H. Liya, F. Yuanyuan, Z. Yuting, Z. Hao, W. Hua, L. Jian and Y. Tiejun (2020). "IGF2BP3 May Contributes to Lung Tumorigenesis by Regulating the Alternative Splicing of PKM." Front Bioeng Biotechnol **8**: 679.
Yamamoto, N., T. Oshima, K. Yoshihara, T. Aoyama, T. Hayashi, T. Yamada, T. Sato, M. Shiozawa, T. Yoshikawa, S. Morinaga, Y. Rino, C. Kunisaki, K. Tanaka, M. Akaike, T. Imada and M. Masuda (2017). "Clinicopathological significance and impact on outcomes of the gene expression levels of IGF-1, IGF-2 and IGF-1R, IGFBP-3 in patients with colorectal cancer: Overexpression of the IGFBP-3 gene is an effective predictor of outcomes in patients with colorectal cancer." Oncol Lett **13**(5): 3958-3966.
Yamanaka, Y., E. M. Wilson, R. G. Rosenfeld and Y. Oh (1997). "Inhibition of insulin receptor activation by insulin-like growth factor binding proteins." J Biol Chem **272**(49): 30729-30734.

Yan, A., C. Wang, L. Zheng, J. Zhou and Y. Zhang (2020). "MicroRNA-454-3p inhibits cell proliferation and invasion in esophageal cancer by targeting insulin-like growth factor 2 mRNA-binding protein 1." Oncol Lett **20**(6): 359.
Yan, J., Y. Zhang, Q. She, X. Li, L. Peng, X. Wang, S. Liu, X. Shen, W. Zhang, Y. Dong, J. Lu and G. Zhang (2017). "Long Noncoding RNA H19/miR-675 Axis Promotes Gastric Cancer via FADD/Caspase 8/Caspase 3 Signaling Pathway." Cell Physiol Biochem **42**(6): 2364-2376.
Yan, L., J. Zhou, Y. Gao, S. Ghazal, L. Lu, S. Bellone, Y. Yang, N. Liu, X. Zhao, A. D. Santin, H. Taylor and Y. Huang (2015). "Regulation of tumor cell migration and invasion by the H19/let-7 axis is antagonized by metformin-induced DNA methylation." Oncogene **34**(23): 3076-3084.
Yang, B., N. Damaschke, T. Yao, J. McCormick, J. Wagner and D. Jarrard (2015). "Pyrosequencing for accurate imprinted allele expression analysis." J Cell Biochem **116**(7): 1165-1170.
Yang, B., J. Wagner, N. Damaschke, T. Yao, S. M. Wuerzberger-Davis, M. H. Lee, J. Svaren, S. Miyamoto and D. F. Jarrard (2014). "A novel pathway links oxidative stress to loss of insulin growth factor-2 (IGF2) imprinting through NF-kappaB activation." PLoS One **9**(2): e88052.
Yang, J., J. Wen, T. Tian, Z. Lu, Y. Wang, Z. Wang, X. Wang and Y. Yang (2017). "GLUT-1 overexpression as an unfavorable prognostic biomarker in patients with colorectal cancer." Oncotarget **8**(7): 11788-11796.
Yang, M., Y. Guo, X. Liu and N. Liu (2020). "HMGA1 Promotes Hepatic Metastasis of Colorectal Cancer by Inducing Expression of Glucose Transporter 3 (GLUT3)." Med Sci Monit **26**: e924975.
Yang, W., N. Ning and X. Jin (2017). "The lncRNA H19 Promotes Cell Proliferation by Competitively Binding to miR-200a and Derepressing beta-Catenin Expression in Colorectal Cancer." Biomed Res Int **2017**: 2767484.
Yao, L., M. Liu, Y. Huang, K. Wu, X. Huang, Y. Zhao, W. He and R. Zhang (2019). "Metformin Use and Lung Cancer Risk in Diabetic Patients: A Systematic Review and Meta-Analysis." Dis Markers **2019**: 6230162.
Ye, P., Y. Xi, Z. Huang and P. Xu (2020). "Linking Obesity with Colorectal Cancer: Epidemiology and Mechanistic Insights." Cancers (Basel) **12**(6).
Ye, S., W. Song, X. Xu, X. Zhao and L. Yang (2016). "IGF2BP2 promotes colorectal cancer cell proliferation and survival through interfering with RAF-1 degradation by miR-195." FEBS Lett **590**(11): 1641-1650.
Yong, F. L., C. W. Law and C. W. Wang (2013). "Potentiality of a triple microRNA classifier: miR-193a-3p, miR-23a and miR-338-5p for early detection of colorectal cancer." BMC Cancer **13**: 280.
Yoshimizu, T., A. Miroglio, M. A. Ripoche, A. Gabory, M. Vernucci, A. Riccio, S. Colnot, C. Godard, B. Terris, H. Jammes and L. Dandolo (2008). "The H19 locus acts in vivo as a tumor suppressor." Proc Natl Acad Sci U S A **105**(34): 12417-12422.
Yu, H. and T. Rohan (2000). "Role of the insulin-like growth factor family in cancer development and progression." J Natl Cancer Inst **92**(18): 1472-1489.
Yuan, F., L. Deng, X. Sun, Z. Chen, N. Shivappa, A. K. Sheth, G. S. Cooper, J. R. Hebert and L. Li (2021). "Dietary inflammatory index and risk of colorectal adenoma: effect measure modification by race, nonsteroidal anti-inflammatory drugs, cigarette smoking and body mass index?" Cancer Causes Control.
Yun, J. M., I. Jialal and S. Devaraj (2011). "Epigenetic regulation of high glucose-induced proinflammatory cytokine production in monocytes by curcumin." J Nutr Biochem **22**(5): 450-458.
Yun, K., H. Soejima, A. E. Merrie, J. L. McCall and A. E. Reeve (1999). "Analysis of IGF2 gene imprinting in breast and colorectal cancer by allele specific-PCR." J Pathol **187**(5): 518-522.
Zapf, J. and E. R. Froesch (1981). "Comparison of pancreatic human and biosynthetic human insulin with respect to their action on adipocytes and chick embryo fibroblasts." Diabetes Care **4**(2): 257-259.
Zemel, S., M. S. Bartolomei and S. M. Tilghman (1992). "Physical linkage of two mammalian imprinted genes, H19 and insulin-like growth factor 2." Nat Genet **2**(1): 61-65.

Zhan, S., D. N. Shapiro and L. J. Helman (1994). "Activation of an imprinted allele of the insulin-like growth factor II gene implicated in rhabdomyosarcoma." J Clin Invest **94**(1): 445-448.
Zhang, H., C. Gao, L. Fang, H. C. Zhao and S. K. Yao (2013). "Metformin and reduced risk of hepatocellular carcinoma in diabetic patients: a meta-analysis." Scand J Gastroenterol **48**(1): 78-87.
Zhang, L., W. Zhou, V. E. Velculescu, S. E. Kern, R. H. Hruban, S. R. Hamilton, B. Vogelstein and K. W. Kinzler (1997). "Gene expression profiles in normal and cancer cells." Science **276**(5316): 1268-1272.
Zhang, L., Y. Zhou, T. Huang, A. S. Cheng, J. Yu, W. Kang and K. F. To (2017). The interplay of lncRNA-H19 and its binding partners in physiological process and gastric carcinogenesis. International Journal of Molecular Sciences**:** E450.
Zhang, M., C. H. Wu, X. L. Zhu and Y. J. Wang (2014). "Loss of imprinting of insulin-like growth factor 2 is associated with increased risk of primary lung cancer in the central China region." Asian Pac J Cancer Prev **15**(18): 7799-7803.
Zhang, T. J., J. D. Zhou, W. Zhang, J. Lin, J. C. Ma, X. M. Wen, Q. Yuan, X. X. Li, Z. J. Xu and J. Qian (2018). "H19 overexpression promotes leukemogenesis and predicts unfavorable prognosis in acute myeloid leukemia." Clin Epigenetics **10**: 47.
Zhang, X., D. Wang, B. Liu, X. Jin, X. Wang, J. Pan, W. Tu and Y. Shao (2020). "IMP3 accelerates the progression of prostate cancer through inhibiting PTEN expression in a SMURF1-dependent way." J Exp Clin Cancer Res **39**(1): 190.
Zhang, Z. J., Z. J. Zheng, H. Kan, Y. Song, W. Cui, G. Zhao and K. E. Kip (2011). "Reduced risk of colorectal cancer with metformin therapy in patients with type 2 diabetes: a meta-analysis." Diabetes Care **34**(10): 2323-2328.
Zhao, L., Y. Liu and X. Wang (2021). "TNF-alpha promotes insulin resistance in obstructive sleep apnea-hypopnea syndrome." Exp Ther Med **21**(6): 568.
Zhao, X., X. Liu, G. Wang, X. Wen, X. Zhang, A. R. Hoffman, W. Li, J. F. Hu and J. Cui (2016). "Loss of insulin-like growth factor II imprinting is a hallmark associated with enhanced chemo/radiotherapy resistance in cancer stem cells." Oncotarget **7**(32): 51349-51364.
Zhao, Z., M. Lan, J. Li, Q. Dong, X. Li, B. Liu, G. Li, H. Wang, Z. Zhang and B. Zhu (2019). "The proinflammatory cytokine TNFalpha induces DNA demethylation-dependent and -independent activation of interleukin-32 expression." J Biol Chem **294**(17): 6785-6795.
Zheng, Z. H., D. M. Wu, S. H. Fan, Z. F. Zhang, G. Q. Chen and J. Lu (2019). "Upregulation of miR-675-5p induced by lncRNA H19 was associated with tumor progression and development by targeting tumor suppressor p53 in non-small cell lung cancer." J Cell Biochem **120**(11): 18724-18735.
Zhong, T., Y. Men, L. Lu, T. Geng, J. Zhou, A. Mitsuhashi, M. Shozu, N. J. Maihle, G. G. Carmichael, H. S. Taylor and Y. Huang (2017). "Metformin alters DNA methylation genome-wide via the H19/SAHH axis." Oncogene **36**(17): 2345-2354.
Zhou, Y., B. Sheng, Q. Xia, X. Guan and Y. Zhang (2017). "Association of long non-coding RNA H19 and microRNA-21 expression with the biological features and prognosis of non-small cell lung cancer." Cancer Gene Ther **24**(8): 317-324.
Zhu, M., Q. Chen, X. Liu, Q. Sun, X. Zhao, R. Deng, Y. Wang, J. Huang, M. Xu, J. Yan and J. Yu (2014). "lncRNA H19/miR-675 axis represses prostate cancer metastasis by targeting TGFBI." FEBS J **281**(16): 3766-3775.
Zuo, Q. S., R. Yan, D. X. Feng, R. Zhao, C. Chen, Y. M. Jiang, M. Cruz-Correa, A. G. Casson, X. D. Kang, F. Han and T. Chen (2011). "Loss of imprinting and abnormal expression of the insulin-like growth factor 2 gene in gastric cancer." Mol Carcinog **50**(5): 390-396.

INTERNET REFERENCES

ATCC.org, 2016. Accessed 1st June 2021. https://www.atcc.org/

Bowelcancer.org.uk., 2019[2]. "Staging and grading". Accessed 22nd February 2021. https://www.bowelcanceruk.org.uk/about-bowel-cancer/diagnosis/staging-and-grading/

Bowelcanceruk.org.uk., 2019[1]. "Symptoms of bowel cancer". Accessed 22nd February 2021. *https://www.bowelcanceruk.org.uk/about-bowel-cancer/symptoms/?gclid=CjwKCAiAyc2BBhAaEiwA44-wW8uNiMgiCPzuu26jUZaNmTw38ZoCepZnc9l0H2lvELMsXgpQmgd9LxoCyg8QAvD_BwE*

Cancer.net (2019). "Colorectal Cancer: Introduction". Accessed 17th February 2021. *https://www.cancer.net/cancer-types/colorectal-cancer/introduction*

Cancer.org (2018). "What Are Wilms Tumours?". Accessed 12th February 2021. *https://www.cancer.org/cancer/wilms-tumor/about/what-is-wilms-tumor.html*

Cancerresearchuk.org., 2019[1]. "The Gleason score and Grade Groups". Accessed 11th February 2021. *https://www.cancerresearchuk.org/about-cancer/prostate-cancer/stages/grades*

Cancerresearchuk.org., 2019[2]. "Treatment". Accessed 22nd February 2021. *https://www.cancerresearchuk.org/about-cancer/bowel-cancer/treatment*

cancerresearchuk.org., 2020[1]. "Prostate cancer incidence statistics: Prostate cancer incidence by UK country". Accessed 11th February 2021. *https://www.cancerresearchuk.org/health-professional/cancer-statistics/statistics-by-cancer-type/prostate-cancer/incidence#heading-Zero*

cancerresearchuk.org., 2020[2]. "Prostate cancer incidence statistics: Prostate cancer incidence by age". Accessed 11th February 2021. *https://www.cancerresearchuk.org/health-professional/cancer-statistics/statistics-by-cancer-type/prostate-cancer/incidence#heading-One*

cancerresearchuk.org., 2020[3]. "Bowel cancer statistics: Bowel cancer statistics". Accessed 7th February 2021. *https://www.cancerresearchuk.org/health-professional/cancer-statistics/statistics-by-cancer-type/bowel-cancer#heading-Zero*

cBioPortal.org. Accessed 9th May 2021. https://www.cbioportal.org/

Diabetes.co.uk., 2019. "Diabetes and Hyperglycemia". Accessed 11th February 2021. https://www.diabetes.co.uk/Diabetes-and-Hyperglycaemia.html

Macmillan.org., 2018. "Staging of prostate cancer". Accessed 11th February 2021. https://www.macmillan.org.uk/cancer-information-and-support/prostate-cancer/staging-and-grading-of-prostate-cancer

NHS.uk (2018). "Should I have a PSA test?" Prostate cancer. Accessed 11th February 2021. *https://www.nhs.uk/conditions/prostate-cancer/should-i-have-psa-test/*

NHS.uk (2019). "Diagnosis - Bowel cancer". Accessed 22nd February 2021. https://www.nhs.uk/conditions/bowel-cancer/diagnosis/

NICE, 2012. "Type 2 diabetes in adults: management ". Accessed 9th March 2017. https://www.nice.org.uk/guidance/ng28/ifp/chapter/blood-glucose-and-target-levels

niddk.nih.gov., 2020. "Insulin resistance & Prediabetes". Accessed 1st June 2021. https://www.niddk.nih.gov/health-information/diabetes/overview/what-is-diabetes/prediabetes-insulin-resistance

Prostatecanceruk.org (2019). “What are the symptoms of prostate cancer?”. Accessed 11th February 2021. *https://prostatecanceruk.org/prostate-information/about-prostate-cancer/prostate-cancer-symptoms*